D.Phil Thesis

by

Dennis Kätzel

under supervision of

Prof. Gero Miesenböck

submitted in

Hilary Term 2011

OPTOGENETIC ANALYSIS OF INHIBITORY CIRCUITS IN THE NEOCORTEX

Und da

war der heilige Hain

nur noch Holz.[1]

G.W.F. Hegel

[1] "And thus, the sacred grove was only wood."

Optogenetic Analysis of Inhibitory Circuits in the Neocortex

Dennis Kätzel, Keble College, D.Phil Physiology, Anatomy and Genetics, HT2011

Abstract

Information processing in the brain involves circuits composed of different classes of neurons. Inhibitory interneurons are by far the most diverse subgroup in terms of physiology and morphology, and the principles that govern their connectivity are far from understood. Their excitatory counterparts, pyramidal and spiny stellate cells, have been found to be governed by a compartmentalized horizontal and vertical structure – forming layers and columns – as well as by a stereotypic or "canonical" pattern of connections between them.

However, it has remained unclear whether similar, general organizing principles exist for inhibitory circuits. To map the sources of inhibitory inputs to neocortical pyramidal cells, a Cre-lox-based mouse knock-in line, that conditionally expresses the light-sensitive ion channel channelrhodopsin-2 in GABAergic neurons, was generated. Expression levels were sufficient to drive interneuron spiking at up to 40 Hz, but too low to activate synaptic terminals allowing perisomatic activation and thus mapping of local connections. I found, that inhibitory inputs to excitatory cells in all layers in primary motor (M1), somatosensory (S1), and visual cortex (V1) derive largely from the same layer and putative column. However, four translaminar inhibitory connections were found, which differ significantly both, between as well as within a cortical area. Most notably, (some) excitatory cells in layers 2/3, 4 and 5B of V1 receive prominent, putative feedback inhibition from their direct or indirect output layers. Furthermore, while a columnar structure is visible also in inhibitory circuits, their laminar organization is degenerate in an area-specific manner. Neocortical inhibitory microcircuits thus display significant variations, which potentially reflect the localization of function.

ACKNOWLEDGEMENTS

I wish to thank Drs. Michael Kohl, Tommas Ellender, Karri Lamsa, Louise Upton, as well as Wiebke Nissen, Robert Roorda and Yan Tan for their very helpful continuous support and advice during the research presented in this thesis. I am furthermore very grateful to Drs. Boris Zemelman and Markus Woelfel for providing the three transgenic mouse lines deployed in this project and starting its characterization. Moreover, I thank “my” former student, Christina Buetfering, for her sedulous help during the initial evaluation of the ChR2 mouse line.

I owe an overwhelming gratitude to my supervisor, Prof. Gero Miesenböck, for providing me with the conditions and materials, the direction and scientific advice, as well as the inestimable general support of – and beyond - my thesis project.

Finally, I deeply thank my family, Elisa and Niklas, for everything.

DECLARATION

I declare that I have produced this thesis myself in its entirety, under supervision of Prof. Gero Miesenböck. Parts of the results, methods and discussion are taken from my previous paper (Kätzel et al., 2011), for which I have conducted all experiments and analyses published therein as well as provided the basic manuscript. All experiments contained in this thesis have been done by myself unless stated otherwise.

WORD COUNT

43,203 (excl. references)

Contents

Chapter 1 – Introduction

Functional dissection of the neuronal machine

To truly understand how the brain processes information one requires knowledge of the structure as well as the function (or: computational goal) of its computational elements, like neurons, circuits and regions (Glimcher, 2004; Marr, 1982; Marr and Poggio, 1976). A description of the pure structure of a neural network is prerequisite for a mechanistic conception of how neural signals flow within the circuit, but if this structure cannot ultimately be related to the circuit's computational function, it lacks explanatory power (Martin, 2009)[2].

Nonetheless, the 'default' strategy is to at first adopt a reductionist approach, which decomposes the system into its parts, that are individually easier to analyze. In circuit neuroscience the most obvious of these routes is connectomics (Eisenstein, 2009): 'If you want to understand the neural circuits of the brain, decompose them into the neurons and connections between them and describe both at a biophysically and morphologically detailed level.' However, this endeavour is hampered by many problems. For example, descriptions of axonic and dendritic morphology (Binzegger et al., 2004; Helmstaedter et al., 2009a, b, c) do not capture the actual physiological connectivity (e.g. synaptic strength) between neurons. Approaches using electrophysiology (Brown and Hestrin, 2009; Gupta et al., 2000; Thomson et al., 1996a; Thomson et al., 1996b; Thomson et al., 2002) can only look at few neurons at a time (Scanziani and Hausser, 2009), often not knowing their type; they thus remain blind to the organization of the network as a whole.

[2] These arguments date back to Immanuel Kant's *Critique of Judgement* (chap. 81) (Kant, 2001), where he states that any account claiming to be an 'explanation' in biology must involve two criteria: Its contents need to be *mechanistic*; and they need to be *functional*. Either one alone gives rise to a solely descriptive account.

In my DPhil research I therefore capitalize on a novel technology originally pioneered by my supervisor Gero Miesenböck (Lima and Miesenböck, 2005; Miesenböck and Kevrekidis, 2005; Zemelman et al., 2002; Zemelman and Miesenböck, 2001; Zemelman et al., 2003) and termed optogenetics (Deisseroth et al., 2006). Optogenetics — encoding responsiveness to light genetically — allows the observation or control of the activity of genetically specified subtypes of neurons within intact neural tissue at a large scale with optical methods (Miesenböck and Kevrekidis, 2005). In my project, I focus on a brain area, which is not only central to human cognitive abilities, but also encompasses a wide variety of cell subtypes, which – to a large extent – are poorly understood: the neocortex. Once I have studied parts of its connectivity, as demonstrated in this thesis, I will be able to formalize this knowledge in a computational model and derive functional predictions (Martin, 2009) that are to be tested *in vivo,* in future. In this way, structural, mechanistic insight can be linked back to a functional, computational goal.

The organization of the neocortex

The neocortex is usually thought to be the most complex of all brain areas and also the largest (in terms of volume) and most recently evolved (Hawkins and Blakeslee, 2004; White, 1989). Neuroscientists are used to refer to four organizational principles when they study and talk about neocortical connectivity. First, neocortex is organized into – roughly six – layers horizontally. Second, it is divided into columns vertically. Third, there is a more or less stereotypic ("canonical") flow of information between layers (Douglas and Martin, 2004). Fourth, individual connections are cell-specific rather than random (Thomson and Morris, 2002; Yoshimura and Callaway, 2005; Yoshimura et al., 2005). The main purpose of my

dissertation project was to examine whether these organizational principles also hold for inhibitory circuits. I will return to these four central tenets after discussing the connections formed by excitatory and inhibitory neocortical neurons.

The neocortex contains three anatomical types of connections: local, inter-areal or sub(neo)cortical projections (Douglas et al., 2004; White, 1989). Functionally, connections can be inhibitory, excitatory or modulatory. While excitatory connections, can be of all three types, inhibitory ones are mainly local, while modulatory ones[4] are mostly subcortical long-range projections (Douglas et al., 2004; Douglas and Martin, 2004; Petreanu et al., 2007; White, 1989).

The quantitative or physiological description of excitatory and inhibitory connections within the cortex has largely been based on data from primary sensory cortices – especially visual cortex – of monkeys, cats (Binzegger et al., 2004; Gilbert, 1983; Gilbert and Wiesel, 1979, 1983; Martin and Whitteridge, 1984; Thomson et al., 2002), tree shrew (Fitzpatrick, 1996), ferrets and rodents (Dantzker and Callaway, 2000; Thomson et al., 2002) and (later on) the somatosensory (particularly: barrel) cortex of rodents (Gupta et al., 2000; Thomson et al., 2002). In the last two decades, much effort has been devoted to investigating specific individual connections in great anatomical and physiological detail using electro- and/or optophysiology in combination with morphological reconstructions, as described below.

[4] Modulatory input is thought to arise mainly from nuclei in the midbrain and brainstem (substantia nigra pars compacta and ventral tegmental areal providing dopamine, raphe nucleus for serotonin, locus coeruleus for norepihephrine), the hypothalamus (tuberomammilary nucleus providing histamine) and the forebrain (Nucleus basalis Meynert giving rise to cholinergic projections) (Purves et al., 2004).

Excitatory connections

Intrinsic or **local neocortical excitatory connections** by far outnumber (both with respect to the absolute numbers as well as types of connections) inter-areal and inter-regional (cortical-subcortical) connections (Douglas et al., 2004; White, 1989). Their sources, excitatory pyramidal neurons and spiny stellate cells of layer 4 represent about 80 % of all neocortical neurons. The notion that they represent a rather uniform population, though common, is debated (e.g. (Chang and Luebke, 2007; Schubert et al., 2001)) and will be addressed below.

Determining the "flow of information" within a cortical circuit, local excitatory connections appear to conform, with only minor variations (Barbour and Callaway, 2008; Koralek et al., 1988; Shepherd and Svoboda, 2005; Weiler et al., 2008), to the "canonical" laminar organization first described in cat visual cortex (Binzegger et al., 2004; Douglas and Martin, 2004; Gilbert, 1983; Gilbert and Wiesel, 1979, 1983; Thomson and Bannister, 2003; Thomson et al., 1996a; Thomson and Lamy, 2007; Thomson et al., 2002), independently of the cortical area or species: Thalamic afferents arrive in layer 4, whose spiny stellate neurons project to the superficial layers 2 and 3. Axonal projections of pyramidal cells in these layers terminate in layer 5 and some of those from layer 5 in layer 6. Pyramidal neurons in layer 6 in turn excite the thalamic input layer 4. In addition, strong recurrent connections – although existing in all layers – are especially numerous in layer 2/3 (Binzegger et al., 2004; Thomson et al., 2002).

Area-specific variations of this "canonical" scheme include a second, so-called paraleminiscal thalamic input stream into somatosensory cortex (S1) terminating in the septal regions in layers 5A to 1 (Koralek et al., 1988; Lu and Lin, 1993), a strong excitatory feedback-projection from layer 3 to 4 in auditory cortex (A1) (Barbour and

Callaway, 2008), a strongly diminished layer-6-to-4 connection in S1 (Schubert et al., 2003) compared to V1, a 5A-to-2 (septum) excitatory projection in S1 (Shepherd and Svoboda, 2005) as well as an apparently exclusive top-down organization in primary motor cortex (M1), which lacks both a prominent thalamorecipient middle layer (4) with densely packed spiny stellate cells and the layer-6-to-4 connection (Douglas et al., 2004; Hooks et al., 2011; Weiler et al., 2008).

Inter-areal excitatory projections mostly originate in layer 2/3 and target layer 4 (if projecting to functionally higher cortical areas), or derive mainly from 5 or 6 and target all layers except for 4 (if projecting to lower cortical areas). Inter-hemispheral (callosal) projections between homologous areas originate mainly from layers 2/3 and 5 and target especially layers 2/3 and 5 and, to a lesser extent, also layer 6 but never layer 4 (Douglas and Martin, 2004; Petreanu et al., 2007; White, 1989).

Subcortical output (efferent) projections usually originate in layer 5 – if targeting the tectum, striatum, pons, medulla or spinal cord – or in layer 6 – if targeting the thalamus or the claustrum (Brown and Hestrin, 2009; Douglas et al., 2004; White, 1989).

Subcortical excitatory input (afferent) projections into the neocortex – especially to its primary sensory areas - in turn is mainly provided by the thalamus (White, 1989). While the excitatory input to hierarchically higher neocortical areas mainly derives from other neocortical areas (see below), these areas may also receive some specific subcortical excitation. For example, the magnocellular component of the superior colliculus is disynaptically connected to the higher visual areas V3 and V5 (dorsal stream) involving only the thalamus (pulvinar), but not the primary visual cortex V1 – and thus potentially allowing the phenomenon of “blindsight” (Lyon et al., 2010).

Excitatory inputs from both, neocortical and subcortical sources, innervate pyramidal cells in layers 2/3, 5A and 5B of S1 at different stereotypic subcellular positions, thus mapping the different input channels onto their somato-dendritic axis (Petreanu et al., 2009): Layer 2/3 neurons receive excitation from the following sources and onto the dendritic area given in brackets: ventral posterior medial (VPM) thalamic nucleus (basal dendrites below cell body), layer 4 (proximal dendrites above VPM-input-zone), layer 2/3 itself (proximal apical dendrite), M1 (distal dendrite/tuft) and posterior medial (POM) thalamic nucleus (apical dendrite). Pyramidal neurons in 5B are excited by the following sources: VPM (proximal and distal apical dendrite), layer 4 (proximal apical dendrite), layer 2/3 (middle apical dendrite), M1 (middle apical dendrite), while POM input is lacking. Neurons in layer 5A are innervated from the following sources: POM (basal dendrites and tuft), layer 2/3 (basal dendrites) and otherwise like described for layer 5B target cells. In addition, for layer 5 cells the location of layer 2/3-input correlates linearly with the distance (depth) of the somatic location of the cell. The fact that both, POM- as well as M1-derived input – both carrying information about whisker position and movement – arrive, if present, in the apical dendrite or tuft of pyramidal cells of all three layers (2/3, 5A, 5B), suggests a common principle regarding the precise placement of excitatory synapses along the dendritic axis, which in turn might reflect a stereotypic pattern of dendritic integration of distinct input streams (Petreanu et al., 2009). Functionally, however, inputs may not be obviously segregated along the dendritic tree, creating ”minimaps” of tuning preference. Rather, synapses transmitting inputs with largely distinct visual orientation-tuning

may be found in immediate vicinity on a dendritic branch, while those with similar tuning are dispersed among dendrites (Jia et al., 2010).

Inhibitory connections and inhibitory cell types

It has been difficult to determine whether general principles, similar to the excitatory canonical microcircuit, also hold for the laminar organization of inhibitory neocortical neurons and their (local) projections (Douglas and Martin, 2009; Gupta et al., 2000). Systematic studies of inhibitory connectivity, which are prerequisite for abstracting wiring diagrams, have been hampered by the relative sparseness of inhibitory neurons and a bewildering diversity of cell types (Blatow et al., 2005; Gupta et al., 2000; Markram et al., 2004; Soltesz, 2006)(see below). Inhibitory interneurons represent about 15 % of neocortical neurons in rodents, and 20-25 % in primates (DeFelipe et al., 2002).

In general, however inhibitory connections are mainly thought to be local (Douglas and Martin, 2004). Few exceptions to this rule have been found, including interregional connections found in older cortical structures (Apergis-Schoute et al., 2007; Buzsáki et al., 2004), millimeter-long axonal arborizations of Martinotti cells (Markram et al., 2004; Wang et al., 2004), long-range projections from nNOS-positive neocortical interneurons into other target areas and even the hippocampus (Higo et al., 2009), as well as GABAergic input into neocortical from subcortical structures (Douglas et al., 2004).

Interneuron types and their target-specific connectivity

Interneurons form synapses that release the small-molecule neurotransmitter GABA[5], which generally acts on ionotropic $GABA_A$-receptors[6] and thus gates a chloride-permitting conductance. Depending on the chloride-reversal potential[7] and the actual membrane potential, chloride ions will either flow inward and hyperpolarize the cell (at high membrane potential) or may be repelled outward by particularly negative (low) membrane potential leading to a depolarization of the cell[8]. In each case – and also in its common intermediate of nearly no net flow of chloride – the opening of the conductance reduces membrane resistance and thus shunts the cell membrane locally (shunting or divisive inhibition) (Mann and Paulsen, 2007; Staley and Mody, 1992). During development, intracellular chloride concentration is high due to reduced expression of the potassium-chloride-co-transporter 2 (KCC2), and the action of GABA therefore depolarizing (Rivera et al., 1999), which is supposed to regulate the formation of neural circuits, e.g. by providing a broad integration window for glutamatergic plasticity (Akerman and Cline, 2007).

GABA may also bind to $GABA_B$ receptors, which are metabotropic, namely G_i-protein coupled receptors, which inhibit voltage-gated calcium channels while opening inward-rectifying potassium channels (GIRK) producing a prolonged outward current and thus sustained inhibition (Bowery et al., 2002; Chalifoux and

[5] At the hippocampal basket-to-granule-cell synapse, the opening of only three or fewer presynaptic Ca^{2+}-channels is required to trigger GABA release, which – despite the highly stochastic nature of the Ca-channel opening – occurs with high temporal precision (Bucurenciu et al., 2009).

[6] A second form of ionotropic GABA-receptors, GABAC receptors, have been found to be expressed during cortical development in the intermediate zones and have been implicated in the regulation during neuronal migration (attraction of cells) (Denter et al., 2010) (apart from functions outside the cortex).

[7] The driving force for GABA-mediated chloride-currents may also be altered due to activity- and location-dependent changes in extracellular chloride concentration (Kroeger et al., 2010).

[8] GABAergic synapses mature postnatally, in that sense, that they are actually excitatory (depolarizing) on both, pyramidal cells, as well as interneurons (Sauer and Bartos, 2010; Tyzio et al., 2006), but become inhibitory between the first and second postnatal week.

Carter, 2011; Kohl and Paulsen, 2010; Padgett and Slesinger, 2010). In addition, many interneurons may release a variety of neuropeptides, which generally seem to decrease the activity in a local network (Baraban and Tallent, 2004). In general, an interneuron forms more synapses (according to one reference, up to 30, 15 on average) onto one pyramidal-cell-target than pyramidal cells do; those synapses are usually highly distributed (Markram et al., 2004). In addition, the weight of inhibitory synapses, like that of excitatory ones, can be acutely strengthened by nicotinergic cholinergic innervation (Aracri et al., 2009; Lawrence, 2008; von Engelhardt et al., 2007). Finally, GABA is not only present during active (spike-mediated) synaptic transmission of inhibitory interneurons, but also on a continuous basis providing tonic inhibition, potentially due to GABA-release from glia cells as shown in cerebellum (Lee et al., 2010). Tonic $GABA_A$-activation does not change the membrane potential in the resting state, but introduces a negative offset, when the neuron is driven near to spiking threshold (Pavlov et al., 2009). Also, GABA-release from astrocytes, induced upon glutamate-uptake, may add to tonic inhibition (Heja et al., 2009).

Subcellular targetting of GABAergic connections

The rules governing the interneuron-type-specific positioning of inhibitory synaptic terminals on the surface of postsynaptic target cells are increasingly well understood, and, in fact, provide the primary basis of classification of interneurons in hippocampus and neocortex of all species investigated, including rodents, cats and monkeys (Douglas et al., 2004; Douglas and Martin, 2004; Klausberger and Somogyi, 2008; Markram et al., 2004; White, 1989):

It is generally thought that in both brain regions one cell type preferentially forms synapses at axons – the axo-axonic or chandelier cell – while a second type

primarily forms synapses at the soma and proximal dendrites ("perisomatically targeting"). The latter cell type is referred to as the basket cell and further subdivided in small, large and nest basket cells[9]. The remaining interneurons – most prominently bipolar cells, double-bouquet cells, bitufted cells, and Martinotti cells – comprise a heterogeneous group whose members target preferentially the dendrite, with more or less specificity for the proximal or distal dendritic shafts, the apical tuft or maybe dendritic spines (Table 1.1) (Douglas and Martin, 2004; Halasy et al., 1996; Markram et al., 2004).

Although the (sub-)cellular location of presynaptic terminals is a primary criterion to define interneuron types (see below and Table 1.1 for other classification schemes), it is worth noting that targeting preferences are mostly qualitative rather than absolute. For example, Martinotti cells, known to from the majority of inhibitory synapses on the dendritic tufts of pyramidal cells, also target along the entire dendrite as well as at the soma (Markram et al., 2004; Wang et al., 2004). Conversely, small basket cells in layer 4 of the cat (clutch cells) make the majority of their synapses (35-50%) on dendritic shafts, and, in addition, form about as many synapses on dendritic spines as on somata (<=30%) (Kisvarday et al., 1985). Nevertheless, basket cells can be generally distinguished from all other interneurons by having a considerable number of synapses (20-50%) in the perisomatic region, while all dendrite-targeting cells have many fewer. According to this criterion (as well as their general morphology), basket cells have been identified in all mammalian species investigated, including mouse, rat, cat, monkey and human (White, 1989). Only in the latter two (i.e. in primates), however, do their

[9] The distinction between those is again mainly made based on (axonal) morphology: large basket cells, predominating in layer 4 (compared to 2 and 3), are multipolar and have long horizontal axon collaterals. Small basket cell in contrast have dense, local axon collaterals.The nest basket cell, forms long axons forming nests around the soma (Gupta et al., 2000; Markram et al., 2004).

axonal terminals form the dense “pericellular nests” (originally discovered by Cajal in human tissue), which inspired their name, “basket” cell, and sparked considerable discussion regarding a primate-specific interneuron subtype (White, 1989).

An exception to this “rule” of fuzzy targeting profiles are the Chandelier cells, which have been found to contact the axonal compartment of their postsynaptic partners with high specificity in all species examined including mouse, rat, rabbit, cat, monkey and human (White, 1989).

Morphology of interneurons

In addition to the axonal targeting pattern, axonal as well as dendritic morphology can be used to classify interneurons into one of the subgroups listed in Table 1.1, while somatic morphology is usually less informative. For example, interneurons can be broadly classified into three main categories, based on whether their axonal arbours are local (neurogliaform cell, small basket cell, chandelier cell, etc.), vertical (double bouquet cell, Martinotti cell, bipolar cell), or horizontal (large basket cell, Cajal-Retzius cell) (DeFelipe, 2002; Douglas and Martin, 2009). Historically, the categorization of interneurons according to their axonal and dendritic morphology provided the one and only means of their classification for more than half a century (White, 1989). During those anatomical studies it turned out, that all major morphological subtypes of interneurons are qualitatively present in various mammals such as marsupials, rodents, rabbits, cats and monkeys, while their quantitative abundance may vary from species to species or area to area (DeFelipe et al., 2002; Douglas and Martin, 2004; Tyler et al., 1998; White, 1989). For example (Douglas and Martin, 2004), double-bouquet or bipolar cells are present in rat frontal cortex (Kawaguchi and Kubota, 1997) and rat V1 (Peters and Harriman,

1988), cat V1 (Peters and Regidor, 1981) and monkey V1 (Lund and Wu, 1997). Although in primate neocortex morphological diversity of interneurons is more advanced compared to rodent neocortex (in the sense, that the former contains morphologically very specialised cell types, while in the latter morphologies are more uniform), this does not imply a greater diversity of function of interneurons in general (Douglas and Martin, 2004; Tyler et al., 1998; White, 1989), i.e. “novel, primate-specific” functional interneuron types such as the “true” wide arbor basket cell with dense pericellular nests (White, 1989) or the double bouquet cell (DeFelipe et al., 2002) as sometimes argued.

	AAC/CC	LBC	SBC	NBC	BTC	NGC	BPC	DBC	MC	CRC
Name	Chandelier	Large Basket	Small Basket, Clutch (in V1 L4)	Nest Basket	Bitufted	Neurogliaform	Bipolar	Double Bouquet	Martinotti	Cajal Retzius
Proteins (according to H. Markram)	CB, PV	CB, PV, NPY, SOM (rare), CCK; never VIP	CB, PV, **VIP**, CCK	CB, PV, NPY, SOM, CCK	CB, CR, NPY, VIP, SOM, CCK; Never PV	?	**CR & VIP**, CCK	**CB & CR**, VIP or CCK Never PV, SOM, NPY	CB, CR, **SOM**, CCK; never PV or VIP	
Target - Compartment	axon	soma & proximal dendrite	soma	soma & proximal dendrite	dendrite	dendrite	basal dendrites of PCs	basal dendrites of PCs; spines & shafts of dendrites	all dendrite & tuft, soma	dendrite & tuft
Layers of soma location	2/3 & 5 (5%) 4 & 6 (1%)	2/3 (30%) 4 (30%) 5 (40%) 6 (30%)	2/3 & 5 (5%) 4 (10%) 6 (2%)	2/3 (20%) 4 (25%) 5 & 6 (8%)	2/3 (15%) 4 & 6 (8%) 5 (5%)	2-4 (1-2%)?	2/3 (10%) 4-5 (5%) 6 (10%)	**2/3** & 5 (8%) 4 (3%)	2/3 (15%) 4 (25%) 5 (33%) 6 (50%)	1
Soma		large	medium		ovoid	very small, button-like	small, spindle or ovoid	ovoid?		large
Firing pattern (classical)		FS		-		LS (late-s.), (2/3, 5)	RSNP (2/3, 5); IS (2/3, 5)	LTS/BSNP (L5); RSNP (2/3, 5)	LTS/BSNP (L5), RSNP (2/3, 5)	
Firing pattern (Markram)	AC, cNAC, bNAC, dSTUT, rBST	AC, NAC, cSTUT, cIS, dSTUT, rBST,	AC, NAC, STUT	bAC, cAC, cNAC, dNAC, cIS	bAC, cAC, NAC, cSTUT	dNAC	bAC, cAC, bNAC, cSTUT, bIS, cIS	bAC, cAC, bNAC, bIS, cIS	bAC, cAC, cNAC, bSTUT, cSTUT, cIS	-
Axon	local clusters frequent branching chandeliers	expansive, translaminar transcolumnar	local, dense, varicose, curvy, branchy	local (cluster), longer; less frequ. branching	wide horizontal span across columns, but only to adjacent layers	dense, intertwined arboziation of ultra-thin axons with very frequ. branching	narrow band crossing all layers; low bouton density / target #	tight fascicular axonal cylinder with highly varicose collaterals extending across all layers, dense boutons, frequ. branching	projecting towards L1 and horizontally in L1 for mms; target L1-L5 (selectively); form spiny boutons	only in L1, extensive

	AAC/CC	LBC	SBC	NBC	BTC	NGC	BPC	DBC	MC	CRC
Dendrite	multipolar bitufted	large, mostly multipolar, but also bipolar, bitufted or pyramidal	multipolar (L4), bitufted,& bipolar (L2/3)		bitufted	many fine radiating dendrites, finely beaded & rarely branched; symmetrical & spherical arbour	mostly bipolar, rarely bitufted; Extending up to L1 and down to L6	bitufted		
Synapse # onto PCs	?	14.5 ± 1.7	20.5 ± 10.5	15.8 ± 4.1	15 ± 7	?	?	?	11.2 ± 5.5	?
Synapse type (IN pre)	2d	2d	1f (AC) - only 1 2d (dNAC) 3c (cNAC)	2d 3c	2d	2d	-	-	2d 3c (bSTUT)	-
Synapse # from PCs	2.5	7	2.5	2.5	7	?	3	?	10	?
Synapse type (PC pre)	2d	2d	-	1f (AC, dNAC); 2d (d-NAC)	-	-	-	2d	1f	-
Comment	powerfully editing output of target cells	primary source of la-teral intralami-nar inhibition between columns					may be excitatory by releasing only VIP		source of transcolum-nar inhibition from layer 1	

Table 1.1: **Diversity of subtypes of neocortical inhibitory interneurons** (Gupta et al., 2000; Markram et al., 2004). ***Abbreviations:*** **Interneuron Markers:** CB, calbindin; PV, parvalbumin, CR; calretinin; NPY, neuropeptide Y; VIP, vasoactive intestinal peptide; CCK, cholecystokinin, SOM, somatostatin. **Firing patterns:** FS, fast-spiking; LS, late-spiking; IS, irregular spiking; RSNP, regular spiking non-pyramidal; BSNP, bust-spiking non-pyramidal, AC, accomodating (=adapting); NAC, non-accomodating (=non-adapting); IS, irregular spiking, rBST, regular bursting; STUT, stuttering; c, classical; d, delayed; b, bursting. **Short-term synaptic plasticity:** 1f, fascilitating; 2d, depressing; 3c, constant.**Misc.:** PC, pyramidal cell, L, layer.

Beyond morphology – further classification schemes for interneurons

In addition to morphological criteria it is usually practical as well as functionally informative to use three additional characteristics for classifying interneurons: the expression of marker proteins, the electrophysiological response properties (in response to a depolarizing step pulse) and the short-term synaptic dynamics of the input and output synapses, i.e. the excitatory synapses targeting the interneuron as well as the inhibitory synapses formed by the interneuron on other postsynaptic neurons.

With respect to **marker proteins** (Blatow et al., 2005; Markram et al., 2004) it is generally assumed that parvalbumin (PV), somatostatin (SOM) and calretinin (CR) in the rat brain (Markram et al., 2004) or parvalbumin, somatostatin and VIP in rat (Kawaguchi and Kubota, 1997) and mouse (Gonchar et al., 2007; Xu et al., 2010b) brain define three mutually exclusive subtypes of interneurons. In rats, in fact, up to 5 largely (but not strictly) non-overlapping cell types have been described: CCK- and α-actinin-positive neurons, in addition to the types defined by PV, CR, and SOM (Uematsu et al., 2008). In contrast to the situation in rats, calretinin can be co-expressed with SOM in mice; and in both rodents it is largely colocalized with VIP (Gonchar et al., 2007; Uematsu et al., 2008; Xu et al., 2010b). The three mutually exclusive subclasses in mice defined by PV, SOM and VIP account for only about 60 % of all inhibtory neurons, while the remainder express markers like calbindin, neuropeptide Y (NPY), cholecystokinin (CCK) and CR (in addition to others), which however partially overlap with SOM or VIP (Xu et al., 2010b). The mature immunohistochemical identity defined by neuropeptide expression patterns (NPY, SOM, CCK, VIP) is established in the first four postnatal weeks (Gonchar et al., 2007; Kowianski et al., 2008). Also in other (non-rodent) species such as monkeys,

cats and marsupials, all major calcium-binding proteins (PV, CR and CB) as well as neuropeptides (SOM, NPY, VIP) are present in certain subtypes of interneurons, which are generally similar in morphology and laminar or areal distribution to those found in rodents (Douglas and Martin, 2004; Hof et al., 1999). In monkeys, the three calcium-binding proteins have been traditionally used to label three interneuron subclasses (Douglas and Martin, 2004; Hof et al., 1999), as calbindin and parvalbumin are expressed in a largely mutually exclusive fashion (Hendry et al., 1989). While the latter was also reported in rat frontal cortex initially (Kawaguchi and Kubota, 1993), it became a matter of debate later on to what extent it holds true for rodent neocortex in general (Markram et al., 2004).

The **electrophysiological response properties** are not as uniform as molecular ones, as different authors use different classification schemes altogether, e.g. compare (Gupta et al., 2000; Otsuka and Kawaguchi, 2009; Xu and Callaway, 2009). In general, they imply a categorization based on the spiking behaviour of an interneuron evoked by a depolarizing step-current injected during whole-cell current-clamp recordings. The most advanced scheme (Ascoli et al., 2008), is largely based on the classification suggested by Henry Markram's lab, which distinguishes between accommodating (= adapting, inter-spike intervals increase substantially over time), non-accommodating (inter-spike intervals remain (nearly) constant), irregular spiking and stuttering (firing clustered spikes followed by pauses of spiking) (Gupta et al., 2000; Markram et al., 2004) – in the three flavours of classical (firing uniformly throughout), delayed onset and bursting onset (Table 1.1). Classically, and in the practical context today, fewer groups are assumed: Mostly, fast-spiking cells are distinguished from a range of others, including irregular

spiking, adapting etc. In addition to the overall response pattern to a step-pulse current injection, other characteristics of the resulting spike train, such as spike-width, are usually used to classify intrinsic electrophysiological properties[10]. Although largely defined in rodents, such electrophysiological interneuron types are also found in other species, with probably only minor variations. For example, while also the monkey cortex contains fast-spiking and adapting interneurons, some types of the latter express very brief spikes – as short as usually only found in fast-spiking cells in rodents; also, neurogliaform cells in layer 1 (identified by NPY-expression like in rodents), did not show delayed-onset spike-responses as typical in rodents (Zaitsev et al., 2008).

The **short-term plasticity** of excitatory synapses onto interneurons as well as of the inhibitory synapses themselves have also been found to vary with some regularity. Most notably, excitatory synapses[11] onto regular-spiking interneurons with bitufted morphology, often expressing somatostatin (i.e. putative Martinotti cells) are facilitating – the amplitude of consecutive EPSPs increases from input to input. In contrast, EPSPs in multipolar, fast-spiking PV-positive interneurons (i.e. putative basket cells) as well as those in double-bouquet cells and irregular spiking bipolar cells are generally depressing, like those in excitatory cells: the amplitude of EPSPs in a train decreases over time (Kapfer et al., 2007; Reyes et al., 1998;

[10] Originally all interneurons were described as FS, then some were singled out as a different group and defined as LTS (low-threshold-spiking) and synonymously as BSNP (burst spiking non-pyramidal) as well as after-hyperpolarization-burst-firing; those cells were mostly found in layer 5 and correspond to Martinotti cells or double-bouquet cells. Then, thirdly, some RSNP (regular spiking non-pyramidal) cells were found in layers 2/3 and 5, and separated out as another group, which correlates morphologically with Martinotti cells, double-bouquet cells or bipolar cells, etc.; (Markram et al., 2004).

[11] Excitatory synapses onto interneurons from clusters on the surface of dendrites and even the soma (while those on pyramidal cells target only the dendrite). A pyramidal cell forms ca. 6 synapses onto a connected basket cell; those synapses display different AMPA-receptor subunit composition and contain few NMDA-receptors (Wang et al., 1999).

Wang et al., 1999). (Other non-fast-spiking interneurons in layer 2/3, however, may also receive depressing inputs, while nest-basket cells may receive facilitating excitation (Gupta et al., 2000; Kapfer et al., 2007; Markram et al., 2004)). In addition, the short-term plasticity of excitatory synapses onto interneurons varies with respect to the home layer of the interneuronal target, even if excitation arises from one and the same pyramidal neuron, providing a potential correlate for layer-specific information processing (Wang et al., 1999).

Inhibitory synapses themselves may show facilitating, depressing or constant (neither depressing nor facilitating) behaviour (Gupta et al., 2000; Reyes et al., 1998). Like excitatory connections, inhibitory ones are mostly depressing, in many cases also constant (recovering); facilitating inhibitory synapses, in turn, seem to be specific to small basket cells (Gupta et al., 2000)[12] – one and the same small basket cell can form a facilitating connection with an interneuron and a constant connection with a pyramidal cell. Similarly, one and the same pyramidal cell can receive both constant as well as depressing inhibitory inputs. This complexity illustrates that the specific combination of pre- and postsynaptic cell type determines short-term synaptic dynamics — the presynaptic-postsynaptic interaction principle (Gupta et al., 2000).

Functional diversity of inhibitory interneurons?

Altogether, a considerable list of morphological, electrophysiological and molecular criteria has been put together by researchers, so far, and consolidated by the Petilla

[12] GABAergic synapses can be *facilitating*, F1 (8% (all from small basket cells) on pyramidal cells, 29% on interneurons), *depressing*, F2 (76% on pyramidal cells, 58% on interneurons) or recovering/unchanged, F3 (16% on pyramidal cells, 13% on interneurons; displaying the largest vesicular release). Both phenomena can co-exist in a single input-train, but one will be more dominant. F2 synapses use multiple release sites, while F1 and F3 probably do not. These classifications can be frequency dependent (Gupta et al., 2000).

consortium (Ascoli et al., 2008) to allow for a standardized description of interneurons[13]. However, given that the various classification schemes hardly map onto each other (Markram et al., 2004), it is perhaps not surprising that the consortium did not manage to produce an unequivocal consensus classification (Douglas and Martin, 2009).

Indeed, it is probably no exaggeration to state that the question of how morphological, electrophysiological and molecular diversity translates into *functional* diversity (computational division of labour) lies at the heart of current interneuron research. The notion that *molecular* diversity translates into functional diversity is the principal hypothesis of any *optogenetic* dissection of inhibitory circuits as envisioned as the primary follow-up project of my D.Phil: This is because, genetic targeting of optical actuators relies on molecular markers (calcium-binding proteins, neuropeptides, and eventually developmental regulators (Huang et al., 2007)) and their genetic control elements to address one putative interneuronal subtype, while leaving all others unresponsive to light. It is only the variety of molecular markers, which provides a handle to cut through the diversity of interneurons in the context of physiology at the network level, while all other classifications do not provide any similar access to manipulate circuitry based on *a priori* knowledge. Thus, the less molecular diversity maps onto morphological and electrophysiological diversity – or: the less it matters for actual diversity of function – the less informative will an optogenetic dissection of interneurons be.

Where, then, does interneuronal classification translate into diversity in interneuron function?

[13] The Petilla nomenclature mentions types of dendrites (aspiny and normal, spiny, aspiny and beaded), types of somata (fusiform, round, polygonal, else), dendritic structure (unipolar, bipolar, bitufted, multipolar), and electrical firing-pattern (fast-spiking (FS), adapting (AC), non-FS-non-AC, accelerating, irregular spiking, intrinsic bursting) which variably mix with the firing modes (initial burst, continuous, delayed, stuttering) (Ascoli et al., 2008).

Target compartment and axonal morphology

It is easiest to see how interneurons targeting different subcellular compartments could play different functional roles: Interneurons forming synapses at the axon or soma are ideally positioned to delay or erase action potentials and thus edit the "output" of their postsynaptic partners. In contrast, interneurons targeting dendritic compartments effectively control synaptic input and its integration (Douglas and Martin, 2004, 2009). Since excitatory inputs from various sources map onto distinct parts of the somatodendritic axis (Petreanu et al., 2009), interneurons targeting the tuft, spines, the distal or the proximal dendrite (Markram et al., 2004) may control distinct input channels.

Likewise, axonal morphology may determine the effective spatial range of an interneuron and thus its function. For example, the wide horizontal, intralaminar arborizations of large basket cells may provide lateral inhibition between columnar units in neocortex (Mountcastle, 1978). In contrast, the narrow but long vertical extensions of double-bouquet cells, bipolar cells and Martinotti cells may subserve feed-forward or feedback inhibition of excitatory signals flowing between layers within a column. Finally, the widely, superficially extending axons exclusive to Martinotti cells make them the only source of transcolumnar inhibition from layer 1 (Markram et al., 2004; Wang et al., 2004). In conclusion, axonal morphology, especially if specific to one interneuronal subclass as defined by other criteria, may confer and reflect functional specialisation.

In one study interneurons were solely classified based on the horizontal and vertical extent of their axons without resort to any other criteria: L2/3 interneurons were classified into local (intralaminar/intracolumnar; 40%), lateral (transcolumnar, 30%), translaminar-L2/3-to-L4/5A (20%) and translaminar-L2/3-to-L1 (8%) inhibitors in

addition to chandelier cells (4%); lateral inhibitors extend to the neighbouring columns potentially providing surround-inhibition (Helmstaedter et al., 2009b).

Dendritic and somatic morphology

Although it is conceivable that dendritic and somatic morphology determines interneuronal function, this possibility appears not to have received much attention in the literature. On the one hand, theoretical studies predict that neuronal morphology has a significant impact on electrophysiological behaviour (Mainen and Sejnowski, 1996; Weaver and Wearne, 2008), suggesting that some correlation between somato-dendritic morphology and electrophysiological characteristics might exist. On the other hand, the principal cause of different functional properties of excitatory pyramidal cells in enthorhinal cortex appeared to be the differential expression and subcellular localisation of ion channels, not systematic changes in morphology (Garden et al., 2008). If this principle holds generally for neocortical cells, cell morphology might indeed not matter much for functional specialisation.

Molecular diversity

The functional relevance of molecular interneuron diversity is much debated. In hippocampus, where interneuronal diversity is much better understood than in neocortex, it has indeed been found that interneurons with different marker proteins – e.g. PV-positive (CCK-negative) vs. CCK-positive (PV-negative) basket cells - form networks with distinct electrical connectivity, synaptic plasticity, subcortical inputs, pyramidal cell targets and oscillatory rhythms (Freund, 2003; Klausberger et al., 2005; Somogyi and Klausberger, 2005). In neocortex, however, our understanding of functional diversity is much less advanced. Nevertheless, groups of molecules used for classification are all likely to confer some functional meaning in any brain region. Empirical investigations have revealed a large diversity of

differential expression of electrically and functionally relevant ion channels (e.g. potassium channel subtypes), gap junction proteins and receptors (e.g. for serotonin) in interneurons (Blatow et al., 2005; Martina et al., 1998; Toledo-Rodriguez et al., 2004). Most intriguingly, some of these marker proteins are mutually exclusive, providing some indirect hint that the cell populations they label are functionally distinct. Most importantly, PV, SOM and VIP are found in distinct interneuron populations (see above). These molecular markers also correlate with some morphological subtypes; e.g. SOM (and never PV or VIP) is mainly expressed in Martinotti cells (and some bitufted cells), VIP in some small basket cells, double bouquet cells and bipolar cells, and PV in chandellier and many basket cells (Markram et al., 2004), providing some degree of overlap across two major classification schemes and suggesting functionally relevant diversity.

A study based on single-cell reverse-transcriptase real-time PCR (Monyer and Lambolez, 1995), combined with additional principal-component and cluster analysis, found three expression clusters thought to comprise genes that confer particular electrophysiological characteristics. The first cluster contains the genes for calretinin (CR) as well as for the ion channel subunits SK2, Kv3.4, Caα1B, all of which mediate slower kinetics and lead to the accommodating (AC) or irregular spiking (IS) electrophysiological phenotype found most prominently in dendrite-targeting interneurons (see Table 1.1). A second cluster includes the calcium-binding protein calbindin and the ion-channel subunits Caα1G, Caβ1, Caβ3, Caβ4, HCN3, HCN4, Kv1.4, and Kv3.3, and confers a bursting behaviour. A third class, probably the most prominent, corresponds to the classical fast-spiking interneuron type – mostly basket and chandellier cells – which is created by a synergy of the fast calcium buffer parvalbumin (PV) and the ion channel subunits HCN1, HCN2,

Kv1.1, Kv1.2, Kv1.6, Kv3.1, Kv3.2, Kvβ1, and Caα1A (Markram et al., 2004; Toledo-Rodriguez et al., 2004; Toledo-Rodriguez et al., 2005). Especially the Kv3.1 and Kv3.2 fast delayed-rectifier potassium channels, which contribute >90% of the outward current during spike-like events, are essential for shaping fast-spiking behaviour as they feature a high activation threshold (permitting a fast rise of the action potential) and a fast deactivation in absence of inactivation (entailing short but strong hyperpolarization) (Jonas et al., 2004). These potassium channel subunits synergize with electrical compactness (including a small membrane time constant, i.e. a small window for temporal summation), spine free dendrites, fast transmitter clearance, and AMPA-mediated EPSCs that are fast, strong and synchronous in quantal release, to mediate extremely rapid signal flow (1-2 ms from synapse to synapse) and fast-spiking (several 100 Hz) phenotype observed in those fast-spiking interneurons (Jonas et al., 2004).

The first (CR) and the last (PV) class are largely mutually exclusive while the expression of calbindin partly – but not completely - overlaps. In addition, there is a near-perfect inversion of expression patterns between delayed-onset and burst-onset-spiking neurons (Markram et al., 2004; Toledo-Rodriguez et al., 2004).

Thus, calcium-binding proteins and some ion-channel subunits represent genetic markers – potentially to exploit in optogenetics – that do not just define arbitrary cell groups but rather correlate with a whole cluster of functionally connected genes giving rise to a specific electrophysiological subtype. The three best characterized (if not the only) examples, where most classification schemes converge on an interneuron subtype whose function in the network is quite well understood, are detailed below.

Such functional meaning of marker molecules is also suggested by the fact, that both, their expression (i.e. the presence of all major peptides and calcium-binding proteins) in general as well as their correlation with certain morphological and/or electrophysiological interneuron types is at least partially conserved not only across neocortical areas, but also across species such as monkey, cat, marsupial, rat and mouse (Douglas and Martin, 2004; Hof et al., 1999): For example, calbindin is expressed by some double bouquet and Martinotti cells (both featuring vertically oriented, translaminar axons) in both, macaque and rat, and show mainly adapting electrophysiological responses (Kawaguchi and Kubota, 1997; Zaitsev et al., 2008). Similarly, parvalbumin labels basket and Chandelier cells in macaque and rodents (Hendry et al., 1989; Hof et al., 1999; Kawaguchi and Kubota, 1997) and correlates in both, rats and monkeys, with fast-spiking electrophysiological behaviour (Kawaguchi and Kubota, 1997; Zaitsev et al., 2008).

Martinotti cells - mediating frequency-dependent disynaptic dendritic inhibition

In the case of the — morphologically defined – Martinotti cell, some coarse correlations exist between all major classification schemes: Martinotti cells are (1) morphologically characterized by upward projecting, broad axonal trees ramifying extensively in layer 1 and bitufted dendrites as well as (2) by the presence of the molecular marker SOM and the absence of PV and VIP (Kawaguchi and Kondo, 2002; Kawaguchi and Kubota, 1996; Markram et al., 2004; Wang et al., 2004). Their (3) electrophysiological response patterns involve accommodating (90 %), non-accommodating (8 %) and stuttering (2 %) types, which are further specified in dependence of initial burst or delay of the response (Wang et al., 2004) (other classification-schemes denote them as either intrinsically bursting (IB) or low-

threshold spiking (LTS)); and they receive (4) facilitating excitatory synapses (Kapfer et al., 2007; Reyes et al., 1998; Silberberg and Markram, 2007).

Apart from fast-spiking neurons, the Martinotti cell is probably the best-characterized (according to the above criteria) interneuron subtype: Due to the supra-linear recruitment of deep layer (layer 5) Martinotti cells via facilitating synapses, the strong axonal arborization in upper layers and the placement of their synapses in dendritic tufts (in layer 1) in the home as well as adjacent and distant columns (Berger et al., 2009; Berger et al., 2010; Kapfer et al., 2007; Markram et al., 2004; Silberberg and Markram, 2007; Wang et al., 2004), Martinotti cells are ideally suited to control the dendritic integration and thus the neuronal gain of layer 5 cells (Berger et al., 2009; Berger et al., 2010; Murayama et al., 2009; Silberberg and Markram, 2007) as well as layer 2/3 cells (Kapfer et al., 2007).

In the former case, they represent the inhibitory component of a very prevalent motif of frequency-dependent disynaptic inhibition between layer 5 pyramidal cells, while in the latter case they might form a layer-5-to-layer-2/3 translaminar inhibitory feedback loop. In both cases they control excitation very effectively by powerful normalizing, gain-modulating inhibition directed mainly towards the dendritic tufts (Larkum et al., 2009; Murayama et al., 2009). Just one layer 2/3 pyramidal cell needs to be active to trigger enough Martinotti cells for widespread inhibition, which in turn increases tenfold when two pyramidal neurons are activated simultaneously (10 spikes, 100 Hz) (Kapfer et al., 2007). And: Only four layer 5 pyramidal cells are sufficient to disynaptically inhibit all layer 5 pyramidal cells in a cortical column via these interneurons (Berger et al., 2010). Such inhibition directed towards the dendritic tuft strongly impedes the transmission of distal-dendritic excitatory inputs towards the soma (Murayama et al., 2009; Pérez-Garci et al., 2006). This is

because apical-dendritic voltage-sensitive Ca^{2+}-channels normally lead to dendritic plateau potentials and dendritic calcium spikes that increase the gain (output/input-relation) and switch the cell to a bursting firing mode (Larkum et al., 2004), while the strength of sensory stimulation is encoded in the dendritic Ca^{2+}-response of layer 5 pyramidal neurons. Thus, the inhibitory control of the distal dendritic excitation and calcium dynamics by Martinotti cells, which are driven by pyramidal neurons in layer 5, may effectively control the gain of many neighbouring pyramidal neurons and thus enable them to encode stimuli adaptively. Although layer 5 Martinotti cells might also be activated by thalamocortical input, only their facilitating excitation by layer 5 pyramidal cells (i.e. their participation in feedback inhibition) has a strong and proportional effect on the gain and enables adaptive coding (Murayama et al., 2009). In fact, thalamocortical activation of Martinotti interneurons is particularly weak or even non-existing, compared to other interneuron subtypes (Beierlein et al., 2003; Cruikshank et al., 2010).

In agreement with this view, it has been found that the activity of non-fast-spiking interneurons (potentially comprising Martinotti cells) increases strongly during active behaviour (Gentet et al., 2010), while FS-interneuron firing dominates during quiet wakefulness. In addition, SOM-positive interneurons in layer 2/3 of primary visual cortex respond to a visual stimulus with significant delay (compared to PV-positive and pyramidal cells) (Ma et al., 2010), as would be expected for a feedback element, especially if activated in a non-linear fashion. Both findings, would confirm a specific role for SOM-interneurons in mediating normalizing feedback-inhibition during active and intense processing of sensory information in the behaving animal.

This is not to say, that other interneurons may not be involved in normalizing inhibition - i.e. a divisive form of inhibition, which scales with the activity of the local

excitatory circuit (Douglas et al., 1995; Douglas and Martin, 2009). Any inhibitory mechanism that reduces the output firing rate per unit of synaptic input current by definition reduces the gain of a neuron's spiking mechanism and is modelled as a divisive action. Reducing the input resistence of a neuron is a common final path of achieving such gain reduction and may result from inhibition-independent mechanisms, such as increasing background synaptic activity, as well as inhibition-dependent mechanisms, in case they take the form of shunting inhibition (i.e. the shunting effect of inhibition is the stronger inhibitory component compared to the hyperpolarization component) (Chance et al., 2002; Douglas and Martin, 2009). Although it is been noted, that shunting inhibition might nevertheless not have a divisive (but rather subtractive) effect on firing rates, because the spiking mechanism clamps the membrane potential above the chloride reverse potential (leading to hyperpolarizing, i.e. dominantly subtractive inhibition) where additional spikes do not influence the strength of inhibition very much, the same work has demonstrated, that – if at all – shunting inhibition is indeed divisive when directed to the more distal dendrites (Douglas and Martin, 2009; Gabbiani et al., 1994; Holt and Koch, 1997). Although this modeling work strengthens the case for the typically distal-dendritically targeting Martinotti cell as mediating normalizing, divisive inhibition (Murayama et al., 2009), a note of caution is appropriate here: The model assumes that naturalistic spike rates are indeed so high, that the spiking clamps the cell close to spiking threshold and above chloride reverse potential – based on calculations regarding energy consumption of the brain, this, however, is unrealistic, since even cells responding to a stimulus will mostly fire rather sparsely (Olshausen and Field, 2005). In this case, i.e. if an even responding cell assumes a resting potential close to or below the chloride reverse potential, inhibitory inputs from *any*

interneuronal source may exert shunting inhibition, which has a divisive rather than a subtractive effect on firing rates, at least if timed appropriately (shortly after driving excitatory inputs). Thus, interneurons mediating feedforward or lateral inhibition might act divisively on firing rates of a postsynaptic neuron, too, which could even realize a normalization, in case their activity has some proportional relation to the activity in the local recurrent excitatory network (Douglas et al., 1995).

The multipolar bursting cell

Another interneuron type, described in one study, exemplifies the correlation of morphological, molecular and electrophysiological characteristics with functional aspects: the multipolar bursting cell (MBC) in L2/3 of neocortex (Blatow et al., 2003).

The MBC is PV- and CB-positive, but VIP-negative and mostly CR-negative. Compared to fast-spiking, PV-positive/CB-negative basket cells (which are also often VIP- and CR-negative), the MBC has (1) a distinct morphology featuring a more local axon, and (2) a different electrophysiological step-pulse response pattern displaying initial bursts of 2-3 action potentials at around 70 Hz followed by regular (~13 Hz) firing. Also, MBCs cannot follow sustained spiking above 15 Hz, while FS-cells can even follow far above 50 Hz. (3) MBCs are distinguished by connectivity, innervating other MBCs via synapses and gap junctions as well as other FS and pyramidal cells via synapses without being innervated by FS cells themselves (Blatow et al., 2003).

Especially the latter aspect of a specific (i.e. non-random) connectivity most likely directly translates into functional specialisation, as the asymmetry of the connections between MBCs and normal FS-basket cells establishes a hierarchy

between them, in which FS-basket cells are inhibited by MBCs. Interestingly, carbachol application reliably induces gap-junction-mediated and $GABA_A$-synapse-mediated oscillatory transmission. These carbachol-induced oscillations are not glutamate dependent, but are reduced in synchrony and amplitude, if $GABA_A$-receptors are blocked. They spread as both sub- and suprathreshold synchronized theta oscillations (5.2 Hz) in the MBC-cell network (at least up to 200 µm wide) and are reliably transmitted as IPSPs onto pyramidal cells with 1 ms delay. In conclusion, the multipolar bursting cell represents an interneuronal cell type that generates well-synchronized theta-oscillations and transmits them widely to other, hierarchically subordinate neurons in the circuit (Blatow et al., 2003).

PV-positive basket cells – mediating perisomatic feedforward inhibition

In the case of PV-positive neurons, functional correlation extends even further, as many of these neurons correspond morphologically to basket and chandelier cells, i.e. they target perisomatically or at the axon, respectively, and thus control the spiking of their postsynaptic partner. A molecular marker can thus identify a functional subclass of cells, which is furthermore defined by the expression of certain receptors and ion channels often conferring very specific (fast-spiking) electrophysiological properties (see above). However, even in this case nature does not quite “stick to the beauty of simplicity”: parvalbumin is expressed in only about 50 % of basket cells; and neither are all basket cells of the fast-spiking (FS) electrophysiological type, nor are all FS-cells PV-positive (Markram et al., 2004).

Nevertheless, the correlation of morphological, molecular, electrical and targeting properties is intriguing, and points to a very specific functional role in the neocortical network which can only be elucidated once the actual connectivity of these cells is understood. In (primary sensory) neocortex the PV-positive basket cell is largely

presumed to engage in a motif of fast feedforward inhibition (Sun et al., 2006). Although a range of regular-spiking interneuron subtypes have been found to mediate such feedforward inhibition in the neocortical input layers as well (Porter et al., 2001), inhibition by fast-spiking interneurons is 10 times more powerful than alternative connections and very reliable as well as precisely timed (Gabernet et al., 2005; Sun et al., 2006). Low-threshold spiking interneurons (which include Martinotti cells), in turn, are hardly activated by thalamocortical input (Beierlein et al., 2003; Cruikshank et al., 2010).

The feedforward motif is as follows: At the level of layer 4, both excitatory spiny stellate cells as well as basket cells receive strong thalamocortical excitation (Agmon and Connors, 1991; Gil et al., 1999). However, basket cells in turn innervate their excitatory neighbours and thus inhibit them strongly, providing only a small temporal window of 1-10 ms and/or a high activity threshold within/above which spiny stellate cells can integrate and transmit the thalamocortical input onto their postsynaptic partners (Sun et al., 2006; Swadlow, 2002, 2003). Thus, basket cells have been suggested to fulfill a dual function of gating the input into the neocortical network in both the temporal as well as the tuning domain. This role is aided by reliable, precisely timed and powerful inhibition as well as the very broad tuning (for example, with respect to the direction of whisker deflection in barrel cortex) of basket cells: precisely timed inhibition controls the timing of excitatory cell responses and increases the temporal resolution of the circuit, while broadly tuned inhibition sharpens excitatory tuning by ensuring that only the most optimal stimuli, featuring the preferred orientation of whisker deflection, are transmitted by a specific excitatory cell (Gabernet et al., 2005; Sun et al., 2006; Swadlow, 2002, 2003; Swadlow and Gusev, 2002).

A similar function in sensory gating and tuning has been suggested in primary visual cortex, particularly for the construction of the push-pull visual receptive fields of so-called simple cortical neurons (Hubel and Wiesel, 1959, 1962). Since the input into the cortex is excitatory and blocking of inhibition reduces stimulus selectivity, it is assumed that the inhibitory "pull" of simple receptive fields is of cortical origin and consequently mediated by interneurons with phase-shifted simple or complex receptive fields, at least in rodents (Borg-Graham et al., 1998; Hirsch and Martinez, 2006; Liu et al., 2009b; Monier et al., 2003)[14]. The latter are also thought to explain the contrast invariance of orientation tuning in both simple and complex receptive fields: In a pure feedforward model, stimuli with high contrast but non-preferred orientation should exert a similar drive as stimuli with low contrast but preferred orientation – this is however not the case, as the former evoke hardly any excitation (i.e. tuning is preserved equally across contrasts), while the contrast of preferred stimuli is nevertheless encoded in proportional cortical activation. This specificity strongly suggests that orientation selectivity is achieved at the cortical level, by means of lateral and feed-forward inhibition, blocking non-preferred stimuli. Just as in primary somatosensory cortex, where fast-spiking interneurons are broadly tuned to directions of whisker deflection, parvalbumin-positive neurons are tuned very broadly with respect to different orientations and directions of visual stimuli as well as spatial phase, thus possessing non-linear response properties (Hirsch and Martinez, 2006; Kerlin et al., 2010; Liu et al., 2009a; Ma et al., 2010; Niell and Stryker, 2008) (but note also a report suggesting high orientation

[14] More precisely, however, the typical linear responses of simple cells – evident in a linear increase of spike-frequency with more preferred spatial phase - which cannot be explained in a purely feedforward model as the thalamic output is already non-linear (due to the non-linearity of the spiking mechanism), could be achieved by means of lateral inhibition: The non-linearities in thalamocortical excitation can be cancelled out by the non-linearities in intracortical, lateral inhibition (Wielaard et al., 2001), providing an overlapping, but spatially mismatched inhibitory receptive field (Liu et al., 2009b).

selectivity of PV-cells (Kerlin et al., 2010)). In both cortical areas, PV cells could raise the threshold of their postsynaptic partners to filter out suboptimally tuned stimuli (Douglas et al., 1995; Hirsch and Martinez, 2006; Liu et al., 2009a; Liu et al., 2009b; Swadlow, 2003). In agreement with that, their (weak) orientation (and spatial frequency) preference corresponds to the net aggregated tuning preference of their surrounding, potentially interconnected excitatory neurons (Bock et al., 2011; Kerlin et al., 2010) as predicted by an early computational study (Douglas et al., 1995).

Although the evidence for inhibition in shaping visual receptive fields is ample and compelling (but see (Priebe and Ferster, 2008; Priebe et al., 2004) for a dissenting opinion), it is worth noting that the identity of the interneuron subtype involved is not equally well established in primary visual cortex as it is in barrel cortex. This is, at least in part, because the functional connectivity of different interneuron subtypes is less well known and the visual response properties of different subtypes of interneurons are not drastically distinct (Kerlin et al., 2010; Ma et al., 2010). Notably, parvalbumin-positive neurons always exhibit broad (unspecific) tuning and complex-like receptive fields, at least in the input layers 4 and upper 6 (Hirsch and Martinez, 2006) as well as layer 2/3, while somatostatin-positive interneurons in layer 2/3 and 4 show a large variation from untuned, complex to highly tuned, simple receptive fields (Ma et al., 2010)[15].

[15] Computational division of labour in the construction of receptive fields might however arise rather at the level of subtype-specific input and output connectivity and its dynamics: Having discussed both, the motif of dendritic feedback inhibition by Martinotti cells as well as perisomatic feedforward inhibition by basket cells, it is important to note, that a *dynamic* division of labour or routing of activity through the circuit has been found in the putative analogues of these two cell types in hippocampus: During stimulation of its outer layer, the alveus containing afferent excitatory fibres, with multiple (10) stimuli at 50 Hz, firstly putative fast-spiking basket cells are activated by recurrent excitation and provide perisomatic inhibition. Just like in neocortex, however, excitatory synapses onto basket cells are strongly depressing (see above), leading to a quick abortion of perisomatic inhibition. Secondly, and more slowly dendrite-targeting interneurons (putative somatostatin-positive OLM cells) are activated by – again like is the case for their neocortical analogues, Martinotti cells – facilitating excitatory inputs, providing rising and persistent dendritic inhibition (Pouille and Scanziani, 2004).

Finally, feedforward inhibition may also enable the time-invariant representation and recognition of stimulus sequences (e.g. the recognition of a melody independent of how fast it is played, or of a movement independent of its speed) as has been shown in the grasshopper (Creutzig et al., 2009) (Creutzig et al., 2010): If an excitatory input is not only transmitted to a higher-order neuron but in parallel low-pass filtered by an interneuron, which then also synapses onto the former, the bursting spike response to the second stimulus in a sequence will contain the more spikes the longer the pause between first and second stimulus was (since the inhibition has already decreased more). Thus the total spike-count per second in the higher order neuron remains constant, invariant of the speed of the input sequence (Creutzig et al., 2010).

Oscillations and fast-spiking cells

As illustrated by the example of the multipolar bursting cell, inhibitory neurons are implicated in oscillatory network activity; in fact, one of the major functions – at least of some subtypes of interneurons – might be to generate, transmit or "decode" oscillations in local as well as distant circuits (Buzsaki, 2006; Mann and Paulsen, 2007). Different interneuron types are likely to underlie different oscillatory frequencies, since distinct sets of subthreshold active conductances – an interplay

---

Due to the similarity of cell types and their characteristics regarding synapses and connectivity between neocortex and hippocampus, it can be assumed, that a computational division of labour exists in visual cortex in the dynamic – rather than the static – regime. In that way, the two inhibitory subtypes – PV- vs. SOM-positive – might contribute to temporally distinct phases in the transient formation of a visual representation: Perisomatically targeting basket cells, innervated largely also by thalamic inputs or by the first receiving excitatory cells (Beierlein et al., 2003; Cruikshank et al., 2010; Sun et al., 2006), provide a stable cancellation of non-linearities with subtractive inhibition shaping simple receptive fields instantly in a few milliseconds (see above), while – if excitation gets strong and long enough – Martinotti-cells are activated henceforth in a supralinear fashion to provide sustained normalizing, gain modulating dendrite-targeting inhibition to preserve the optimal dynamic range of the cells in the local circuit (Kapfer et al., 2007; Murayama et al., 2009). In agreement with this, the visual responses of somatostatin-positive interneurons have found to be delayed compared to PV- and excitatory cells (Ma et al., 2010).

of certain Na_v and K_v channels - can confer resonance properties with distinct preferred frequencies on distinct interneurons (Jonas et al., 2004). As a result, sustained subthreshold depolarization (by pharmacological agonists or current injection) may evoke subthreshold oscillations in particular frequency bands, mostly either theta or gamma, while sinusoidal input evokes resonant behaviour (amplitude increase at preferred frequencies). In the suprathreshold range, the reliability and temporal precision of spiking is highest at preferred frequencies of the subthreshold resonance behaviour which can endow certain interneuron types with band-pass filter characteristics – supporting the transmission of information, and thus network oscillations, at one frequency but not another (Jonas et al., 2004).

How do perisomatically-targeting interneurons contribute to network oscillations?

Because fast-spiking basket cells are coupled to each other via gap junctions (Amitai et al., 2002; Gibson et al., 1999) and transmit their activation swiftly and with high reliability, they may be easily synchronized by shared excitatory input and thus support the restriction of excitatory activity to a specific temporal phase uniformly in the local network (Sejnowski and Paulsen, 2006). This allows them to cause and detect oscillations, as described in detail below.

Individual GABAergic perisomatically-targeting basket cells – just like Martinotti cells in frequency-dependent disynaptic inhibition – may exert a powerful influence on the local network. For example, in rat hippocampus it has been shown that an individual basket cell can force a pyramidal cell into an oscillatory rhythm of a certain frequency band (theta) and – by highly divergent projections – synchronize the activity of a local network of its target cells (Cobb et al., 1995).

More often, however, basket cells are implicated in oscillations of the gamma-frequency band[16]. Hippocampal gamma-oscillations displaying high coherence across cells are thought to depend on fast-spiking parvalbumin-positive, perisomatically-targeting basket cells, partly forming a gap-junction mediated syncytium and requiring AMPA receptor-mediated glutamatergic excitation (Bartos et al., 2002; Bartos et al., 2007; Mann et al., 2005). The exact frequency of the oscillations depends (probably) on synaptic time constants, and on the precise connectivity via gap junctions and synapses (Bartos et al., 2002) as well as on the strength of NMDA-mediated excitation of interneurons (which in turn is counteracted by tonic inhibition) (Mann and Mody, 2009).

Gamma oscillations in hippocampus may emerge from either one of two independent "gamma generators" (Buzsaki, 2006) – the dentate gyrus (requiring cortical/enthorhinal drive) (Chrobak and Buzsaki, 1996) and the highly recurrent CA3 network (requiring cholinergic innervation from the septum as a permissive factor and entraining CA1 via its interneurons) (Csicsvari et al., 2003); the latter can be reproduced experimentally in the hippocampal brain slice by applying the muscarinic-cholinergic agonist carbachol (Fisahn et al., 1998) or the glutamatergic agonist kainate (Hormuzdi et al., 2001), while gamma oscillations in the neocortex (in slice) can be induced by application of carbachol and kainate in combination (Buhl et al., 1998; Traub et al., 2005). Gamma rhythms are abolished when basket cells are electrically uncoupled, i.e., when gap junctions are disrupted in a connexin-36 knock-out mouse (Buhl et al., 2003; Hormuzdi et al., 2001). Also, a

[16] Reflecting their historical origins in EEG recordings, oscillatory rhythms are somewhat arbitrarily assigned to different frequency bands: delta (0.5-4 Hz), theta (4-8 Hz), alpha (8-12 Hz), beta (12-30 Hz), and gamma (30-80 Hz), varying with species (Buzsaki, 2006). A more useful classification would consider the physiological mechanisms that generate periodic behaviour at different frequencies, but clues to potential mechanisms have often remained elusive. One exception is the role of basket cells in gamma oscillations.

reduction of the activity of parvalbumin-positive cells by *Cre* -mediated GluRA (GluR1) subunit knockout impairs recruitment of fast-spiking neurons into the network activity of the hippocampus, with consequences for working memory (Fuchs et al., 2007) [17].

Furthermore, basket cells have fast, temporally precise (see above), and highly divergent signalling properties and display spiking activity that is phase-locked to the gamma cycle (Bartos et al., 2002; Bartos et al., 2007; Klausberger et al., 2003). In fact, certain hippocampal interneuron subtypes generally fire in a specific phase relation to a particular rhythm depending on the subtype, which again illustrates that morphological and molecular diversity likely translates into functional division of labour (Klausberger et al., 2003; Klausberger et al., 2005; Klausberger and Somogyi, 2008; Somogyi and Klausberger, 2005). This concept is further supported by the existence of striking anatomical relationships: the axonal arborizations of distinct types of hippocampal interneurons separate the gamma- and theta-rhythms in the transverse and longitudinal directions of the hippocampus, respectively, allowing different temporal activity patterns to be remapped onto different spatial domains (Gloveli et al., 2005). In general, the phase angle of inhibitory inputs with respect to gamma and other oscillations seems to depend on the kinetics of the particular $GABA_A$-receptor type involved (Bartos et al., 2007; Buzsaki, 2006).

From the pharmacological experimental model and the accumulated data described above, two principal models of the causation of gamma oscillations have emerged. Both depend critically on fast-spiking basket cells: In one version excitatory drive is provided to interneurons – among them basket cells – by AMPA receptor mediated excitation from pyramidal cells, which in turn are quickly feedback-inhibited, leading

[17] This study also serves as a fine example of the successful use of genetic engineering in clarifying the subtype-specific roles of interneurons in intact circuits (Fuchs et al., 2007)

to an oscillation that sharpens in synchrony by means of gap-junction mediated spread of excitation among basket cells and subsequent swift truncation of activity by GABAergic inhibition, which is much faster than inhibition onto pyramidal cells. In the other model, high-frequency oscillations can be generated in the basket cell network alone (e.g. as shown under glutamatergic antagonists) via mutual gap-junction mediated excitation and subsequent fast synaptic inhibition, while the increasing entrainment and incorporation of glutamatergic phasic excitation actually decreases the oscillation frequency (Mann and Paulsen, 2007). While the electrical coupling mediates coherence of the oscillation, the time course of glutamatergic and GABAergic transmission onto interneurons (in addition to intrinsic resonance properties) determines both coherence and oscillation frequency (Jonas et al., 2004). Importantly, the selective involvement of fast, perisomatically-targeting interneurons displaying selective gap-junction coupling among each other (but none with other interneuron types), is likely essential for achieving such high-frequency oscillations and thus demonstrates a vital division of labour among interneurons (Mann and Paulsen, 2007). Such mechanism of synchronization of network activity by interneurons is likely to actually happen in the neocortex *in vivo*, as under these conditions interneurons, specifically FS-cells, fire much more synchronously than excitatory neurons (Gentet et al., 2010).

Cortical fast-spiking interneurons may not only be generators but also detectors of partially synchronized pyramidal cell activity that is then distributed, enhanced and precisely timed within the electrically and synaptically connected interneuron network (Galarreta and Hestrin, 2001; Sejnowski and Paulsen, 2006). This ‚detector' function is partially mediated by the strong excitatory input into

interneurons as well as their resonance properties (see above), which allows them to function as band-pass or band-stop filters for certain frequency bands (Buzsaki and Draguhn, 2004; Izhikevich, 2006; Jonas et al., 2004; Soltesz, 2006).

This model likely translates to neocortex whose basket cells display similar properties, selective mutual gap-junction coupling (Beierlein et al., 2003; Galarreta and Hestrin, 1999; Galarreta and Hestrin, 2002; Gibson et al., 1999; Hestrin and Galarreta, 2005) and are likewise selectively (however see: (Porter et al., 2001)) involved in a motif of feedforward inhibition, which can effectively restrict the timing of pyramidal cell activity to specific phases (Beierlein et al., 2003; Gibson et al., 1999; Sun et al., 2006) and thus produce oscillations (Sohal et al., 2009). Also, gamma oscillations in neocortical slices can be induced pharmacologically in the same way as they can in hippocampus, suggesting a common mechanism (Buhl et al., 1998; Traub et al., 2005). Finally, using optogenetic activation of parvalbumin(PV)-positive interneurons in a closed-loop design experiment (feeding non-gamma-modulated pyramidal cell firing into optical activation of PV-cells), an emergent increase of power in the gamma frequency band of spontaneous oscillatory network activity could be observed, while selective optical inhibition of PV-cells decreased gamma power of spontaneous oscillations *in vivo* (Sohal et al., 2009).

What might be the function of network oscillations?

Network oscillations may provide precise temporal frames for neural computation (Buzsaki, 2006), which can aid four central but interrelated tasks in cortical information processing (Sejnowski and Paulsen, 2006): (1) the representation of sensory information by “binding” its aspects, (2) precise timing of individual spikes in neurons and populations, which might increase information content, (3) the

regulation of the flow of information leading to filtering and attention, and (4) the regulation of memory formation and retrieval.

The oscillatory behaviour of inhibitory interneurons can restrict the activity of pyramidal cells to distinct repetitive time slots with high accuracy (Bartos et al., 2007; Fricker and Miles, 2001). Such temporal frames and frequency bands may also regulate the information transmission between brain regions, which is supposed to be aided (e.g. by blocking simultaneous signals from other sources) by the synchronization of the network oscillations in these two regions (Fries, 2005).

Mechanistically, such synchrony-dependent interregional information transmission and inhibition of other, non-synchronized inputs could be achieved by means of an input layer of inhibitory neurons involved in feedforward inhibition (Akam and Kullmann, 2010), just as implemented by the basket cells of layer 4 (see above). Oscillations are detected by allowing only phase-locked input from other regions into the local network while non-phase-locked inputs are blocked out by feedforward inhibition (Akam and Kullmann, 2010; Azouz and Gray, 2003).

Such information routing by synchronization may also underlie perceptual binding between brain/neocortical areas or within an area by means of synchronized gamma oscillations (Eckhorn et al., 1988; Gray et al., 1989) as well as multi-modal integration or representation (Senkowski et al., 2008). With respect to the latter it is particularly interesting that somatosensory input into auditory cortex can reset the phase of network oscillations in the latter, and thus determine input selection by blocking activity that is not in the appropriate phase of the novel oscillation (Lakatos et al., 2007). In addition, synchronization between cortical areas and subcortical brain regions in the gamma or theta frequency bands has been observed in relation to certain behaviour. For example, the ventral striatum is synchronized with the

piriform cortex in the 50 Hz band, but with frontal cortex in the 80-100 Hz band. Receipt of reward or psychomotor stimulants decreases the power of the former, but increases that of the latter oscillations (Berke, 2009). Furthermore, LFP and single units in the ventral striatum (nucleus accumbens) synchronize with the hippocampus during exploration, but switch to synchronization with the prefrontal cortex (PFC) during task execution, potentially based on the fact that bursting activity in the PFC can generate up-states in nucleus accumbens neurons (Gruber et al., 2009). Likewise, synchronisation between the ventral (but not dorsal) hippocampus and the medial prefrontal cortex is observed in states of anxiety and partly controlled by 5-HT1A-receptor-dependent synaptic transmission (Adhikari et al., 2010). And synchronisation between CA1 and the lateral amygdala (in the theta-frequency band) increases strongly upon presentation of a fear-conditioned stimulus, potentially underlying the retrieval of fear-related memory (Seidenbecher et al., 2003). In conclusion, switching synchronization of distinct frequency bands between different brain areas might be a mechanistic underpinning of information transfer needed for different behavioural tasks.

Gamma oscillations may also increase information transmission through the local network, as gamma-modulated EPSCs provided to pyramidal cells using dynamic clamp, enhance mutual information (i.e. the information that the spiking output of the cells contain about their input) compared to non-gamma-modulated input; also, gamma-modulated optical activation of layer 5 pyramidal cells enhances mutual information in FS-cells (i.e. the information contained in their spiking about the stimulation) – but not in other interneurons – compared to non-gamma-modulated stimulation (Sohal et al., 2009). This might represent the mechanistic underpinning of the implementation of attention - and resulting behavioural increase in

performance and speed - by raising the gamma-band synchronization of neurons representing the attended stimulus (Fries et al., 2001; Womelsdorf et al., 2006).

Finally, theoretical studies have suggested that coherent oscillations (and thus precisely timed phasic inhibition), especially in the theta and gamma frequency bands (and particularly in hippocampus), are crucial to the formation and retrieval of memory (Axmacher et al., 2006; Lisman, 1999; Lisman and Idiart, 1995; Paulsen and Moser, 1998; Sejnowski and Paulsen, 2006).

The larger diversity of interneuron function

Distinct subtypes of interneurons participate in different connectivity motifs and hence fulfill particular functions within a circuit. Martinotti cells enable normalizing feedback inhibition controlling the gain or dynamic range of a neuron. Fast-spiking interneurons participate in feedforward inhibition gating the input into the cortical network and may also cause or decode theta and gamma oscillations. Multipolar bursting cells, in turn, may entrain the circuit in theta oscillations. Indeed, these examples illustrate how electrophysiological, optical and genetic methods in combination may allow for a synthesis of anatomical and physiological knowledge about a particular subtype of interneuron and the circuit context it is operating in. Repeated application of similar approaches may eventually uncover the functional roles of all interneuron types, including the far less abundant ones, in neocortical circuits.

What might be these roles? The function of inhibitory neurons is often presumed to balance excitation. However, if this were the main, or only, role of inhibition, why could excitation not be made smaller in the first place? Indeed, many computational models do “work” completely without inhibition and many more by including just a global measure of inhibition, neglecting any division of labour among inhibitory

neurons. Alternatively, the near-ubiquitous short-term synaptic depression of excitatory synapses may, in itself, prevent over-excitation in the network (Abbott et al., 1997; Chance et al., 1998; Rothman et al., 2009). Moreover, excitatory networks and individual layer 2/3 pyramidal cells can self-regulate their activity by endocannabinoid-mediated self-innervation (Marinelli et al., 2009).

However, inhibition is likely to be useful when excitation simply cannot be made smaller in the first place because strong amplification of excitation is an essential part of the computational process. Consider the highly recurrent network found in the neocortex, especially in layer 2/3 (Binzegger et al., 2004; Chance et al., 1999; Douglas et al., 1995; Douglas and Martin, 2007b), which may be important (Douglas and Martin, 2007b) for generating complex (Chance et al., 1999) or simple (Douglas et al., 1995) visual receptive fields. Normalizing inhibition can serve to avoid the potential (Douglas et al., 1995) disadvantages of recurrent networks, namely that they are prone to overexcitation (explosion), bimodality (being either near-silent or saturated) as well as sluggish in their responses, as the sensitivity to external inputs is decreased in favour of local mutual excitation (“old” stimuli are still transmitted and amplified in the network while new ones do not provide any further, detectable excitation) (Chance and Abbott, 2000). In this scenario, however, it is essential that inhibition is not simply a “mirror” image balancing excitation, but that disproportions between excitation and inhibition are key to enable efficient computation (Chance and Abbott, 2000; Douglas et al., 1995).

Likewise, sparse coding – suggested to enhance computational and energetic efficiency – might be promoted by inhibition. Interneurons are very likely involved in the sparsification of neural responses that is observed at both, the developmental onset of visual processing (Rochefort et al., 2009) as well as during visual

stimulation with complex scenes (as opposed to receptive-field-optimized single stimuli). In development, it has been found with photostimulation-assisted circuit mapping, that GABAergic connectivity increases before and refines around the time of eye opening – at least partially due to a decline in the excitatory action of GABA. The refinement coincided specifically with the development of orientation tuning in visual cortex (Dalva, 2010). In the processing of naturalistic visual stimuli, an increase in RS-spiking interneuron firing has been observed *in vivo* , potentially contributing to sparser and temporally more precise stimulus representation (Haider et al., 2010).

Furthermore, interneurons might regulate the formation of long-term synaptic memory, whose induction is dependent on the amplitude and timing or pre- and postsynaptic activity in a mechanism known as spike-timing-dependent plasticity (STDP) (Bi and Poo, 1999; Bi and Poo, 1998; Magee and Johnston, 1997; Markram et al., 1997b). As illustrated above, due to the precise, subtype-specific placement of inhibitory synapses as well as their temporal coordination of activity, interneurons are perfectly suited to control both, *amplitude* and *timing* of excitatory activity of a cell and of a local circuit, and might thereby also regulate synaptic plasticity (Sejnowski and Paulsen, 2006)[18]. The GABAergic regulation of STDP-like synaptic plasticity, resulting in stimulus-dependent alteration of visual receptive field structure, was indeed found in the optic tectum of Xenopus larvae (however, in this case, GABA is still depolarizing) (Richards et al., 2010).

[18] Although inhibitory synapses are generally not thought to be long-term plastic in the adult cortex (with few exceptions), excitatory synapses onto interneurons *are* - and in fact via an “anti-hebbian” mechanism, decreasing the synaptic weight upon coincident activity (Kullmann and Lamsa, 2007; Lamsa et al., 2007). Deploying that mechanism, interneurons can in principle contribute to synaptic long-term plasticity, involving potentiation via a depression of the interneuron excitation, as demonstrated at the CA3-to-CA1 (Schaffer collateral) synapse (Ormond and Woodin, 2009). However, the timing (and strength) of individual inhibition or inhibition evoked within network oscillations might also locally and directly control the induction or readout of synaptic memories (Paulsen and Moser, 1998).

Although many principles remain to be elucidated, it appears that molecular and morphological diversity gives rise to different subtypes of interneurons, which display distinct electrophysiological characteristics and regulate different aspects of target cell function in cortical microcircuits.

Inhibitory connections in the neocortex

In spite of a wealth of knowledge about morphological, electrical and molecular characteristics of individual interneurons, the rules according to which intra- and translaminar inhibitory *connections* are wired in the neocortex, and the extent to which these connectivity patterns generalize across cortical areas, remain largely unknown.

Although examples of translaminar and transcolumnar projections of interneurons have been described (Helmstaedter et al., 2009a, b; Lund, 1988; Markram et al., 2004), it is widely believed that inhibition is local and largely intralaminar (Binzegger et al., 2004; Brill and Huguenard, 2009; Dantzker and Callaway, 2000; Gupta et al., 2000; Kapfer et al., 2007; Silberberg and Markram, 2007; Thomson and Lamy, 2007; Thomson and Morris, 2002; Thomson et al., 2002; Xu and Callaway, 2009; Yoshimura and Callaway, 2005; Yoshimura et al., 2005). Intracellular filling of neurons and extensive reconstruction of their morphology (Binzegger et al., 2004) as well as intracellular recordings from multiple neurons (which, however, naturally favour the analysis of nearby cells) (Gupta et al., 2000; Thomson and Lamy, 2007; Thomson et al., 1996b; Thomson et al., 2002) form the basis of this view, which has been supported also by experiments using laser scanning photostimulation in rodent primary sensory cortex: inhibition appears to derive to a large extent from

the home layer and putative home column, with some inhibition also coming from adjacent layers (Brill and Huguenard, 2009; Dantzker and Callaway, 2000; Xu and Callaway, 2009). For example, all neurons in layer 2/3 of rat V1 receive most of their inhibition from the home-layer (proportions are for pyramidal cells: 78%, for fast-spiking cells: 76%, for adapting interneurons: 62%) and the rest from layer 4 (feedforward inhibition) (Dantzker and Callaway, 2000).

In addition, some inhibition clearly originates in other layers. It is likely that the extent of translaminar and transcolumnar inhibition depends on interneuron subtype. For example, large basket cells with their wide horizontal axonal arborizations are thought to mediate transcolumnar (lateral) inhibition within the same layer (Binzegger et al., 2004; Kawaguchi and Kubota, 1993; Markram et al., 2004). Conversely, the majority of dendrite-targeting cells (Martinotti cells, double-bouquet cells, bipolar cells, and bitufted cells) may actually cross multiple layers and thus mediate translaminar inhibition (see Table 1.1) (Markram et al., 2004). However, much of this evidence is anecdotal. Translaminar inhibition from layer 5 to about 25% of layer 2/3 pyramidal cells (4/14) has been noted but not further characterized (Dantzker and Callaway, 2000). There are also three documented cases of layer-5-Martinotti-cell-mediated translaminar inhibition of layer 2/3 pyramidal cells in S1 in individual paired patch-clamp recordings (Kapfer et al., 2007). For inhibitory postsynaptic cells – and to a very small extent also for pyramidal cells – in layer 2/3 of S1, inhibition from all layers (1 to 6) has been found and quantified using photostimulation (Xu and Callaway, 2009). In addition, the layer-4-to-2/3 translaminar connection is well-documented in paired recordings (Thomson et al., 2002).

Apart from connecting to excitatory neurons, interneurons are also known to connect to other interneurons in both, an excitatory fashion via gap junctions as well as in the usual inhibitory mode via chemical synapses (Blatow et al., 2003; Galarreta and Hestrin, 1999; Galarreta and Hestrin, 2002; Gibson et al., 1999). Gap-junction mediated connections are thought generally to interconnect interneurons of the same type, such as fast-spiking PV-basket cells in layer 4 or low-threshold spiking SST-positive cells in layer 5 (Hestrin and Galarreta, 2005) and display a strong linear decrease in connection probablity and coupling strength as a function of distance, dropping to zero after ~200µm and including 20-50 connected cells per interneuron altogether (Amitai et al., 2002; Gibson et al., 1999). However, preferential gap-junction coupling between PV-positive multipolar bursting cells and calretinin-positive bipolar cells has also been described, suggesting that gap-junction coupling is governed by strict subtype-specificity but not necessarily by the rule that only cells of the same subtype are connected (Caputi et al., 2008). Inhibitory synaptic connections between interneurons can interconnect different cell types, e.g. to establish a hierarchy among interneurons as described above in the case of the multipolar-bursting cell (Blatow et al., 2003), or the same type of interneurons (Gibson et al., 1999), e.g. to promote well-synchronized network oscillations. CR-positive interneurons, in particular, seem to preferentially target other interneurons (Caputi et al., 2008; Gonchar and Burkhalter, 1999). A comprehensive depiction of excitatory and inhibitory neocortical connections can be found at the homepage of the Yuste lab at Columbia University[19] as well as in (Thomson and Lamy, 2007).

[19] http://www.columbia.edu/cu/biology/faculty/yuste/databases.html

I now return to the principles of neocortical organization, discussing first the specificity of neocortical neuronal connections and subsequently the three concepts which dominate our understanding of neocortical structure.

Specificity or stochasticity in neuronal wiring?

It has been a matter of intense debate (Kozloski et al., 2001; Markram, 2008; Thomson and Morris, 2002; Yoshimura and Callaway, 2005) whether and to what extent the synaptic connections between neurons are random, in the sense that whenever the neurites of two potential partners meet in close enough proximity a synapse of a specific kind is established with a certain probability. The alternative view is that neuronal connections are made with high specificity, i.e. the probability of a synaptic connection varies drastically in dependence of the subtype of both, the pre- and the postsynaptic neuron. 'Subtype', here, may refer not only to the identity of the cell as an actual molecular or morphological subtype, but also to its laminar or columnar location, its local connectivity and even its individual function in the network (e.g. simple cell vs. complex cell in V1 (Hirsch and Martinez, 2006; Hubel and Wiesel, 1959)), as illustrated below.

Surprisingly, computational models of biological neural networks, including those of the neocortex, do not assume much structure or specificity of neuronal connections, even if they purport to reproduce neocortical information processing (Maass et al., 2002; Sussillo and Abbott, 2009). On the other hand, as described below, there are many indications that neuronal connections are wired with high specificity. Since specific wiring carries an informational cost compared to non-specific wiring, one can assume that specificity is important for biologically realistic neocortical information processing.

A first hint that synaptic connections are not random comes from the highly bimodal distribution of the number of synaptic interconnections between any two neurons – with many neurons forming (nearly) no contacts at all and a few forming multiple (3-8) contacts (Markram, 2008; Markram et al., 1997a). This is not a trivial observation, as the axon of virtually every cell comes in close approximation with the dendritic tree of virtually any other cell in a column (Kalisman et al., 2005; Markram, 2008). Furthermore, multisynaptic connections between pyramidal neurons can be erased or newly formed over the course of just a few hours, depending on suprathreshold activity (Le Be and Markram, 2006).

Other examples of wiring specificity are the determination of synaptic short-term dynamics by both, the subtype of the pre- and postsynaptic cell (Gupta et al., 2000; Kapfer et al., 2007; Pouille and Scanziani, 2004) and the selective formation of electrical and chemical synapses between interneurons of certain subtypes, but not others (see above). For instance, those pyramidal cells in layer 5 that feature a very extensive dendritic arborization preferentially innervate fast-spiking cells with facilitating synapses and one or multiple release sites. Pyramidal cells with less arborized dendrites preferentially innervate FS-interneurons with depressing synapses and only multiple release sites (Angulo et al., 2003).

Optophysiologal readout – functional imaging - has aided the search for cell-type- and spatial specificity of neuronal connections, and has revealed that postsynaptic partners of layer 5 pyramidal cells with a certain subcortical projection (tectum) are local pyramidal cells and interneurons with a distinct electrophysiology, synaptic dynamics and stereotyped spatial position (Kozloski et al., 2001). Similarly, the subcortical projection target of layer 5 cells can determine their connection probabilities with local layer 5 cells (Brown and Hestrin, 2009).

Photostimulation-assisted mapping of network connectivity has provided the means to address the question of selectivity in an even more informative fashion than multiple intracellular recordings and morphological reconstructions, because global presynaptic connectivity patterns of one or more postsynaptic cell(s) can be delineated (Yoshimura and Callaway, 2005; Yoshimura et al., 2005). However, particulars of synaptic dynamics, amenable to analysis during dual-recordings cannot be derived with photo-stimulation, since the presynaptic neuron cannot be precisely controlled. Using this approach, it was found that pyramidal cells in layer 2/3 of S1 receive their dominant excitation from layer 4 – unless, they are situated in layer 2 and above the septal region, in which case they are rather driven by layer 5A (Shepherd and Svoboda, 2005). This finding is highly significant as it illustrates functional specialisation among seemingly uniform pyramidal cells within one layer – i.e. a “break” or dissociation in laminar homogeneity. Importantly, in S1 two different thalamic input streams arrive in distinct compartments – the lemniscal input from the ventral posterior medial (VPM) nucleus in layer 4 (barrel) and the paralemniscal input from the posterior medial (POM) nucleus in layer 5A, 4 (septum) and 1 (Koralek et al., 1988; Lu and Lin, 1993). Thus, the differential excitation of layer 2/3 pyramids from either layer 4 or 5A suggests that these input streams are kept relatively separate and run as parallel interdigitating pathways even in the next processing layer. If cells are located in the same barrel, their input sources are very similar; however, similarity drops off on the edge of the barrels and thus gives rise to a columnar organization even in layer 2/3 (Shepherd and Svoboda, 2005). An earlier study had furthermore shown that the specific connectivity just described is plastic: the minor layer 4 to layer 2/3(septum)

connection strengthens significantly upon whisker-deprivation, while the initially strong layer 4 to layer 2/3(barrel) projection weakens (Shepherd et al., 2003).

A similar dissociation among pyramidal cells exists in layer 5, where intriniscally bursting (IB) cells featuring large, triangular cell bodies, extensive dendrites and axonal arborizations in deep layers can be clearly distinguished from regular spiking pyramids (RS) displaying a more roundish soma, less dendritic arborizations and axonal ramifications in supragranular layers (Chagnac-Amitai et al., 1990). Notably, these contrasting morphological and electrophysiological characteristics again predict the presynaptic connectivity of these cells: IB-cells receive most of their excitation from layers 4 and 6, while RS cells are connected mainly to inputs from layers 2 to 5. IB cell receive very little inhibition, while RS cells are strongly inhibited, especially from layers 2/3 and 5 (Schubert et al., 2001).

In layers 2/3 and 5 in V1, layer 2/3 pyramidal cells share common input from layers 2/3 and 4 if they are connected to each other, while the amount of shared input from L5 (and shared inhibitory input from layers 2-4) does not depend on local connectivity (Yoshimura et al., 2005). Similarly, if layer 2/3 pyramidal cells are connected with each other, their probability of exciting the same layer 5 pyramidal cell is at chance level, while if they are not connected, the likelihood of innervating the same cell is enhanced > 3-fold. In turn, if layer 5 cells are connected, their chance of receiving input from the same layer 2/3 cell is increased > 4-fold, while if they are not connected, that chance is below random level (Kampa et al., 2006).

Specific subtypes of interneurons, in turn, receive differential amounts of excitation and inhibition from specific layers. For example, fast-spiking interneurons in layer 2/3 of V1 receive most of their excitation mainly from layer 4 (just as their excitatory

neighbours) and minor amounts from layers 2/3 and 5A, while adapting interneurons receive their dominant excitation either from deeper layers, especially 5B, or laterally from their home layer (Dantzker and Callaway, 2000). In layer 2/3 of S1, SOM-positive Martinotti cells, some fast-spiking (FS) and some bipolar cells receive excitation from layer 4 (again: like their excitatory neighbours), while chandelier cells, neurogliaform and irregular spiking (IS) cells receive inhibition from layer 5A (Xu and Callaway, 2009). Assuming that these laminar excitatory connections transmit distinct inputs from different thalamic nuclei (VPM vs. POM) (Petersen, 2007), there is a significant division of labour between interneuron subtypes based on spatiotemporal activity patterns alone.

In layer 2/3 of V1, translaminar connectivity, on a fine scale, depends not only on inhibitory cell type, but also on the intralaminar connectivity itself: Fast-spiking cells connect preferentially to neighbouring pyramids, if these also provide them with excitation; and such reciprocally connected FS-interneuron-pyramidal cell pairs largely share their excitatory input, while pairs that are only unidirectionally connected do not. Adapting inhibitory neurons, in turn, do not significantly share excitatory input with connected pyramids, independent of their intralaminar connectivity. Likewise, reciprocally connected FS-interneuron-pyramid pairs in layer 5 do not significantly share excitatory drive from layer 2/3, while interconnected non-FS-interneuron-pyramid pairs do, suggesting that this specific connectivity motif is a laminar specialisation of layer 2/3 (or the cortex: frontal cortex vs. V1), and not of the interneuron subtype as such (Otsuka and Kawaguchi, 2009). In agreement with this, fast-spiking cells receive less translaminar feedforward excitation (from layer 2/3) compared to non-fast-spiking cells (Otsuka and Kawaguchi, 2009), while the relationship is again reversed for FS- vs. non-FS-

interneurons in layer 2/3 with respect to their translaminar feedforward excitation (from layer 4) (Dantzker and Callaway, 2000).

These and further data have suggested essentially non-random, fine-scale patterns of neocortical connectivity between interneurons and pyramidal cells, that are dependent on the neuronal subtype as well as its layer- and target-related location and connections.

Layers

The probably most fundamental principle regarding neocortical structure is that neocortex – in any area - is organized into layers. This view may be interpreted in two ways: The weak interpretation is that neocortical layers *do* exist and that they *do* matter – i.e. that, when descending from the pia vertically down to the white matter, anatomical and physiological alterations occur in an abrupt or step-wise manner, and that the areas of continuity between such quantal alterations are more or less uniform computational compartments akin to the layers in artificial neural networks. The strong interpretation is that there is a stereotypic number of such compartments or layers across the entire neocortical mantle; currently that number is assumed to be 6 (White, 1989).

The layered architecture of neocortex was first established based on differences in shading – due to differential cell and fiber densities, which can be emphasized by using various stains (e.g. Nissl for cell bodies) – along the vertical axis from the pia to the white matter (White, 1989). Although it is widely assumed that the neocortex features a 6-layered organization throughout, this concept is rather a historical convention established in the 1970s, after systems with different numbers of layers (ranging between 5 and 9) and different localization of their borders in different areas had already been proposed (Douglas and Martin, 2007a; White, 1989). This

is important to note since the fact that neocortex is subdivided into 6 layers across the entire mantle (the strong interpretation) is often taken as an indication of a “canonical” neocortical architecture and information processing algorithm (Hawkins and Blakeslee, 2004). In fact, it was the histological *differences* in lamination patterns that allowed neuroscientists like Brodmann to *distinguish* the various neocortical areas from each other in the first place (White, 1989), long before the functional or physiological specialisations of these areas were established and found to coincide with the histologically differentiated areas. These histological differences were incorporated into the “canonical” 6-layer framework by assuming different sublayers in different cortical areas and species (White, 1989).

While a lamination pattern based purely on histological differences, such as density of cells and fibres, could have been considered artificial and biologically meaningless, functional relevance has been added to the laminar concept by a rich variety of findings indicating that neurons and their connections (and thus presumably their function) display distinct characteristics based on their laminar location. Indeed, there is the (debatable) claim that, among the relatively homogenous group of neocortical pyramidal cells, the cortical layer where the cell body is situated represents the strongest predictor of cell physiological as well as anatomical variation, so that five ‚subtypes’ of excitatory cells – according to their locations in layers 2 to 6 - are distinguished (Buzsaki, 2006: 58). Interneurons of different subtypes, in turn, vary in their type-specific-density depending on the layer (Markram et al., 2004), and at least for one type, the fast basket cell, a difference in somatic size has been found between those in layer 2/3 and those in layer 5 (Uematsu et al., 2008).

More importantly, cells in different layers are connected to distinct inputs and outputs. Connectivity patterns thus display layer-specific motifs, the most prominent ones being the major connections of the canonical microcircuit described above: e.g. layer 2/3 pyramids display a high degree of recurrent connectivity and are "extrinsically" excited by layer 4 or intracortical long-range projections, while layer 4 cells are clearly distinct, in that they receive prominent thalamic excitation and many fewer recurrent inputs, and so forth. (Douglas and Martin, 2004). Based on functional criteria, the lamination also became slightly re-organized (at least for rodents), as layers 2 and 3 were merged together, since their cells display no such obvious difference in anatomy and connectivity, while layer 5 has been separated into 5A and 5B. In the latter case, the anatomical (but not electrophysiological) distinctness of the sublayers could be clearly supported by differential extrinsic and intrinsic connectivity, as layer 5A (but not 5B) pyramidal cells are targeted by a thalamic input stream (Lu and Lin, 1993) and receive their local excitation and inhibition almost exclusively from layer 4 and 5A (potentially integrating the lemniscal and paralemniscal thalamic input into the neocortex), but not from layer 5B and 6 (Schubert et al., 2006).

Studies in the hippocampus have also suggested that the synaptic properties of inhibitory inputs are layer-specific, as interneurons from different layers influence the same pyramidal cell via different $GABA_A$ receptors (slow vs. fast) (Kozhemiakin et al., 2004; Pearce, 1993). The observation of slow-$GABA_A$-mediated IPSCs emitted by neurogliaform cells in neocortical layer 1 (Szabadics et al., 2007) as well as the diversity of $GABA_A$- as well as $GABA_B$-mediated IPSCs in the neocortex (Benardo, 1994; Ing and Poulter, 2007) suggests that there might be layer-specific receptors and kinetics of inhibitory connections, here too.

Apart from cellular morphology and intrinsic and extrinsic connectivity, physiological phenomena also obey laminar borders. For example, it could be shown that network oscillations display a laminar pattern in visual cortex *in vivo*, involving 2-3 Hz oscillations in layer 2/3 and 10-15 Hz oscillations in layer 5 (Sun and Dan, 2009). The frequency of ongoing activity is strongly correlated with the spatiotemporal window of visual integration: Neurons with fast-oscillating spontaneous inputs exhibit transient visual responses and small receptive fields (RFs), whereas those with slow inputs show prolonged responses and large RFs (Sun and Dan, 2009). Also, receptive field structure in primary visual cortex varies with laminar location, featuring mostly simple cells in the thalamorecipient layer 4 (~70%) and (partly) 6, while layer 5 is dominated by complex cells (~ 75%) (Martinez et al., 2005; Niell and Stryker, 2008). Similarly, it was shown in primary auditory cortex that the spiking probability, response predictability, temporal latency and spatial extent of spontaneous and acoustically evoked activity varied significantly between layers – most notably between layers 2/3 and 5/6. Importantly, layer 6 displayed not only the shortest latencies but also the lowest response probability (highest sparseness) and the smallest response predictability (= mutual information regarding the sensory event). This suggests a relative autonomy of layer 6 (Harris, 2010; Sakata and Harris, 2009). However, it has to be noted, that most of these physiological investigations (since they are conducted *in vivo*), do not actually point to the question, of a strict laminar – that is, step-wise or quantal – vertical organization as opposed to a continuity of alterations.[20]

[20] It is important to note, that the principle of laminar unity and the principle of cell-specific wiring (explained before) necessarily contradict each other the more, the stricter they are expressed.

Columns

While layers provide a vertical separation of neocortical tissue into distinct functional compartments, columns are thought to represent vertically separated computational modules – each endowed with the rich multilayered processing architecture of layers 1 through 6. Columns are often viewed as identical and independent modules whose sole distinguishing characteristic is their extrinsic connections (Mountcastle, 1997; Mountcastle, 1978). Each column is thought to contain the complete "set" of layers, cells and motifs, thus giving rise to a vastly parallel neocortical processing architecture (Mountcastle, 1978). Needless to emphasize, that the concept of the cortical column as the processing module is key to models of how the neocortex is organized; the proposal that the entire neocortical mantle is just made of those modular units tiled one next to the other, is an almost inevitable prediction of that concept. However, the proof of this prediction and its underlying idea — that a columnar structure is essential for neocortical computational function — has remained elusive (Horton and Adams, 2005).

The idea of the vertical arrangement of largely independent processing units was first brought about by Lorente de No's observation that the vast majority of axons, and thus neuronal connections, run vertically between the layers (Lorente De Nó, 1922; Lorente De Nó, 1938). Horizontal connections were surprisingly sparse. This suggested that neocortical information processing involves cells communicating with other neurons in layers above or below them, but hardly with neurons situated at a horizontal distance of more than 200-400 µm away. In addition, Lorente de No discovered the septae in layer 4 (Lorente De Nó, 1922) of what much later became known to be the whisker-related barrelfield (see below); these septae appear as

vertical streaks “dividing” the neocortex into regular intervals of 200-400 µm, depending on the species.

Importantly, however, the concept of the column – in sharp contrast to that of the layer – is largely a physiological one, and thus had to await psychophysical and electrophysiological investigations to be clearly articulated (Horton and Adams, 2005). In 1957 and 1962, two studies laid the ground for the current concept of the cortical column. First, Vernon Mountcastle showed that the electrophysiological representation of superficial (from skin or hair) vs. deep (e.g. from joints) touch sensation remained constant along vertical electrode penetrations into the cat somatosensory cortex, but switched abruptly from time to time upon more horizontal tracks (Mountcastle, 1957). Secondly, Hubel and Wiesel showed that upon near-horizontal penetration of cat V1, the orientation preference of the visual receptive field switches abruptly, while cells roughly aligned vertically share the same orientation preference (i.e. constitute one functional minicolumn) (Hubel and Wiesel, 1962, 1963). The principle that cells representing the same stimulus property (i.e. having similar tuning characteristics) cluster together and eventually form vertical arrangements has been repeatedly found in other cortical areas and their incoming projections such as M1, S1, A1, V2, V3, MT, IT (Horton and Adams, 2005). In V1, several of the relatively thin (20-35µm) orientation columns representing different orientations cluster together in larger columnar arrangements – ocular dominance columns — whose cells share the extent to which they are driven by the input from one eye (Horton and Adams, 2005; Hubel and Wiesel, 1969)[21]. These again might have some spatial relationship with the occurence of cytchrome-c oxidase-rich patches (“blobs”), each of which contains cells which

[21] The spatial extension of ocular dominance columns is plastic during development and is regulated by GABAergic signalling involving the α1-subunit of the GABA receptor (Fagiolini et al., 2004; Hensch and Stryker, 2004).

preferentially represent a certain colour-contrast (colour-opponency) (Horton and Hubel, 1981; Ts'o and Gilbert, 1988). In contrast to other columnar representations, this physiological feature of colour preference across layers coincides with an identifiable anatomical landmark across all layers (except 4A and 4C) once the tissue is stained for cytochrome oxidase.

The only other obvious correlation of physiological and anatomical columns is the barrelfield in somatosensory cortex representing the whiskers at the snout of the animal. Here, input deriving mostly (but not exclusively) from one whisker is mapped onto one and the same “barrel”-like structure in layer 4, which is separated by septae from neighbouring barrels representing neighbouring whiskers (Woolsey and Van der Loos, 1970). Although septa are only visible in layer 4 – without any staining, which is crucial for physiological experiments – they can be extrapolated into the other layers to imagine the column. And indeed, that “imaginary” column corresponds to a real physiological column, as cells in all layers within one column are driven mostly be signals form one whisker (Petersen, 2007; Woolsey and Van der Loos, 1970). In agreement with this, it has been shown, using voltage sensitive dye imaging, that selective electrical stimulation in one barrel of layer 4 causes neuronal excitation that is confined to a barrel-related column in layer 4 and – largely – also in layers 2/3 and 5 (Petersen and Sakmann, 2001). Importantly, block of inhibition by a GABA-antagonist breaks this columnar constraint in layers 2/3 and 5 – but not in layer 4 – allowing neighbouring columns to be excited as well. This predicts that the columnar flow of information is maintained by lateral inhibition between neighbouring columns, potentially provided by horizontally ramifying large basket cells (Markram et al., 2004; Mountcastle, 1978; Petersen and Sakmann, 2001). Interestingly, this columnar organization is also plastic, as pairing layer-4-

stimulation in one column with stimulation in layer 2/3 of an adjacent column subsequently enables – in a mechanism dependent on NMDA-receptor induced plasticity – a spreading of the activity into layer 2/3 of the previously co-stimulated (adjacent) column upon single stimulation of layer 4 in the primary column (Petersen and Sakmann, 2001).

In essence, the column means that there are some “quantal”, “discrete” or “step-wise” – i.e. non-continuous – changes when one examines the functional properties, usually the stimulus preference, while moving horizontally across the neocortex, while such tuning characteristics do not change systematically upon vertical penetration, since cells within one column “compute on” the same input or stimulus. In a few instances, such physiological columnar arrangements may coincide with anatomical markers, as in the case of the barrel-related column.

However, it has been pointed out that, unlike the functional clustering in primary visual minicolumns, barrel-related columns are in a way trivial, since the “discrete” nature of stimulus-representation in their case results simply from the fact that the external sensory surface, the whiskers, are also discrete – much in contrast to the continuous sensory surface in the visual system (retina) or the auditory system (cochlea) (Horton and Adams, 2005). This criticism however, does not invalidate the understanding of whisker-related barrel-columns as a proper cortical column, as it conforms to all its definitions and provides a superb example of a modular information processing unit. However, it does question the validity of transferring the findings from such a highly special system to other cortical areas, most of which do not operate on naturally discrete input.

A final and more serious criticism regarding the concept of cortical columns recognizes their existence[22] but questions their importance for cortical processing. Such criticism emerges from data, mostly from certain mammalian species that lack a columnar organization in cortical areas where other species do feature it. Examples include the visual cortex in rodents, where both orientation columns and ocular-dominance columns have not been identified (Horton and Adams, 2005; Ohki et al., 2005), the whisker-related somatosensory cortex of the beaver and cat, which do not feature barrels (Woolsey et al., 1975), as well as mutant mice, which do not feature barrels and a much decreased columnar structure of single-whisker representation, but seem functionally normal, with only minor physiological alterations (Cases et al., 1996; Horton and Adams, 2005; Welker et al., 1996)[23]. In general, it seems that the columnar organization, especially in visual areas, is more flexible and changes with stimulus type (Horton and Adams, 2005). In conclusion, the highly influential concept of vertical processing units is likely true, while the columns as such are much less spatiotemporally static or bound to anatomically fixed, discrete modules than initially thought. In fact, they might form transiently as vertical units of processing centred around any input that reaches the neocortex (Markram, 2008).

[22] There is, of course, also further criticism on the “discrete” nature, that makes a column a module, since already in the experiments of Hubel and Wiesel in 1974, it became obvious, that stimulus-preferences may change rather gradually. Periodicity and clustering of functionally related cells – central tenets of the columnar organization - does in fact, not necessarily exclude gradual changes at the borders of the module (Horton and Adams, 2005).

[23] However, this argument is likewise questionable, since the columnar organization is not necessarily abolished, just because septae and discrete segregation of thalamocortical afferents is lacking.

Canonical connectivity

As already implicit in the concept of the cortical column, the anatomical fine structure of different neocortical regions is remarkably uniform, suggesting that a limited number of conserved microcircuit motifs are replicated extensively (Mountcastle, 1997). In support of this view, the local connections between excitatory neurons of different neocortical areas in different species appear to conform to the "canonical" laminar organization (the canonical neocortical microcircuit) first derived in cat visual cortex (Douglas and Martin, 2004; Douglas et al., 1989; Gilbert, 1983; Gilbert and Wiesel, 1979, 1983) and described above (see "Excitatory connections"). Although variations to this scheme exist in various cortical areas and species as outlined above (see "Excitatory connections") (Barbour and Callaway, 2008; Hooks et al., 2011; Koralek et al., 1988; Shepherd and Svoboda, 2005; Weiler et al., 2008), it is argued that these variations may fine-adapt a cortical area to its specific function, while the general principles of how information flows and thereby is processed within a local neocortical circuit or module (eventually corresponding to a column) is identical (Douglas and Martin, 2004; Hawkins and Blakeslee, 2004). If structure defines function, a common architecture across functionally distinct neocortical areas could mean a common algorithm of information processing that "runs" "everywhere" across the neocortical mantle (Hawkins and Blakeslee, 2004). However, areas differ with respect to the input they process as well as the regions which receive their output – i.e. they differ with respect to their extrinsic, but not their intrinsic connections (Mountcastle, 1978). As one of the fathers of the idea of 'canonical organization and processing throughout the neocortex', Vernon Mountcastle (1978: p. 9) put it: "there is nothing intrinsically motor about the motor cortex, nor sensory about the sensory cortex."

The appealing idea that principles of cortical organization generalize has inspired comprehensive attempts, such as the ‘blue brain project,’ to model the precise wiring and electrophysiology of a cortical column (Markram, 2006) and to transfer principles of neuronal organization from simpler spinal systems to cortical function (Yuste et al., 2005).

The idea of a canonical neocortical microcircuit is an important extension and refinement of Mountcastle’s original hypothesis of a seemingly ubiquitous columnar organization. It formalizes the concept of a common neocortical computational algorithm and has provided an important working hypothesis to guide both theory and experiment. Although the idea is not proven in the strictest sense, since numerous variations have been discovered as described above, it is highly valuable as a default blueprint or filter, which allows deviations from the canonical wiring scheme to be identified as such, and thus be interpreted as a specialisation that relates to the function of a particular neocortical area.

Therefore, it is important to extend the canonical wiring scheme beyond excitatory connections and also incorporate stereotypic elements of inhibition as well as their area-specific variations. The only example for which this has been done thoroughly so far is the motif of frequency-dependent disynaptic dendritic inhibition between pyramidal cells in layer 5 by Martinotti cells of the same layer (Berger et al., 2009). This motif has been found in all of the five neocortical areas investigated in the rat (S1, A1, M1, V2, and mPFC), with just minor quantitative variations in prevalence (being somewhat more common in primary sensory areas) and the kinetics of disynaptic inhibition. The authors interpreted this observation by concluding that inhibitory motifs are likewise canonical (Berger et al., 2009). However, this interpretation remains to be tested by analysing all inhibitory connectivity motifs

across neocortical layers and areas. Detailed anatomical maps of inhibitory connections in neocortical circuits thus promise to reveal general principles of cortical organization.

Optical and genetic methods of circuit dissection

Information processing in the brain involves circuits that are composed of many different classes of neurons, as illustrated above. To understand brain function and brain pathology, the individual roles of these different classes have to be examined in the context of the circuits in which they operate (Callaway, 2005; Miesenböck and Kevrekidis, 2005; Zemelman and Miesenböck, 2001).

Key to the approach used here is the optical control of neurons with the help of light-sensitive ion channels that can be genetically targeted to any neuronal subtype for which a specific genetic control element is known. These light-gated actuators represent the logical counterpart of genetically encodable fluorescent sensors for calcium (Miyawaki et al., 1997; Romoser et al., 1997), voltage (Siegel and Isacoff, 1997), synaptic transmission (Miesenböck et al., 1998; Miesenböck and Rothman, 1997), and chloride (Kuner and Augustine, 2000) which allow neuronal activity to be read out in a cell-type specific manner. Encodable optical sensors have now reached the sensitivity to measure subthreshold events like synaptic inputs and single action potentials (Miesenböck and Kevrekidis, 2005; Tian et al., 2009). They represent the "readout" arm of a suite of methods that includes optical tools for both reading and writing neuronal signals and was later renamed as "optogenetics" (Deisseroth et al., 2006).

The concept of genetically targeted optical control as a logical counterpart to genetically targeted optical detection was introduced thus in 2001:

"Genetics and protein engineering are invading what not long ago was the exclusive domain of synthetic chemistry and pharmacology. Protein-based sensors of neural activity are emerging opposite synthetic indicator dyes; drugs that silence neurons or synapses are finding genetically encoded counterparts. A conspicuous void, however, exists in the genetic line-up at the position that photostimulants and caged neurotransmitters (that is, inactive precursors activated by light) occupy in the synthetic arsenal. We feel that filling this void constitutes a challenging but particularly rewarding area for future developments.
Whereas conventional photostimulation must localize the stimulus in the form of the uncaging light beam, genetic schemes would localize the response (in the form of an encoded sensitivity to light),

and illumination could then be broad. Patterns of distributed activity might be fed directly into a genetically circumscribed population of neurons, irrespective of the anatomical location of its members or their connection to sensory input.
Like metabolic pathways, neural pathways are arranged as graphs of interconnected nodes. The ability to probe individual nodes with pure, often synthetic substrates proved instrumental for the dissection of metabolism. Perhaps the ability to probe defined groups of neurons with synthetic information will hold the key to an understanding of neural systems." (Zemelman and Miesenböck, 2001)

Not long after this proposal, the Miesenböck group conceived and demonstrated the two principal modes of genetically targeted optical control of neural activity:

ChARGe – the prototype of direct photoactivation

The first light-controlled actuator used to fire action potentials in a neuron was a *Drosophila* rhodopsin (Zemelman et al., 2002). This light-activated G-protein-coupled receptor conferred light-sensitivity to mammalian neurons (hippocampal pyramidal cells in culture) once heterologously expressed alongside a minimal signaling cascade, consisting of arrestin-2 and the compatible G_{α}-subunit. Illumination activated endogenous ion channels to cause multiple action potentials. As the photoreceptor is absent from mammalian central neurons, light-sensitivity can be specifically targeted to a genetically determined subset of cells, while all other neurons remain unresponsive to light. Thus, this is the first demonstration of what later became known as optogenetics (in the sense of optical control, not readout) (Deisseroth et al., 2006). Furthermore, as chARGe is intrinsically (or directly) light-sensitive, i.e. does not require a repeated activation by an (un)caged ligand (see below), it is the principle prototype of all later optogenetic approaches using mammalian or microbial opsins (see below), and theoretically ideal for least invasive remote control.

However, just like all its successors, chARGe does in fact depend on a retinal as its intrinsic light sensor, which has to be covalently bound to the opsin to form rhodopsin (Zemelman et al., 2002). Since no protein has been found to date which

gains truly intrinsic light-sensitivity (apart from fluorescent proteins), just from a certain arrangement of amino acids, this is a fundamental limitation to any form of optical control. Fortunately, it was found later, that retinal is present at sufficient levels in vertebrate central neurons to support the action of opsin-based phototransduction, so that this limitation did not actually pose significant problems (Boyden et al., 2005; Li et al., 2005). (The reason for the presence of retinal is unknown, however). In invertebrate neurons, such as adult *Drosophila*, it does, however, create a hindrance for using such opsin, and favours retinal-independent approaches.

Indirect photoactivation via ligand-gated ion channels and uncaging

The first examples of retinal-independent – however, only indirectly light-sensitive – optogenetic tools were again published by the Miesenböck group (Zemelman et al., 2003). In this case, a ligand-gated ion channel, which is not present in the nervous system of interest, is again expressed exclusively in a genetically determined population of neurons, while the tissue is perfused with a caged (i.e. inactive) form of its ligand (Zemelman et al., 2003). Light-sensitivity of the activation of the channel – and thus the neuron – is conferred by the photosensitivity of the cage: Upon illumination (usually with UV-light) and photon-absorption, the cage is removed from the ligand due to photoconversion, and the released agonist may gate open its channel (Sjulson and Miesenböck, 2008). The first truly optogenetic experiment - that is, the use of light-gated ion channels under a cell-type-specific gene-regulatory element to control intact neural circuits and behaviour - was achieved using this strategy, namely P2X2 in behaving fruit flies (Lima and Miesenböck, 2005).

The approach is an extension of the principle of optical activation by uncaging active neurotransmitters from biologically inert, “caged” precursors (Callaway and Katz, 1993; Walker et al., 1986; Wieboldt et al., 1994a; Wieboldt et al., 1994b; Wilcox et al., 1990). The original approach, most notably using caged glutamate, but also acetylcholine and GABA, had overcome the restriction imposed by the inflexibility of intracellular electrodes in terms of studying multiple cells at a time, and instead map tens or hundreds of connections between neurons at high speed by rastering neural tissue with an uncaging light beam (Callaway and Katz, 1993; Katz and Dalva, 1994). The use of nonlinear optics to restrict photoactivation to small, diffraction-limited volumes ranging from the size of a single synapse to that of a neuron provided many more applications of photoactivation to dissect neural circuits and stimulate multiple cells simultaneously to provide highly complex spatio-temporal input patterns into brain circuits (Denk, 1994; Denk et al., 1990; Nikolenko et al., 2007; Svoboda et al., 1996). However, as photoreleased glutamate activates all neurons, regardless of their type, this approach faced a fundamental limitation in studying the diverse functions of the various elements of neuronal circuits.

Thus, replacing photocontrol via glutamate receptors with optical activation of heterologously expressed ligand-gated ion channels represented a transformative step towards targeted interference with neural circuits. Such remote excitation of neurons became possible in the uncaging-regime by deploying P2X2 and caged ATP, TRPM8 and (potentially caged) menthol or TRPV1 and caged capsaicin (Zemelman et al., 2003). The suggested TRP-channels had the additional advantage of being activated by temperature changes using heat (TRPV1) or cold (TRPM8), which indeed has been widely deployed in flies, where remote activation by temperature is feasible (however, instead of TRPV1, TRPA1 has ultimately been

used for heat-mediated activation) (Krashes et al., 2009; Pulver et al., 2009; Rosenzweig et al., 2005).

P2X-channels in turn provide a particular promising candidate for improvement by genetic engineering (Zemelman et al., 2003). In particular, a tethered P2X2-agonist, as described below for the light-gated glutamate receptors (Volgraf et al., 2006), would greatly improve the temporal properties of neuronal activation, while featuring the advantage of almost two orders of magnitude higher single-channel conductance and independent subcellular sorting (to the soma, instead of dendrites) over the latter (Sjulson and Miesenböck, 2008). Unfortunately, such optimization requires knowledge of the three-dimensional structure of the protein, which (for P2X4) was only solved in 2009 (Kawate et al., 2009), while that for glutamate receptors as well as rhodopsin was solved much earlier allowing their fine-scale engineering (see below).

The approach of using heterologously expressed ligand-gated ion channels for optical remote control entails four potential advantages over current methods of direct light-activation: (1) The single-channel conductance of the ligand-gated ion channels is significantly higher than those of currently used microbial opsins; e.g. the single-channel conductance of P2X2 is 40 pS, while that of channelhrodopsin-2 (ChR2) is 40-50 fS (Jarvis and Khakh, 2009; Nagel et al., 2005a; Nagel et al., 2003). Thus, reliable excitation is possible even in expression systems (such as transgenic conditional expression), where the expression level is relatively low (approximately as high as that of endogenous house-keeping genes, if at all). Indeed, the first – and before publication of the present study: only – optogenetic activator, expressed conditionally from a targeted transgenic locus and allowing for robust neuronal excitation is TRPV1 (Arenkiel et al., 2008). (This transgenic mouse

has, however, never been used so far for optical activation via uncaging.) (2) Partly as a result of (1), these tools are much more amenable to two-photon excitation, and thus to the yet unachieved goal of optogenetic control with single-cell resolution in intact brain tissue: Two-photon mediated uncaging of glutamate has been widely applied (Matsuzaki et al., 2001), also for circuit-mapping (Nikolenko et al., 2007) without genetic resolution. Two-photon-uncageable compounds to gate heterologously expressed ion channels, should achieve single-cell resolution of genetically targeted cells. A two-photon-uncageable capsaicin (to gate TRPV1) already exists (Zhao et al., 2006). It should also be possible to cage ATP with chromophores possessing larger two-photon cross-sections. (3) Ionotropic receptors can be equally used for optical as well as for chemical activation, since the (non-caged) ligands can be applied (puffed or injected) into tissue directly. This might provide advantages for sustained activation, or activation in deeper brain structures, which cannot be reached by light (no matter if 1- or 2-photon) applied at the surface of the brain, e.g. with LEDs. Although optical fibres can be inserted into brain tissue to reach deeper structures, their (lateral) radius of activation is presumably limited to less than 300 µm, while chemical compounds can be quickly distributed in brain tissue *in vivo* (Busche et al., 2008; Konnerth, 2009). (4) A fourth advantage is that these systems do not require endogenous retinal, which is difficult to add *in vitro* as well as *in vivo*.

The two principal disadvantages of indirectly light-gated ion channels are (1) the lack of temporal precision – due to the slowness and relative unreliability of the uncaging process, ligand-binding kinetics, and wash-out (dilution) of uncaged agonist and the (2) requirement to add (and wash out) caged ligands, which is particularly problematic *in vivo* (Zhang et al., 2006).

From SPARK to LiGluR – artificial channels and click-chemistry

To unite the advantages of direct and indirect photoactivation or avoid their disadvantages, a research group comprising chemists and biologists has set-out to pursue an intermediate approach by generating synthetic ion channels (just like originally intended for P2X2 (Zemelman et al., 2003)). Their general principle is to use a photoisomerizable molecule – in all cases an azobenzene – as a linker, which has a reactive group, mostly a maleimide (interacting with the amino acid cysteine), on one side and an agonist or antagonist of the respective channel on the other side (Gorostiza and Isacoff, 2008). In contrast to the two approaches described previously, this three-partite photosensitizer needs to be added only once at the beginning of an experiment (e.g. zebrafish larvae need to be bathed in it for 45 min (Wyart et al., 2009)) – neither internal retinal nor external continuous caged agonist supply is needed. The reactive group will attach the photosensitizer covalently to a specifically placed amino acid in the engineered, heterologously expressed receptor, which allows the ligand on the other side of the azobenzene-linker to reach its binding site. Photoisomerization of the azobenzene linker allows to switch back and forth between either one of two configurations, thereby mediating binding and unbinding of the ligand, each of which requires light of a distinct wavelength (Gorostiza and Isacoff, 2008).

Their first creation, named SPARK (synthetic photoisomerizable azobenzene-regulated K^+) channel and published already one year after ligand-gated ion channels were proposed as optogenetic tools (2004), was the first light-gated ion channel ever “made” (in the true sense) and the first genetically targetable *silencer* (Banghart et al., 2004). It was an engineered potassium channel gated by unbinding (short wavelength) and binding (long wavelength) of an azobenzene-

tethered channel blocker. Just like most other prototypes of opogenetic tools, it had a severe limitation, namely, that the engineered, heterologously expressed channel actually constituted a significant leak, thus altering the membrane properties of the cells studied. The approach was taken further, however, yielding a light-gated glutamate-receptor (LiGluR) for reliable and strong excitation of neurons with spike-timing precision up to 50 Hz and above (Szobota et al., 2007; Volgraf et al., 2006). Later, a light-gated, potassium-selective glutamate-receptor was engineered allowing silencing of neural activity with high fidelty (Janovjak et al., 2010). Apart from the fact that these channels are sorted like endogenous glutamate-receptors (i.e. accumulate in the dendrite rather than in the soma) and require the external addition of the photosensitizer malemeide-azobenzene-glutamate (MAG), these creations represent superb, 2nd-generation tools for genetically targeted photocontrol (Gorostiza and Isacoff, 2008; Wyart et al., 2009) and open the road for further development (such as two-photon-isomerizable linkers).

Microbial opsins for genetically targeted excitation and inhibition

Although microbial opsins where only applied for optogenetic intervention almost half a decade after the first formulation of the principle of optogenetics, they have since then become the most widely used tools in the field. Their original drawbacks – the requirement for all-trans-retinal and their tiny single-channel conductance (hence weak excitation or inhibition) – were not faced in mammalian neurons or overcome, either by increasing the gene dose (delivering the gene for the microbial opsin via viral vectors) or by increasing the single-channel conductance by means of genetic engineering. Once these strategies were successful, the convenience of the absence of any requirement for an external chemical compound could be

harnessed, while the temporal fidelity largely excelled the indirectly light-gated ion channels and reached the level of LiGluR.

The protoype and up to now (in modified form) most widely used microbial opsin is channelrhodopsin-2 (ChR2), which originates from the algae *Chlamydomonas reinhardtii* and was molecularly identified by Peter Hegemann in 2001. The sequence was directly submitted to GenBank, thus largely escaping the notice of the neuroscience community (Kateriya et al., 2001) – likewise so, when it was discovered independently by another group one year later (Sineshchekov et al., 2002). When expressed in oocytes, ChR2 encodes a light-sensitive proton pump, which has a leak cation-conductance of ~40-50 fS associated with the light-induced pump cycle. Notably the conductance desensitizes from an initial and transient high-conductance state reached within τ ~ 1 ms to a persistent low conductance state (τ ~ 6.8 ms), which is only ~40% of the former and recovers very slowly (τ = 6.4 s) (Nagel et al., 2003). The gain-of-function mutation H134R improves the steady-state conductance, while, however, maintaining slow off-kinetics (reaching the closed state with τ ~ 20 ms) (Nagel et al., 2005a). ChR2 can be genetically targeted to muscle cells or neurons of the invertebrate *C. elegans* and result in the electrical activation of these cells upon illumination with blue light. This was the second optogenetic study ever published; it effectively established ChR2 as a convenient optogenetic tool (Nagel et al., 2005a). Slightly earlier that same year Edward Boyden and Karl Deisseroth (Boyden et al., 2005) as well as Peter Hegemann and Stefan Herlitze (Li et al., 2005) demonstrated that ChR2 could be used to activate also mammalian neurons in culture and control their individual action potentials, evoked with peak-latencies of 10-15 ms with an accuracy of less

than 5 ms, without producing significant side effects resulting from the overexpression of the channel in the membrane (Boyden et al., 2005).

In addition to designing optimized viral vectors, which allowed the strong and (by means of the *Cre-lox* system) cell-type specific genetically targeted remote control *in vivo* (Adamantidis et al., 2007; Aravanis et al., 2007), the lab of Karl Deisseroth – mostly in close collaboration with that of Peter Hegemann - has further improved the toolbox of microbial opsins in four directions: Firstly, another microbial opsin VChR1, derived from the algae *Volvox carteri* and similar to ChR2, was introduced, which has the peak of its activation wavelength 70 nm shifted into the red spectrum, compared to ChR2 (540 nm instead of 470 nm), and thus can still be activated by long-wavelength (~590 nm) light effectively, where the activation of ChR2 is almost vanished. Thus, these two tools, expressed in different cell-types of the same circuit, can be deployed to control different neuronal populations independently from each other (Zhang et al., 2008). Secondly, another mutation (C128S) was introduced into ChR2 which extends the life-time of the open state rendering the channel open - once “switched on” by blue light - until it is “switched off” by yellow light (Berndt et al., 2009). Not requiring any further illumination throughout the open state, this bistable ChR2 also improves the light-sensitivity of ChR2 by about two orders of magnitude and thus makes it ideal for *in vivo* application (as it is activated already by dim, scattered light), especially when longer activation is needed, without risking to overheat the tissue with the light-source (Berndt et al., 2009). Thirdly, the problem of relatively slow on- and off-rates of the ChR2-kinetics and sustained plateau potentials, usually preventing reliable activation with spike-timing precision above 20 Hz, was addressed. To achieve this, a different mutation was engineered, E123T, which has a faster onset (flash-to-peak time < 1 ms, compared

to > 2 ms in wildtype ChR2), a faster off-rate (τ ~ 5 ms, instead of ~10 ms), a higher steady-state current (~55 % instead of 40 % of peak current) and a significantly improved recovery of the peak-current (τ ~ 1 s, instead of > 6 s), thus supporting extended spike trains of up to at least 200 Hz in neocortical PV-interneurons with high spike-timing precision – however, at the cost of much reduced single-channel conductance even compared to the wildtype ChR2 (Gunaydin et al., 2010). Potentially even better prospects, especially regarding high conductance, would be achievable using the engineered ChR1/2 variants ChEF and ChIEF from Roger Tsien's lab, which display a steady-state current of ~70 % of the peak current and likewise a faster kinetics than wt-ChR2 (Lin et al., 2009) or the strongly calcium-permeable ChR2-variant CatCh (Kleinlogel et al., 2011).

A fourth development is the optimization of microbial opsins which can mediate neuronal silencing. Although the approach of optical inhibition had been spearheaded by synthetic ion channels (see above, (Banghart et al., 2004; Janovjak et al., 2010), a technology that would be independent of externally added ligands would be desirable. The first opsin-based neuronal silencing was developed by the groups of Peter Hegemann and Stefan Herlitze, using the rat rhodopsin 4, which, by means of Gi-mediated signalling, could effectively silence spiking neurons, however only relatively weakly and with low temporal resolution (Li et al., 2005). The Deisseroth and the Boyden labs in collaboration with others published a second approach, this time based on a microbial opsin, which constituted the light-induced chloride pump NpHR from *Natronomons pharaonis* and could effectively silence individual as well as multiple action potentials evoked by strong current injections (200-300 pA) in cultured hippocampal neurons (Han and Boyden, 2007; Zhang et al., 2007). Since its optimal wavelength of activation is strongly red-shifted

by about 100 nm (to 580 nm) with respect to ChR2, one and the same cell population or circuit – expressing both ChR2 and NpHR - can be excited and inhibited using distinct wavelengths, as demonstrated *in vivo* in *C. elegans* (Zhang et al., 2007). However, as the “single-channel conductance” of that chloride pump (which does not actually contain a channel) is very small and the sorting to the cell membrane of mammalian cells is significantly hampered, the effective use of this tool, especially *in vivo* , had to await significant genetic engineering, yielding enhanced NpHR (eNpHR) (Gradinaru et al., 2008; Zhao et al., 2008). Also, microbial (namely archael) opsins, that constitute light-driven proton (not chloride) pumps with large “conductances”, have been found to be much more efficient in optical silencing (Chow et al., 2010).

The application of these microbial opsins have been broad (exceeding the space of this introduction), ranging from mapping of neural circuits in the brain slice to *in vivo* control of circuits and behaviour in the rodent and monkey brain. Likewise, the dissection of the function of different, genetically specified subtypes of interneurons – one of the central goals of and beyond the present study – has been pioneered for parvalbumin-positive interneurons *in vivo* and *in vitro* (Cardin et al., 2009; Sohal et al., 2009). Neocortical excitatory long-range connectivity has been mapped using ChR2 – however, not genetically targeted to any specific cell type (Petreanu et al., 2007; Petreanu et al., 2009). Importantly, the mapping and functional dissection of local inhibitory (or excitatory) circuits has not yet been achieved, due to the fact that the fusion protein of ChR2 and a fluorescent protein, introduced with either viral vectors or *in utero* electroporation, tends to accumulate in axons and synapses, thus preventing the exclusive determination of the location of the cell body of a stimulated neuron (Petreanu et al., 2007; Petreanu et al., 2009). The publication of

the present study is the first report of the application of an optogenetic tool (ChR2) for the mapping of local circuits, i.e. circuits where pre- and postsynaptic neurons are arbitrarily intermingled (Kätzel et al., 2011).

The D.Phil project

The considerable morphological and physiological diversity of interneurons - in addition to their small number - poses significant challenges to traditional electrophysiological approaches but might benefit greatly from genetically based methods of analysis (Miesenböck and Kevrekidis, 2005; Monyer and Markram, 2004; Zemelman and Miesenböck, 2001). As the molecular taxonomy of interneuron subclasses is refined with the discovery of more and more characteristic marker genes, promoters will be identified that can grant selective genetic access to defined cell types, and thus enable the anatomical and functional dissection of interneuron networks by means of genetically targeted photostimulation or optogenetics.

In my DPhil project, I establish for the first time an optogenetic method of mapping *local* circuits using *conditional* expression of the actuators ChR2 and P2X2 from a targeted genomic locus. As outlined above, such attempts have so far been hampered by the small single-channel conductance of the actuator channelrhodopsin-2 and by the tendency of virally expressed ChR2 to accumulate in axons and synapses – thus promoting their direct excitation. Synaptic activation makes the currently published optogenetic tools ideal for mapping long-range projections, but obviously prevents the dissection of local circuits, where actuator-expressing presynaptic neurons are intermingled with their postsynaptic targets. With predominantly somatic expression of the actuator, scanning a stimulating beam across neural tissue (Callaway and Katz, 1993) will generate light-evoked

inhibitory currents in electrophysiologically recorded postsynaptic partners whenever the focal spot activates a presynaptic interneuron. The resulting “IPSC images” reflect the laminar and tangential distributions of sources of inhibition.

Beyond the establishment of such a technology, I deploy it to test if the four principles of neocortical organization derived from an analysis of excitatory cells and their connections – layers, columns, canonical connectivity and specificity of individual connections – also hold true for inhibitory circuits. My work centres around the question: „Where does a single pyramidal cell of a certain layer receive its inhibitory inputs from and what are its characteristics?“ It involves neocortical brain slices, obtained from genetically modified mice expressing light-activated ion channels. These slices largely preserve the cortical microcircuitry in functional form but provide an experimentally accessible setting.

My first working hypothesis is that the anatomical location of an interneuron in a specific cortical layer as well as in relation to its postsynaptic target neuron is a significant predictor of functional differences in its inhibitory output, and thus, that inhibitory connections are wired with high specificity with respect to the individual cell.

My second working hypothesis is that inhibitory circuits, like excitatory ones, display a relatively stereotypic organization (Douglas and Martin, 2004; Mountcastle, 1997; White, 1989), which features a canonical wiring pattern of inhibitory connections. To test the validity of this notion, I compare the connection schemes of inhibitory neurons in primary visual cortex (V1), somatosensory or barrel cortex (S1), and motor cortex (M1) of the mouse.

My third working hypothesis is that inhibitory circuits, like excitatory ones, are structured clearly into a laminar and (where applicable) columnar organization. [24]

[24] This "core programme" may be considered as the start-up of a comprehensive attempt towards an optogenetic analysis of inhibitory circuits involving the following central research questions:
A. How are GABAergic interneurons wired into microcircuits?
A.1 For a genetically defined interneuron subtype, e.g. a small basket cell, in a given cortical layer, to which cortical layer do inhibitory connections project? What are the synaptic targets (pyramidal cells and/or other interneurons)? Which receptors are involved (fast or slow variants of $GABA_A$ or $GABA_B$)?
A.2 How strong is the synaptic connection, i.e. what is the 'normalized evoked input' (Dantzker and Callaway, 2000)? What synaptic dynamic (e.g. plasticity) does it display?
A.3 What is the preferred firing frequency of a certain interneuron subtype, and how are oscillations transduced to pyramidal cells (i.e. what is the synaptic transfer function)?
A.4 Is there a canonical connectivity pattern across cortical areas?
B. What is the impact of GABAergic interneurons on collective circuit activity?
B.1 What alteration of the spontaneous activity of single pyramidal cells does the collective excitation of interneurons of a certain subtype lead to, and what is the dose-response-relationship?
B.2 In spontaneously occurring or pharmacologically induced coherent network states, such as oscillations or 'up' and 'down' states , how many interneurons of what type are necessary to alter collective network behavior? For example, what does it take to elicit oscillations of local field potentials or multiple units, to produce or disrupt synchrony, or to switch a pyramidal cell from an 'up'into a 'down' state (Mann et al., 2009)?
Further research questions include: Which interneurons of which cortical layer innervate other interneurons of which layer via electrical (i.e. gap junction) or chemical synapses, respectively? Interneuronal innervation of interneurons as well as electrical coupling of interneurons represents a central field within the functional micro-anatomy of the cortex (Soltesz, 2006). In particular, a profound understanding of cortical rhythm generation will have to await a detailed dissection of inter-interneuronal circuits (Buzsaki, 2006). Interaction studies between interneurons (i.e. stimulating one neuron, while recording from a potential postsynaptic partner) have become feasible due to the high throughput and specificity of genetically targeted photostimulation. This opens entire new fields for analysis: Do some interneurons target preferentially interneurons whereas others target preferentially pyramidal cells? Do interneurons of a certain class only synapse electrically on interneurons of the same class? Can rhythmic oscillations be triggered and maintained within isolated populations of one interneuron type? Are those populations sufficient to entrain specific rhythms in pyramidal cells (Buzsaki, 2006; Söhl et al., 2005)? Are long-range projections of GABAergic interneurons central for synchronized neural activity (Mann and Paulsen, 2007)? Can interneuronal networks and thus their rhythms be selected or regulated by peptidergic innervation (Koch, 2004)? Further extension is possible by adopting the analysis of "transfer functions" of inhibitory circuits within a closed-loop-design, i.e. building an artificial circuit where the activity of a post-synaptic pyramidal cell directs the optical actuation of the pre-synaptic interneuron, so that the dynamics of this neuronal interaction can be studied in a controlled setting somewhat analogous to a 'dynamic clamp' (Sohal et al., 2009).

Chapter 2 – Materials and Methods

Mouse construction

The three novel (i.e. previously unpublished) mouse strains used in this thesis work were generated by Dr. Boris Zemelman under supervision of Prof. Gero Miesenböck at Sloan-Kettering Center for Cancer Research (New York) and Yale University (New Haven). They have the following structure:

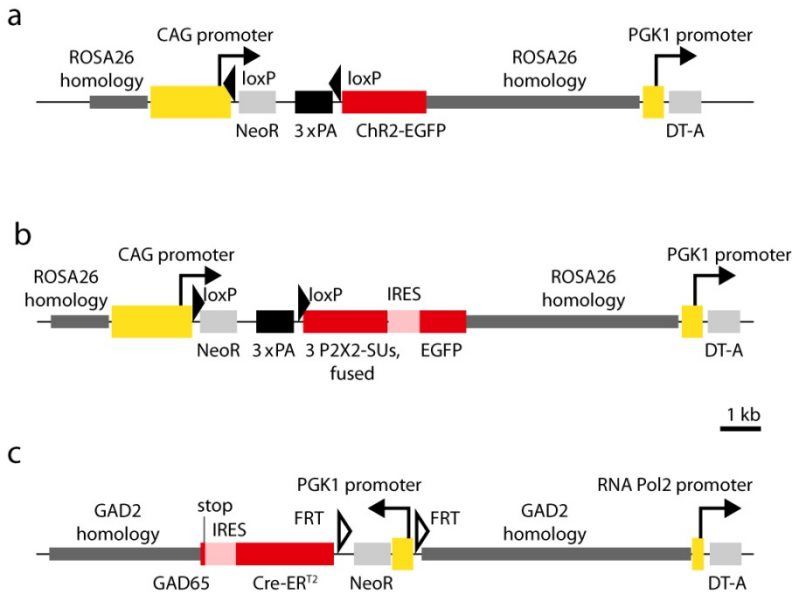

Figure 2.1. Targeting Constructs for ChR2 (a) and P2X2 (b) responder lines and for the Gad65/Gad2 driver line (c). Homology sequences are indicated in dark grey, promoters in yellow, open reading frames in red, IRES in light red and selection markers in light grey. PA, poly-A stop-sequence, black. SUs, subunits. (a, b) Constructs used to generate the R26::ChR2-EGFP or the R26::P2X2-IRES-EGFP allele. Cre-mediated excision of a triple-polyA transcriptional STOP cassette (3x PA, black) flanked by loxP sites enables ChR2- or P2X2-EGFP expression from the CAG promoter. (c) Construct used to generate the Gad2::Cre-ERT2 allele. An internal ribosome entry sequence (IRES, light red) separates the Gad65 and Cre-ERT2 reading frames.

Generation of a Cre-responsive R26::ChR2-EGFP or R26::P2X2-IRES-EGFP allele

To generate a *Cre*-responsive actuator (Kateriya et al., 2001; Miesenböck and Kevrekidis, 2005; Zemelman et al., 2002) allele whose expression could be restricted to genetically circumscribed groups of neurons, the *GT(ROSA)26Sor* (*R26*) locus was targeted with an actuator transgene driven by an ubiquituously

active, strong promoter (CAG): In the case of the channelrhodopsin-2 responder line, a codon-optimized de novo synthesized DNA fragment encoding the 315 N-terminal amino acids of channelrhodopsin-2 (ChR2) (Kateriya et al., 2001; Nagel et al., 2003), including the H134R mutation, that increases the conductance in the desensitized state (Nagel et al., 2005a) was fused via a 10-amino acid linker (EAGAVSGGVY) to EGFP (Clontech). ChR2-EGFP expression was driven by the synthetic CMV early enhancer/chicken β actin (CAG) promoter (Niwa et al., 1991) after Cre-mediated excision of a *lox*P-STOP cassette (Soriano, 1999a) interposed between transcription and translation start sites. Recombination brings the ChR2-EGFP coding sequence in frame with an initiating ATG in the *lox*P site, resulting in translation of ChR2-EGFP with an 11-amino acid N-terminal "*lox*P tag" (MYAIRSYELAT). The expression unit was targeted to the *GT(ROSA)26Sor* (*R26*) locus after insertion into the ROSA26-PA vector (Soriano, 1999a; Srinivas et al., 2001) (Fig. 2.1a).

The P2X2-responder line was generated similarly, with three minor variations: The loxP-sites were inverted, so that translation starts from the endogenous ATG of the P2X2-gene. In contrast to the native P2X2-gene, the three P2X2-subunits, which usually comprise a P2X2-channel trimer were fused artificially with two linkers. And, the EGFP was not fused directly to the end of the P2X2 channel gene, but is expressed independently from an IRES (Fig. 2.1b).

Generation of a Gad2::CreER^{T2} allele

To generate the potential for conditional *Cre* recombinase activity in all GABAergic interneurons, a cassette encoding tamoxifen-inducible *Cre*-ER^{T2} (Feil et al., 1996; Indra et al., 1999; Leone et al., 2003; Metzger et al., 1995) was inserted into the *Gad2* locus. The GFP coding sequence of plasmid pIRES2-EGFP (Clontech) was

replaced with a DNA fragment encoding *Cre*-ER^{T2}, and this IRES-*Cre* unit was fused to an *FRT*-NeoR-*FRT* selection cassette. The assembly was ligated into a *Gad2* targeting vector, which contained a 3168-bp 5' homology arm (spanning a portion of the last intron and exon of the *Gad2* gene, up to and including the stop codon) and a 5571-bp 3' homology arm (consisting of *Gad2* 3' untranslated region immediately following the stop codon). A selection cassette containing the diphteria toxin (DT-A) open reading frame, driven by the RNA polymerase II promoter and terminated by the SV40 polyadenylation signal, was inserted downstream of the 3' homology arm (Fig. 2.1c).

R1 embryonic stem (ES) cells (129Sv X 129SvJ F1 hybrid) were transfected with the linearized targeting vectors, and after G418 selection and expansion, homologous recombinant ES cell clones were identified by PCR and confirmed by Southern blotting. Recombinant ES cells were injected into C57Bl/6J blastocysts to produce germline chimeras. The *FRT*-NeoR-*FRT* selection cassette present in the *Gad2* targeting construct was deleted by breeding founders with the *FLPeR* strain (Farley et al., 2000). Mice are in a mixed (129 x C57Bl/6J) background.

Genotyping

Genotyping was applied when experimental animals, including Pcp-*Cre*>ChR2, Gad65-*Cre*>ChR2, Gad65-*Cre*>ChR2–Gad65-GFP, Gad65-*Cre*>ChR2–Gad67-GFP, CamKIIα-*Cre*>ChR2 (two different drivers (Casanova et al., 2001; Tsien et al., 1996b) were tested, the latter available from JAX (stock# 005359}), and Gad65-*Cre*>P2X2, CamKII-*Cre*>P2X2, were created by crossing driver (CamKIIα-*Cre*, Gad65-*Cre*, Pcp-*Cre*) and responder (ChR2, P2X2) to obtain the resulting experimental strain. To allow sufficient expression of ChR2 or P2X2, the responder

locus was always used in homozygous state for experiments, i.e. required at least two generations (usually more) of mouse crossing to be obtained. After achieving animals with homozygous responder but hemizygous driver locus, mice were tested for functional expression and crossed to obtain animals homozygous also in the driver locus ("double-homozygous"). Some driver lines could not be bred to homozygosity, since they are either transgenic, e.g. BAC-transgenic mice carrying the *Cre* in a random location (the CamKIIα-driver of (Casanova et al., 2001)) or CDS knock-in, where *Cre* disrupts an endogenous gene (as is the case in the Pcp-*Cre*). To obtain homozygous lines, two genotyping reactions were performed in principle, one confirming the presence of the *Cre* (termed mut- or *Cre*-PCR), another one confirming the disruption of the wildtype locus (wt-PCR). Double-homozygous lines are advantageous for reducing animal numbers and procedures, as 100 % of offspring can be used for experiments without further requirement for tissue sampling and genotyping[25].

Genotyping was performed by PCR, using the following primers: For detecting the wild-type ROSA26 locus (in responder strains) the forward primer 5' tgcagtggagtaggcggggagaag and the reverse primer 5' cgggagaaatggatatgaagtactgggc were used yielding a 550 bp product (T_m = 66°C). For detecting the ChR2-EGFP in the ROSA26 locus (Fig. 2.1a) the forward primer 5' attgaggtcgagacgctggt and the reverse primer 5' agcctttaagcctgcccaga were applied yielding a 852 bp product (T_m = 55°C). For detecting P2X2 in the ROSA26 locus the forward primer 5' gctctgactgagcaggtggtggac and the reverse primer 5' ttccgctgcctgcaaagggt were used yielding a 413 bp product (T_m = 61°C) (Fig. 2.1b).

[25] However, a homozygous driver locus, might result in alterated expression of the endogenous gene, e.g. of Gad65, and entail phenotypes. Ideally, if larger colony size and more time can be afforded, double-homozygous lines should be bred with responder-homozygous (driver-negative) lines, to obtain hemizygous driver loci in all experimental mice.

Genotyping for the Gad2-wildtype locus was performed using the forward primer 5' gacttccttattgaagaaatcgaacg and the reverse primer 5' ctgattagaacacagccttttgtca yielding a 449 bp product (T_m = 55°C) (Fig. 2.1c). Generic *Cre* (in Gad65-*Cre*, CamKIIα-*Cre*) was detected using the forward primer 5' ccgggctgccacgaccaa and the reverse primer 5' ggcgcggcaacaccattttt yielding a 445 bp product (T_m = 61°C). The primers were designed, tested and established by Christina Buetfering, a diploma student working under my supervision, Yan Tan, a lab technician in the Miesenböck lab, and myself.

The genotyping reaction was performed using tissue from one or two ear notches (avoiding tail clipping as the more severe procedure), which was obtained either by myself or animal technicians. Further processing was mostly performed by Yan Tan, rarely by myself. DNA was extracted from tissue samples using the Promega Maxwell 16 system and Mawell 16 Tissue DNA purification Kit (Promega, Cat.# AS1030) and dissolved in 300 µL elution buffer to yield about 1ng/µl.

The Invitrogen accuPrime™ Taq DNA Polymerase System (Invitrogen, SKU# 12339-016T) was used for the PCR reaction, which was performed in thin-walled tubes in a Bio-Rad PCR machine (Bio-Rad PTC-0200G DNA-Engine, Peltier Thermal Cycler) with a heated lid, using a total reaction volume of 15 µl.

The lypholized primer molecules were diluted upon arrival to achieve 100 µM. For further use, a primer mix was created, diluting 10µl of forward(fw)- and 10µl of reverse(rev)-primer solution in 80µl dH2O (10 µM final concentration). This primer mix (0.6 µl) was used to create a master mix containing dH_2O (11.5 µl), 10x AccuPrime PCR Buffer II (blue lid, 1.5 µl) and AccuPrime™ Taq DNA Polymerase (0.2 µl). After gentle mixing, 13.8 µl of the mix was dispensed into thin-walled PCR

tubes and 1.2 µl of genomic DNA solution (~ 1ng/µl) added. The generic PCR program used was:

step 1	94°C	2 minutes
step 2	93°C	20 seconds
step 3	[Tm]°C	30 seconds
step 4	68°C	≥ 60 seconds / 1kb of product
repeat steps 2 to 4 for 33 cycles		
step 5	68°C	5 minutes
step 6	12°C	hold

After the PCR reaction was finished, PCR samples were analyzed by gel electrophoresis at 120 V for approximately 20 minutes using a 1 % agarose gel. Ethidium-bromide-stained bands were visualized under UV-illumination.

Experimental animals and induction of transgene expression

Experimental animals were homozygous at both targeted loci. They were maintained on a 12 hour light/dark cycle on standard diet RM3 (Special Diet Services), containing 19,9 IU/g vitamin A and 9,58 µg/g retinol. For some later experiments with ChR2-mice, the food was replaced with a Vitamin-A enriched version, containing 100 IU/g vitamin A, in order to potentially improve the availability of the ChR2-co-factor all-trans-retinal and thus its functional expression levels. At 4 to 7 weeks, mice with inducible driver lines were injected i.p. on five consecutive days with 0.5-1 mg 4-OH-tamoxifen (Sigma-Aldrich) dissolved in sterile sunflower oil at a concentration of 5-10 mg/ml. The mice were used within 7 days after the last injection.

All procedures conformed to the UK Animals (Scientific Procedures) Act 1986.

Immunohistochemistry

Animals were perfused with phosphate-buffered saline (PBS, pH 7.4) containing 4 % (w/v) paraformaldehyde (PFA) and 0.2 % (w/v) picric acid under general ketamine-medetomidine anesthesia (see below). The brain was removed and incubated for 24 h in perfusion solution and subsequently infiltrated with 30 % (w/v) sucrose in PBS for at least 24 h. Coronal sections of 40–60 µm were cut on a Leica SM 2000R sliding microtome. To minimize the PFA exposure of calcium binding proteins for analyzing specificity of ChR2 expression (Fig. 3.2 and Table 3.1), 150 µm thick sections were cut acutely in ice-cold aCSF (see below) and incubated in fixation solution (PBS containing 4 % PFA and 0.2 % picric acid) for 2 h instead.

Sections were washed three times in Tris-buffered saline (TBS, Sigma), three times in TBS containing 3 % (w/v) Triton X-100 (TBS-T), and once for 1 h in TBS-T containing 20 % (v/v) horse serum (Vector Labs). After a short rinse in TBS, slices were incubated for 48 h at 4 °C in TBS-T containing 1 % horse serum and combinations of the following primary antibodies: anti-GFP (rabbit, 1:500, Sigma; chicken, 1:500, AbCam); anti-*Cre* recombinase (mouse, 1:500, Millipore); anti-Gad65 (rabbit, 1:500, Millipore; mouse, 1:100 Santa Cruz); anti-Gad67 (mouse, 1:1000, Millipore); anti-CaMKIIα (rabbit, 1:400, Epitomics); anti-parvalbumin (mouse, 1:2000, Swant); anti-calretinin (mouse, 1:500, Swant); anti-calbindin (mouse, 1:250, Swant); anti-somatostatin (rabbit, 1:400, Millipore); anti-neuropeptide Y (rabbit, 1:800, abcam); and anti-vasoactive intestinal peptide (rabbit, 1:500, immunostar). The sections were rinsed 4 times in TBS and stained in TBS-T containing 1 % horse serum and Alexa488- and Alexa546-labeled

secondary antibodies (Invitrogen). After four rinses in TBS, slices were mounted in VectaShield (Vector Labs) and imaged on a Zeiss LSM510 confocal microscope.

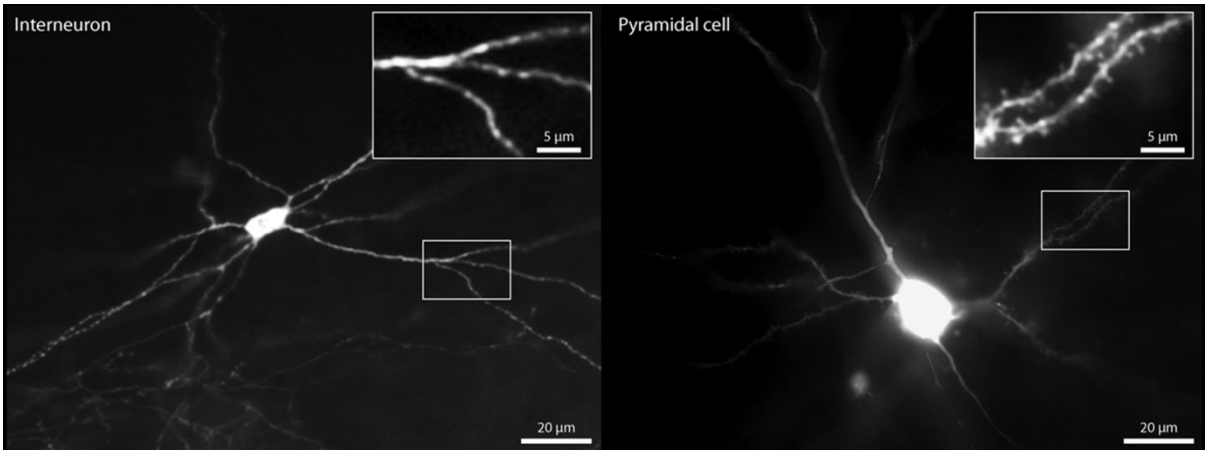

Figure 2.2. Presence (right) or absence (left) of dendritic spines define cell type. Wide-field fluorescence images of cells filled with neurobiotin during electrophysiological recordings, followed by fixation and staining with fluorescently labeled streptavidin. Insets reproduce contrast-enhanced images of boxed areas, showing spiny and spineless dendrites of pyramidal cells and interneurons, respectively, at 2.5-fold higher magnification.

Brain slices harboring neurobiotin-filled cells were fixed overnight in PBS containing 4 % PFA and 0.2 % picric acid, rinsed in TBS, and incubated overnight in TBS-T containing 1 % (v/v) horse serum, 4 µg/ml Alexa-546-labeled avidin (Invitrogen), and 0.0001 % DAPI (Sigma). Further processing was as described above. Neurons were classified as excitatory vs. inhibitory based on the presence vs. absence of mushroom-like spines on dye-filled dendritic arbors (Fig. 2.2); however, presence or absence of ChR2-induced inward currents during mapping experiments served (in addition to a large membrane time constant and cell capacitance as well as a low holding current at 0 mV in excitatory cells) as a reliable preliminary criterion on-line.

Sensory deprivation

For one experimental series sensory deprivation was performed to study the plasticity of inhibitory circuits in S1. Whiskers of > 2 month-old animals were

trimmed unilaterally under transient ketamine/medetomidine anaesthesia in whisker rows A, B, D, and E (leaving the middle row, C, intact). Whiskers were re-trimmed every other day over a period of 2-3 weeks before experimental usage.

In vitro electrophysiology

Experiments were performed on mice mostly aged 5–8 weeks, 1–7 days after the last 4-OH-tamoxifen injection. Whisker-trimmed mice and corresponding controls were used at an age of more than 2 month. The animals were anesthetized by injection of 100 µl ketamine (100 mg/ml; Fort Dodge) plus 50 µl medetomidin (1 mg/ml; Pfizer) and perfused cardially with ice-cold solution containing (in mM): 2.5 KCl, 1.25 NaH_2PO_4, 25 $NaHCO_3$, 10 glucose, 240 sucrose, 0.5 $CaCl_2$, 7 $MgCl_2$, pH 7.4, 320 mosm. The brain was recovered into perfusion solution, and coronal neocortical slices of 310 µm were cut on a Leica VT1000S and, later, VT1200S vibratome.

Cells were recorded as described below in M1 using slices between Bregma +1.2 until Bregma +0.5 mm, S1-barrelfield using sections between Bregma +0.3 until Bregma -0.9 mm, as well as in V1 using slices between Bregma -2.5 until -3.3. Sections of M1 from further anterior than Bregma +1.2 mm are usually too thick with respect to their cortical depth so that they cannot be visualized in their entirety with the optics used, while M1 slices which also contained significant barrelfield were not used anymore (as then M1 starts fading out). The somatosensory barrelfield was usually best visible on the more anterior slices not containing hippocampus (given that the area-adapted slicing angle was used, see below). V1 was usually used from where hippocampus starts to draw towards ventral significantly (more anterior to that, V1 is too thin in its lateral extension) until the point where the cortices easily detach from the central part of the brain slice (since

from then onwards, V1 is too thin with respect to its cortical depth, so that each layer would be covered by only few spots of the stimulation grid).

The lateral location of each brain area was usually determined according to certain landmarks. In M1 cells were used that are at or slightly lateral from the lateral edge of the ventricle. The S1-barrelfield was easily identified by the layer 4 barrels, which were often made better visible by defocusing the objective (or the condensor) slightly. V1 circuits were located lateral from the triangle-shaped dorsal hippocampal commissure and *forceps major* of the *corpus callosum*, which on the more anterior V1-containing slices also corresponds roughly to the region right above the dorsal dentate gyrus in the direction perpendicular to the pia.

The slices were incubated for one hour at 34 °C and subsequently maintained at 25 °C in modified aCSF containing (in mM): 125 NaCl, 2.5 KCl, 1.25 NaH_2PO_4, 25 $NaHCO_3$, 25 glucose, 1 $CaCl_2$, 2 $MgCl_2$, pH 7.4, 315 mosm. Eventually 1.25 mM $CaCl_2$ were used instead of 1 mM. Recordings were performed at room temperature in aCSF containing (in mM): 125 NaCl, 3.5 KCl, 1.25 NaH_2PO_4, 25 $NaHCO_3$, 25 glucose, 1.25 $CaCl_2$, 1 $MgCl_2$, pH 7.4, 300-310 mosm. All extracellular solutions were bubbled with 95 % O_2/5 % CO_2. If spontaneous network activity (up-states) occured repeatedly due to high potassium and/or low magnesium levels (Shu et al., 2003), $MgCl_2$ was raised to up to 1.5 mM. For experiments involving P2X2 2.5 mM KCl was used to counteract basal overexcitation from accumulating ATP levels, while the relatively low calcium concentration was maintained as stated to counteract the use-dependent block of P2X2 by calcium ions (Jarvis and Khakh, 2009).

Patch pipettes had tip resistances of 4-6 MΩ and contained the following internal solutions (in mM): For whole-cell recordings of IPSCs in voltage clamp: 110 CsOH,

110 gluconic acid, 0.2 EGTA, 30 Hepes, 2 MgATP, 0.3 Na_2GTP, 4 NaCl, 5 QX-314-bromide, 0.2 % neurobiotin. For whole-cell recordings of optically evoked activity in current clamp: 120 K-gluconate, 10 KCl, 10 Hepes, 4 MgATP, 0.3 Na_2GTP, 10 phosphocreatine, 0.2 % neurobiotin. For cell-attached recordings: 125 NaCl, 3.5 KCl, 1.25 NaH_2PO4, 25 $NaHCO_3$, 25 glucose, 1.5 $CaCl_2$, 1 $MgCl_2$, 0.5 % neurobiotin. All internal solutions were adjusted to pH 7.2–7.25 and an osmotic strength of 270-280 mosm. Signals were amplified and lowpass-filtered at 2 kHz by a Multiclamp700a amplifier (Molecular Devices) and digitized at 5–10 kHz (Digidata 1440, Molecular Devices).

Optical stimulation

Optical stimulation experiments were performed on a Zeiss Axioskop 2FS microscope. A 40x, 0.8 NA water immersion objective with DIC optics was used for electrode placement and a 10x, 0.3 NA water immersion objective, without DIC optics, for optical stimulation. For channelrhodopsin-2 experiments, the output of a continuous-wave solid-state laser with a maximum power of 325 mW at 473 nm (LRS-473-AH-300-10, Laserglow) was digitally switched and intensity-modulated by an acousto-optic deflector (IntraAction model ASN-802832 with ME-802 driver), positioned by a pair of galvanometric mirrors (GSI Lumonics VM500 with MiniSAX servo controllers), and merged with the epi-illumination path of the microscope via custom-built optics (Fig. 2.3).

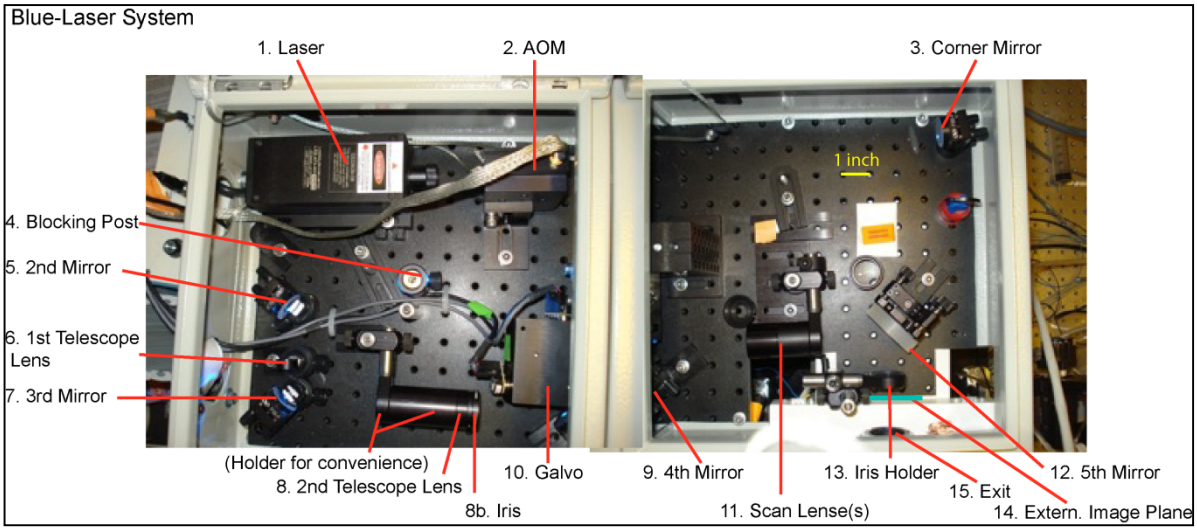

Figure 2.3. Blue-laser-system.

For experiments involving P2X2 and photo-release of ATP from its DMNPE-caged form (~125 μM in aCSF, Invitrogen) a UV-Laser (DPSS) with maximum power of ~300 mW was used in conjunction with a similar scan system, however featuring UV-coated galvanometric mirrors (Fig. 2.4). Power-levels were adjusted manually between a maximum output power at the objective of 90 mW and a minimum power of 0.9 mW using a set of neutral density filters combined within a pair of filter-wheels (ThorLabs).

In channelrhodopsin-2 based experiments, light pulses carried 1.0-2.0 mW of optical power at the exit pupil of the objective; in the case of Purkinje cells, the optical power was attenuated (to a minimum of 0.5 mW) given their higher sensitivity to blue light (or lower spike-threshold as measured in light-intensity). Often, lower power levels would be used at the first stimulation sweeps, while afterwards power levels were gradually increased, to counteract the reversible light-induced desensitization as well as a notable light-induced degradation of functional ChR2.

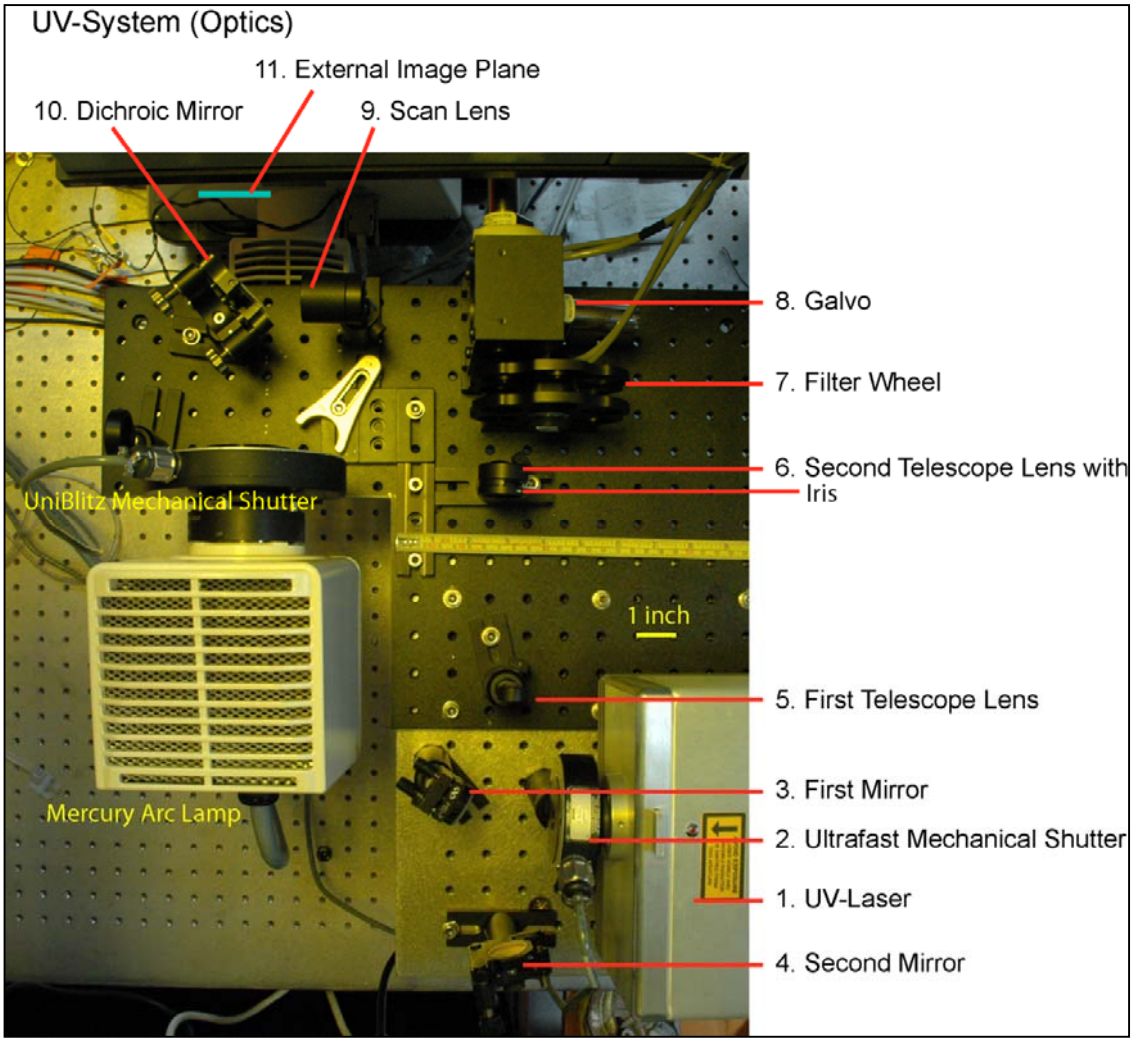

Figure 2.4. UV-laser-system.

To generate maps of inhibitory inputs, a virtual instrument written in LabVIEW 8.5 delivered focussed stimulation light pulses of 20 ms duration at intervals ranging between 400 and 850 ms to grids encompassing 14 x 14 to 14 x 22 locations, depending on the cortical area. While initially 14 x 14 maps with variable point spacing (55 – 70 µm lateral distance) were used for all mapping experiments, soon the grid design was adjusted to the thickness of the cortex in each area, using 14 x 16 grids in V1, but 14 x 20 in S1 and M1 (occasionally 14 x 22 was used in M1), with a constant inter-spot distance of 60 µm. For estimating the spatial resolution of photoactivation, grids of 8 x 8 spots were generally used. Wide-field stimuli were

generated by defocusing the objective by ~200 µm (upward) and increasing the optical power to ~20 mW. Pseudo-randomized stimulation sequences were used to maximize the time between illuminating neighbouring spots.

Data analysis

Data were analyzed in Igor 6 (Wavemetrics), MatLab 7.9 (The Mathworks), and SPSS 17 (SPSS Inc.). Maps of inhibitory inputs were constructed from electrophysiological signals recorded during 8-10 sweeps of the whole stimulation sequence. IPSCs were identified by three criteria. First, the amplitude of the upward deflection in the averaged trace had to exceed 3 times the average standard deviation of current fluctuations in the absence of an optical stimulus (rms noise). In exceptional cases, factors of 2.5–3.5 rms noise were applied to compensate for unusually low or high baseline activity in the recordings (Silberberg and Markram, 2007). Second, IPSCs had to reach half-maximal amplitude within 5–70 ms after optical stimulus onset, accommodating the longest expected delays of 25 ms for spiking (see below) and 40 ms for dendritic conductance (Silberberg and Markram, 2007). Third, IPSCs had to occur in at least three of the 8–10 sweeps and exhibit a temporal jitter of < ± 10 ms.

The presynaptic sources of reproducible ("verified") inhibitory inputs (IPSCs) were allocated to individual cortical layers, which were identified by differences in shading and cell density (Anderson et al., 2009; Dantzker and Callaway, 2000; Weiler et al., 2008; Yoshimura and Callaway, 2005; Zilles and Wree, 1995) (Fig. 2.5).

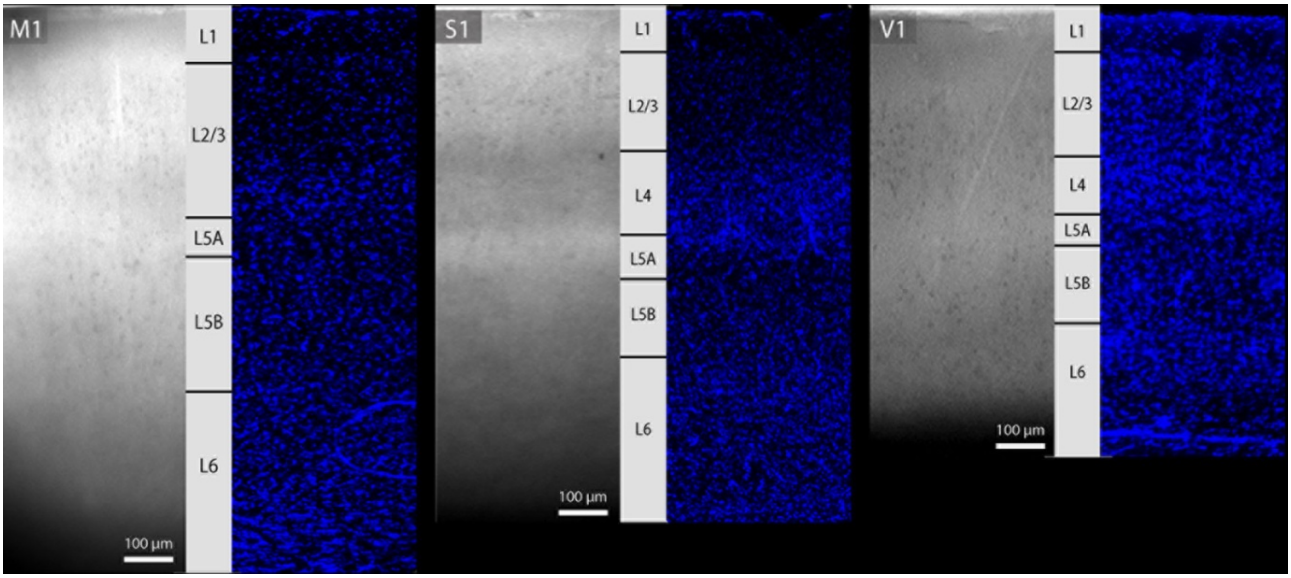

Figure 2.5. Laminar borders and cell morphologies. (a) Slices of primary motor cortex (M1), primary somatosensory cortex (S1), and primary visual cortex (V1) under brightfield (left panels) and epifluorescence illumination highlighting DAPI-stained nuclei (right panels). Left and right panels are from different specimens.

The synaptic strength of each individual inhibitory input source was measured by integrating the average recorded current between 5 ms before and 95 ms after the time point where the corresponding rising IPSC reached its half-maximum amplitude, thus representing the amount of charge flowing during the IPSC in units of Coulomb. To estimate the strength of each *laminar* source of inhibition for the individual target cells, the number of identified inhibitory input sources from each layer was multiplied by the average amount of charge flow of IPSCs from that layer. This product was standardized to 100 within each cell before statistical analysis was performed across individual target cells. Alternatively, the strength of each *laminar* input source was measured by adding the number of individual inhibitory input sources from each layer and dividing by the total of identified inhibitory input sources of the cell, thus arriving at an estimate of what percentage of inhibitory input sources are situated in each layer while discarding any information about their synaptic strength. Most of the statistical findings described were true for both

measures, the normalized charge-weighted number of input sources as well as the normalized number of input sources.

Discriminant functions were constructed using SPSS (SPSS Inc.) to examine whether the overall laminar source distributions of inhibitory inputs differed systematically among cortical areas M1, S1, and V1. These functions incorporated as predictor variables the laminar input strength from all cortical layers but layer 4 (which is not present in M1). Layer-by-layer differences among cortical areas were evaluated by classical one-way ANOVA and nonparametric Kruskal-Wallis test, followed by post-hoc analysis using Tukey's honestly significant difference criterion.

The horizontal spread of input sources was quantified by summing the number of confirmed inputs for each of the 14 columns of the stimulation grid, i.e. perpendicular to the pia. Since inhibitory input maps could be shifted with respect to the target cell location, and since columnar borders, in turn, were only visible in barrel cortex, the vertical sums of inhibitory inputs were aligned with respect to the column of stimulation spots that together with its left neighbours included 50 % of all inputs (i.e. to the median of each profile). The aligned horizontal input profiles of each target cell were interpolated to µm scale and averaged across all cells of the same layer and cortical area. In addition, the distance between the leftmost and the rightmost occurrence of at least one input was measured for each target cell and used for statistical analysis via one-way ANOVA followed by pair-wise Tukey-HSD across cortices within the same layer as well as across layers within the same cortical area.

To examine the columnar organization of inhibitory inputs in S1, I performed paired recordings from pyramidal cells located in the same or in adjacent somatosensory barrels. Three measures were used to quantify the relative tangential displacement of the two inhibitory input maps: the distance between the centres of mass (weighted centroids) of the normalized charge flow maps; the spatial cross-correlation of the two horizontal input profiles (obtained from a normalized two-dimensional cross-correlation of the two individual input maps, which was summed in the vertical direction and interpolated to µm-scale); and the temporal crosscorrelation of the "linearized" IPSC sequences recorded during 6–10 sweeps of the stimulation raster. To generate these linearized sequences, the IPSCs in each recording were reordered so that progression in time corresponds to a strictly sequential—as opposed to pseudo-random—sweep of the stimulation grid; a temporal shift of e.g. 400 ms (the interval between successive optical stimuli at the standard stimulation frequency of 2.5 Hz) then equals a spatial shift of one grid spacing. The three measures were averaged into a single index of map displacement. Intercell distances (estimated from brightfield images) and map displacements were converted from µm-scale to barrel units (bu), by dividing the values by the horizontal extent of the individual barrels the cells were located in. Correlation and curve fitting analyses were used to relate map displacements to intercell distance and barrel-related location of the pairs.

To identify subpopulations of pyramidal cells with distinct inhibitory connectivity patterns, data from M1, S1, and V1 were pooled across cortices for each layer (2/3 to 6) and cluster analyses were performed based on the amount of inhibition deriving from the home layer as well as from the one or two strongest translaminar

sources. Thus, neurons in layers 2/3 were characterized by the amount of inhibition deriving from layers layers 2/3, 5 and 5B, and neurons in layer 5B by inhibition from layers 5, 5B and 6. Observations were partitioned into hierarchical clusters, using the between-groups linkage method and a cosine metric to quantify distances between data points. The relative length of branches in the resulting dendrogram was used to estimate the optimal number of clusters. The robustness of the cluster solutions retrieved was estimated by non-parametric bootstrapping with 1000 repetitions: The three parameters of laminar input used for the clustering were averaged for layer 2/3 as well as layer 5B targets, respectively. A new population of maps featuring the same mean and standard deviation as the original population was generated and the cluster analysis repeated on this dataset. Means and standard deviations of relative distances in the dendrogram (scaling between 0 and 1) were calculated across the 1000 repetitions performed in each of the two cases.

To examine the uniformity of layer-specific connectivity, a cluster analysis orthogonal to the previous one was conducted using the same method: cells were pooled across postsynaptic home layers, but within one cortex at a time. Since prominent translaminar inhibition was not the focus of this analysis, the amounts of inhibitory input from *all* layers (1 through to 6) were used as clustering variables. Furthermore, the center of mass, already used for the columnar analysis, was used to capture the location of the map along the vertical axis in a single number and examine its relation to the vertical cell location (again, with reference to the stimulation grid). For this, and other investigations, input sources of the stimulation grid were assigned to a particular bin of a 25-bin vertical scale spanning the whole

cortical depth. Bins were assigned stereotypically to a certain layer, depending on the specific cortical area.

Using the same standardized scale, the laminar organization at the input side (i.e. at the specific location of presynaptic input sources) was investigated: Here, for each cell, a vertical profile plotting the amount of inhibitory input sources in each of the 14-to-22 rows of the stimulation grid along the vertical direction was calculated and numerically differentiated. The peaks and troughs of the first derivative correspond to the locations of the most drastic increases and decreases in input numbers, the location of which was assigned to a specific bin in the standardized vertical scale and summed up across the profiles of all cells of each target cell population, in order to check for possible coincidences with laminar borders.

Results

Chapter 3 – Optogenetic targeting and photoactivation of GABAergic interneurons using Channelrhodopsin-2

Conditional expression of channelrhodopsin-2 from a genomic locus

The channelrhodopin-2 (ChR2) responder line was designed to express a channelrhodopsin-2–EGFP fusion protein (ChR2-EGFP) after Cre-mediated excision of a transcriptional STOP cassette (Fig. 2.1a). ChR2-EGFP expression in the majority of GABAergic neurons was achieved by crossing this mouse line with a driver strain carrying a tamoxifen-inducible *Cre* recombinase (Cre-ER^{T2}) cassette, preceded by an internal ribosome entry site (IRES), in the 3'-untranslated region of the *Gad2* gene (Fig. 2.1b). Transcription of the targeted *Gad2*-locus produces a bicistronic message, which is translated into the 65 kDa isoform of glutamic acid decarboxylase (Gad65) and Cre-ER^{T2} protein. Because recombination of the *R26::ChR2-EGFP* locus requires tamoxifen-mediated induction of *Cre* activity, ChR2-EGFP expression can be timed to the appropriate developmental stage.

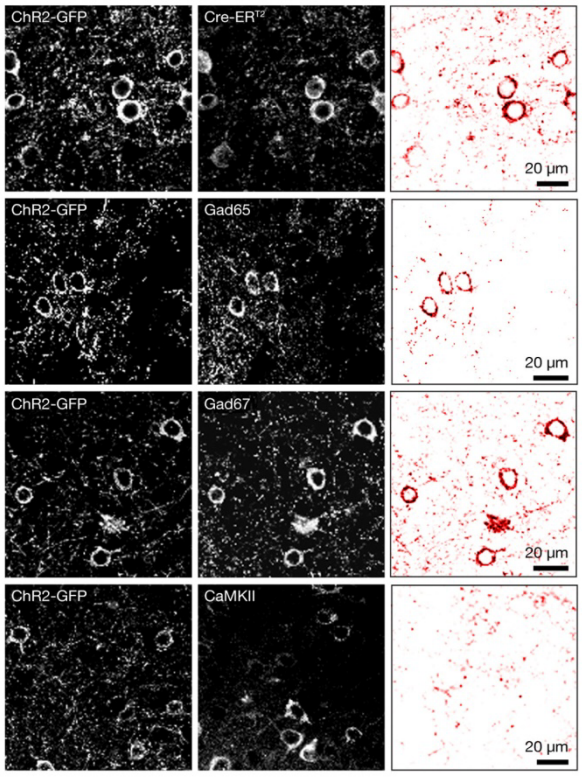

Figure 3.1. Targeted ChR2 expression in GABAergic interneurons.
Gad2::CreT2 R26::ChR2-EGFP mice after tamoxifen induction express ChR2-GFP in *Cre*-positive cells (top), which comprise both Gad65- and Gad67-positive interneurons (middle), but not CamKIIα–positive pyramidal cells (bottom). See Table 3.1 for statistics. The left and center columns show raw confocal images; the right column displays the corresponding colocalization maps, which were produced by multiplying the two fluorescence channels on a pixel-by-pixel basis and normalizing the resulting product image to 8 bits.

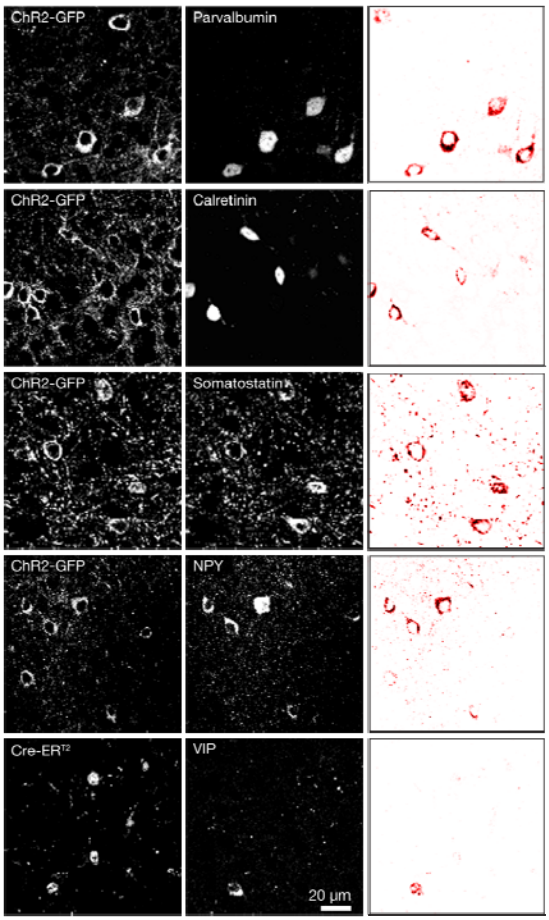

Figure 3.2. Cell-type specificity of ChR2-EGFP expression. Neocortical slices were obtained from *Gad2::Cre-ER^{T2} R26::ChR2-EGFP* mice 1–7 days after tamoxifen induction and immunolabeled. The left and center columns show raw confocal images after staining with fluorescently labeled secondary antibodies; the right column displays the corresponding colocalization maps, which were produced by multiplying the two fluorescence channels on a pixel-by-pixel basis and normalizing the resulting product image to 8 bits. ChR2-EGFP expression is detected in all major interneuron subclasses, which are defined by the expression of calcium binding proteins and neuropeptides.

Identifier	Marker	% Coexpression	*n*
Cre	GFP	98.7	234
GFP	Cre	99.5	219
Gad65	GFP	96.4	139
GFP	Gad65	100.0	121
Gad67	GFP	95.1	143
GFP	Gad67	89.7	146
Parvalbumin	GFP	100.0	215
Calretinin	GFP	88.3	196
Calbindin	GFP	89.4	104
Somatostatin	GFP	98.7	151
Neuropeptide Y	GFP	98.0	150
VIP	Cre	94.7	95

Table 3.1. Cell-type specificity of ChR2-GFP expression in the Gad65>ChR2-GFP line. Percentages of cells expressing the indicated identifier proteins that also express the indicated marker proteins (*n* = number of cells counted).

Following *Cre* induction between the fourth and sixth postnatal weeks, double immunolabeling of neocortical slices demonstrated comprehensive and selective ChR2-EGFP expression in all major subclasses of GABAergic interneurons (Blatow et al., 2005; Markram et al., 2004; Xu et al., 2010a) (Fig. 3.1c, Fig. 3.2, Table 3.1). These include neurons positive for Gad65 (96 %), Gad67 (95 %), parvalbumin (100 %), calretinin (88 %), somatostatin (99 %), neuropeptide Y (98 %), and VIP (95 %). ChR2-EGFP expression was undetectable in CaMKIIα-positive pyramidal cells (Fig. 3.1c).

Genetically targeted photostimulation of GABAergic interneurons

Focal illumination (473 nm, 20 ms pulses, 1-2 mW of optical power) of acute neocortical slices from mice carrying homozygous recombined *R26::ChR2-EGFP* loci in *Gad2*-positive cells elicited action potentials in interneurons but not in pyramidal cells (Fig. 3.3a, b). The comparatively low expression levels of ChR2 from the genomic cassette required longer stimulating light pulses than those used to activate virally transduced or transfected neurons (Petreanu et al., 2007; Petreanu et al., 2009); a 20-ms pulse duration was found to represent a favorable trade-off between reliable action potential intiation (100 % in cell-attached mode, *n* = 10 cells; 91.1 % in whole-cell mode, *n* = 45 cells) and the maintenance of an approximate 1:1 ratio of spikes per optical pulse (20-ms pulses evoked single action potentials in 80 % of recorded cells and occasional doublets in the remaining 20 %; *n* = 10 cells in cell-attached mode).

Interneurons at native resting potential followed optical pulse trains with maximal frequencies of 0.5–40 Hz in cell-attached (*n* = 10; Fig. 3.3a) or whole-cell recordings (*n* = 41; Fig. 3.3b). Action potentials occured with latencies of 15.8 ± 3.7 ms from the onset of illumination (means ± s.d., *n* = 4 cells in cell-attached

mode; Fig. 3.3d). Two cells, displaying a fast-spiking phenotype, could follow optical stimulation up to 40 Hz if light pulses lasted 6-8ms (1.5 mW), but responded with mostly 2 (75%) but up to 3 spikes/pulse (5% of pulses) when stimulated with pulses of 20 ms at 2.5 Hz (2 mW).

Individual 20-ms pulses caused non-desensitized peak depolarizing photocurrents of –188 ± 106 pA at holding potentials of –70 mV and –145 ± 82 pA at –60 mV (means ± s.d.; *n* = 4 cells each; Fig. 3.3c), displaying considerable cell-to-cell-variability. When stimulating at higher frequencies subsequent inward currents were smaller due to light-induced desensitization of ChR2 (Fig. 3.3c, left), but amplitudes recovered within 5-10 s (Fig. 3.3c, right) (Nagel et al., 2005b).

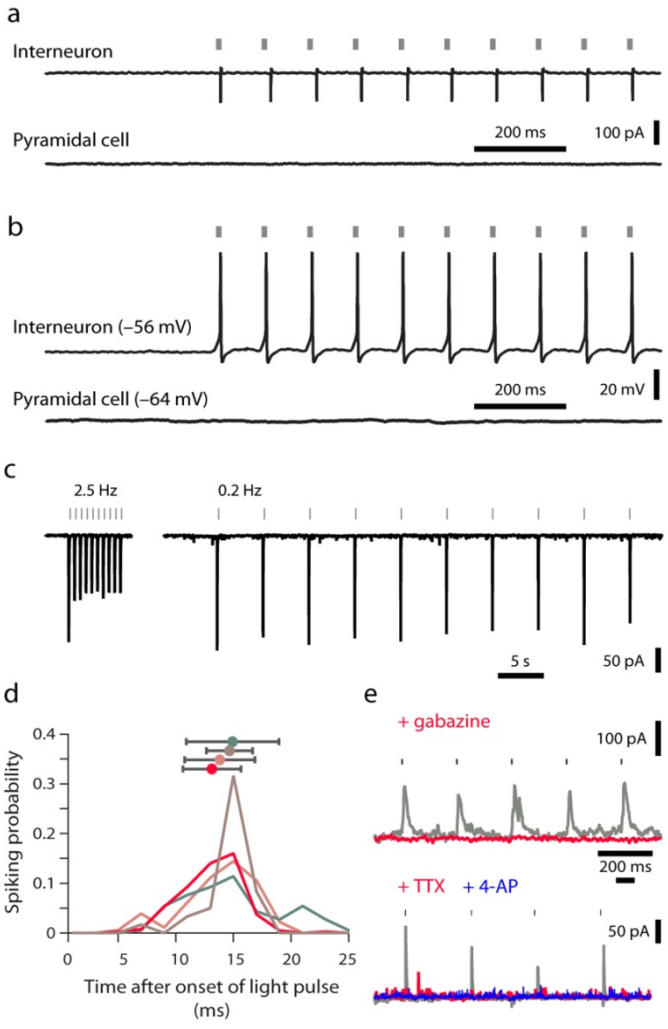

Figure 3.3. Genetically targeted photostimulation of GABAergic interneurons. (a, b) Responses to photostimulation in cell-attached (a) and whole-cell current-clamp recordings (b); native resting potentials are indicated in parentheses. Interneurons follow trains of 20-ms optical pulses at 10 Hz with action potentials; pyramidal neurons are unresponsive to light. (c) ChR2-mediated photocurrents recorded in voltage-clamp. Photocurrents desensitize during repeated optical stimulation of a cell at frequencies > 1 Hz (left) but remain stable at stimulation frequencies ≤ 0.2 Hz (right). (d) Temporal precision of light-evoked action potentials. Spiking probabilities as a function of time after stimulus onset were estimated by analyzing 29–198 light-evoked action potentials per cell (*n* = 4 interneurons in cell-attached recordings; colored traces). Spike times are defined as the times at which the upstroke of an action potential reaches half-maximal amplitude. Average spike latencies (± s.d.) are indicated in matching colors. (e) Wide-field optical stimulation at 5 or 1 Hz (grey bars) with a slightly diverging ~100 µm beam carrying 20 mW of optical power evokes IPSCs in pyramidal cells voltage-clamped at 0 mV (grey traces). IPSCs are abolished after bath application of 10 µM gabazine (red trace, top) or 0.5 µM TTX (red, bottom) and 100 µM 4-AP (blue, bottom).

Interneurons in cortical areas M1, S1, and V1 were equally responsive to light, and no significant interregional differences in the ability to control fast- or non-fast-spiking cells were detected (Fig. 3.4; P = 0.704 and 0.235 for fast- and non-fast-spiking cells, respectively; one-way ANOVA).

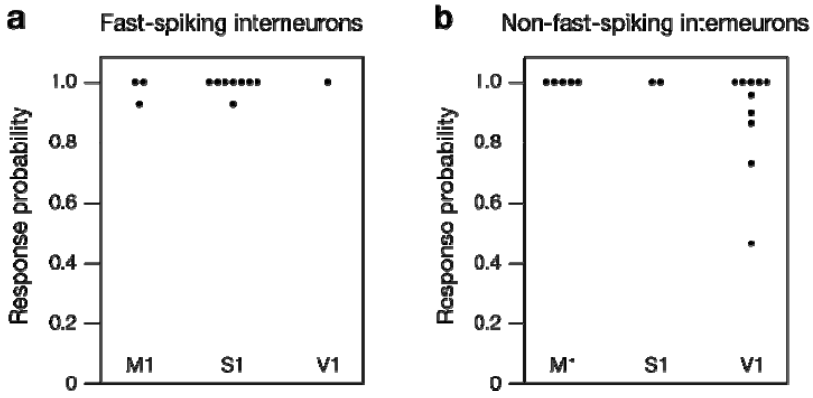

Figure 3.4. Responsiveness of interneurons to optical stimulation. Spiking probabilities were estimated by stimulating neocortical interneurons in layer 5B of M1, S1, and V1 with a sequence of 30 light pulses (473 nm, 20 ms pulses, 2.0 mW of optical power, 0.2 Hz). Each data point represents one cell. Three criteria were used to distinguish fast- from non-fast-spiking neurons: fast-spiking neurons *i*) attained firing rates > 100 Hz during a 500-ms depolarizing current step of 300 pA; *ii*) exhibited a ratio > 0.7 of the average interspike interval (ISI) at the beginning and end of the depolarizing current step (averages of 3 ISIs each); and *iii*) displayed a spike width of ≤ 1ms at half-maximal amplitude. Cells that met all three criteria were classified as fast-spiking (**a**); cells that failed all three criteria as non-fast-spiking (**b**). Six neurons were excluded because they met some but not all criteria; four neurons were unresponsive to light. No significant differences in the responsiveness of fast- and non-fast-spiking interneurons in different cortical areas were detected by parametric one-way ANOVA (P = 0.704 and 0.235 for fast- and non-fast-spiking cells, respectively).

Driving inhibitory neurons periodically by wide-field illumination caused stimulus-locked IPSCs in pyramidal cells (Fig. 3.3e). Bath application of the $GABA_A$ receptor antagonist SR95531 (gabazine, 10 μM) blocked these optically evoked IPSCs (Fig. 3.3e, top), as did application of the sodium channel blocker tetrodotoxin (TTX, 0.5 μM, Fig. 3.3e, bottom). In contrast, if ChR2 is expressed using viral delivery or *in utero* electroporation (Petreanu et al., 2007; Petreanu et al., 2009), expression levels are often sufficiently high in synaptic terminals to allow for direct activation of synaptic release, not requiring TTX-sensitive somatic (or axonal) action potentials. In one report, however, the blocking of the entire Na_V-population (including synaptic/axonal ones) by TTX does abolish synaptic release, unless repolarizing

potassium channels are also blocked by 100 µM 4-aminopyridine (4-AP) to leave the calcium-excitation through synaptic ChR2 and calcium-channels unrestrained (Petreanu et al., 2009). In the transgenic system developed here, however, 4-AP application does not recover synaptic inputs (Fig. 3.3e, blue trace), suggesting that only perisomatically triggered action potentials can evoke transmission. Consistent with this interpretation, axonic stimulation of GABAergic Purkinje cells in cerebellar slices failed to produce back-propagating action potentials or enhanced somatic depolarizations (*n* = 7 cells; Fig. 3.5).

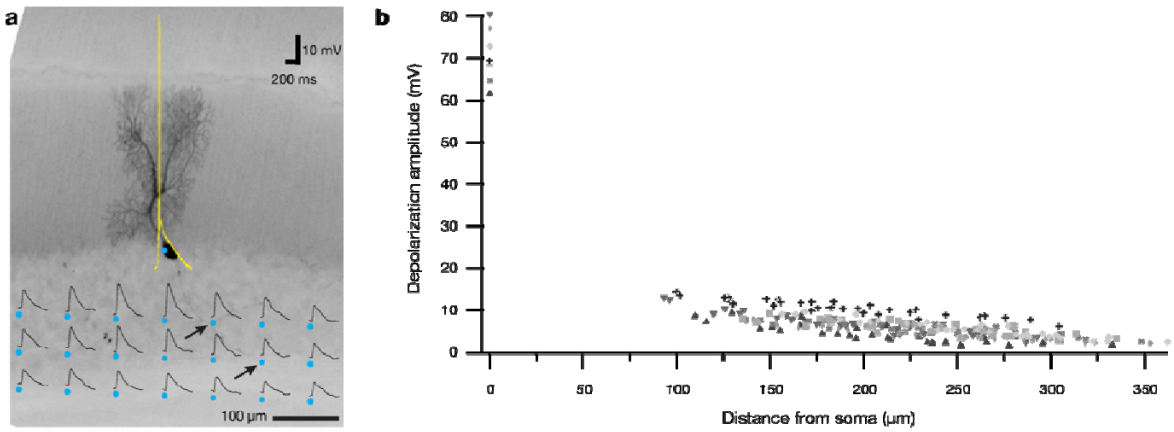

Figure 3.5. Perisomatic but not axonal photostimulation evokes action potentials. To examine the possibility of eliciting action potentials by axonal photostimulation, GABAergic Purkinje cells, which possess anatomically well-separated dendritic and axonal compartments, were analyzed in cerebellar slices obtained from *Gad2::Cre-ER*^{T2} *R26::ChR2-EGFP* mice 1–7 days after tamoxifen induction. (**a**) In the representative example shown, optical raster stimulation of cerebellar white matter (blue dots; 20-ms pulses of 0.5 mW optical power) fails to elicit backpropagating action potentials in a Purkinje cell under current clamp (native resting potential –68 mV), even when the stimulating laser beam directly overlaps the axon of the recorded cell (arrows). Somatic stimulation reliably elicits spiking (yellow trace). (**b**) The amplitudes of light-evoked depolarizations as a function of the distance of the focused stimulation beam from the soma (*n* = 7 Purkinje cells, represented with different symbols). All data points follow a linear trend without stimulation hotspots, demonstrating the absence of direct axonal stimulation.

Light-evoked depolarizations generated by illuminating the dendritic arbours of neocortical interneurons (*n* = 5 cells) were similarly insignificant. Contour plots revealed that depolarization amplitudes and spiking probabilities decayed in a nearly radial-symmetric manner as a function of somatic distance; stimulation

hotspots corresponding to the locations of underlying dendrites were absent (Fig. 3.6a).

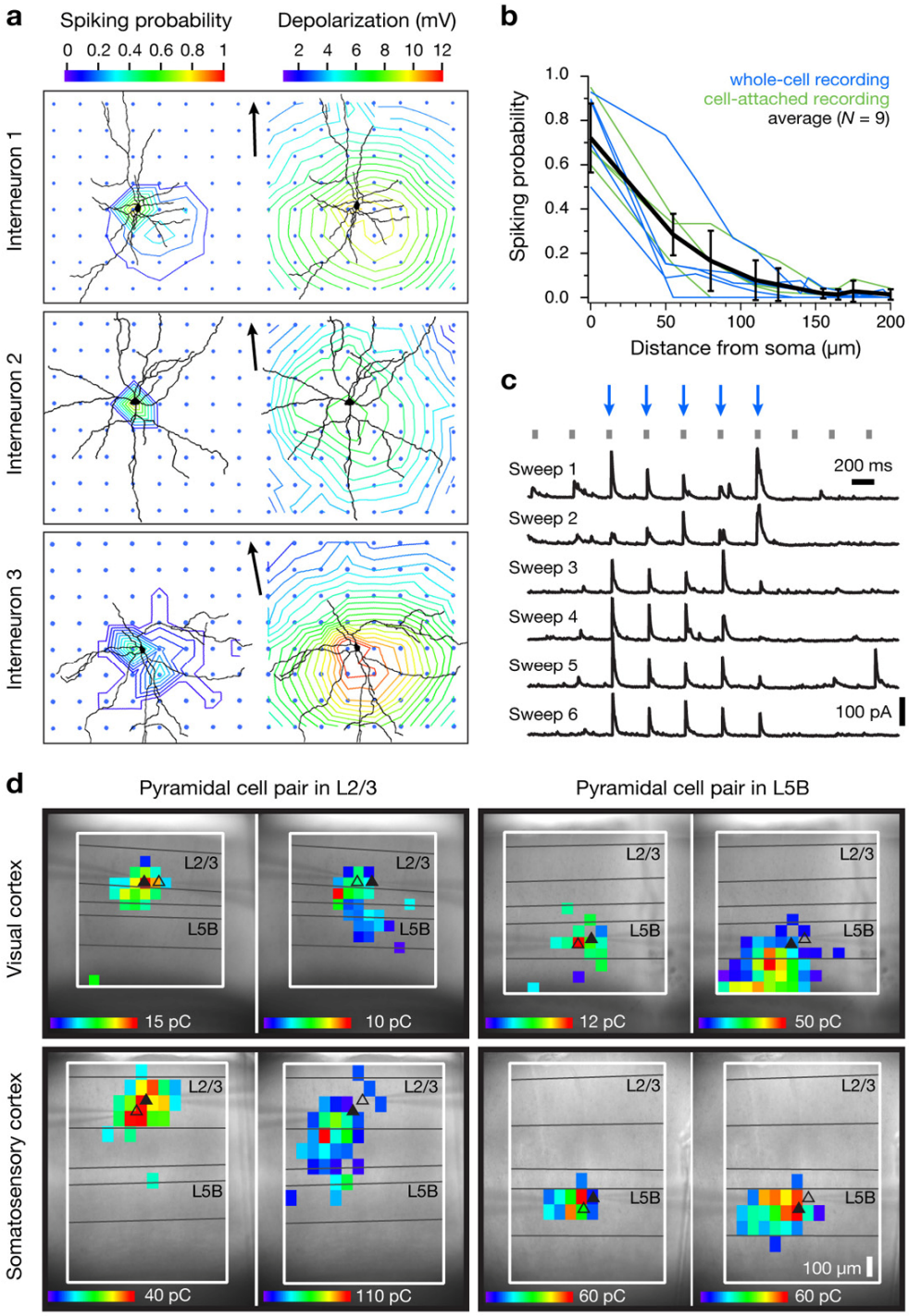

Figure 3.6. Optogenetic mapping of inhibitory connectivity. (a, b) Optical resolution of genetically targeted photostimulation. Contour plots depict spiking probabilities (left) and depolarization amplitudes (right) as functions of stimulus location for three interneurons. The neurons were filled with neurobiotin during whole-cell current-clamp recordings and reconstructed. Perisomatic illumination reliably elicits action potentials (left), but positioning the focus of the stimulating beam near dendritic branches does not cause higher spiking probabilities or larger depolarizations than illumination of dendrite-free neuropil equidistant from the soma (right). Arrowheaded bars represent 100 µm and point to the pia. (b) Spiking probabilities of 9 interneurons as functions of the distance of the stimulation spot from the soma. Cells were recorded in the cell-

attached (*n* = 4 cells, green traces) or whole-cell configuration (*n* = 5 cells, blue traces). (c) Sequential illumination of 10 different locations at 2.5 Hz (20 ms, 2 mW optical power, grey tick marks). Stimulus locations marked by blue arrows give rise to IPSCs in the recorded pyramidal cell and thus harbour synaptically connected interneurons; these inputs are reproducible in 6 consecutive trials (top to bottom). (d) Maps of inhibitory inputs to four pyramidal neurons in V1 (top row) or S1 (bottom row). The cells are located in layers 2/3 (left column) or 5B (right column) at comparable depths (± 7 µm) from the surface of the slice. The neurons were recorded simultaneously in pairs to test whether cells within the same local network could exhibit different connectivity patterns. Cell positions are marked by triangles; a filled triangle denotes the postsynaptic target for each map. Colour on a heat scale symbolizes the average amount of charge flowing during 100 ms following the onset of the IPSC, at a holding voltage of 0 mV.

The approach thus offers two hitherto unrealized advantages for mapping connectivity: First, it can distinguish synaptic inputs originating locally (that is, from neurons whose somata lie within the illumination cone) from axonal or dendritic projections into the illuminated volume, which is a crucial prerequisite for mapping local circuits (as opposed to long-range connections). And second, the optical stimulus selectively targets inhibitory neurons. Focal photolysis of caged glutamate, in contrast, elicits responses in both inhibitory (Brill and Huguenard, 2009; Xu and Callaway, 2009) and excitatory (Dantzker and Callaway, 2000; Xu and Callaway, 2009; Yoshimura and Callaway, 2005; Yoshimura et al., 2005) neurons and is therefore prone to mapping polysynaptic connections, because interneurons at some distance from the stimulation site may be activated indirectly.

However, it is formally possible also for a purely inhibitory input to propagate polysynaptically if the targets of inhibition generate rebound spikes. I tested this scenario and found no evidence in its favour (Fig. 3.7). Pyramidal cells (*n* = 19 cells) and fast-spiking (*n* = 13 cells) as well as non-fast-spiking interneurons (*n* = 24 cells) were hyperpolarized to increasingly negative holding potentials. Rebound spikes appeared in 4/19 pyramidal cells and 3/13 fast-spiking interneurons, but only when these neurons were released from holding potentials below –150 mV (Fig. 3.7 a, b).

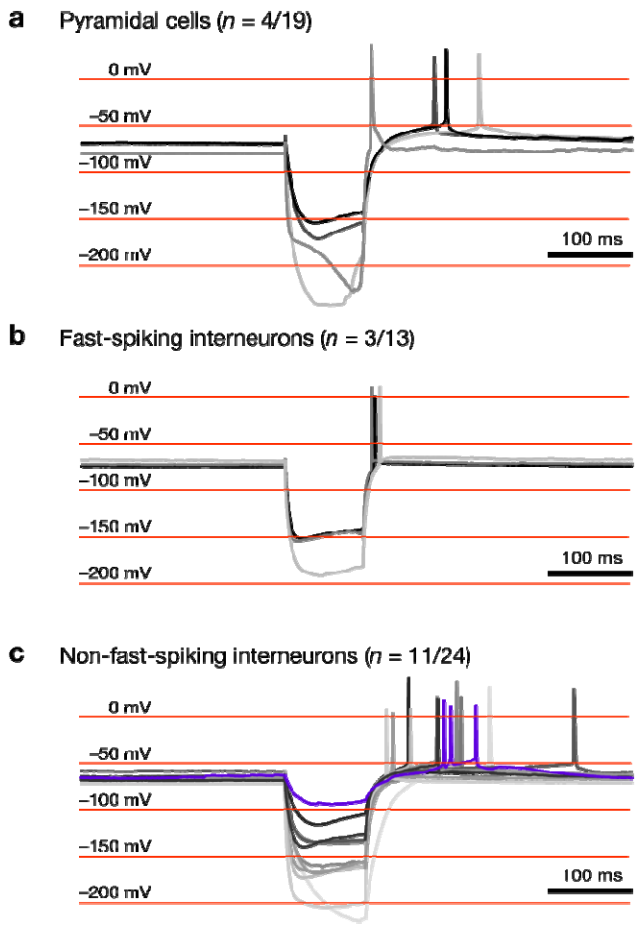

Figure 3.7. Rebound spiking requires strong hyperpolarization. To define the requirements for eliciting rebound spikes, hyperpolarizing 100-ms current steps of increasing amplitudes (maxima between –200 and -–1100 pA) were injected into (**a**) neocortical pyramidal cells (*n* = 19 cells), (**b**) fast-spiking interneurons (*n* = 13 cells), and (**c**) regular-spiking interneurons (*n* = 24 cells). The traces shown indicate the most positive voltages at which cells emitted rebound spikes from hyperpolarization offset; traces of cells that did not generate spikes (15/19 pyramidal cells, 10/13 fast-spiking interneurons, and 13/24 non-fast-spiking interneurons) are omitted for clarity. The average current amplitudes (± s.d.) required to elicit at least one rebound spike were 765 ± 526 pA for pyramidal cells (**a**), 800 ± 175 pA for fast-spiking interneurons (**b**), and 431 ± 211 pA for non-fast-spiking interneurons (**c**). Three criteria were used to distinguish fast- from non-fast-spiking neurons: fast-spiking neurons *i*) attained firing rates > 100 Hz during a 500-ms depolarizing current step of 300 ms; *ii*) exhibited a ratio > 0.7 of the average interspike interval (ISI) at the beginning and end of the depolarizing current step (averages of 3 ISIs each); and *iii*) displayed a spike width of ≤ 1ms at half-maximal amplitude. Cells that met all three criteria were classified as fast-spiking (**b**); cells that failed all three criteria as non-fast-spiking (**c**). The "rebound spike thresholds" of pyramidal cells (**a**) and fast-spiking interneurons (**b**) lie around –150 mV, those of non-fast-spiking interneurons (**c**) around -120 mV. One non-fast-spiking interneuron (blue trace in **c**) generated rebound spikes from a hyperpolarization offset of –84 mV, but with spike latency > 100 ms. Any IPSCs triggered by such spikes would have fallen outside the applied detection window of 5–70 ms after optical stimulus onset (see Methods).

Non-fast-spiking interneurons emitted rebound spikes more frequently (11/24 cells) and, in one extreme cases, upon release from a hyperpolarized potential above –100 mV (–84 mV; Fig. 3.7.c). However, the latencies of rebound spikes from the offset of shallow hyperpolarizations were so large (> 100 ms) that any IPSCs caused by them would have been excluded in the mapping experiments because the temporal contingency between light pulse and postsynaptic event was broken. (Due to the temporal precision (Petreanu et al., 2007; Petreanu et al., 2009; Zhang et al., 2006) of ChR2, the appearance of light-evoked IPSCs is highly predictable,

making it possible to average trials and employ much shorter detection windows than with glutamate uncaging (Dantzker and Callaway, 2000; Shepherd et al., 2005; Shepherd and Svoboda, 2005); see Methods.) To generate short-latency (≤ 50 ms) rebound spikes, non-fast-spiking interneurons needed to be hyperpolarized at least below –117 mV (Fig. 3.7.c).

However, for GABAergic IPSCs to achieve this degree of hyperpolarization would require chloride reversal potentials of –120 mV or less and, therefore, unphysiologically low (Thomson et al., 1996a; Thomson et al., 1996b) intracellular chloride concentrations of ≤ 1 mM. This allows me to exclude the activation of polysynaptic chains with confidence: the IPSC images recorded depict the origins of monosynaptic inhibitory connections.

Optogenetic mapping of inhibitory input distributions

To analyze the laminar and columnar organization of local inhibitory connections, one or two excitatory neurons were voltage-clamped at 0 mV (to maximize chloride currents through $GABA_A$ receptors and minimize spontaneous EPSC amplitudes), while a focused laser beam (20 ms pulses at 2 mW, spot size 3–5 μm) rastered a rectangular grid of locations spaced at 55-to-65-μm intervals. The grid spacing reflects the lateral resolution of photostimulation, limited by light scattering in the slice, which was estimated by moving the focus of the stimulating beam away from the soma of a recorded interneuron and measuring the decrease in spiking probability as a function of distance (Fig. 3.6a, b).

Stimulus-locked IPSCs could be evoked by focal illumination of certain locations but not others, revealing the somatic positions of inhibitory interneurons providing input to the recorded excitatory cell(s) (Fig. 3.6c, d). The distributions of input sources were reproducible for the same postsynaptic neuron during repeated sweeps of the

stimulation grid (Fig. 3.6c) but differed for two simultaneously recorded cells located nearby in the same slice (Fig. 3.6d).

However: The practice of holding the excitatory targets of inhibition at 0 mV could lead to depolarization-induced suppression of inhibition (Llano et al., 1991; Pitler and Alger, 1992) (DSI), which might mask some inhibitory inputs. DSI is mediated by a retrograde signalling system (Kano et al., 2009; Wilson et al., 2001) that communicates the depolarization of a postsynaptic neuron via the release of endocannabinoids to inhibitory presynaptic terminals, which downregulate GABA release upon activation of cannabinoid receptor-1 (CB-1). To test for a possible confound of my experiments due to DSI, I compared the inhibitory input structure of 6 pyramidal cells, first when these cells were voltage-clamped at –70 mV and subsequently when the same cells were held at 0 mV (Fig. 3.8). When adjusting the detection threshold for IPSCs appropriately, no differences in the number and distribution of inhibitory input sources were found (P = 0.821 for rejecting the null hypothesis of equal input numbers).

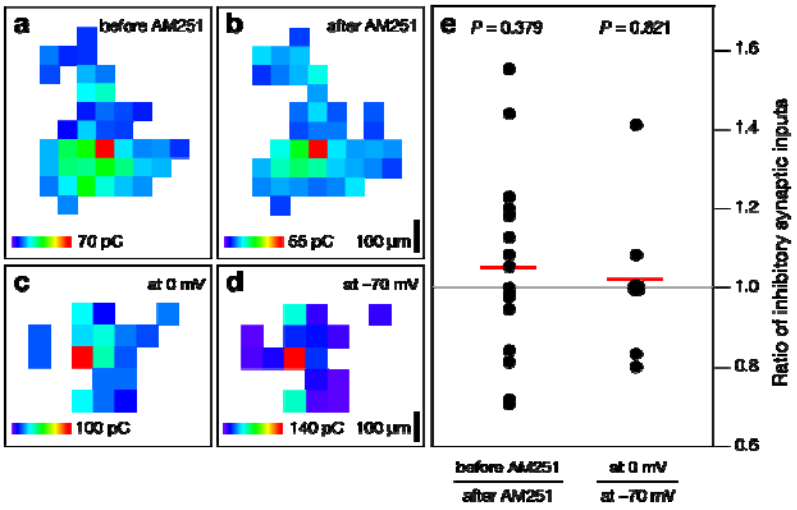

Figure 3.8. Lack of a confound due to depolarization-induced suppression of inhibition (DSI). (**a-d**) Maps of inhibitory inputs to pyramidal neurons in layer 5B. Color on a heat scale symbolizes the charge flowing during the IPSC. To test whether DSI (potentially caused by holding the recorded target neuron at 0 mV) might lead to detection failures of inhibitory inputs, two types of control experiment were performed. (**a**, **b**) In the first type of control experiment, inhibitory input maps were recorded at a holding potential of 0 mV, first in the absence (**a**) and then in the presence of the CB-1 antagonist AM251 (**b**, 2 µM, n = 17 cells). (**c**, **d**) In the second type of control experiment, input maps were first recorded at a holding potential of –70 mV (**d**) and subsequently at a holding potential of 0 mV (**c**, n = 6 cells). Note that in each case the number and distribution of inhibitory input sources are well-preserved. (**e**) Statistical comparisons of the ratio of

inputs detected in each experimental condition in both types of control experiment show no significant deviations from unity (one-sample *t*-test). Each data point represents one cell; population means are indicated by horizontal red lines.

In a second set of control experiments, I compared inhibitory input maps recorded in the presence and absence of the CB-1 antagonist AM251 at 2 μM (*n* = 17 cells, Fig. 3.8). Again, no differences in input number or map structure were detected (*P* = 0.379).

Genetically targeted photostimulation using P2X2-channels

As explained in the introduction, ChR2 suffers from a small single-channel conductance (50 fs, (Nagel et al., 2005a; Nagel et al., 2003), which impedes its usage for driving neurons above spike threshold if ChR2 is not expressed at high enough density, or the spike threshold (rheobase) of a neuron relative to its resting potential and input resistance is too high, as is the case in our conditional transgenic expression system for pyramidal neurons (Fig. 3.9b). Ligand-gated ion channels like P2X2, in contrast, can help to circumvent this problem, given that their single-channel conductances range up to more than two orders of magnitude higher (e.g. 20 pS for P2X2 (Jarvis and Khakh, 2009)): At similar age and using the same CamKIIα-*Cre* driver line in combination with a homozygous actuator gene, the activation of pyramidal neurons achieved is dramatically stronger using the P2X2-actuator (Fig. 9a) - even at short illumination times of 1 ms. When ChR2 is driven to saturation in the same cell type, it produces a 10 mV depolarization in the most favourable circumstances (Fig. 9b). (The fact that saturation is reached, is determined from the fact that the depolarization amplitude achieved with a power of 6 mW or 50 ms stimulation time was not larger than that achieved with 2 mW power and 20 ms.) Spiking in pyramidal cells could be evoked in CamKIIα>P2X2 mice in

almost all cases (15/16), albeit at different power levels and pulse lengths, probably depending on the functional P2X2 expression levels, which in turn were found to be dependent on age, among other factors. Likewise, activation of interneurons in Gad65>P2X2 could be reliably achieved (n = 4/5 putative interneurons).

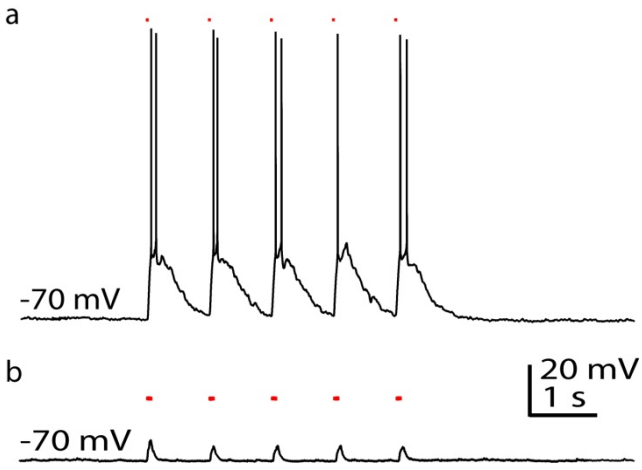

Figure 3.9. Photoactivation of layer 2/3 pyramidal neurons using conditional transgenic expression of P2X2 (a) vs ChR2 (b) at 1 Hz stimulation frequency. (a) A UV-laser (365 nm peak wavelength) and an output power at the objective of up to 27 mW was directed at the soma of pyramidal cells expressing P2X2 for ca. 1 ms, causing depolarization and spiking due to uncaging of ATP (250µM DMNPE-ATP in standard ACSF). (b) A blue laser (473 nm peak wave length) with an output of up to 6 mW at the objective was illuminating the recorded ChR2-expressing pyramidal neuron for up to 50 ms causing up to 10 mW peak depolarization but never spiking.

However, despite featuring a strong activation of all cell types as well as a better spatial resolution compared to ChR2 (not shown), certain problems were observed, which require resolution before this responder mouse line can be used for mapping experiments:

(1) The response of individual neurons to photoactivation displays less temporal reliability and high cell-to-cell variability compared to those in the ChR2 line. To achieve ideally 1 spike/pulse, optimal power levels varied from 0.9 to 27 mW, and optimal stimulation times varied between 1 and 50 ms. In addition, the delay to the occurence of the spike is larger and more variable compared to ChR2 (likely due to the additional stochasticity and kinetics of uncaging, diffusion, and ligand binding), ranging from 30 to 60 ms. Compared to glutamate uncaging, however, the within-cell variation of the spiking response is not as large – usually 1-2 spike(s)/pulse compared to 0-5 spikes/pulse for glutamate uncaging (Dantzker and Callaway, 2000). Further evaluation is needed under strictly constant conditions regarding

mouse age, sex and time after tamoxifen-injections (while concentration in caged ATP seems to be less relevant) to determine the sources of this variation.

(2) The activation is not subtype-specific in the adult mouse: Interneurons were at least equally photo-activatable as pyramidal neurons in the adult (> P62) CamKIIα>P2X2 mouse – as determined by direct measurement of interneurons (n = 2) as well as by $GABA_A$-dependent, spatially specific light-evoked IPSCs in pyramidal neurons (n = 2) (both under 20 µM CNQX) . In reverse, pyramidal cells (n = 2/3) could be activated in older (P106) Gad65>P2X2 mice. Since the stimulation intensity does not differ between specific and unspecific activation in these cases within the same mouse (in contrast to what would be expected,if the stop-cassette were leaky, as found in viral expression systems), this is probably due to endogenous expression of P2X2 receptors in adult wildtype neocortical cells, as has been reported for layer 2/3 and 5 in adult rat neocortex (Pankratov et al., 2002, 2003). In agreement with this, I found not all pyramidal cells in Gad65>P2X2 mice to be ATP-sensitive (as reported before) and I found pyramidal cells in adult wildtype mice to respond with bursts of action potentials, if free ATP (5-100 mM in reservoir) is applied to them locally (n = 3). Furthermore, I have developed primers for sequencing the knock-in part of the ROSA26-locus in experimental P2X2-mice, and found – from the sequencing results - that the stop-cassette was present as expected, excluding that the responder mouse line had become unspecific by losing the stop-cassette in the germline. Finally, and providing a preliminary solution to this problem, I found that pyramidal cells (n = 8) in younger Gad65>P2X2 mice (P17, P38), were indeed unresponsive to photostimulation via ATP-uncaging, while interneurons (n = 2) in these mice emitted stimulus-locked spikes (at even lower stimulation intensity than used for testing the pyramidal cells). (Unfortunately, the

late onset of both of the CamKIIα-drivers tested (see Methods), does not allow for the reverse experiment.) To what extent endogenous P2X-expression in interneurons starts already before 3-5 weeks of age – i.e. if specificity can be reached between different *subtypes* of interneurons if using subtype-specific drivers – remains to be tested.

(3) Although sometimes light-evoked, $GABA_A$- (n = 2) and TTX- (n = 1) sensitive IPSCs were recorded upon illumination of nearby neural tissue, in other cases (n = 2) reproducible IPSCs or EPSCs were not evoked upon repeated illumination. Reliable and spatially highly selective IPSCs (in Gad65>P2X2 mice) could be evoked however, upon local pressure delivery of ATP (n = 2), which might suggest, that synapses could be blocked by adenosine residues (acting on A1 receptors) in the caged ATP stock, as has been shown for hippocampal excitatory synapses (Canals et al., 2008). Interestingly, if mapping was performed under application of a selective A1 antagonist, strong, spatially highly selective and reproducible IPSCs could be evoked by light-stimulation – albeit they arrived with a significant delay of 0.5 – 5 s (n = 4, in 2 mice), which was reflected in a similar delay of light-evoked spiking in an interneuron recorded in the same mouse.

These three examples demarcate the current front of implementing this mouse line and illustrate that its deployment might be more complicated than initially thought, mainly due to endogenous interactions with the (un)caged ligand or its by-products as well as due to variation in response reliability across days/mice: despite powerful activation of cells, mapping of synaptic connections is not automatically straightforward.

Chapter 4 – A columnar centre-surround organization of inhibitory circuits

Optical raster stimulation allowed me to identify sources of inhibitory inputs to excitatory cells in M1, S1, and V1 and assemble individual input maps for 6–22 excitatory neurons per layer and cortical area in the first mapping study (Table 4.1), yielding a data set of 3,823 input sources or putative connections. Unless stated otherwise, the results shown in chapter 4, 5 and 6 are based on this dataset.

	L2/3	L4	L5A	L5B	L6	Sum
M1	9	-	6	9	6	*30*
S1	22	8	8	8	8	*54*
V1	15	12	6	12	8	*53*
Sum	*46*	*20 20*	*29*		*22*	

Table 4.1. Summary statistics of optical mapping experiments. Number of excitatory neurons in the indicated cortical areas (rows) and layers (columns) whose inhibitory input distributions were mapped.

Sources of inhibition were confined within horizontal domains spanning at most 550 μm, or the width of 3 somatosensory barrels (180 ± 22 μm per barrel; n = 17, Fig. 4.1c), suggesting that inhibitory microcircuits interconnect adjacent columns (Table 4.2). The horizontal reach of inhibitory connections, however, varied from layer to layer, giving rise to hourglass-shaped inhibitory input profiles with notable constrictions in layer 4 of sensory cortices (284 μm in S1 and 310 μm in V1) (Fig. 4.1c, Table 4.2). This observation is consistent with the idea that lateral inhibition constrains the flow of information to columnar units in supra- and infragranular layers (Petersen and Sakmann, 2001), whereas columns in layer 4 are largely defined by the parcellation of thalamocortical projections. Inhibitory connections thus follow a pericolumnar “centre–surround” arrangement, which provides an

anatomical substrate by which activity in one column can suppress that of its immediate neighbors (Mountcastle, 1978; Petersen and Sakmann, 2001).

	M1	S1	V1	*P*-value (ANOVA)
L2/3	302 ± 134 µm	374 ± 104 µm	433 ± 113 µm	0.054
L4	-	284 ± 65 µm	310 ± 121 µm	0.594
L5A	405 ± 61 µm	478 ± 78 µm	303 ± 85 µm	0.002
L5B	553 ± 153 µm	431 ± 99 µm	466 ± 169 µm	0.228
L6	556 ± 97 µm	526 ± 128 µm	399 ± 167 µm	0.109
***P*-value (ANOVA)**	0.002	0.000	0.032	
Significant interlaminar differences ($P < 0.05$)	L2/3 - L5B L2/3 - L6 (L5A - L6)	(L2/3 - L4) (L2/3 - L5A) L2/3 - L6 L4 - L5A L4 - L5B L4 - L6	(L4 - L5B) (L5A - L5B)	

Table 4.2. Horizontal (columnar) organization of inhibitory connections. Horizontal distances (means ± s.d.) between the leftmost and the rightmost inhibitory input to an excitatory neuron in the indicated cortical area (columns) and layer (rows). Comparisons of group means by one-way ANOVA revealed only a single significant difference between M1, S1, and V1 (crimson shaded background): the horizontal domain providing input to pyramidal cells in L5A was smaller in V1 than in S1. Within each cortical area, the horizontal spread of inhibitory connections varied significantly from layer to layer (blue shaded background). The pairwise interlaminar differences responsible for the overall intra-areal variation are listed below each column (Tukey-HSD post-hoc test and independent-sample *t*-test; entries in parentheses reached significance levels of $P < 0.05$ only in independent-sample *t*-tests).

Because the columnar structure is visible in S1, it was possible to probe the columnar organization of inhibitory circuits directly by recording simultaneously from pairs of layer 2/3 pyramidal neurons in either the same (n = 5 pairs) or in adjacent (n = 6 pairs) barrel-related columns. While the input maps of layer 2/3 neurons in the same column overlapped to a large degree (Fig. 4.1a), those of cells in adjacent columns were shifted by about one barrel diameter (Fig. 4.1b).

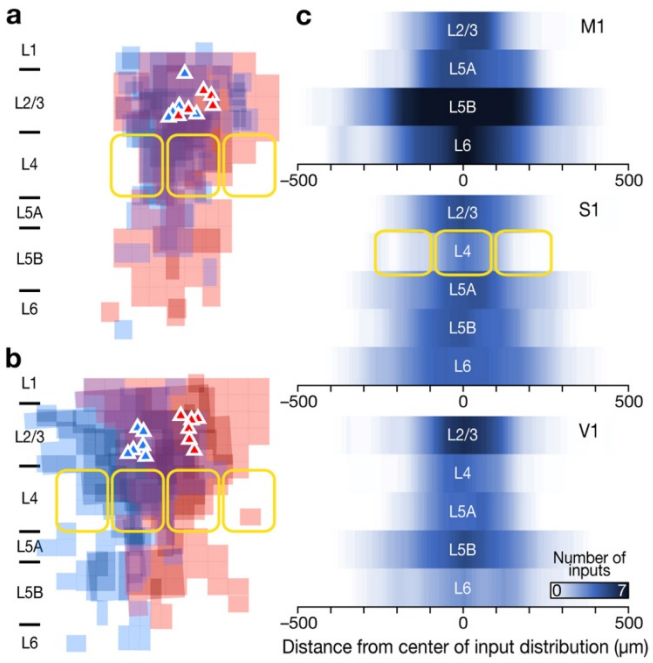

Figure 4.1. Horizontal (columnar) organization of inhibitory connections.
(a, b) Maps of inhibitory inputs to pairs of simultaneously recorded pyramidal neurons in layer 2/3 of S1 are overlaid. The maps are in binary input count format (that is, they depict the locations of inhibitory inputs but not their strength) and have been scaled to the size of a standard somatosensory barrel (yellow outlines). Cell positions are marked by triangles. Data from the left cell in each pair are coded in blue, data from the right cell in red. (a) Pairs of pyramidal neurons in the same barrel-related column. (b) Pairs of pyramidal neurons in adjacent barrel-related columns. (c) Horizontal profiles of input distributions. The profiles depict the interpolated number of inhibitory inputs as a function of horizontal distance from the centre of the input distribution for each layer, ignoring the laminar (vertical) location of these inputs. Data from pyramidal neurons in all cortical layers of M1 (n = 28 neurons, top), S1 (n = 52 neurons, centre), and V1 (n = 53 neurons, bottom) were analyzed. Horizontal distances were scaled to the size of a standard somatosensory barrel (yellow outlines) and centre aligned; the number of inhibitory inputs to an excitatory neuron in a given layer at a given distance from the map centre was then averaged. The intensity of blue colour symbolizes the density of input sources. See Methods and Table 4.2 for statistical detail.

Spatial cross-correlation analysis (see Methods) confirmed that the input maps of two neurons in the same barrel-related column were displaced by slightly less than the average distance between the two cells (0.36 ±0.28 bu vs. 0.39 ± 0.11 bu, means ± s.d., bu = barrel unit, horizontal size of the individual barrel), whereas the maps of cells in different columns were shifted by approximately a single column width (0.90 ± 0.14 bu; P = 0.002). If map displacements occurred in discrete, barrel-sized steps, the correlation between map shift and intercell distance should be small if calculated for the two groups individually (partial correlation, r_p) , but large if calculated across all pairs (r), since in the latter case it is mediated by the barrel-related location of the cells. This was indeed the case (r = 0.826, P = 0.002; r_p = 0.280, P = 0.434), supporting the notion of a discrete columnar structure of inhibitory circuits. In fact, map displacements were fitted better by a step function of

intercell-distance than by a linear function (Fig. 4.2), which might hint towards the notion of discrete, barrel-related shifts of inhibitory circuits of pyramidal cells in S1.

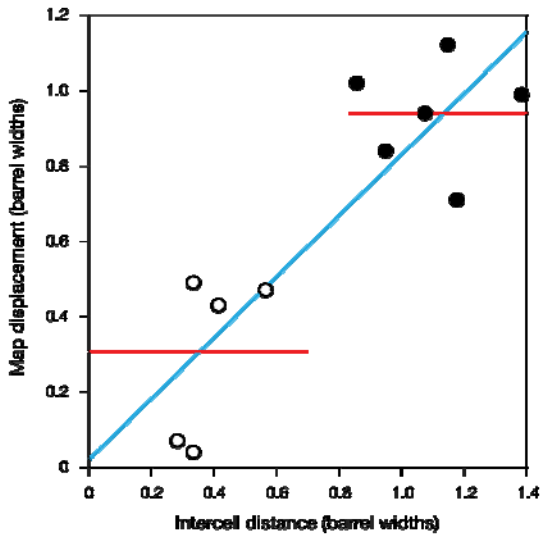

Figure 4.2. Columnar organization of inhibitory inputs. To examine the columnar organization of inhibitory inputs in barrel cortex (S1), paired recordings from layer 2/3 pyramidal neurons located in either the same (open symbols, *n* = 5 pairs) or in adjacent (filled symbols, *n* = 6 pairs) barrel-related columns were performed. The scatterplot shows the tangential displacement between the inhibitory input maps of each cell pair, which was determined by cross-correlation analysis (see Methods), as a function of intercell distance. Both measures were normalized by dividing measurements on a µm-scale by the horizontal distances between barrel septa. A step function (red) captures the relationship between intercell distance and map displacement better than a linear fit (blue): the summed squares of residuals (or sums of squares due to error, SSE) are 0.3065 and 0.3601, respectively.

It is furthermore notable, that layer 5B of M1 displays the widest horizontal extent and the strongest (majorly intralaminar: see Fig. 5.1) inhibition (Fig. 4.1c), which could reflect a significant amount of competition via lateral inhibition at the main output stage of motor cortex.

Chapter 5 – The laminar organization of inhibitory circuits

Area-specific differences in the laminar organization of inhibitory connections

In contrast to a horizontal structure that appeared largely identical across cortical areas (Fig. 4.1c, Table 4.2), the vertical organization of inhibitory connections showed clear area-specific variations. With the exception of neurons in layer 6, excitatory cells in different cortical areas displayed distinct laminar source distributions of inhibitory inputs (Fig. 5.1, Tables 5.1 - 5.4).

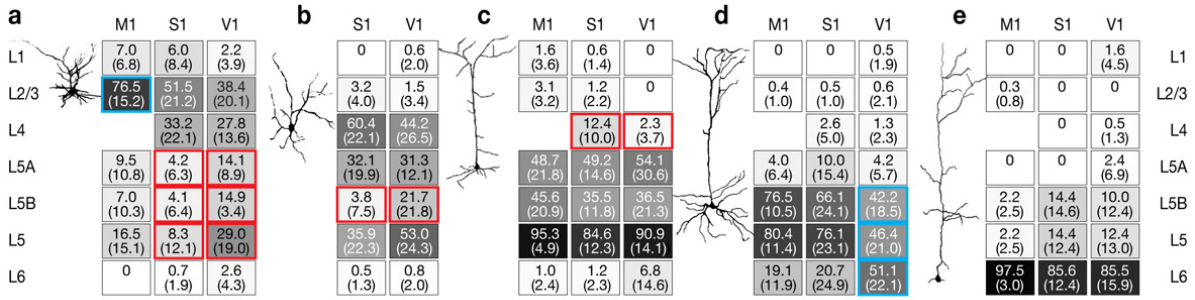

Figure 5.1. Vertical (laminar) organization of inhibitory connections. (a–e) Average strength of inhibitory input from the indicated source layers (rows) to excitatory neurons located in layers 2/3 (a), 4 (b), 5A (c), 5B (d) and 6 (e). An example of a neurobiotin-filled excitatory neuron, recovered after recording, is shown to the left of each panel. The figure summarizes data from 30 neurons in M1, 54 neurons in S1, and 53 neurons in V1. The strength of a connection is expressed as the average percentage of inhibitory charge flow arising from identified inputs in a layer. L5 represents the sum of L5A and L5B. Values are represented numerically (s.d. in parentheses) and by the intensity of grey shading. Coloured boxes indicate significant differences ($P < 0.05$), either between two cortical areas (red) or between one area and the other two (blue), as determined by one-way ANOVA and subsequent Tukey-HSD post-hoc tests. See Tables 4.1 and 5.1 for statistical detail.

While the dominant source of inhibition was usually intralaminar — that is, originating from interneurons residing in the same layer as the soma of the excitatory neuron (Binzegger et al., 2004; Brill and Huguenard, 2009) — striking exceptions to this rule were found, particularly in V1. Here, pyramidal cells in layer 5B were strongly inhibited by interneurons in layer 6 (Fig. 5.1d, Tables 5.1 - 5.3) and cells in layers 2/3 and 4 by interneurons in layer 5, especially sublayer 5B (Fig.

5.1a, b; Tables 5.1 - 5.3). Quantitatively, the total inhibitory charge flow (Fig. 5.1) as well as the normalized numbers of inhibitory inputs (Table 5.2) from the dominant translaminar source (layer 6 for neurons in layer 5B, and layer 5B for neurons in layers 2/3 and 4) were at least twice as large in V1 as in M1 and S1 (see also Fig. 5.2c).

a Parametric ANOVA

Source layer \ Target layer	2/3	4	5A	5B	6
1	0.167	0.429	0.425	0.509	0.438
2/3	0.000	0.324	0.073	0.948	0.275
4	0.403	0.171	0.039	0.426	0.334
5A	0.003	0.903	0.895	0.340	0.438
5B	0.011	0.039	0.553	0.001	0.136
5	0.001	0.131	0.307	0.001	0.123
6	0.157	0.700	0.376	0.002	0.158

b Non-parametric (Kruskal-Wallis) ANOVA

Source layer \ Target layer	2/3	4	5A	5B	6
1	0.107	0.414	0.323	0.492	0.417
2/3	0.001	0.239	0.017	0.655	0.264
4	0.370	0.105	0.035	0.786	0.317
5A	0.002	0.643	0.945	0.760	0.417
5B	0.055	0.009	0.711	0.002	0.297
5	0.001	0.123	0.393	0.003	0.289
6	0.015	0.804	0.798	0.003	0.295

c Post-hoc analysis of pairwise differences

Comparison of S1 and V1

Source layer \ Target layer	2/3	4	5A	5B	6
1	0.230	0.429	0.881	0.600	0.488
2/3	0.134	0.324	0.582	0.986	1.000
4	0.403	0.171	0.027	0.426	0.334
5A	0.002	0.903	0.913	0.385	0.488
5B	0.008	0.039	0.990	0.022	0.705
5	0.001	0.131	0.586	0.006	0.937
6	0.321	0.700	0.427	0.008	1.000

Comparison of M1 and S1

Source layer \ Target layer	2/3	5A	5B	6
1	0.935	0.632	1.000	1.000
2/3	0.007	0.268	0.988	0.325
4				
5A	0.251	0.999	0.403	1.000
5B	0.752	0.557	0.483	0.116
5	0.371	0.295	0.890	0.127
6	0.743	0.998	0.986	0.204

Comparison of M1 and V1

Source layer \ Target layer	2/3	5A	5B	6
1	0.236	0.406	0.579	0.538
2/3	0.000	0.063	0.943	0.325
4				
5A	0.384	0.908	0.998	0.538
5B	0.177	0.673	0.001	0.383
5	0.137	0.867	0.001	0.218
6	0.165	0.444	0.004	0.196

Table 5.1 Vertical (laminar) organization of inhibitory connections, as inferred from total laminar charge flow measurements (see Fig. 5.1). P-values of comparisons by parametric one-way ANOVA (a) or Kruskal-Wallis test (b) of differences between M1, S1, and V1 in the amount of inhibitory charge flow from the indicated source layers (rows) to excitatory neurons in the indicated target layers. (c) P-values of pairwise differences by Tukey-HSD post-hoc test. Significant differences ($P < 0.05$) between cortical areas are highlighted by crimson shaded backgrounds. Data for L4 target cells, which is assumed to not be resolvable in M1, were analyzed by independent-sample t-test (a, c) or Mann-Whitney U-Test (b).

Evidence of putative feedforward inhibition between layers, or of descending inhibition from superficial to deeper laminae, was scant, with two important

exceptions. In the sensory cortices S1 and V1, an inhibitory layer 4-to-2/3 connection (Thomson et al., 2002) ran parallel to the flow of excitatory signals (Binzegger et al., 2004) from spiny stellate neurons of layer 4 (Fig. 5.1a). And in S1, a 5-fold larger amount of layer 4-derived inhibition than in V1 entered layer 5A, via marginally faster synaptic connections (Fig. 5.1c; 20-80 % rise time = 5.8 ± 1.1 ms in S1 vs. 7.6 ± 1.5 ms in V1, P = 0.06).

		Source layer					
		1	**2/3**	**4**	**5A**	**5B**	**6**
Target layer							
2/3	**M1**	9.2 ± 8.9	75.2 ± 15.4	-	8.2 ± 10.1	7.4 ± 8.9	0
	S1	12.8 ± 8.9	47.5 ± 18.3	30.1 ± 18.9	7.0 ± 10.1	5.9 ± 8.6	0.7 ± 1.9
	V1	3.1 ± 4.4	36.5 ± 15.2	27 ± 11.1	13.1 ± 6.8	17.3 ± 15.3	3.0 ± 4.6
4	**S1**	0	4.1 ± 4.8	58.5 ± 17	31.2 ± 13.2	4.7 ± 7.9	1.6 ± 4.4
	V1	1.2 ± 4.1	2.0 ± 4.2	40.4 ± 20	33.4 ± 10.0	21.9 ± 15.6	1.1 ± 2.7
5A	**M1**	3.6 ± 4.7	4.0 ± 2.7	-	43.5 ± 17.8	48.4 ± 15.9	1.9 ± 4.5
	S1	1.3 ± 2.6	2.9 ± 4.8	14 ± 9.9	41.9 ± 17.2	37.8 ± 12.6	2.1 ± 3.9
	V1	0	0	3.3 ± 5.1	50.8 ± 29	37.8 ± 18.5	8.1 ± 17.7
5B	**M1**	0	0.8 ± 2.1	-	5.9 ± 6.5	68.9 ± 10.5	23.8 ± 12.0
	S1	0	1.1 ± 2.3	3 ± 5.5	13.2 ± 18.4	60.0 ± 24.9	22.7 ± 23.3
	V1	0.7 ± 2.5	0.7 ± 2.5	2 ± 2.8	3.9 ± 4.6	42.2 ± 12	50.5 ± 15.6
6	**M1**	0	0.7 ± 1.7	-	0	2.6 ± 3.1	96.7 ± 4.3
	S1	0	0	0	0	16.9 ± 14.6	83.1 ± 14.6
	V1	3.8 ± 7.5	0	0.9 ± 2.5	0.9 ± 2.5	10.7 ± 11.8	83.7 ± 17.1

Table 5.2. Normalized numbers of inhibitory connections. Percentages of inhibitory inputs (means ± s.d.) from the indicated source layers to excitatory neurons in the indicated target layers. The table summarizes data from 30 neurons in M1, 54 neurons in S1, and 53 neurons in V1 (Table 4.1). Percentages were obtained by counting the number of inputs from a particular layer and dividing by the cell's total number of identified inputs. Colours indicate significant differences ($P < 0.05$), either between two cortical areas (crimson shaded background) or between one area and the other two (blue shaded background), as determined by parametric and non-parametric one-way ANOVA and subsequent Tukey-HSD post-hoc tests. Data for L4 target cells, which is assumed to be not resolvable in M1, were analyzed by independent-sample t-test and Mann-Whitney U-Test.

Target layer		Source layer: 1	2/3	4	5A	5B	6
2/3	M1	2.2 ± 1.9	16.4 ± 8.4	-	2.7 ± 3.6	1.2 ± 1.2	0
	S1	1.3 ± 1.6	9.5 ± 3.9	7.3 ± 5.3	2.4 ± 3.7	1.8 ± 3.0	0.2 ± 0.5
	V1	0.8 ± 1.3	9.5 ± 4.9	6.7 ± 2.6	3.3 ± 1.7	5.0 ± 4.9	0.7 ± 1.0
4	S1	0	0.8 ± 0.9	8 ± 3.7	4.6 ± 3.1	0.9 ± 1.5	0.1 ± 0.4
	V1	0.2 ± 0.6	0.3 ± 0.7	6.3 ± 3.5	4.9 ± 1.5	3.9 ± 4.1	0.3 ± 0.9
5A	M1	1 ± 1.3	1.2 ± 1.0	-	12.2 ± 5.5	12.8 ± 3.6	0.7 ± 1.6
	S1	0.6 ± 1.4	1.0 ± 1.6	4.1 ± 3.3	11.6 ± 5.3	11.0 ± 5.5	0.9 ± 1.8
	V1	0	0	0.7 ± 1.0	7.2 ± 1.8	7.7 ± 5.3	2.7 ± 6.1
5B	M1	0	0.4 ± 1.0	-	3.7 ± 4.0	40.2 ± 15.0	16.3 ± 13.4
	S1	0	0.3 ± 0.5	0.8 ± 1.5	3.5 ± 5.8	15.3 ± 7.0	7.8 ± 10.7
	V1	0.3 ± 0.9	0.3 ± 0.9	0.6 ± 0.8	1.2 ± 1.5	11.6 ± 6.1	15.8 ± 10.8
6	M1	0	0.3 ± 0.8	-	0	1.2 ± 1.5	42.3 ± 12.1
	S1	0	0	0	0	6.9 ± 7.7	23.6 ± 11.9
	V1	0.6 ± 1.0	0	0.1 ± 0.4	0.1 ± 0.4	2.4 ± 4.0	13.9 ± 9.1

Table 5.3. Absolute numbers of inhibitory connections. Numbers of inhibitory inputs (means ± s.d.) from the indicated source layers to excitatory neurons in the indicated target layers. The table summarizes data from 30 neurons in M1, 54 neurons in S1, and 53 neurons in V1 (Table 4.1). Colours indicate significant differences ($P < 0.05$), either between two cortical areas (crimson shaded background) or between one area and the other two (blue shaded background), as determined by parametric and non-parametric one-way ANOVA and subsequent Tukey-HSD post-hoc tests. Data for L4 target cells were analyzed by independent-sample *t*-test and Mann-Whitney U-Test.

Target layer		Source layer: 1	2/3	4	5A	5B	6
2/3	M1	14.3 + 13.9	14.7 + 8.5	-	16.1 + 14.2	12.3 + 7.3	0
	S1	18.6 + 12.9	29.1 + 21.1	27.1 + 21.8	12.0 + 7.4	12.8 + 8.2	12.8 + 8.2
	V1	5.6 + 7.0	10.6 + 6.5	13.4 + 17.8	14.1 + 19.7	10.2 + 9.0	10.0 + 4.4
4	S1	-	27.1 + 19.8	41.8 + 27.0	37.2 + 18.2	11.1 + 6.4	21
	V1	-	13.4 + 5.9	17.3 + 17.6	18.9 + 29.3	13.7 + 15.4	5.1 + 0.4
5A	M1	10.4 + 15.2	8.4 + 7.5	-	13.8 + 4.8	14.1 + 10.8	4
	S1	15.2 + 7.1	16.0 + 7.7	31.4 + 12.6	53.7 + 27.2	44.4 + 30.1	18.7 + 5.4
	V1	0	0	6.5 + 4.3	17.4 + 13.9	11.7 + 6.8	5.3 + 0.3
5B	M1	0	7.3 + 2.5	-	9.4 + 4.8	21.2 + 7.7	15.2 + 6.7
	S1	0	6.6 + 1.4	13.4 + 1.6	15.8 + 9.3	26.9 + 15.4	15.3 + 15.0
	V1	7.1	8.1	5.3 + 2.9	8.1 + 4.6	10.1 + 4.7	10.5 + 6.4
6	M1	2	0	-	0	6.3 + 3.1	7.4 + 2.8
	S1	0	0	0	0	13.7 + 11.3	14.3 + 10.5
	V1	0.8 + 1.4	0	0	0	6.3 + 3.3	7.4 + 3.8

Table 5.4. Charge flow per IPSC. Average charge flow per IPSC in pC (means ± s.d.) from the indicated source layers to excitatory neurons in the indicated target layers. The table summarizes data from 30 neurons in M1, 54 neurons in S1, and 53 neurons in V1 (Table 4.1). Colors indicate

significant differences (P < 0.05), either between two cortical areas (crimson shaded background) or between one area and the other two (blue shaded background), as determined by parametric and non-parametric one-way ANOVA and subsequent Tukey-HSD post-hoc tests. Data for L4 target cells, were analyzed by independent-sample t-test and Mann-Whitney U-Test.

Area-specific differences in vertical inhibitory connectivity were so characteristic that a discriminant analysis could assign a substantial fraction of excitatory neurons of all layers (> 70 %) correctly to their cortical areas of origin, based on the laminar distribution of their inhibitory inputs alone (Fig. 5.2a, Table 5.5). This was true irrespective of whether inhibition was quantified by measuring total inhibitory charge flow or the number of synaptic input sources from a layer (Table 5.5). The classification was most accurate in M1 (96 %) and V1 (75 %) but less accurate in S1 (63 %; averages across layers 2/3 to 5B).

a Charge flow (%)		**Target layer**				
		L2/3	**L4**	**L5A**	**L5B**	**L6**
***P*-value**	Y1	0.000	0.292	0.017	0.021	0.251
	Y2	0.003	-	0.2	0.438	0.462
Correct prediction	M1	100.00%	-	100.00%	89.00%	83.30%
	S1	68.00%	87.50%	62.50%	25.00%	62.50%
	V1	73.00%	75.00%	83.30%	75.00%	12.50%
	Mean	76.10%	80.00%	80.00%	65.50%	50.00%
Incorrect prediction	M1	0%	-	0%	11% V1	16.7% V1
	S1	18% M1 14% V1	12.5% V1	37.5% V1	37.5% M1 37.5% V1	37.5% M1
	V1	7% M1 20% S1	25% S1	16.7% S1	8.3% M1 16.7% S1	50% M1 37.5% S1

b Number of inputs (%)		Target layer				
		L2/3	L4	L5A	L5B	L6
P-value	Y1	0.000	0.134	0.047	0.042	0.139
	Y2	0.019	-	0.141	0.415	0.141
Correct prediction	M1	100%	-	100%	100%	100%
	S1	60%	87.50%	62.50%	25%	62%
	V1	80%	83.30%	100%	83.30%	37.50%
	Mean	73.80%	85%	85%	72.40%	63.60%
Incorrect prediction	M1	0%	-	0%	0%	0%
	S1	20% M1 20% V1	12.5% V1	12.5% M1 25% V1	37.5% M1 37.5% V1	37.5% M1
	V1	20% S1	16.7% S1	0%	16.7% M1	50% M1 12.5% S1

Table 5.5. Classification of excitatory neurons by their inhibitory input patterns (see Fig. 5.2a). Discriminant functions were constructed to examine whether the overall laminar source distributions of inhibitory inputs to excitatory neurons in different target layers differed among cortical areas M1, S1, and V1 (Fig. 6a). Discriminant functions take the form of linear combinations: $Y = b_0 + b_1 * X_1 ... + b_n * X_n$, rendering a certain discriminant variable Y from predictor variables X1 to Xn. in dependence of discriminant coefficients b_i . Here, these functions incorporated as predictor variables X the total laminar inhibitory charge flows (a, see Fig. 5.1) or input counts (b; see Table 5.2) from all cortical layers but L4 (which cannot be resolved in M1), and hence, produce a discriminant variable Yj for every individual cell j.
Arithmetic means (centroids, Y_C) and standard deviations (S) over Y_j are caluculated within each of the three groups (cortices, Y_{Cw}, S_w) as well as between Y_{Cb}, S_b). Discriminant coefficients b_i are optimized with respect to a maximal ratio of between-group-to-within-group variance (S_b/S_w), resulting in the following discriminant functions:

For L2/3: Y1 = 0.09 L1 + 1.32 L2/3 + 0.87 L5A + 0.34 L5B – 0.27 L6
Y2 = –0.13 L1 – 0.03 L2/3 + 0.58 L5A + 0.49 L5B + 0.43 L6

For L5A: Y1 = 0.65 L1 + 1.28 L2/3 + 3.07 L5A + 2.81 L5B + 0.84 L6
Y2 = –0.11 L1 – 0.28 L2/3 + 1.88 L5A + 1.34 L5B + 1.22 L6

For L5B: Y1 = 1.43 L1 – 1.03 L2/3 + 1.25 L5A + 0.7 L5B + 1.88 L6
Y2 = –0.10 L1 + 1.74 L2/3 + 3.26 L5A + 6.67 L5B + 7.6 L6

P-values for significance tests comparing the means (centroids) of the discriminant values Y1 and Y2 for excitatory neurons in M1, S1, and V1, were calculated to estimate, if cortices could be successfully separated by the retrieved functions. P-values are tabled for the indicated layers (crimson backgrounds indicate $P < 0.05$). Percentages of correct and incorrect predictions are given below.

Multiple factors could be responsible for the observed regional differences in vertical inhibitory connectivity, singly or in combination. The principal source layers of translaminar inhibition (layers 4, 5B, and 6) could be populated with interneurons,

or particular subtypes of interneurons, at different densities. Alternatively, the translaminar connection probabilities of interneurons and excitatory cells could vary in an area-specific manner. Finally, regional variations could be due to differences in the functional properties of these connections, such as their release probabilities, synaptic conductances, and the distribution of synapses along the somatodendritic axis of pyramidal cells.

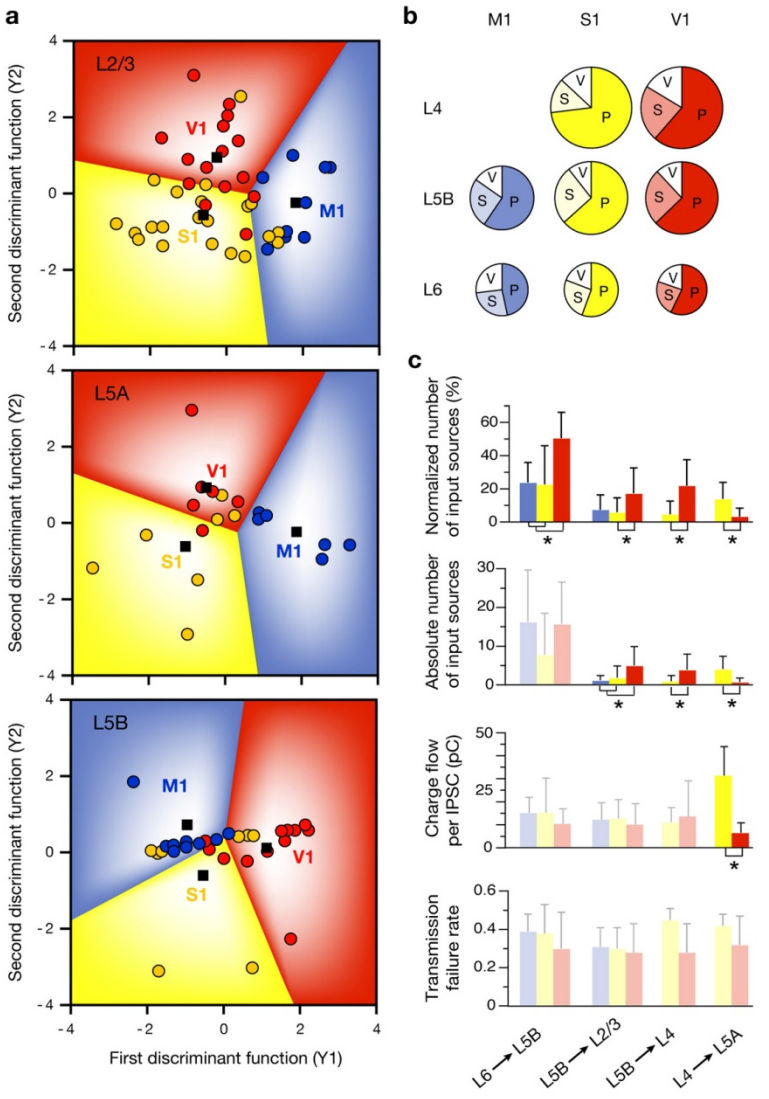

Figure 5.2. Area-specific differences in the laminar organization of inhibitory connections.
(a) Discriminant functions were constructed to examine whether the overall laminar source distributions of inhibitory inputs to excitatory neurons in different target layers differed systematically between cortical areas M1, S1, and V1. These functions, which are given in Table 5.5, incorporated as predictor variables the amount of inhibitory charge flow from all cortical layers but layer 4 (which cannot be resolved in M1). The discriminant plots summarize data from neurons in layers 2/3 (top), 5A (middle), and 5B (bottom), for which a successful classification could be found (Table 5.5). Each recorded cell is represented as a point in the coordinate system spanned by the two orthogonal discriminant functions Y1 and Y2. Borders between colored areas indicate decision boundaries for assigning neurons to M1 (blue), S1 (yellow), and V1 (red). Data points whose fill color matches the background color are classified correctly. Black squares indicate the centroid positions for all cells in each cortical area. (b) Abundance of the three major interneuron subtypes defined by the expression of parvalbumin (P), somatostatin (S), and VIP (V) in layers 4 (top), 5B (center), and 6 (bottom) of M1 (left), S1 (center), and V1 (right). Pie chart diameters represent the interneuron density (cells/volume) in the respective cortical layer; areas of wedges symbolize the percentages of PV-, SOM-, and VIP-positive interneurons. See Table 5.6 for numerical and statistical detail. (c) Properties of translaminar inhibitory connections. Colored bars symbolize data for M1 (blue), S1 (yellow), and V1 (red). The bar graph shows normalized and absolute numbers of inputs, charge flow, and failure rates (means + s.d.) for the four translaminar motifs found to exhibit area-specific differences (see Fig. 5.1). These motifs include inhibitory-to-excitatory connections from L6

to L5B, from L5B to L2/3, from L5B to L4, and from L4 to L5A. Asterisks denote statistically significant differences between cortical areas ($P < 0.05$), as determind by parametric and non-parametric ANOVA and subsequent Tukey-HSD post-hoc tests. Data for layer 4 target cells, which cannot be resolved in M1, were analyzed by independent-sample *t*-test and Mann-Whitney U-Test. See Tables 5.2, 5.3, 5.4 and 5.7 for statistical detail.

	Layer	Cells per 0.05 mm^3			*P*-value				*n*		
		M1	S1	V1	ANOVA	M1-S1	M1-V1	S1-V1	M1	S1	V1
PV	4	-	611 ± 106	525 ± 115	-	-	-	0.021	-	18	22
	5B	309 ± 84	430 ± 71	419 ± 97	0.000	0.000	0.001	0.925	21	16	18
	6	132 ± 32	207 ± 111	184 ± 59	0.025	0.024	0.163	0.732	23	17	16
SOM	4	-	116 ± 43	188 ± 47	-	-	-	0.000	-	13	14
	5B	130 ± 44	175 ± 64	168 ± 68	0.043	0.050	0.110	0.921	20	21	22
	6	91 ± 46	93 ± 54	74 ± 27	0.308	0.988	0.430	0.339	20	21	21
VIP	4	-	109 ± 63	139 ± 67	-	-	-	0.198	-	18	15
	5B	79 ± 29	71 ± 34	79 ± 50	0.841	0.870	0.999	0.873	12	13	9
	6	93 ± 26	71 ± 37	63 ± 29	0.125	0.234	0.150	0.859	11	13	7

Table 5.6. Abundance of interneuron subtype. Neocortical slices were obtained from Gad2::Cre-ERT2 R26::ChR2-EGFP mice 1–7 days after tamoxifen induction and immunolabeled with antibodies against GFP plus parvalbumin (PV), somatostatin (SOM), and vasoactive intestinal peptide (VIP), respectively. Numbers of PV-, SOM-, and VIP-positive interneurons were determined in image stacks of n 50 µm-thick slices; cell counts are reported as cells per 0.05 mm^3 (means ± s.d.). Crimson shaded backgrounds indicate significant differences ($P < 0.05$) between two cortical areas, as determined by parametric one-way ANOVA and subsequent Tukey-HSD post-hoc tests. Data for L4 target cells were analyzed by independent-sample t-test.

To distinguish between these possibilities, I began by comparing the abundances of the three principal interneuron subtypes defined cytochemically in mice (Xu et al., 2010b) for layers 4, 5B and 6 of V1, S1, and M1. No consistent covariation between the density of inhibitory neurons or the subtypes expressing parvalbumin, somatostatin, or VIP and the strength of inhibition originating in a layer was detected (Fig. 5.2b, Table 5.6).

Furthermore, the absolute and normalized numbers of identified translaminar connections (Fig. 5.2c, Tables 5.2 and 5.3) as well as three of their functional properties (Fig. 5.2c, Tables 5.4, 5.7, and 5.8) were compared: the frequency of transmission failures (differences in which serve as an index of intercortical differences in release probability, given the uniform light sensitivity of interneurons

across cortical areas, as documented in Fig. 3.4); the inhibitory charge flow per IPSC (which is proportional to synaptic conductance); and the 20-80% rise time of IPSCs (which can reflect the electrotonic distance of a synapse from the soma (Jack and Redman, 1971), and may therefore serve as a crude proxy of anatomical distance).

Connection		Transmission failure rate			*P*-value			
Source	Target	M1	S1	V1	ANOVA	M1-S1	M1-V1	S1-V1
2/3	2/3	0.31 ± 0.10	0.30 ± 0.11	0.28 ± 0.15	0.918			
5A	2/3	0.33 ± 0.11	0.34 ± 0.11	0.33 ± 0.18	0.593			
5B	2/3	0.43 ± 0.13	0.33 ± 0.16	0.37 ± 0.20	0.946			
4	4	-	0.45 ± 0.06	0.28 ± 0.15	0.004	-	-	0.004
5B	4	-	0.43 ± 0.18	0.32 ± 0.09	0.150			
5A	5A	0.27 ±0.18	0.23 ± 0.12	0.25 ± 0.13	0.821			
4	5A	-	0.42 ± 0.06	0.32 ± 0.15	0.162			
5B	5B	0.22 ± 0.07	0.27 ± 0.10	0.34 ± 0.13	0.046	0.557	0.038	0.349
6	5B	0.39 ± 0.09	0.38 ± 0.15	0.30 ± 0.19	0.401			

Table 5.7. Transmission failure rates. Failure rates of IPSCs from the indicated source layers onto excitatory postsynaptic cells in the indicated target layers (means ± s.d.). The table only includes inhibitory circuit motifs with characteristic area-specific differences (Fig. 5.1). Failure rates were estimated as the fraction of optical stimuli which failed to elicit supra-threshold IPSCs (see Methods). Because no significant area-specific differences in optical responsiveness were detected (Fig. 3.4), differences in transmission failure rate reflect predominantly differences in *synaptic* transmission. Crimson shaded backgrounds indicate significant differences ($P < 0.05$) between two cortical areas, as determined by parametric one-way ANOVA and subsequent Tukey-HSD post-hoc tests. Data for L4 target cells were analyzed by independent-sample *t*-test.

Connection		20–80 % rise time (ms)			*P*-value			
Source	Target	M1	S1	V1	ANOVA	M1-S1	M1-V1	S1-V1
2/3	2/3	9.0 ± 2.4	6.9 ± 2.3	6.2 ± 2.1	0.037	0.255	0.029	0.304
5A	2/3	10.3 ± 5.5	6.7 ± 2.7	7.5 ± 2.4	0.215			
5B	2/3	11.0 ± 3.5	6.6 ± 2.1	8.3 ± 2.0	0.113			
4	4	-	5.6 ± 1.3	7.5 ± 2.8	0.094	-	-	
5B	4	-	4.8 ± 3.2	8.8 ± 1.6	0.008	-	-	0.008
5A	5A	10.7 ± 2.9	5.8 ± 1.2	5.3 ± 1.7	0.000	0.000	0.000	0.884
4	5A	-	5.7 ± 1.1	7.5 ± 1.4	0.063	-	-	
5B	5B	5.7 ± 1.6	5.2 ± 1.2	5.9 ± 1.4	0.665			
6	5B	8.4 ± 2.3	4.8 ± 1.3	5.4 ± 2.0	0.004	0.009	0.01	0.731

Table 5.8. IPSC rise times. IPSC rise times from the indicated source layers onto excitatory postsynaptic cells in the indicated target layers (means ± s.d.). Rise times were measured for single

IPSCs on individual trials and represent the interval between the rising IPSC reaching 20 % and 80 % of its maximal amplitude. The table only includes inhibitory circuit motifs with characteristic area-specific differences (Fig. 5.1). Crimson shaded backgrounds indicate significant differences ($P < 0.05$) between two cortical areas, as determined by parametric one-way ANOVA and subsequent Tukey-HSD post-hoc tests. Data for L4 target cells were analyzed by independent-sample *t*-test.

Fig. 5.2c indicates that regional differences in inhibitory connectivity arose to a large extent from variable connection probabilities; in one instance (the layer 4-to-5A motif), there was an additional increase in inhibitory charge flow per IPSC (Fig. 5.2c). The relative prominence of translaminar inhibition from layer 6 to layer 5B in V1, in contrast, was not due to an absolute increase in the number of layer 6-to-5B connections but rather a reduction of inputs from other laminar sources (Table 5.2). Thus, in this case, the *relative* amount of translaminar inhibition from layer 6 – namely relative with respect to the other layers providing inhibition – is significantly increased in V1 compared to the other cortices. (Such a relative measure assumes the "view of the cell" with respect to where it is inhibited from the most.)

Differences in transmission failures (Fig. 5.2c) or the putative somatodendritic locations of inhibitory synapses, as inferred from IPSC rise times measured on individual trials (Table 5.8), played no discernible role.

Cell-specific differences in the laminar organization of inhibitory connections

Characteristic differences in average inhibitory connectivity among cortical areas were not reflected in equally characteristic, region-specific wiring patterns of individual cells. Rather, an inspection of individual input maps revealed that laminar patterns of inhibitory connectivity showed striking cell-to-cell variation within the same cortical layer and area. For example, some excitatory neurons in layers 2/3 and 5B of V1 and S1 received strong translaminar inhibition from layers 5 and 6, respectively, whereas others did not. Cells with dramatically different inhibitory input distributions could be found immediately next to each other in the same cortical slice, suggesting that cell-to-cell variability is not a slicing artefact (Fig. 3.6d).

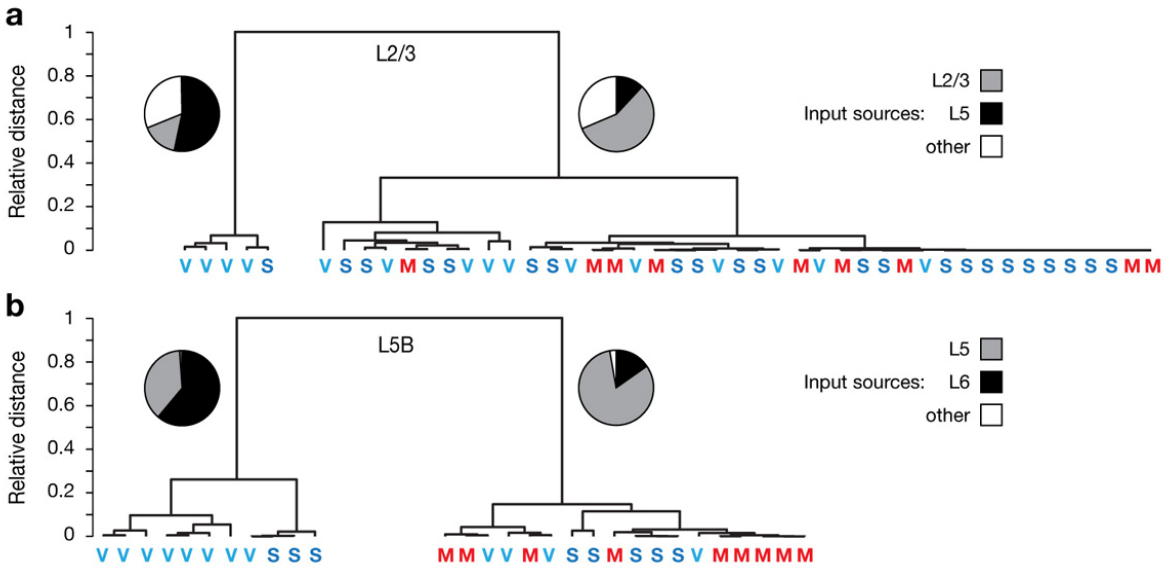

Figure 5.3. Cell-specific differences in the laminar organization of inhibitory connections. (**a, b**) Hierarchical clustering of pyramidal cells in layers 2/3 (**a**) and 5B (**b**) of M1, S1, and V1. Classification variables were the strengths of intra- and translaminar inhibitory inputs, quantified as normalized inhibitory charge flow. Neurons in both layers fall into two well-separated clusters: a minor population of neurons receiving strong translaminar inhibition (left cluster), and a major population of predominantly home-layer inhibited neurons (right cluster). The robustness of the cluster solutions found has been assessed by non-parametric bootstrapping, which confirmed a large separation distance with low variation for the two-cluster solution in both, layer 2/3 cells (0.64 ± 0.11) and layer 5B cells (0.71 ± 0.09; mean ± s.d.), while further bifurcations displayed increasingly larger relative variability. Pie charts indicate the average strengths of inhibitory input from the dominant

translaminar layer in black (layer 6 for neurons in layer 5B, and layer 5 for neurons in layers 2/3), the home layer in grey, and other layers in white. Coloured letters denote the cortical area from which each observation is derived. Note the high frequency of V1 neurons and the absence of M1 neurons in the clusters receiving dominant translaminar inhibition.

Hierarchical cluster analysis using the between-groups linkage method and a cosine metric indicated the presence of two distinct subpopulations of pyramidal cells in layers 2/3 and 5B of the primary sensory cortices V1 and S1 (Fig. 5.3). Members of one of these populations received the overwhelming majority of inhibitory inputs from their respective home layers; the inhibitory input distribution of these cells therefore resembled that of pyramidal neurons in layers 2/3 and 5B of motor cortex (Fig. 5.1a, d). The other subpopulation of cells appeared specific to sensory cortex; it was found only in V1 and - albeit in smaller numbers - S1 (Fig. 5.3a, b). This group of neurons is defined by prominent translaminar inhibition, which serves as the dominant source of GABAergic input (Fig. 5.3a, b). Neurons receiving translaminar inhibition accounted for 26.6 and 4.5 % of recorded cells in layer 2/3 of V1 and S1, respectively (Fig. 5.3a), and for 66.6 and 37.5 %, respectively, of all neurons in layer 5B (Fig. 5.3b). Differences in average inhibitory connectivity among cortical areas thus arise, at least in part, because two subpopulations of excitatory neurons with distinct inhibitory input patterns are present in different proportions.

The existence of such strikingly different subpopulations suggests that inhibitory connections are wired with high specificity: E.g. interneurons in layer 5 connect preferentially to one pyramidal neuron in layer 2/3, while collectively avoiding its immediate neighbour. Interestingly, in layer 2/3 (but not 5B) of V1, the presence of such dominant translaminar inhibition is negatively correlated with the lateral extent of inhibition; i.e. predominantly home-layer inhibited neurons receive significantly

broader lateral inhibition than do neurons in the translaminar cluster (means ± s.d. = 471 ± 102 vs. 330 ± 76 μm; *P* = 0.02; Fig. 5.4).

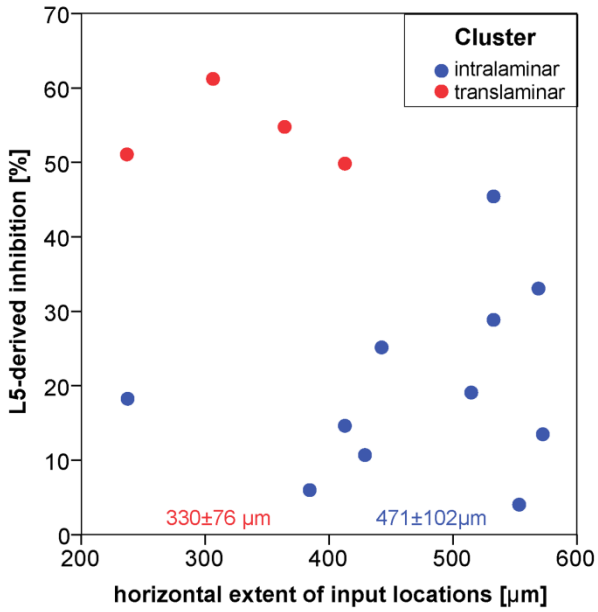

Fig. 5.4: Translaminar inhibition is negatively associated with lateral extent of (intralaminar) inhibition. Layer-5-derived inhibition plotted against horizontal extent of input locations (as determined for Fig. 4.1c and Table 4.2) across layer 2/3 cells in V1. The two clusters retrieved by hierarchical cluster analysis (Fig. 5.3) are colour-coded as indicated.

Chapter 6 – Degeneracy in the laminar organization of inhibitory circuits

The cell-specific differences in the laminar organization of inhibitory circuits described above underline the specificity of individual inhibitory connections, but raise the question how *uniform* layer-specific inhibitory circuits are as well as whether laminar borders are significant for structuring such circuits. To test these notions, the vertical organization of inhibition was assessed regarding both, the (1) pre- and the (2) postsynaptic side: In the former case, the question is raised, whether the vertical distribution of presynaptic interneurons innervating a pyramidal cell, is obviously structured by layers, or their borders, respectively. In the latter case, one has to ask, if the overall pattern of inhibitory inputs found for every neuron, is more similar for neurons within one and the same layer, compared to neurons from a different layer, i.e. whether there is a layer-specific input structure (despite some variation already described).

To analyze the inhibitory input distribution of pyramidal cells, a cluster analysis, orthogonal to the one shown in Fig. 5.3, was conducted by pooling recorded cells from all layers within each of the three cortical areas and using the amount of inhibition received from all layers (1 to 6) as clustering variables (Fig. 6.1).

The optimal solutions retrieved involve 3 clusters in M1 and 4 clusters in S1 and V1, which roughly represent cells dominated by inhibition from layers 2/3 (cluster 1), 4 (cluster 2 in S1 and V1), 5 (cluster 2 in M1, 3 in S1 and V1) and 6 (last cluster in all cases). Thus, the optimal number of clusters is always one less than the expected number, i.e. the number of cortical layers.

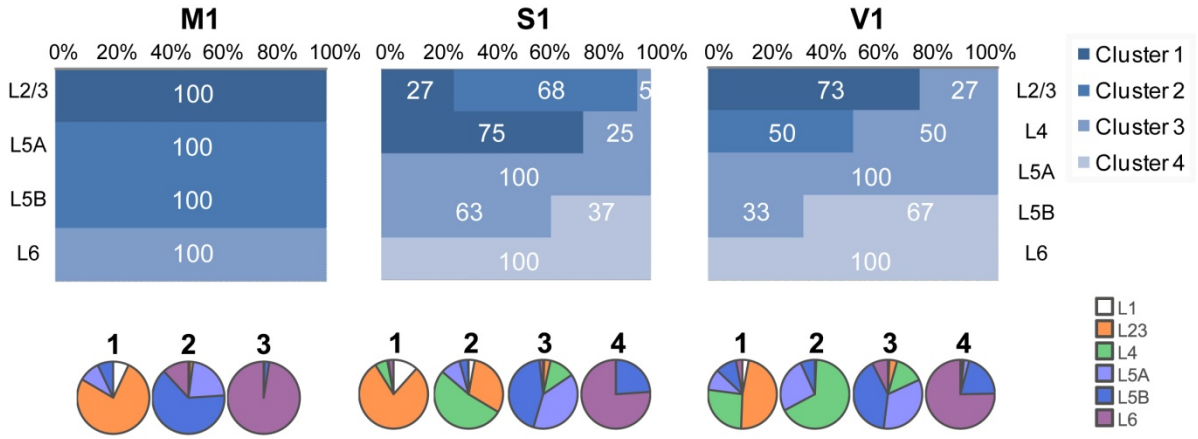

Figure 6.1. Cluster analysis reveals degeneracy in laminar uniformity of inhibitory circuits. Cells were pooled within each cortical area and clustered in dependence of the amount of inhibition received from all layers (L1 through to L6). Bar diagrams represent percentage of recorded cells – drawn along the x-axis - from each layer (2/3 through to 6) – drawn along the y-axis - in each cortex (M1, S1, and V1). White numbers give the share of each laminar cell population sorted to the respective cluster (1 through to 4) indicated by the background colour of the bar. The pie charts, numbered by the cluster they represent in each of the cortical areas, display the average amount of inhibition cells in that cluster receive from each layer (as colour-coded at the bottom right).

In M1, this finding reflects the simple fact that cells from sublayers 5A and 5B are combined into one cluster (or: functional layer), while otherwise the laminar organization is maintained: pyramidal cells within layers 2/3, 5, and 6 are – despite some variation – so similar within and so distinct from each other with respect to the inhibitory connectivity patterns they “sample” that purely based on such a pattern they can be assigned to their home layer. If inhibitory laminar connection patterns are indeed important for information processing, then – purely based on inhibition – the layers form rather uniform computational compartments distinct from one another.

In the sensory cortices, however, this laminar uniformity appears broken. Most notably, neurons from cluster 3 (i.e. pyramidal cells dominated by layer 5 derived inhibition) can be found in all layers from 2/3 through to 5B. In other words, a

proportion of cells in each layer receives dominant – putative feedback - inhibition from the major output layer of the neocortical circuit.

Also, a subset of neurons in layer 4 in V1 is so distinct (featuring dominant layer-4-derived inhibition) from any other population of excitatory neurons in the visual cortex that they form an independent cluster, while the remaining layer 4 neurons are predominantly inhibited by layer 5. In S1 in contrast, a majority of layer 4 neurons shares prominent layer 2/3- (instead of layer 4-)derived inhibition. (The remaining minority of layer-4 cells in S1 is again dominated by layer 5 derived inhibition, analogous to V1). Nevertheless, there exists a cluster also in S1, that is dominated by layer-4-derived inhibition. In contrast to V1, however, where that cluster consists of layer-4 cells, in S1 that cluster consists exclusively of layer 2/3 cells – obviously featuring strong feedforward inhibition from the neocortical input layer. Finally, layer 6 seems to be a largely independent and uniform compartment with respect to its sources of inhibition, providing inhibition to layer 6 pyramidal cells and a subset of layer 5B neurons in sensory cortical areas.

In conclusion, in sensory areas, pyramidal cells located in different layers can have similar patterns of inhibitory input, while pyramidal cells located in the same layer can have patterns that are vastly distinct from those of their immediate neighbours. This suggests that inhibitory circuits are wired with high specificity, and that cortical layers are not the only organizing principle of inhibitory circuits. Functional constraints or division of labour, especially in sensory cortices, seem to transcend laminar borders.

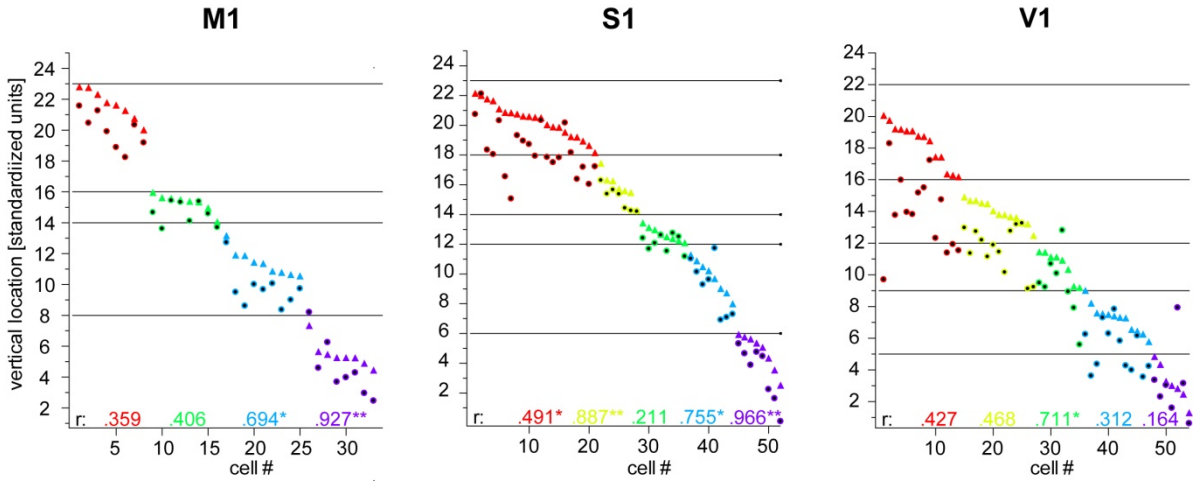

Figure 6.2. Vertical location of map centroid and target cell. For cells in all three cortical areas M1, S1 and V1 the vertical location of the cells (triangles) – as determined from brightfield images – and their corresponding map centroids (colour-matched circles right above or below each cell) was plotted using a standardized, area-specific 25-row scale. Home layers of the cells are colour-coded (2/3, red; 4, yellow, 5A, green; 5B, blue; 6, purple). Bivariate correlations between centroid and cell distance from the white matter were computed within each of these target cell layers and plotted below in the matching colour; their statistical significance is indicated (* $P < 0.05$; ** $P < 0.01$).

In order to investigate if such a degeneracy of laminar uniformity within a layer is simply due to and predicted by the vertical location of the target cell itself - or, put differently, if vertical somatic position is a continuous rather than discrete organizing variable – the laminar location of the weighted centroid of each map and of the corresponding cell were plotted and tested for a linear, correlative association (Fig. 6.2). The plot was generated by subdividing the vertical axis into a standardized scale of 25 rows, each of which is assigned to a particular layer, depending on the average laminar boundaries in each cortex (obtained from n = 15 brightfield images per cortex), so that the vertical locations of cells and weighted map centroids could be compared across brain slices of one and the same cortical area. As in the case of layers, it appears that the vertical location of a cell does indeed give some indication of the location of the map. However, this relationship does not come as a fixed, stereotypic rule, which would be valid across cortical areas: For example, significant correlations between those two variables occur in layer 5A of V1, but in all layers *except* for 5A in S1. M1 again conforms to neither of these two patterns,

showing significant correlations only in layers 5B and 6 (Fig. 6.2). Even for those populations, where significant correlations exist, this “rule” is not valid for all cells and thus the vertical location of a cell is insufficient to predict the location of the input map generally. Like the layers, the vertical location of a cell seems to provide a default organizing principle with respect to the location of inhibitory input maps, which is however, frequently overridden by specific, potentially computationally meaningful, connectivity patterns of individual cells.

Finally, the compartmental laminar organization was assessed on the “input side” as well: If layers are meaningful for organizing inhibitory circuits, then the number of inhibitory inputs a cell receives should abruptly change at laminar borders. The inspection of individual maps (Fig. 3.6d) already suggests that, while the number of input sources can indeed change abruptly from one vertical row to the next, these rows may as well be located at laminar borders as in the middle of a layer (compare for example the two cells in each of the two pairs in S1 in Fig. 3.6d).

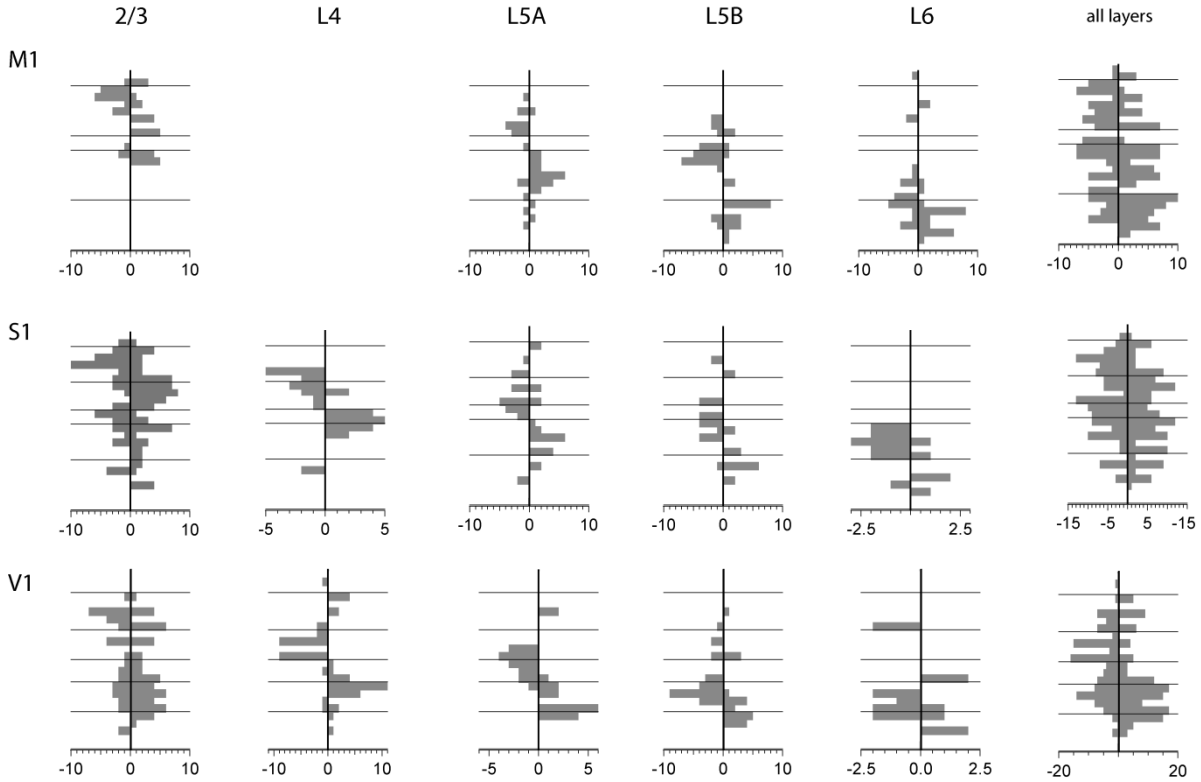

Figure 6.3. Summed incidences of decreases and increases (when moving towards the pia) in the horizontal sum of input numbers (grey bars), plotted along the negative and positive x-axis, respectively. The y-axis represents cortical depth from pia to white matter, standardized within a 25-bin scale stereotypic for each cortical area (M1, S1, V1). Horizontal black lines indicate the location of laminar borders, starting from the layer 1-to-2/3 border at the very top of each graph, and ending with the layer 5B-to-6 border at its bottom.

To investigate this more systematically, the positions of maximal changes in input numbers along the vertical profile of all maps were derived by differentiating them numerically to extract the vertical locations of maximal increases or decreases in input numbers, which were again standardized using the 25-bin vertical scale already employed in Figure 6.2. For each population of pyramidal cells (e.g. layer 2/3 neurons in M1), minima and maxima were counted (i.e. summed up) for each of the vertical bins, and plotted along the negative and positive x-axis, respectively (Fig. 6.3). It is evident that changes in input numbers along the vertical axis do not systematically coincide with laminar borders.

Chapter 7 – Layer-specific structural plasticity in inhibitory circuits

It has been reported that alterations in inhibitory connections may underlie the adaptations of deprived or otherwise plastic cortical circuits (Fagiolini et al., 2004; Hensch and Stryker, 2004; Jasinska et al., 2010; Ni et al., 2011; Yazaki-Sugiyama et al., 2009). In addition, the current finding that inhibitory circuits display large within- and between-area variation suggests that it may be the wiring of inhibitory connections, in addition to extrinsic connectivity (Mountcastle, 1978), which causes the functional specialization of a cortical area (e.g., sensory vs. motor) or of an individual cell (e.g., simple vs complex). If this notion were correct, and if connections remained plastic in the adult, one would assume that inhibitory wiring patterns would change and adapt under conditions of sensory deprivation in a rather predictable manner. Historically, there is only one study published so far, which investigated (excitatory) functional connectivity in a quantitative way (using glutamate-uncaging) in deprived (barrel) cortex (Shepherd et al., 2003).

To examine the plasticity of inhibitory circuits, primary whisker-related somatosensory cortex was deprived of sensory input in > 2 month-old Gad65>ChR2 mice by means of repeated whisker trimming. Whiskers of all rows, except for the middle (C) row, were cut unilaterally and repeatedly every two days over at least two weeks to induce circuit plasticity. In order to see the five rows, slices of somatosensory cortex were cut at an 45°-oblique angle (Finnerty et al., 1999; Shepherd et al., 2003), and inhibitory connections were mapped and analyzed as before (see Methods).

In order to study inhibitory circuit plasticity, the input profile of layer 2/3 cells was analysed, as they (compared to cells in other layers) feature the two functionally most relevant types of translaminar inhibition segregated by layer: layer 4 provides strong putative feedforward inhibition, and layer 5(B) gives rise to – somewhat smaller – putative feedback inhibition (Fig. 5.1, 6.1, chap. 8).

Consistent with the hypothesis that inhibitory circuits adapt a cortical area to its specific function, the putative feedback-inhibition motif from layer 5B to layer 2/3 decreased by almost 4-fold in deprived barrel-related columns compared to control mice (P = 0.033; Fig. 7.1). Interestingly, the motif was weakened also in the remaining non-deprived column (corresponding to the C row); however, this change did not reach statistical significance (P = 0.366). This significant plasticity is specific to inhibition from layer 5B, i.e. it is neither present for layer 5A-derived inhibition, nor for layer-4- as well as homelayer-derived putative feedforward inhibition.

	whisker-trimmed mice				
	trimmed whiskers	non-trimmed whiskers	control	Tukey	ANOVA
L1	35.1 (17.0)	27.1 (10.3)	24.9 (14.9)	.084	.071
L2/3	50.8 (18.9)	59.6 (12.2)	54.0 (15.8)		
L4	9.9 (11.9)	8.4 (6.5)	9.6 (9.1)		
L5A	2.8 (4.4)	1.9 (3.0)	5.7 (5.9)		
L5B	1.5 (2.5)	3.0 (5.9)	5.7 (5.3)	.033	.043
L5	4.3 (6.2)	4.9 (8.3)	11.5 (10.4)	.083	.085
L6	0	0.1 (0.3)	0.1 (0.2)		
N	26	12	15		

Figure 7.1. Somatosensory deprivation leads to specific adaptation of translaminar inhibition. Numbers and grey values indicate amount of inhibition (normalized product of charge and input numbers, see Fig. 5.1) received from each layer (indicated on the left) by layer 2/3 pyramidal neurons; S.D. in brackets below each mean value. Groups were formed according to a cell being inside a barrel-related column that was deprived (left) or not-deprived (middle) of its principal whisker in whisker-trimmed mice. The right column shows values for cells in non-deprived mice. Numbers of cells (N) in each group are indicated at the bottom. Significant differences as estimated by one-way ANOVA and subsequent pair-wise Tukey-HSD post-hoc test at P < 0.05 are indicated by red boxes, those at P < 0.1 by blue boxes. No differences were found between the middle group and any other group.

This difference in layer-5B-derived inhibition is mainly due to a significant decrease in absolute (P = 0.012) as well as normalized (P = 0.042) input numbers in deprived columns compared to control mice. Although the absolute size of the 5B-derived inputs measured as charge flow per average ISPC is also significantly reduced (P = 0.007), the relative size is not (P = 0.791) – an indication, that IPSCs are scaled down roughly equally across all layers (i.e. layer-unspecifically) in deprived neocortex compared to controls. Connection probabilities[26], in contrast, are altered in a layer-specific fashion, i.e. specifically for layer 5B-derived inputs. (All P-values refer to a pairwise independent-sample T-Test).

It is interesting to note that layer-1 derived inhibition increases in the opposite direction, potentially indicating some inter-areal top-down silencing to prevent uncontrolled activity. Also note that the values for some layers (1 and 4) differ from those obtained before (Fig. 5.1), which is most likely due to the fact of a vastly different slicing angle.

[26] A decrease in numbers of input sources could be due to either a decrease in interneuron numbers, assuming constant connection probability of inhibitory connections, or due to a decrease in connection probability, while interneuron numbers remain the same. The former case would imply that in the adult (older than 2 month), potentially transiently deprived neocortex interneurons actually die (specifically in that layer) in response to the deprivation, which is rather unlikely. Therefore, the latter case is assumed here: A decrease in input numbers is in all likelihood due to a decrease in connection probability.

Chapter 8 – Discussion

I have assembled maps of inhibitory-to-excitatory synaptic connections in three neocortical areas (Fig. 8.1). The features depicted in those maps are the somatic locations of presynaptic inhibitory neurons and of postsynaptic excitatory cells as well as the strengths of the connections between them. These maps are by no means a substitute of our current, often remarkably detailed knowledge regarding subcellular target preferences, synaptic dynamics, actual axonal arborizations or physiological specifications of interneurons of various subtypes. It will require repeated application of the optogenetic method of local circuit mapping developed here – featuring the various advantages of the conditional expression from a defined genomic locus – albeit using driver lines that target specific subtypes of interneurons, only, to dissect the inhibitory circuits element by element. Relating such subtype-specific connectivity data to other physiological and morphological features of different interneurons, which are partly already well established, will eventually lead to a comprehensive understanding of functional inhibitory connectivity in the neocortex.

Technical achievements

This study was the first to achieve sufficient conditional expression of ChR2 from a genomic locus to perform optogenetic mapping of local circuits. Before, only few attempts of expressing ChR2 from a genomic locus were successful, and those did neither target a specific locus nor did they involve conditional expression (Ren et al., 2011; Wang et al., 2007). An alternative attempt, expressing ChR2 from the parvalbumin-locus directly, to achieve subtype-specific expression, failed (Sohal et al., 2009).

Using this technique has enabled me to provide a quantitative image of the laminar source distribution of inhibitory inputs to all excitatory target cells of three cortical areas. While extensive multiple intracellular recordings have revealed much about the presence or absence of inhibitory synaptic connections, as well as their synaptic characteristics (like short-term dynamics), they cannot offer a comprehensive view of how much inhibition neocortical cells actually receive from which layer or column. Likewise, morphological studies of axonal projection patterns of inhibitory neurons may provide a quantitative account regarding putative connections in certain locations. However, they are obviously not well suited to depict physiological connectivity. Only comprehensive mapping using photostimulation can reveal such quantitative, physiological connectivity schemes. Before the present study, only three publications existed (Brill and Huguenard, 2009; Dantzker and Callaway, 2000; Xu and Callaway, 2009), which had mapped neocortical inhibitory connections systematically – mainly for cells in layers 2/3 and 5 of S1 or V1 - albeit using glutamate uncaging, which activates all cell types alike and is thus prone to mapping polysynaptic connections, via low-threshold spiking interneurons (Kozloski et al., 2001; Wang et al., 2004). Because pyramidal cells can also be activated by glutamate uncaging in their dendritic tufts (Dantzker and Callaway, 2000), the high percentage of inhibition onto S1 layer 2/3 targets apparently deriving from layer 1 found in one of these studies might be due to such polysynaptic activation. In addition, high levels of caged glutamate blocks $GABA_A$-receptors (Peterka, 2009), which may lead one to underestimate inhibitory connectivity. The present technology combines genetic resolution of cell types with perisomatic restriction of optical activation and a broad, uniform expression across the cortex, as is

necessary for mapping local circuits (but not achieved using viral expression systems).

Nevertheless, the technical achievements presented here are rather a proof-of-principle than an ultimate tool for optogenetic local circuit mapping – mainly due to the low functional ChR2 expression level, prohibiting the application in some cell types, certain conditions (e.g. *in vivo*) or in paradigms of high-frequency or two-photon stimulation (Andrasfalvy et al., 2010; Rickgauer and Tank, 2009; Sohal et al., 2009). As I will argue below, using actuators with higher single channel conductances or better temporal fidelity, including engineered versions of ChR2, LiGluR or P2X2 will be necessary to optimize the present approach (Gunaydin et al., 2010; Lin et al., 2009; Szobota et al., 2007). Likewise, the use of multiple actuator copies, stronger promoters, insulators, introns, or RNA-stabilizing sequences, BAC-transgenics (Heintz, 2001; Ren et al., 2011), or targeting genomic loci different from the ROSA26 locus (Freese and Seeburg, 2004), may provide additional benefits.

Furthermore, although the slice preparation enables us to expose all cortical layers equally for comprehensive quantitative investigation, it entails the risk of cutting axons and dendrites during the slicing process. To minimize distortions of the data set it proved vital to choose a slicing angle that is not strictly coronal, but slightly tilted, so that the tissue is cut exactly perpendicular to the local cortical surface (i.e. parallel to apical dendrites of deep layer pyramidal neurons). Also, as in the current data set, cells should be filled with neurobiotin or biocytin to inspect their gross integrity reducing the risk of misrepresentations of input data due to heavily cut dendrites. However, over-adjusting the angle to protect the apical dendrites as much as possible should also be avoided, as then axons approaching from below

(but invisible to the experimenter) will be compromised. Finally, cells should be patched as deep as possible (30-90 µm) in the slice to ensure that many of their processes as well as presynatic axons are intact. In the preparation in this study, increasing the cell depth was complicated (especially for cells in layers 5 and 6, for which it would matter the most), because in adult mouse neocortex, visibility of cells (which is crucial to patching success) deteriorates strongly with increasing depth due to heavy myelination. Even if all those measures are taken, risks for distortions cannot be completely avoided; for example average cell size decreases from anterior to posterior neocortex, potentially rendering cells in M1 more prone to slicing-related damage than cells in V1. Also, the difference in input from layer 4 into layer 2/3 cells of S1 between the two strongly different cutting angles applied to achieve figures 5.1a vs. 7.1 illustrates, that slicing angle is indeed a strong determinant of the appearance of input maps, and thus comparisons between network connectivity data can only be made, if very similar angles were used for the compared data sets.

Future directions of optogenetic intervention

While optogenetic tools have experienced significant improvement within just one decade, their applications yet largely remain to be explored. Major routes are the following:

(1) Single-cell optogenetics via two-photon excitation represents a major current goal. Despite all success, the final objective of evoking exactly a single spike (at whatever frequency in a series) in exactly a single cell (or a well-defined set of cells) which is a prerequisite for feeding precise artificial messages into neural circuits, yet remains to be achieved. While temporal precision has been greatly improved (Chow et al., 2010; Gunaydin et al., 2010; Janovjak et al., 2010; Szobota

et al., 2007), spatial resolution has not, since all tools published require single-photon excitation, and will thus entail an excitation volume that vastly exceeds that of one neuron (Denk and Svoboda, 1997). Glutamate- and GABA-uncaging are so far the only methods that allow the reliable activation (or inhibition) of cells by means of two-photon optics – and hence, with single-cell (indeed: single-synapse) resolution (Kantevari et al., 2009; Nikolenko et al., 2007). This approach has been adapted into a quasi-optogenetic application, when stimulating selected, fluorescent neurons in mouse lines that express a fluorescent protein under a cell-type specific promoter (Fino and Yuste, 2011; Peterka, 2009). Spatially complex stimulation paradigms using diffractive optical elements or their digital counter-parts, spatial light modulators, becomes possible with this approach, while temporal resolution and spike-timing precision are as poor as in any uncaging-based photostimulation method (Nikolenko et al., 2007; Nikolenko et al., 2008). Thus, two-photon-isomerizable linkers for synthetic channels are underway (Trauner, 2009), while two-photon-mediated excitation of ChR2 via multiple stimulation spots (spatio-temporal summation in spiral scans) or sculpted light has already been demonstrated (Andrasfalvy et al., 2010; Mohanty et al., 2008; Papagiakoumou et al., 2010; Rickgauer and Tank, 2009). The latter, however, suggested, that the depolarisation achieved might be too weak to evoke reliable spiking in desired settings like *in vivo* or with expression of ChR2 from a transgenic locus. Interestingly enough, in zebrafish, expression levels of ChR2 were high enough, even when transgenically, conditionally and inducibly expressed (using the Tet-system) to allow for reliable two-photon mediated excitation *in vivo* (Zhu et al., 2009). Also, using the most recent ChR2-versions (see above), reliable two-photon activation is probably within reach. This development will finally make one of the

classical questions in neuroscience adressable: What makes a neuron fire? (Dayan and Abbott, 2001). So far, the question could only be asked at the sensory periphery.

(2) Clinical applications of optogenetics have been widely suggested but largely remain to be explored. The most obvious (however, non-optogenetic) application of light sensitive ion channels has been the restoration of vision in models of retinitis pigmentosa by photosensitizing the intact ganglion or the bipolar cell layer (Busskamp et al., 2010; Ivanova and Pan, 2009; Lagali et al., 2008; Tomita et al., 2009). Also, experimental treatment of Parkinsonian rats has been demonstrated (Gradinaru et al., 2009; Kravitz et al., 2010), while silencing of focal, medically resistant epileptic activity (Tonnesen et al., 2009) is another obvious application yet to be achieved *in vivo*.

(3) Optimal molecular targeting systems pose another significant challenge, since none of the current approaches is optimal for all purposes. Optogenetic applications generally require strong and ubiquitous expression exclusively in cells of a well-defined subtype. However, strong expression – usually conferred by ubiquitous house-keeping promoters – and cell-specific expression – usually conferred by very specific (but not strong) promoters – force significant trade-offs. In mice, the *Cre-lox* system provides the most general potential solution (Monyer and Markram, 2004; Rajewsky et al., 1996; Soriano, 1999b; Tsien et al., 1996a): Specificity is provided by a weak cell-specific promoter that drives the expression of the *Cre*-recombinase (driver element). Strong expression is provided by driving the actuator with an ubiquitously active, strong house-keeping promoter, such as EF1α, synapsin 1 or the synthetic chicken-beta-actin/early CMV enhancer (CAG) promoter (Hitoshi et al., 1991; Zhang et al., 2007). Separating the strong promoter from the actuator by

means of a STOP-cassette (triple-polyA-region; “stop-floxed”) or inverting the actuator cassette flanked by two mutually exclusive pairs of *lox*-sites (“double-floxed”), will prevent the ubiquitous expression of the actuator in that responder element. Uniting the driver and the responder in the same organism will allow even a minimally expressed *Cre*-recombinase in a specific cell type, where its upstream promoter is active, to recombine the *lox* sites – either removing the stop-cassette in the stop-floxed construct or inverting the actuator gene in the double-floxed construct – and thus allow strong expression of the actuator driven by its upstream house-keeping promoter in just one specific cell type. The driver element is typically provided by means of a transgenic or knock-in line, while the responder is introduced via *in utero* electroporation or viral vectors (AAV or Lenti), since with these vectors the gene dose and thus the expression level can be boosted maximally (Adamantidis et al., 2007; Callaway, 2005; Kuhlman and Huang, 2008; Petreanu et al., 2007; Petreanu et al., 2009). However, the main disadvantage of this technique is that actuator expression levels are not equal throughout the tissue (due to variation in transfection efficiency from cell to cell), that the spatial extent of transfection is small (limited by the diffusion of the virus, usually <~300µm radius, maximally 1 mm (Callaway, 2005)), and that the transfection is labour intense and causes damage to the very circuit to be tested experimentally. In addition, it has been found that both methods of transfection lead to axonal and synaptic accumulation of ChR2, thus preventing the dissection of local circuits (see above) (Petreanu et al., 2007; Petreanu et al., 2009).

The only alternative is to introduce the phototrigger using a transgenic animal carrying the stop-floxed responder cassette (Monyer and Markram, 2004). However, expression from a transgenic locus, with just two copies of the actuator

gene, has - apart from the present study - only been successfully achieved using an actuator, TRPV1, with a large single-channel conductance (Arenkiel et al., 2008). Future alternatives to increase expression from a transgenic locus include using optimized actuators with higher single-channel conductance (see above), multiple-copy constructs (divided by IRESes or self-cleaving 2A elements (Han et al., 2009; Palmenberg, 1990; Szymczak et al., 2004)), the targeting of different genomic loci (Beard et al., 2006; Freese and Seeburg, 2004) as well as the use of stronger house-keeping promoters.

Alternatives to the combinatorial approach as a whole also exist, and – in case of virally mediated gene transfer – are also the only viable option for clinical applications of optogenetics (since *Cre*-transgenic humans do not exist) (Kaplitt et al., 2007). In this case, cell-type specific promoters need to drive the actuator directly. In the case of virally-mediated expression only few instances exist, where promoter elements were found to be strong and specific enough to drive functional actuator expression in neurons *in vivo*; such as the CamKIIα-promoter to restrict expression to cortical pyramidal cells (Adamantidis et al., 2007; Sohal et al., 2009; Zhang et al., 2008). However, systematic attempts to target any of the many cortical interneuron subtypes using elements of promoter regions from specifically expressed calcium-binding proteins, neuropeptides or other marker proteins have failed. Only three elements (two of them from the fish fugu) were found that restrict expression to interneurons (vs. pyramidal cells) but could not distinguish between subtypes (Nathanson et al., 2009). The alternative of driving ChR2 directly from these promoters using knock-in mice (as achieved before with GFP expression) has failed for the parvalbumin-promoter so far tried for the given reasons (Sohal et al., 2009).

Nevertheless, transgenic expression of ChR2 has been achieved using the Thy1-promoter which gives rise to strong enough expression even for *in vivo* applications, albeit with stochastically varying specificity: Only one line, targeting a specific neocortical cell type, namely layer 5 pyramidal cells (line 18, JAX#007612), has resulted (Arenkiel et al., 2007; Wang et al., 2007). It features a strong accumulation of ChR2 in the dendritic tuft, remarkably allowing for *in vivo* excitation of layer 5 pyramidal cells, but again compromising its usefulness for circuit mapping (Arenkiel et al., 2007). Meanwhile however, the strategy of using BAC-transgenics (Heintz, 2001) to introduce ChR2 at sufficient levels downstream of a cell-type-specific promoter was successful in cholinergic neurons (Ren et al., 2011).

(4) All-optical experimental systems, which can harness the full advantage of massively parallel interference with neural circuits (Miesenböck and Kevrekidis, 2005). Simultaneous optical readout and optical input (control) of neural activity – even in the two-photon mode or *in vivo* – have been published (Airan et al., 2007; Gradinaru et al., 2007; Mohanty et al., 2008; Nikolenko et al., 2007; Zhang et al., 2007) and experimental setups are partly already commercially available (e.g. from Femtonics, Prairie Technology or Olympus). Likewise, fast parallel read-out using EEG or multi-electrode recordings in parallel with photostimulation have been established (Adamantidis et al., 2007; Cardin et al., 2009; Zhang et al., 2009). Also, genetically targetable calcium sensors are by now available that allow precise read-out even of subthreshold activity (Tian et al., 2009).

Devising complex experimental questions, which can harness the technological potential that recently became available to explore how defined messages are processed and stored in neural circuits, is, however, a perhaps even greater challenge (Miesenböck and Kevrekidis, 2005). Closed-loop experiments, where the

output of neural activity is fed back into the circuit to explore the evolution of endogenous activity has recently provided insight into the underpinnings of gamma-oscillations (Sohal et al., 2009). Also, all-optical systems might serve to tackle maybe the largest problem of optophysiological techniques – namely that their precision cannot reach the sub-millisecond and sub-pA or sub-mV range that is achieved by electrophysiological techniques and is prerequiste for a proper voltage-clamp- or current-clamp-like control (Hamill et. al 1981; Sakmann & Neher 1984). Measuring the optically evoked activity via imaging, could be the first step to achieve at least a "suprathreshold" current-clamp – adjusting the power levels so that the number of spikes can be precisely defined by changing the illumination parameters for each stimulated cell.

(5) Anatomical identification of photostimulated neurons will not unlikely prove necessary in many applications to retrieve the ("sub-genetic") identity of those neurons, as well as their dendritic and axonal ramifications. Here also, common single-cell electrophysiological methods excel since recorded cells can be filled with a dye and their morphology retrieved in great detail (Binzegger et al., 2004; Horikawa and Armstrong, 1988; Jankowska et al., 1976; Pinault, 1996). However, if optical stimulation becomes possible with single-cell resolution (using two-photon stimulation or having sparsely light-sensitive populations), anatomical information could be retrieved either by direct labelling (after stimulation) using photoactivatable fluorescent proteins (Lippincott-Schwartz and Patterson, 2009; Patterson and Lippincott-Schwartz, 2002) or by *a priori* labelling of those cells that are to be stimulated, using fluorescent tracers (Brown and Hestrin, 2009; Lammel et al., 2008), GFP reconstitution across synaptic partners (GRASP) enabling genetic specification of putatively connected neurons (Feinberg et al., 2008) or expression

of both, phototrigger and fluorescent label using transsynaptic viruses (Callaway, 2008; Larsen et al., 2007; Wickersham et al., 2007a; Wickersham et al., 2007b)

(6) Genetically targeted optical or chemical control of intracellular signalling displays another important avenue of current development and opens up the possibilities needed by the new field of molecular systems biology (Weston and Hood, 2004), which views cells mainly as computational devices. As is most evident in the process of synaptic plasticity, neurons – just as other cells – compute by means of intracellular signalling cascades, not just by electricity, and to decipher "how much" of the neural computation is actually due to molecular computation – interacting with electrical signalling via various routes (e.g. calcium signalling) - may represent one of the most significant neuroscientific ambitions. Fortunately, the technologies for genetically targeted optical control of intracellular signalling are currently thriving and so far include a light-induced adenylate-cyclase (controlling cAMP levels) (Schroder-Lang et al., 2007), light-activated GPCRs – derivatives of mammalian rhodopsins and native GPCRs - controlling G_i, G_q and G_S mediated signalling (Airan et al., 2009; Li et al., 2005), light-activated Rac (Wu et al., 2009), light-dependent RNA-interference (Mikat and Heckel, 2007; Shah et al., 2009) or transcription, e.g. via intracellular uncaging of estrogen-receptor agonists (Deiters, 2009; Shi and Koh, 2004).

Also, *chemically* activated genetically targetable activators or inhibitors of neuronal activity, usually acting via G-Protein signalling have been developed – up to a degree where they can be switched by biologically inert (i.e. orally available) synthetic compounds (Alexander et al., 2009; Armbruster et al., 2007; Conklin et al., 2008; Pei et al., 2008; Tan et al., 2006).

Are inhibitory neocortical microcircuits canonical?

The hypothesis of canonical wiring of neocortical inhibitory circuits was the primary focus of the present study, as described in the introduction (hypothesis 2). If the term “canonical” is interpreted in the strictest possible sense, to imply that precisely the same laminar and tangential organization of inhibitory connections is replicated across the entire neocortical mantle, the discovery of characteristic area-specific variations in average inhibitory connectivity clearly refutes the notion of such canonical wiring (Fig. 8.1). Still, the same distinctly recognizable – perhaps even “canonical” – motifs of inhibitory-to-excitatory connectivity recur in most of the cortical areas I have examined. It is the frequency with which these structural elements are present, not their qualitative existence, that varies across neocortical regions.

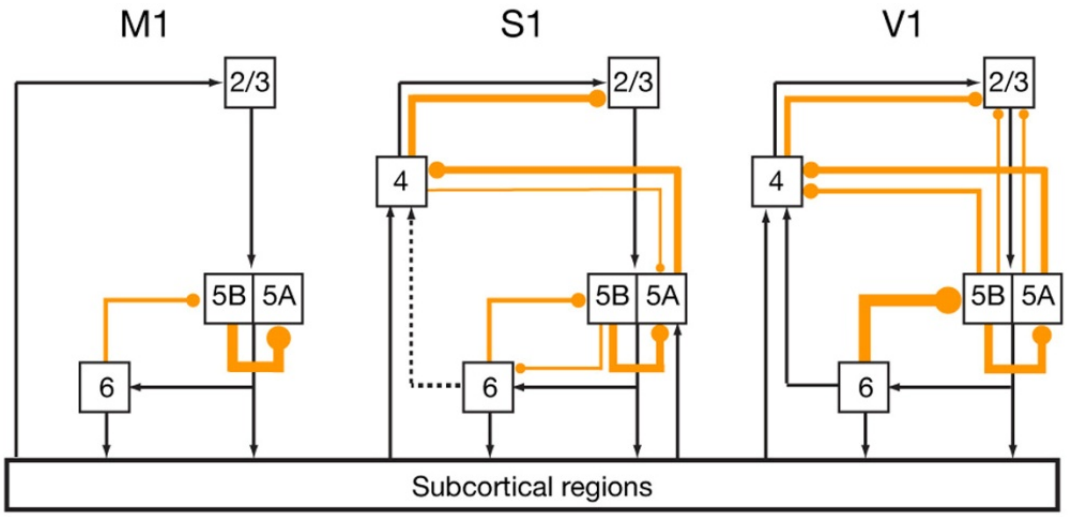

Figure 8.1. Inhibitory circuit motifs. The translaminar inhibitory connections described in this study (yellow, bullet-headed lines) are placed in the context of a “canonical” wiring diagram of excitatory neocortical connections (black, arrow-headed lines; adapted from ref. (Douglas and Martin, 2007a)). Line thicknesses indicate the strengths of inhibitory connections. Intralaminar connections and translaminar motifs contributing ≤ 10 % to the total normalized laminar inhibitory charge flow of a target neuron (see Fig. 5.1) were omitted for clarity.

The most common circuit motif is lateral, intralaminar inhibition of excitatory neurons by interneurons located in either the same cortical column or an immediate

neighbour. In fact, the home layer is always the strongest or – in layers 4 and 5B of V1 – second-strongest source of inhibition (Fig. 5.1). The abundance of this motif in V1, S1, and M1 supports the traditional view that inhibition is largely local, intralaminar, and uniform across functionally distinct areas (Berger et al., 2009; Binzegger et al., 2004; Brill and Huguenard, 2009; Dantzker and Callaway, 2000; Kapfer et al., 2007; Silberberg and Markram, 2007; Thomson and Lamy, 2007; Thomson et al., 2002; Xu and Callaway, 2009). In two (out of six) cases of statistically significant interareal differences in inhibitory connectivity detected, a decreased home-layer-derived inhibition is involved (layer 2/3 in S1 and V1 compared to M1; and layer 5B in V1 compared to S1 and M1; Fig. 5.1). As in both cases, however, the home layer keeps contributing a large share of inhibition, and since almost all subtypes of interneurons form synapses in their home layer (Markram et al., 2004), such interareal differences are difficult to interpret, and thus require further, subtype-specific mapping studies before any conclusion can be drawn.

However, there is also evidence that interneuron axons ramify extensively beyond laminar borders (Helmstaedter et al., 2009b) and that they can form functional synaptic contacts across layers (Kapfer et al., 2007; Thomson et al., 2002; Xu and Callaway, 2009). Here, home-layer derived inhibition via synapses in distant layers, has to be distinguished from genuinely translaminar inhibition, where the somata of pre- and postsynaptic neuron are situated in different layers. For example, the ascending axons of somatostatin-positive, non-fast-spiking Martinotti cells of layer 5 are widely thought to connect preferentially with the apical dendrites of layer 5 pyramidal cells, i.e. mediating intralaminar inhibition (Berger et al., 2009; Murayama et al., 2009; Silberberg and Markram, 2007). However, the existence of their

translaminar axonal ramifications also creates the possibility of truly translaminar inhibition. Indeed there are at least three electrophysiologically documented cases (paired recordings) of a layer 5 Martinotti cell targeting a layer 2/3 pyramidal neuron (Kapfer et al., 2007).

The high experimental throughput of the optogenetic mapping technique developed here has facilitated the detection of these rarer patterns of inhibitory connectivity and allowed for quantitative estimates of motif frequencies. Nine inhibitory translaminar motifs were found (or confirmed) (Fig. 8.1), four of which varied between areas with statistical significance (Fig. 5.1). These motifs include inhibitory-to-excitatory connections (1) from layer 6 to layer 5B, (2) from layer 5 (in particular, sublayer 5B) to layer 2/3, (3) from layer 5B to layer 4, and (4) from layer 4 to layer 5A. Motifs (1) to (3) are particularly prominent in V1, while the fourth motif predominates in S1.

The same connections may generally be present in different cortical regions, but in each area only a subset of excitatory neurons takes part in them to a strong extent (Fig. 5.3). Thus, by strict quantitative measures, inhibitory neocortical circuits are not canonical in two ways: They vary between functionally distinct cortical areas, as well as within one and the same cortical area, i.e. from cell to cell. The latter aspect suggests that inhibitory circuits are wired with high specificity with respect to the individual target cell. Thus, like excitatory synapses (Kozloski et al., 2001; Thomson and Morris, 2002; Yoshimura et al., 2005), inhibitory terminals connect to specific postsynaptic targets with high selectivity – as recently shown for different interneuronal subtypes (in S1 layer 2/3) as postsynaptic targets (Xu and Callaway, 2009).

Do inhibitory circuits follow a columnar and laminar organization?

As explained in the introduction, the concepts of layers and columns implies that neocortical tissue is subdivided into distinct computational compartments in both the horizontal as well as the vertical direction. Revisiting the third hypothesis given in the introduction: Do patterns of inhibitory connectivity reflect this compartmentalization, displaying a laminar and columnar organization?

It has been found, that inhibitory circuits might indeed support a columnar centre-surround architecture, purely based on the lateral spread of inhibitory connections. Moreover, inhibitory circuits obey a step-wise organization in the horizontal direction, which coincides with cortical columns, suggesting, that they themselves are organized in a columnar fashion.

With respect to the vertical or laminar organization, the situation is more complex: Both, the layer (as a categorical variable) as well as the vertical location of a pyramidal neuron (as a continuous variable) predict, to some extent, the overall structure as well as the vertical location of the inhibitory input sources. However, the inhibitory input structure of neurons in most layers – except for layer 6 - is not uniform: instead, some excitatory target cells display an inhibitory connectivity pattern that is vastly different from that of their neighbours and more akin to members of another layer. The principle of laminar uniformity, however, demands a stereotypic inhibitory input structure for all cells in each layer, which – despite some variation – is sufficiently distinct from that of another layer. This is especially violated in sensory cortical areas, arguing for functional specialisations of excitatory cells based on their distinct, cell-specific inhibitory input “supply”. Thus, the principle of wiring specificity overrides the principle of a strict laminar (compartmental) organization of inhibitory circuits. Furthermore, no obvious association exists

between changes in input numbers and anatomical laminar borders. These results recall early morphological observations which gave rise to the idea that inhibitory circuits lack a clear laminar organization (White, 1989).

Functional significance of area- and cell-specific variations in inhibitory connectivity

The variable frequencies at which particular translaminar inhibitory circuit motifs appear in different cortical areas (Fig. 5.1, Fig. 8.1) and the selective participation of pyramidal cells in them (Fig. 5.3) suggest links between these motifs and the functional specialization of areas and cells: For example, the notable layer 4-to-5A connection in S1 may relate to the operation of two thalamocortical input channels in barrel cortex (Koralek et al., 1988; Lu and Lin, 1993). One channel, termed the lemniscal projection, links the ventral posteromedial nucleus (VPM) to cortical layers 3, 4, 5B, and 6, with layer 4 exhibiting the highest density of synaptic terminals. The second, so-called paralemniscal pathway originates in the posterior medial nucleus (POm) and terminates in layers 5A and 1. Prominent reciprocal inhibitory connections between layers 4 and 5A may exist in S1 (but not V1) to enable bidirectional, potentially competitive, communication between these two input streams (Fig. 8.1).

The most striking examples of translaminar inhibition, however, were seen in V1, where some pyramidal cells in layer 5B were strongly inhibited by neurons in layer 6 and cells in layers 2/3 and 4 by interneurons in layer 5, especially sublayer 5B (Fig. 8.1). The likely conductors of these inhibitory signals across laminae are Martinotti cells, which are by far the most abundant deep-layer interneurons with

extensive axonal ramifications in upper layers and are thought to provide normalizing dendritic inhibition through these axonal arbors (Kapfer et al., 2007; Markram et al., 2004; Murayama et al., 2009; Silberberg and Markram, 2007; Wang et al., 2004). Because Martinotti cells are driven intracortically (Berger et al., 2009; Kapfer et al., 2007; Otsuka and Kawaguchi, 2009; Silberberg and Markram, 2007) rather than by thalamic afferents (Cruikshank et al., 2010), and because layer 5 Martinotti cells have been found to innervate pyramidal neurons in layer 2/3 (Kapfer et al., 2007), the translaminar inhibitory connections uncovered here may form part of inhibitory feedback loops from the canonical target layers (Douglas and Martin, 2004; Gilbert and Wiesel, 1979, 1983) of excitatory output: One such loop connects layer 5(B) back to layer 2/3; another loop links layer 6 back to layer 5B (Fig. 8.1). Indeed, empirical evidence for strong excitation of putative Martinotti cells in layer 5 from layer 3 (Otsuka and Kawaguchi, 2009) as well as from layer 5 (Silberberg and Markram, 2007) pyramidal neurons has been described.

In S1, where that 5B-to-2/3 inhibition is also present, albeit weaker than in V1, the specific plasticity of this connection in response to whisker-deprivation detected here (Fig. 7.1) is consistent with its proposed (layer-5B-specific) role of providing normalizing negative feedback: The less input such a network receives, the more the layer-5B-derived inhibition is reduced adaptively. The non-deprived (control) cortex receives more input than the non-deprived C-row barrels in an otherwise deprived cortex, because each row is also partly excited by its neighbours under normal circumstances (Petersen, 2007). Deprived barrels, in turn, receive the least excitation, and thus the least putative normalizing inhibition.

In addition, such structural plasticity following sensory deprivation argues that area- and cell-specific translaminar inhibitory motifs are causally involved in adapting a

circuit to its particular computational function. Furthermore, its layer-specificity hint towards a functional meaning of the home-layer of the presynaptic interneuron (confirming hypothesis 1, as described in the introduction).

Inhibitory circuits and receptive fields

Given the prominence of translaminar (putative) feedback inhibition in V1, and given that V1 is one of the few neocortical areas were a true, individual functional specialisation of neighbouring excitatory cells (simple vs. complex cells) is known (Hubel and Wiesel, 1962; Niell and Stryker, 2008), it is reasonable to hypothesize that such selective connections play a role in the construction of visual receptive fields. Of the two types of pyramidal cells — those receiving exclusively intralaminar inhibition (I term these the home layer-inhibited neurons) and those with translaminar inhibitory inputs (I refer to these as feedback-inhibited neurons) — home layer-inhibited neurons outnumber feedback-inhibited neurons by ~3:1 in layer 2/3 (Fig. 5.3a). In layer 5B, this ratio inverts and reaches ~1:2 in favour of feedback-inhibited neurons (Fig. 5.3b). These numerical ratios match closely the proportions of simple to complex cells in layers 2/3 and 5 (3:1 and 1:3, respectively; (Niell and Stryker, 2008)), raising the possibility that the two cell types described here might correspond functionally to simple and complex cells in visual cortex (Hubel and Wiesel, 1959, 1962).

Assuming this correspondence is genuine, what might be the roles of intra- and translaminar inhibition in the function of simple and complex cells? In layer 2/3, home layer-inhibited neurons (putative simple cells) collect inhibitory inputs from a more extensive horizontal domain than do feedback-inhibited neurons (putative complex cells) (Fig. 5.4). This is expected if lateral inhibition provides a potential mechanism for generating the linear, push-pull receptive fields of simple cells, as

has been suggested based on theoretical (Douglas et al., 1995; Douglas and Martin, 2009; Wielaard et al., 2001) and empirical (Hirsch and Martinez, 2006; Liu et al., 2009b) evidence. However, Priebe and Ferster (2008) have argued that, since the subthreshold modulation ratio across V1 cells does not show the classical bimodal distribution evident at supratheshold level, intrinsic properties of the neurons determining the spike threshold actually cause (by means of its non-linearity) the distinction between simple and complex cells (Priebe and Ferster, 2008; Priebe et al., 2004). The view expressed here has the potential of reconciling both perspectives if, for example, differential inhibition adjusts the spike threshold , i.e. provides a higher threshold for simple cells.

Complex cells, in contrast, have been proposed to achieve their characteristic spatial-phase invariance because of strong recurrent input from other simple and complex cells (Chance et al., 1999). However, the high gain g produced by recurrent networks can render them unstable and sluggish in their responses to rapidly changing signals (Chance and Abbott, 2000). In the original model (Chance et al., 1999), a factor A, dependent on the network gain (i.e. extent of excitatory recurrent connections A = (1-g)) was used to scale down the response of a cell to ensure complex cell behaviour preventing overexcitation. As such an artificial counter-regulation does not have any biological equivalent, inhibition could substitute for this element of the model circuit. Indeed, in theory, the problems of instability and response sluggishness can be solved by adding inhibitory circuit elements that produce a divisive form of shunting inhibition, or inhibition that scales with the output of the circuit, as suggested by the same group and others (Chance and Abbott, 2000; Douglas et al., 1995). In their study, the authors found it necessary to incorporate a motif of disinhibition, in addition, because simple, direct

feedback inhibition effectively just reduces the gain of the recurrent network and thus prevents the emergence of complex receptive fields, altogether. However, for such disinhibition there is, again, no empirical evidence.

Based on the empirical data presented here, however, further qualifications can be suggested, which might solve the problem by providing a suitable form of normalizing inhibitory feedback control of the recurrent network producing complex cells without assuming disinhibition:

(1) The inhibitory neuron is driven by the output of the recurrent circuit and exerts feedback-inhibition in a delayed fashion and proportional to the overall activity in the excitatory local circuit: Mechanistically, layer 5 interneurons are in an ideal position to sample the activity in the local layer 2/3 network, which produces the complex receptive field, since layer 5 is the main output target of layer 2/3 pyramidal neurons. Thus, this output scales the inhibitory layer-5-to-layer-2/3 feedback (as inspired by my finding of such a translaminar motif of inhibition).

(2) The activation of the inhibitory neuron is non-linear, as described for Martinotti cells, where non-linearity results from synaptic facilitation of the synapses that excite them (Berger et al., 2009; Berger et al., 2010; Kapfer et al., 2007; Reyes et al., 1998; Silberberg and Markram, 2007).

In addition to the facilitating activation of Martinotti cells, four further observations, all made in S1 and already described above, suggest that such a Martinotti-cell mediated gain control of a local recurrent layer 2/3 network is a realistic scenario - and might equally hold true for complex cells in V1: (a) The fact, that Martinotti cells are mainly activated intracortically – either from layer 3 or from layer 5 – but not from extrinsic sources like the thalamus; (b) the observation, that layer 5 Martinotti cells exert gain control via normalizing, divisive shunting inhibition over their

intralaminar neighbours; (c) the finding, that supralinear activation of layer 5 Martinotti cells can powerfully inhibit layer 2/3 cells in addition; (d) finally, the finding presented here, that specifically the layer-5B-to-layer-2/3 connection adapts proportionally to decreased input into the neocortical circuit (see above).

Future inverstigations

Apart from a wide range of further technological developments already outlined above (e.g. circuit mapping with two-photon resolution), some rather specific experimental lines can be suggested based on the biological findings presented here. The main goal will be to proceed from the structural or mechanistic insight derived from these (and future) mapping studies towards a functional or computational understanding of the circuit, and especially of the individual motifs of inhibition found.

Although, among those, interareal differences in *intralaminar* inhibition have been discovered, it was rather motifs of *translaminar* inhibition, which predominantly expressed striking variation between – and within - cortical areas, partly breaking the principles of canonical connectivity and laminar uniformity in favour of cell-specific wiring. Such area- and cell-specificity implies, by itself, functional meaning (of those connections and their postsynaptic target cells), which to elucidate remains the major future endeavour implied by this study. In addition, since (1) trans- in contrast to intralaminar connections can display large quantitative variation including being extremely scant or absent in some cells, since (2) they can be manipulated selectively *in vi vo* due to spatial separation from their targets (Murayama et al., 2009), and since (3) only a smaller subset of interneuronal types is known to mediate certain forms of translaminar inhibition (Markram et al., 2004),

those are also much more amenable to a subsequent functional analysis. The following lines of research are therefore proposed to investigate such motifs of translaminar inhibition aiming for a more functional understanding of them:

(1) *Identification of the interneuron-subtype which underlies each connectivity motif.* Knowledge of interneuron subtype will permit conclusions about whether inhibition is predominantly feedback or feedforward, and if it acts to control rather the spiking output or the dendritic integration of the postsynaptic cell. Using the optogenetic approach of local circuit mapping developed, albeit with different, already commercially available driver lines targeting PV-, SOM-, CR-, or NPY-positive interneurons, respectively, will allow to dissect the general inhibitory circuit structure described here, subtype by subtype.

(2) *Functional plasticity of connectivity motifs.* The current result that inhibitory connections display large within- and between-area variation leads to the conclusion, that inhibitory circuits determine the functional or computational specialization of a cortical area and its individual cells to a considerable extent. Thus, if a cortical area is deprived of its usual input – and thus its usual function – one would assume, that inhibitory connectivity will change and adapt rather predictably. This is especially true, if the cortical area assumes a novel function, instead of just remaining idle: For example, if the visual cortex were deprived of visual input, it might be rewired to process somatosensory information, as in congenitally blind humans (Cohen et al., 1997; Sadato et al., 1996), and might therefore lose the V1-specific dominant translaminar inhibition observed in layers 2/3, 4 and 5B (Fig. 5.1).

Therefore, in addition, to the deprivation study in S1 already presented here, connectivity should be studied in deprived primary visual cortex, e.g. in anophthalmic mice.

(3) *Computational modeling.* Modelling allows to bridge the gap between structural descriptive findings and their functional implications, ideally giving rise to predictions that can be tested in the intact, active brain. My mapping results have given rise to a rather specific hypothesis of how normalizing, translaminar feedback inhibition in V1 could be essential for constructing complex receptive fields, building on already existing theoretical studies (Chance and Abbott, 2000; Chance et al., 1999). Those computational models can be further developed incorporating inhibition, as described above, and thereby test the plausibility of such feedback inhibition.

(4) *In vivo experiments.* Finally, such functional predictions can be tested *in vivo*, i.e. in the context of actual cortical information processing. Most importantly, if the model proposed for V1, here, is correct, activating or silencing layer 5 interneurons *in v ivo* should alter the activity of complex – but not simple – cells in layer 2/3: Blocking excitatory synaptic transmission locally in layer 5(B) (Murayama et al., 2009), during optimal visual stimulation of a simultaneously recorded complex cell should lead to a strong increase in its firing rate, since their inhibitory feedback control via layer 5 Martinotti interneurons is abolished. Using a Gad65>P2X2 mouse (see chap. 3) and applying ATP instead, should have the opposite effect – a strong silencing of complex, but not simple cells.

Only via these and similar experimental lines will it be possible to link circuit structure more closely to computational function and clarify if distinct patterns of

inhibitory connectivity not only accompany but actually determine the functional specialization of cortical pyramidal neurons and areas.

References

Abbott, L.F., Varela, J.A., Sen, K., and Nelson, S.B. (1997). *Synaptic depression and cortical gain control*. Science 275, 220-224.

Adamantidis, A.R., Zhang, F., Aravanis, A.M., Deisseroth, K., and de Lecea, L. (2007). *Neural substrates of awakening probed with optogenetic control of hypocretin neurons*. Nature 450, 420-424.

Adhikari, A., Topiwala, M.A., and Gordon, J.A. (2010). *Synchronized activity between the ventral hippocampus and the medial prefrontal cortex during anxiety*. Neuron 65, 257-269.

Agmon, A., and Connors, B.W. (1991). *Thalamocortical responses of mouse somatosensory (barrel) cortex in vitro*. Neuroscience 41, 365-379.

Airan, R.D., Hu, E.S., Vijaykumar, R., Roy, M., Meltzer, L.A., and Deisseroth, K. (2007). *Integration of light-controlled neuronal firing and fast circuit imaging*. Current Opinion in Neurobiology 17, 587-592.

Airan, R.D., Thompson, K.R., Fenno, L.E., Bernstein, H., and Deisseroth, K. (2009). *Temporally precise in vivo control of intracellular signalling*. Nature 458, 1025-1029.

Akam, T., and Kullmann, D.M. (2010). *Oscillations and filtering networks support flexible routing of information*. Neuron 67, 308-320.

Akerman, C.J., and Cline, H.T. (2007). *Refining the roles of gabaergic signaling during neural circuit formation*. Trends in Neurosciences 30, 382-389.

Alexander, G.M., Rogan, S.C., Abbas, A.I., Armbruster, B.N., Pei, Y., Allen, J.A., Nonneman, R.J., Hartmann, J., Moy, S.S., Nicolelis, M.A., McNamara, J.O., and Roth, B.L. (2009). *Remote control of neuronal activity in transgenic mice expressing evolved g protein-coupled receptors*. Neuron 63, 27-39.

Amitai, Y., Gibson, J.R., Beierlein, M., Patrick, S.L., Ho, A.M., Connors, B.W., and Golomb, D. (2002). *The spatial dimensions of electrically coupled networks of interneurons in the neocortex*. J. Neurosci. 22, 4142-4152.

Anderson, L.A., Christianson, G.B., and Linden, J.F. (2009). *Mouse auditory cortex differs from visual and somatosensory cortices in the laminar distribution of cytochrome oxidase and acetylcholinesterase*. Brain Research 1252, 130-142.

Andrasfalvy, B.K., Zemelman, B.V., Tang, J., and Vaziri, A. (2010). *Two-photon single-cell optogenetic control of neuronal activity by sculpted light*. Proc Natl Acad Sci U S A 107, 11981-11986.

Angulo, M.C., Staiger, J.F., Rossier, J., and Audinat, E. (2003). *Distinct local circuits between neocortical pyramidal cells and fast-spiking interneurons in young adult rats*. J Neurophysiol 89, 943-953.

Apergis-Schoute, J., Pinto, A., and Pare, D. (2007). *Muscarinic co ntrol of long-range gabaergic inhibition within the rhinal cortices*. J. Neurosci. 27, 4061-4071.

Aracri, P., Consonni, S., Morini, R., Perrella, M., Rodighiero, S., Amadeo, A., and Becchetti, A. (2009). *Tonic modulation of gaba release by nicotinic a cetylcholine receptors in layer v of the murine prefrontal cortex*. Cereb Cortex 7, 7.

Aravanis, A.M., Wang, L.P., Zhang, F., Meltzer, L.A., Mogri, M.Z., Schneider, M.B., and Deisseroth, K. (2007). *An optical neural interface: In vivo control of rodent motor cortex with integrated fiberoptic and optogenetic technology*. J Neural Eng 4, S143-156.

Arenkiel, B.R., Klein, M.E., Davison, I.G., Katz, L.C., and Ehlers, M.D. (2008). *Genetic control of neuronal activity in mice conditionally expressing trpv1*. Nat Meth 5, 299-302.

Arenkiel, B.R., Peca, J., Davison, I.G., Feliciano, C., Deisseroth, K., Augustine, G.J., Ehlers, M.D., and Feng, G. (2007). *In vivo light-induced activation of neural circuitry in transgenic mice expressing channelrhodopsin-2*. Neuron 54, 205-218.

Armbruster, B.N., Li, X., Pausch, M.H., Herlitze, S., and Roth, B.L. (2007). *Evolving the lock to fit the key to create a family of g protein-coupled receptors potently activated by an inert ligand*. Proc Natl Acad Sci U S A 104, 5163-5168.

Ascoli, G.A., Alonso-Nanclares, L., Anderson, S.A., Barrionuevo, G., Benavides-Peccione, R., Burkhalter, A., Buzsaki, G., Cauli, B., DeFelipe, J., and Fairen, A. (2008). *Petilla terminology: Nomenclature of features of gabaergic interneurons of the cerebral cortex*. Nat Rev Neurosci 9, 557-568.

Axmacher, N., Mormann, F., Fernandez, G., Elger, C.E., and Fell, J. (2006). *Memory formation by neuronal synchronization*. Brain Res Rev 52, 170-182.

Azouz, R., and Gray, C.M. (2003). *Adaptive coincidence detection and dynam ic gain control in visual cortical neurons in vivo*. Neuron 37, 513-523.

Banghart, M., Borges, K., Isacoff, E., Trauner, D., and Kramer, R.H. (2004). *Light-activated ion channels for remote control of neuronal firing*. Nat Neurosci 7, 1381-1386.

Baraban, S.C., and Tallent, M.K. (2004). *Interneuron diversit y series: Interne uronal neuropeptides - endogenous regula tors of neuronal excitab ility*. Trends Neurosci 27, 135-142.

Barbour, D.L., and Callaway, E.M. (2008). *Excitatory lo cal connections of sup erficial neurons in rat auditory cortex*. J. Neurosci. 28, 11174-11185.

Bartos, M., Vida, I., Frotscher, M., Meyer, A., Monyer, H., Geiger, J.R., and Jonas, P. (2002). *Fast synaptic inhibition promotes synchronized ga mma oscillations in hipp ocampal interneuron networks*. Proc Natl Acad Sci U S A 99, 13222-13227.

Bartos, M., Vida, I., and Jonas, P. (2007). *Synaptic m echanisms of syn chronized g amma oscillations in inhibitory interneuron networks*. Nat Rev Neurosci 8, 45-56.

Beard, C., Hochedlinger, K., Plath, K., Wutz, A., and Jaenisch, R. (2006). *Efficient method to generate single-copy transgenic mice by site-specific integration in embryonic stem cells*. Genesis 44, 23-28.

Beierlein, M., Gibson, J.R., and Connors, B.W. (2003). *Two dynamically distinct inhibitory networks in layer 4 of the neocortex*. J Neurophysiol 90, 2987-3000.

Benardo, L.S. (1994). *Separate activation of fast and slow inhibitory postsynaptic potentials in rat neocortex in vitro*. J Physiol 476, 203-215.

Berger, T.K., Perin, R., Silberberg, G., and Markram, H. (2009). *Frequency-dependent disynaptic inhibition in t he pyramidal network: A ubiquitous pathway in the developing rat neocortex*. The Journal of Physiology 587, 5411-5425.

Berger, T.K., Silberberg, G., Perin, R., and Markram, H. (2010). *Brief bursts self-inhibit and correlate the pyramidal network*. PLoS Biol 8.

Berke, J.D. (2009). *Fast oscillations in cortical-striatal networks switch frequency following rewarding events and stimulant drugs*. Eur J Neurosci 30, 848-859.

Berndt, A., Yizhar, O., Gunaydin, L.A., Hegemann, P., and Deisseroth, K. (2009). *Bi-stable neural state switches*. Nat Neurosci 12, 229-234.

Bi, G., and Poo, M. (1999). *Distributed synaptic modification in neural networks induced by patterned stimulation*. Nature 401, 792-796.

Bi, G.Q., and Poo, M.M. (1998). *Synaptic modifications in cultured hippocampal neurons: Dependence on spike timing, synaptic strength, and postsynaptic cell type*. J Neurosci 18, 10464-10472.

Binzegger, T., Douglas, R.J., and Martin, K.A. (2004). *A quantitative map of the circuit of cat primary visual cortex*. J Neurosci 24, 8441-8453.

Blatow, M., Caputi, A., and Monyer, H. (2005). *Molecular diversity of neocortical gabaergic interneurones*. J Physiol 562, 99-105.

Blatow, M., Rozov, A., Katona, I., Hormuzdi, S.G., Meyer, A.H., Whittington, M.A., Caputi, A., and Monyer, H. (2003). *A novel network of multipolar bursting interneurons generates theta frequency oscillations in neocortex*. Neuron 38, 805-817.

Bock, D.D., Lee, W.C., Kerlin, A.M., Andermann, M.L., Hood, G., Wetzel, A.W., Yurgenson, S., Soucy, E.R., Kim, H.S., and Reid, R.C. (2011). *Network anatomy and in vivo physiology of visual cortical neurons*. Nature 471, 177-182.

Borg-Graham, L.J., Monier, C., and Fregnac, Y. (1998). *Visual input evokes transient and strong shunting inhibition in visual cortical neurons*. Nature 393, 369-373.

Bowery, N.G., Bettler, B., Froestl, W., Gallagher, J.P., Marshall, F., Raiteri, M., Bonner, T.I., and Enna, S.J. (2002). *International union of pharmacology. X xxiii. Mammalian î³-*

aminobutyric acidb receptors: Structure and function . Pharmacological Reviews 54, 247-264.

Boyden, E.S., Zhang, F., Bamberg, E., Nagel, G., and Deisseroth, K. (2005). *Millisecond-timescale, genetically targeted optical control of neural activity*. Nat Neurosci 8, 1263-1268.

Brill, J., and Huguenard, J.R. (2009). *Robust short-laten cy perisomatic inh ibition onto neocortical pyramidal c ells detecte d by laser-scanning ph otostimulation*. J. Neurosci. 29, 7413-7423.

Brown, S.P., and Hestrin, S. (2009). *Intracortical circuits of pyramidal neurons reflect their long-range axonal targets*. Nature.

Bucurenciu, I., Bischofberger, J., and Jonas, P. (2009). *A s mall n umber of o pen ca2+ channels trigger transmitter release at a central gabaergic synapse*. Nat Neurosci 13, 19-21.

Buhl, D.L., Harris, K.D., Hormuzdi, S.G., Monyer, H., and Buzsaki, G. (2003). *Selective impairment of hippocampal gamma oscillations in connexin- 36 knock-out mouse in vivo*. J Neurosci 23, 1013-1018.

Buhl, E.H., Tamas, G., and , A.F. (1998). *Cholinergic activation and tonic excitation induce persistent gamma oscillations in mouse somatosensory cortex in vitro*. J Physiol 513, 117-126.

Busche, M.A., Eichhoff, G., Adelsberger, H., Abramowski, D., Wiederhold, K.H., Haass, C., Staufenbiel, M., Konnerth, A., and Garaschuk, O. (2008). *Clusters of hyperactive neurons near amyloid plaques in a mouse model of alzheimer's disease*. Science 321, 1686-1689.

Busskamp, V., Duebel, J., Balya, D., Fradot, M., Viney, T.J., Siegert, S., Groner, A.C., Cabuy, E., Forster, V., Seeliger, M., Biel, M., Humphries, P., Paques, M., Mohand-Said, S., Trono, D., Deisseroth, K., Sahel, J.A., Picaud, S., and Roska, B. (2010). *Genetic reactivation of cone p hotoreceptors restores visual re sponses in r etinitis p igmentosa*. Science 329, 413-417.

Buzsaki, G. (2006). *Rhythms of the brain* (Oxford University Press).

Buzsaki, G., and Draguhn, A. (2004). *Neuronal oscillat ions in cort ical networks*. Science 304, 1926-1929.

Buzsáki, G., Geisler, C., Henze, D.A., and Wang, X.-J. (2004). *Interneuron diversity series: Circuit co mplexity a nd axon wiring eco nomy of cortical int erneurons*. Trends in Neurosciences 27, 186-193.

Callaway, E.M. (2005). *A molecular and genetic arsenal for system s neuroscience*. Trends Neurosci 28, 196-201.

Callaway, E.M. (2008). *Transneuronal cir cuit tracing wit h neurotrop ic viruses* . Current Opinion in Neurobiology 18, 617-623.

Callaway, E.M., and Katz, L.C. (1993). *Photostimulation using caged glutamate reveals functional circuitry in living brain slices*. Proc Natl Acad Sci U S A 90, 7661-7665.

Canals, S., Larrosa, B., Pintor, J., Mena, M.A., and Herreras, O. (2008). *Metabolic challenge to glia activates an adenosine-mediated safety mechanism that promotes neuronal survival by delaying the onset of spreading depression waves*. J Cereb Blood Flow Metab 28, 1835-1844.

Caputi, A., Rozov, A., Blatow, M., and Monyer, H. (2008). *Two calretinin-positive gabaergic cell types in layer 2/3 of the mouse neocortex provide different forms of inhibition*. Cereb Cortex.

Cardin, J.A., Carlen, M., Meletis, K., Knoblich, U., Zhang, F., Deisseroth, K., Tsai, L.-H., and Moore, C.I. (2009). *Driving fast-spiking cells induces gamma rhythm and controls sensory responses*. Nature 459, 663-667.

Casanova, E., Fehsenfeld, S., Mantamadiotis, T., Lemberger, T., Greiner, E., Stewart, A.F., and Schütz, G. (2001). *A camkiialpha iresbac allows brain-specific gene inactivation*. Genesis 31, 37-42.

Cases, O., Vitalis, T., Seif, I., De Maeyer, E., Sotelo, C., and Gaspar, P. (1996). *Lack of barrels in the somatosensory cortex of monoamine oxidase a-deficient mice: Role of a serotonin excess during the critical period*. Neuron 16, 297-307.

Chagnac-Amitai, Y., Luhmann, H.J., and Prince, D.A. (1990). *Burst generating and regular spiking layer 5 pyramidal neurons of rat neocortex have different morphological features*. J Comp Neurol 296, 598-613.

Chalifoux, J.R., and Carter, A.G. (2011). *Gabab receptor modulation of voltage-sensitive calcium channels in spines and dendrites*. J Neurosci 31, 4221-4232.

Chance, F.S., and Abbott, L.F. (2000). *Divisive inhibition in recurrent networks*. Network 11, 119-129.

Chance, F.S., Abbott, L.F., and Reyes, A.D. (2002). *Gain modulation from background synaptic input*. Neuron 35, 773-782.

Chance, F.S., Nelson, S.B., and Abbott, L.F. (1998). *Synaptic depression and the temporal response characteristics of v1 cells*. J. Neurosci. 18, 4785-4799.

Chance, F.S., Nelson, S.B., and Abbott, L.F. (1999). *Complex cells as cortically amplified simple cells*. Nat Neurosci 2, 277-282.

Chang, Y.M., and Luebke, J.I. (2007). *Electrophysiological diversity of layer 5 pyramidal cells in the prefrontal cortex of the rhesus monkey: In vitro slice studies*. J Neurophysiol 98, 2622-2632.

Chow, B.Y., Han, X., Dobry, A.S., Qian, X., Chuong, A.S., Li, M., Henninger, M.A., Belfort, G.M., Lin, Y., Monahan, P.E., and Boyden, E.S. (2010). *High-performance genetically targetable optical neural silencing by light-driven proton pumps*. Nature 463, 98-102.

Chrobak, J.J., and Buzsaki, G. (1996). *High-frequency oscillations in the output networks of the hippocampal-entorhinal axis of the freely behaving rat*. J Neurosci 16, 3056-3066.

Cobb, S.R., Buhl, E.H., Halasy, K., Paulsen, O., and Somogyi, P. (1995). *Synchronization of neuronal activity in hippocampus by individual gabaergic interneurons*. Nature 378, 75-78.

Cohen, L.G., Celnik, P., Pascual-Leone, A., Corwell, B., Faiz, L., Dambrosia, J., Honda, M., Sadato, N., Gerloff, C., Catala, M.D., and Hallett, M. (1997). *Functional relevance of cross-modal plasticity in blind humans*. Nature 389, 180-183.

Conklin, B.R., Hsiao, E.C., Claeysen, S., Dumuis, A., Srinivasan, S., Forsayeth, J.R., Guettier, J.M., Chang, W.C., Pei, Y., McCarthy, K.D., Nissenson, R.A., Wess, J., Bockaert, J., and Roth, B.L. (2008). *Engineering gpcr signaling pathways with rassls*. Nat Methods 5, 673-678.

Creutzig, F., Benda, J., Wohlgemuth, S., Stumpner, A., Ronacher, B., and Herz, A.V. (2010). *Timescale-invariant pattern recognition by feedforward inhibition and parallel signal processing*. Neural Comput 2010, 8.

Creutzig, F., Wohlgemuth, S., Stumpner, A., Benda, J., Ronacher, B., and Herz, A.V. (2009). *Timescale-invariant representation of acoustic communication signals by a bursting neuron*. J Neurosci 29, 2575-2580.

Cruikshank, S.J., Urabe, H., Nurmikko, A.V., and Connors, B.W. (2010). *Pathway-specific feedforward circuits between thalamus and neocortex revealed by selective optical stimulation of axons*. Neuron 65, 230-245.

Csicsvari, J., Jamieson, B., Wise, K.D., and Buzsáki, G. (2003). *Mechanisms of gamma oscillations in the hippocampus of the behaving rat*. Neuron 37, 311-322.

Dalva, M.B. (2010). *Remodeling of inhibitory synaptic connections in developing ferret visual cortex*. Neural Dev 5, 5.

Dantzker, J.L., and Callaway, E.M. (2000). *Laminar sources of synaptic input to cortical inhibitory interneurons and pyramidal neurons*. Nat Neurosci 3, 701-707.

Dayan, P., and Abbott, L.F. (2001). *Theoretical neuroscience: Computational and mathematical modeling of neural systems* (MIT Press).

DeFelipe, J. (2002). *Cortical interneurons: From cajal to 2001*. Prog Brain Res 136, 215-238.

DeFelipe, J., Alonso-Nanclares, L., and Arellano, J.I. (2002). *Microstructure of the neocortex: Comparative aspects*. Journal of Neurocytology 31, 299-316.

Deisseroth, K., Feng, G., Majewska, A.K., Miesenböck, G., Ting, A., and Schnitzer, M.J. (2006). *Next-generation optical te chnologies f or illum inating genetica lly targeted brain circuits*. J Neurosci 26, 10380-10386.

Deiters, A. (2009). *Light activation as a method of regulating and studying gene expression*. Curr Opin Chem Biol 13, 678-686.

Denk, W. (1994). *Two-photon scanning photochemical microscopy: Mapping ligand-gated ion channel distributions*. Proc Natl Acad Sci U S A 91, 6629-6633.

Denk, W., Strickler, J.H., and Webb, W.W. (1990). *Two-photon laser scanning fluorescence microscopy*. Science 248, 73-76.

Denk, W., and Svoboda, K. (1997). *Photon upmanship: Why multiphoton imaging is more than a gimmick*. Neuron 18, 351-357.

Denter, D.G., Heck, N., Riedemann, T., White, R., Kilb, W., and Luhmann, H.J. (2010). *Gabac receptors are fu nctionally e xpressed in the interm ediate zone and regulat e radial migration in the embryonic mouse neocortex*. Neuroscience 167, 124-134.

Douglas, R., Markram, H., and Martin, K.A.C. (2004). *Neocortex*. In *The synaptic organization of the brain*, G.M.G. Shepherd, ed. (Oxford University Press), pp. 499 - 558.

Douglas, R.J., Koch, C., Mahowald, M., Martin, K.A., and Suarez, H.H. (1995). *Recurrent excitation in neocortical circuits*. Science 269, 981-985.

Douglas, R.J., and Martin, K.A. (2004). *Neuronal circuit s of the neocortex* . Annu Rev Neurosci 27, 419-451.

Douglas, R.J., and Martin, K.A. (2009). *Inhibition in cortical circuits*. Curr Biol 19, R398-402.

Douglas, R.J., and Martin, K.A.C. (2007a). *Mapping the matrix: The ways of neocortex*. 56, 226-238.

Douglas, R.J., and Martin, K.A.C. (2007b). *Recurrent neuronal circuit s in the neo cortex*. Current Biology 17, R496-R500.

Douglas, R.J., Martin, K.A.C., and Whitteridge, D. (1989). *A canonical m icrocircuit for neocortex*. Neural Computation 1, 480-488.

Eckhorn, R., Bauer, R., Jordan, W., Brosch, M., Kruse, W., Munk, M., and Reitboeck, H.J. (1988). *Coherent oscillations: A mechanism of feature linking in the visu al cortex? Multiple electrode and correlation analyses in the cat*. Biol Cybern 60, 121-130.

Eisenstein, M. (2009). *Neural circuits: Putting neurons on the map*. Nature 461, 1149-1152.

Fagiolini, M., Fritschy, J.M., Low, K., Mohler, H., Rudolph, U., and Hensch, T.K. (2004). *Specific gabaa circuits for visual cortical plasticity*. Science 303, 1681-1683.

Farley, F.W., Soriano, P., Steffen, L.S., and Dymecki, S.M. (2000). *Widespread recombinase expression using flper (flipper) mice*. Genesis 28, 106-110.

Feil, R., Brocard, J., Mascrez, B., LeMeur, M., Metzger, D., and Chambon, P. (1996). *Ligand-activated site-specific recombination in mice*. Proc Natl Acad Sci U S A 93, 10887-10890.

Feinberg, E.H., VanHoven, M.K., Bendesky, A., Wang, G., Fetter, R.D., Shen, K., and Bargmann, C.I. (2008). *Gfp recon stitution acr oss synaptic partners (grasp) defin es cell contacts and synapses in living nervous systems*. Neuron 57, 353-363.

Finnerty, G.T., Roberts, L.S.E., and Connors, B.W. (1999). *Sensory experience modifies the short-term dynamics of neocortical synapses*. Nature 400, 367-371.

Fino, E., and Yuste, R. (2011). *Dense inhibito ry connectivity in neoco rtex*. Neuron 69, 1188-1203.

Fisahn, A., Pike, F.G., Buhl, E.H., and Paulsen, O. (1998). *Cholinergic induction of network oscillations at 40 hz in the hippocampus in vitro*. Nature 394, 186-189.

Fitzpatrick, D. (1996). *The functional organization of local circuits in visu al cortex: Insights from the study of tree shrew striate cortex*. Cereb. Cortex 6, 329-341.

Freese, S., and Seeburg, P. (2004). *Inaugural-dissertation: Doxycyclin- kontrollierte genexpression im rosa26-lokus der m aus, unpublish ed*. (Universitaets-Bibliothek Heidelberg).

Freund, T.F. (2003). *Interneuron diversity series: Rhyth m and mood in perisom atic inhibition*. Trends Neurosci 26, 489-495.

Fricker, D., and Miles, R. (2001). *Interneurons, spike tim ing, and perception* . Neuron 32, 771-774.

Fries, P. (2005). *A mechanism for cognitive d ynamics: Neuronal communication through neuronal coherence*. Trends in Cognitive Sciences 9, 474-480.

Fries, P., Reynolds, J.H., Rorie, A.E., and Desimone, R. (2001). *Modulation of oscillatory neuronal synchronization by selective visual attention*. Science 291, 1560-1563.

Fuchs, E.C., Zivkovic, A.R., Cunningham, M.O., Middleton, S., Lebeau, F.E., Bannerman, D.M., Rozov, A., Whittington, M.A., Traub, R.D., Rawlins, J.N., and Monyer, H. (2007). *Recruitment of parvalbu min-positive interneurons determ ines hippoca mpal function and associated behavior*. Neuron 53, 591-604.

Gabbiani, F., Midtgaard, J., and Knopfel, T. (1994). *Synaptic integr ation in a model of cerebellar granule cells*. Journal of Neurophysiology 72, 999-1009.

Gabernet, L., Jadhav, S.P., Feldman, D.E., Carandini, M., and Scanziani, M. (2005). *Somatosensory integration controlled by dynamic thalamocortical feed-forward inhibition*. Neuron 48, 315-327.

Galarreta, M., and Hestrin, S. (1999). *A network of fast-spiking cells in the neocortex connected by electrical synapses*. Nature 402, 72-75.

Galarreta, M., and Hestrin, S. (2001). *Spike transmission and synchrony detection in networks of gabaergic interneurons*. Science 292, 2295-2299.

Galarreta, M., and Hestrin, S. (2002). *Electrical and chemical synapses among parvalbumin fast-spiking gabaergic interneurons in adult mouse neocortex*. Proc Natl Acad Sci U S A 99, 12438-12443.

Garden, D.L.F., Dodson, P.D., O'Donnell, C., White, M.D., and Nolan, M.F. (2008). *Tuning of synaptic integration in the medial entorhinal cortex to the organization of grid cell firing fields*. 60, 875-889.

Gentet, L.J., Avermann, M., Matyas, F., Staiger, J.F., and Petersen, C.C. (2010). *Membrane potential dynamics of gabaergic neurons in the barrel cortex of behaving mice*. Neuron 65, 422-435.

Gibson, J.R., Beierlein, M., and Connors, B.W. (1999). *Two networks of electrically coupled inhibitory neurons in neocortex*. Nature 402, 75-79.

Gil, Z., Connors, B.W., and Amitai, Y. (1999). *Efficacy of thalamocortical and intracortical synaptic connections: Quanta, innervation, and reliability*. Neuron 23, 385-397.

Gilbert, C.D. (1983). *Microcircuitry of the visual cortex*. Annual Review of Neuroscience 6, 217-247.

Gilbert, C.D., and Wiesel, T.N. (1979). *Morphology and intracortical projections of functionally characterised neurones in the cat visual cortex*. Nature 280, 120-125.

Gilbert, C.D., and Wiesel, T.N. (1983). *Functional organization of the visual cortex*. Prog Brain Res 58, 209-218.

Glimcher, P.W. (2004). *Decisions, uncertainity, and the brain* (MIT Press).

Gloveli, T., Dugladze, T., Rotstein, H.G., Traub, R.D., Monyer, H., Heinemann, U., Whittington, M.A., and Kopell, N.J. (2005). *Orthogonal arrangement of rhythm-generating microcircuits in the hippocampus*. Proc Natl Acad Sci U S A 102, 13295-13300.

Gonchar, Y., and Burkhalter, A. (1999). *Connectivity of gabaergic calretinin-immunoreactive neurons in rat primary visual cortex*. Cereb Cortex 9, 683-696.

Gonchar, Y., Wang, Q., and Burkhalter, A. (2007). *Multiple distinct subtypes of gabaergic neurons in mouse visual cortex identified by triple immunostaining*. Front Neuroanat 1, 3.

Gorostiza, P., and Isacoff, E.Y. (2008). *Optical switches for remote and noninvasive control of cell signaling*. Science 322, 395-399.

Gradinaru, V., Mogri, M., Thompson, K.R., Henderson, J.M., and Deisseroth, K. (2009). *Optical deconstruction of parkinsonian neural circuitry*. Science 324, 354-359.

Gradinaru, V., Thompson, K.R., and Deisseroth, K. (2008). *Enphr: A natronomon as halorhodopsin enhanced for optogenetic applications*. Brain Cell Biol 36, 129-139.

Gradinaru, V., Thompson, K.R., Zhang, F., Mogri, M., Kay, K., Schneider, M.B., and Deisseroth, K. (2007). *Targeting and readout strategies for fast optical neural control in vitro and in vivo*. J Neurosci 27, 14231-14238.

Gray, C.M., Konig, P., Engel, A.K., and Singer, W. (1989). *Oscillatory responses in cat visual cortex exhibit inter-columnar synchronization which reflects global stimulus properties*. Nature 338, 334-337.

Gruber, A.J., Hussain, R.J., and O'Donnell, P. (2009). *The nucleus accumbens: A switchboard for goal-directed behaviors*. PLoS ONE 4, e5062.

Gunaydin, L.A., Yizhar, O., Berndt, A., Sohal, V.S., Deisseroth, K., and Hegemann, P. (2010). *Ultrafast optogenetic control*. Nat Neurosci 13, 387-392.

Gupta, A., Wang, Y., and Markram, H. (2000). *Organizing principles for a diversity of gabaergic interneurons and synapses in the neocortex*. Science 287, 273-278.

Haider, B., Krause, M.R., Duque, A., Yu, Y., Touryan, J., Mazer, J.A., and McCormick, D.A. (2010). *Synaptic and network mechanisms of sparse and reliable visual cortical activity during nonclassical receptive field stimulation*. Neuron 65, 107-121.

Halasy, K., Buhl, E.H., Lorinczi, Z., Tamas, G., and Somogyi, P. (1996). *Synaptic target selectivity and input of gabaergic basket and bistratified interneurons in the ca1 area of the rat hippocampus*. Hippocampus 6, 306-329.

Han, X., and Boyden, E.S. (2007). *Multiple-color optical activation, silencing, and desynchronization of neural activity, with single-spike temporal resolution*. PLoS ONE 2, e299.

Han, X., Qian, X., Stern, P., Chuong, A., and Boyden, E.S. (2009). *Informational lesions: Optical perturbation of spike timing and neural synchrony via microbial opsin gene fusions*. Frontiers in Molecular Neuroscience 2.

Harris, K. (2010). *Personal communication*.

Hawkins, J., and Blakeslee, S. (2004). *On intelligence*. (New York, Times Books).

Heintz, N. (2001). *Bac to the future: The use of bac transgenic mice for neuroscience research*. Nat Rev Neurosci 2, 861-870.

Heja, L., Barabas, P., Nyitrai, G., Kekesi, K.A., Lasztoczi, B., Toke, O., Tarkanyi, G., Madsen, K., Schousboe, A., Dobolyi, A., Palkovits, M., and Kardos, J. (2009). *Glutamate uptake triggers transporter-mediated gaba release from astrocytes*. PLoS ONE 4, e7153.

Helmstaedter, M., Sakmann, B., and Feldmeyer, D. (2009a). *L2/3 interneuron groups defined by multiparameter analysis of axonal projection, dendritic geometry, and electrical excitability*. Cerebral Cortex 19, 951-962.

Helmstaedter, M., Sakmann, B., and Feldmeyer, D. (2009b). *Neuronal correlates of local, lateral, and translaminar inhibition with reference to cortical columns*. Cerebral Cortex 19, 926-937.

Helmstaedter, M., Sakmann, B., and Feldmeyer, D. (2009c). *The relation between dendritic geometry, electrical excitability, and axonal projections of l2/3 interneurons in rat barrel cortex*. Cerebral Cortex 19, 938-950.

Hendry, S.H.C., Jones, E.G., Emson, P.C., Lawson, D.E.M., Heizmann, C.W., and Streit, P. (1989). *Two classes of cortical gaba neurons defined by differential calcium binding protein immunoreactivities*. Experimental Brain Research 76, 467-472.

Hensch, T.K., and Stryker, M.P. (2004). *Columnar architecture sculpted by gaba circuits in developing cat visual cortex*. Science 303, 1678-1681.

Hestrin, S., and Galarreta, M. (2005). *Electrical synapses define networks of neocortical gabaergic neurons*. Trends Neurosci 28, 304-309.

Higo, S., Akashi, K., Sakimura, K., and Tamamaki, N. (2009). *Subtypes of gabaergic neurons project axons in the neocortex*. Frontiers in Neuroanatomy 3.

Hirsch, J.A., and Martinez, L.M. (2006). *Circuits that build visual cortical receptive fields*. Trends in Neurosciences 29, 30-39.

Hitoshi, N., Ken-ichi, Y., and Jun-ichi, M. (1991). *Efficient selection for high-expression transfectants with a novel eukaryotic vector*. Gene 108, 193-199.

Hof, P.R., Glezer, II, Conde, F., Flagg, R.A., Rubin, M.B., Nimchinsky, E.A., and Vogt Weisenhorn, D.M. (1999). *Cellular distribution of the calcium-binding proteins parvalbumin, calbindin, and calretinin in the neocortex of mammals: Phylogenetic and developmental patterns*. J Chem Neuroanat 16, 77-116.

Holt, G.R., and Koch, C. (1997). *Shunting inhibition does not have a divisive effect on firing rates*. Neural Comput 9, 1001-1013.

Hooks, B.M., Hires, S.A., Zhang, Y.X., Huber, D., Petreanu, L., Svoboda, K., and Shepherd, G.M. (2011). *Laminar analysis of excitatory local circuits in vibrissal motor and sensory cortical areas*. PLoS Biol 9, e1000572.

Horikawa, K., and Armstrong, W.E. (1988). *A versatile means of intracellular labeling: Injection of biocytin and its detection with avidin conjugates*. J Neurosci Methods 25, 1-11.

Hormuzdi, S.G., Pais, I., LeBeau, F.E., Towers, S.K., Rozov, A., Buhl, E.H., Whittington, M.A., and Monyer, H. (2001). *Impaired elect rical signaling disrupts gamma frequency oscillations in connexin 36-deficient mice*. Neuron 31, 487-495.

Horton, J.C., and Adams, D.L. (2005). *The cortical colum n: A structure without a function*. Philosophical Transactions of the Royal Society B: Biological Sciences 360, 837-862.

Horton, J.C., and Hubel, D.H. (1981). *Regular patchy distribution of cytochrome o xidase staining in primary visual cortex of macaque monkey*. Nature 292, 762-764.

Huang, Z.J., Di Cristo, G., and Ango, F. (2007). *Development of gaba innervat ion in the cerebral and cerebellar cortices*. Nat Rev Neurosci 8, 673-686.

Hubel, D.H., and Wiesel, T.N. (1959). *Receptive fields of single neurones in the cat's striate cortex*. The Journal of Physiology 148, 574-591.

Hubel, D.H., and Wiesel, T.N. (1962). *Receptive fields, bino cular interaction and functional architecture in the cat's visual cortex*. The Journal of Physiology 160, 106-154.

Hubel, D.H., and Wiesel, T.N. (1963). *Shape and arrange ment of colu mns in cat's striate cortex*. The Journal of Physiology 165, 559-568.

Hubel, D.H., and Wiesel, T.N. (1969). *Anatomical demonstration of columns in the monkey striate cortex*. Nature 221, 747-750.

Indra, A., Warot, X., Brocard, J., Bornert, J., Xiao, J., Chambon, P., and Metzger, D. (1999). *Temporally-controlled site-specific mutagenesis in th e basal laye r of the epid ermis: Comparison of the recombinase activity of the t amoxifen-inducible cre-er(t) and cre-er(t2) recombinases*. Nucl. Acids Res. 27, 4324-4327.

Ing, T., and Poulter, M.O. (2007). *Diversity of gaba(a) receptor synaptic currents on individual pyramidal cortical neurons*. Eur J Neurosci 25, 723-734.

Ivanova, E., and Pan, Z.H. (2009). *Evaluation of the adeno-associated virus mediated long-term expression of channelrhodopsin-2 in the mouse retina*. Mol Vis 15, 1680-1689.

Izhikevich, E.M. (2006). *Dynamical system s in neuroscien ce: The geometry of excitabil ity and bursting* (MIT Press).

Jack, J.J.B., and Redman, S.J. (1971). *An electrical description of the motoneurone, and its application to the analysis of synaptic potentials*. The Journal of Physiology 215, 321-352.

Jankowska, E., Rastad, J., and Westman, J. (1976). *Intracellular application of horseradish peroxidase and its lig ht and electron microscopical appearance in spino cervical tract cells*. Brain Res 105, 557-562.

Janovjak, H., Szobota, S., Wyart, C., Trauner, D., and Isacoff, E.Y. (2010). *A light-gated, potassium-selective glut amate receptor for the optical inhibition of ne uronal firing*. Nat Neurosci 13, 1027-1032.

Jarvis, M.F., and Khakh, B.S. (2009). *Atp-gated p2x cation-channels*. Neuropharmacology 56, 208-215.

Jasinska, M., Siucinska, E., Cybulska-Klosowicz, A., Pyza, E., Furness, D.N., Kossut, M., and Glazewski, S. (2010). *Rapid, learning-indu ced inhibito ry synaptog enesis in murine barrel field*. J. Neurosci. 30, 1176-1184.

Jia, H., Rochefort, N.L., Chen, X., and Konnerth, A. (2010). *Dendritic organizat ion of sensory input to cortical neurons in vivo*. Nature 464, 1307-1312.

Jonas, P., Bischofberger, J., Fricker, D., and Miles, R. (2004). *Interneuron diversity series: Fast in, fa st out - temporal and spatial signal processing in hippo campal interneurons*. Trends Neurosci 27, 30-40.

Kalisman, N., Silberberg, G., and Markram, H. (2005). *The neocortical m icrocircuit as a tabula rasa*. Proc Natl Acad Sci U S A 102, 880-885.

Kampa, B.M., Letzkus, J.J., and Stuart, G.J. (2006). *Cortical feed-f orward networks for binding different streams of sensory information*. Nat Neurosci 9, 1472-1473.

Kano, M., Ohno-Shosaku, T., Hashimotodani, Y., Uchigashima, M., and Watanabe, M. (2009). *Endocannabinoid-mediated control of synaptic transmission*. Physiol. Rev. 89, 309-380.

Kant, I. (2001). *Kritik der urteilskraft* (Meiner-Verlag).

Kantevari, S., Matsuzaki, M., Kanemoto, Y., Kasai, H., and Ellis-Davies, G.C. (2009). *Two-color, two-photon uncaging of glutamate and gaba*. Nat Methods 7, 123-125.

Kapfer, C., Glickfeld, L.L., Atallah, B.V., and Scanziani, M. (2007). *Supralinear in crease of recurrent in hibition during sparse a ctivity in the som atosensory cortex*. Nat Neurosci 10, 743-753.

Kaplitt, M.G., Feigin, A., Tang, C., Fitzsimons, H.L., Mattis, P., Lawlor, P.A., Bland, R.J., Young, D., Strybing, K., Eidelberg, D., and During, M.J. (2007). *Safety and tolerability of gene therapy with an adeno-associated virus (aav) borne gad gene for parkinson's disease: An open label, phase i trial*. The Lancet 369, 2097-2105.

Kateriya, S., Fuhrmann, M., and Hegemann, P. (2001). *Direct subm ission: Chlamydomonas reinhardtii retinal binding protein (cop4) gene*.

Katz, L.C., and Dalva, M.B. (1994). *Scanning laser photostim ulation: A new approach for analyzing brain circuits*. J Neurosci Methods 54, 205-218.

Kätzel, D., Zemelman, B.V., Buetfering, C., Wölfel, M., and Miesenböck, G. (2011). *The columnar an d lam inar organization o f inhibitory connections to neocortica l excitatory cells*. Nat Neurosci 14, 100-107.

Kawaguchi, Y., and Kondo, S. (2002). *Parvalbumin, somatostatin and cholecystokinin as chemical markers for specific gabaergic interneuron types in the rat frontal cortex*. Journal of Neurocytology 31, 277-287.

Kawaguchi, Y., and Kubota, Y. (1993). *Correlation of physiological subgroupings of nonpyramidal cells with parvalbumin- and calbindind28k-immunoreactive neurons in layer v of rat frontal cortex*. J Neurophysiol 70, 387-396.

Kawaguchi, Y., and Kubota, Y. (1996). *Physiological and morphological identification of somatostatin- or vasoactive intestinal polypeptide-containing cells among gabaergic cell subtypes in rat frontal cortex*. J. Neurosci. 16, 2701-2715.

Kawaguchi, Y., and Kubota, Y. (1997). *Gabaergic cell subtypes and their synaptic connections in rat frontal cortex*. Cereb. Cortex 7, 476-486.

Kawate, T., Michel, J.C., Birdsong, W.T., and Gouaux, E. (2009). *Crystal structure of the atp-gated p2x4 ion channel in the closed state*. Nature 460, 592-598.

Kerlin, A.M., Andermann, M.L., Berezovskii, V.K., and Reid, R.C. (2010). *Broadly tuned response properties of diverse inhibitory neuron subtypes in mouse visual cortex*. Neuron 67, 858-871.

Kisvarday, Z.F., Martin, K.A., Whitteridge, D., and Somogyi, P. (1985). *Synaptic connections of intracellularly filled clutch cells: A type of small basket cell in the visual cortex of the cat*. J Comp Neurol 241, 111-137.

Klausberger, T., Magill, P.J., Marton, L.F., Roberts, J.D.B., Cobden, P.M., Buzsaki, G., and Somogyi, P. (2003). *Brain-state- and cell-type-specific firing of hippocampal interneurons in vivo*. Nature 421, 844-848.

Klausberger, T., Marton, L.F., O'Neill, J., Huck, J.H.J., Dalezios, Y., Fuentealba, P., Suen, W.Y., Papp, E., Kaneko, T., Watanabe, M., Csicsvari, J., and Somogyi, P. (2005). *Complementary roles of cholecystokinin- and parvalbumin-expressing gabaergic neurons in hippocampal network oscillations*. J. Neurosci. 25, 9782-9793.

Klausberger, T., and Somogyi, P. (2008). *Neuronal diversity and temporal dynamics: The unity of hippocampal circuit operations*. Science 321, 53-57.

Kleinlogel, S., Feldbauer, K., Dempski, R.E., Fotis, H., Wood, P.G., Bamann, C., and Bamberg, E. (2011). *Ultra light-sensitive and fast neuronal activation with the ca(2+)-permeable channelrhodopsin catch*. Nat Neurosci 2011, 13.

Koch, C. (2004). *Biophysics of computation: Information processing in single neurons*, New edn (Oxford University Press).

Kohl, M.M., and Paulsen, O. (2010). *The roles of gabab receptors in cortical network activity*. In *Advances in pharmacology* (Academic Press), pp. 205-229.

Konnerth, A. (2009). *Personal communication*.

Koralek, K.-A., Jensen, K.F., and Killackey, H.P. (1988). *Evidence for two complementary patterns of thalamic input to the rat somatosensory cortex*. Brain Research 463, 346-351.

Kowianski, P., Morys, J.M., Dziewiatkowski, J., Wójcik, S., Sidor-Kaczmarek, J., and Morys, J. (2008). *Npy-, som- and vip- containing interneurons in postnatal development of the rat claustrum*. Brain Research Bulletin 76, 565-571.

Kozhemiakin, M.B., Draguhn, A., and Skrebitsky, V.G. (2004). *Layer-specific potentiation of evoked ipscs in rat hippocampal ca1 pyramidal cells by lanthanum*. Brain Res Bull 64, 97-101.

Kozloski, J., Hamzei-Sichani, F., and Yuste, R. (2001). *Stereotyped position of local synaptic targets in neocortex*. Science 293, 868-872.

Krashes, M.J., DasGupta, S., Vreede, A., White, B., Armstrong, J.D., and Waddell, S. (2009). *A neural circuit mechanism integrating motivational state with memory expression in drosophila*. 139, 416-427.

Kravitz, A.V., Freeze, B.S., Parker, P.R.L., Kay, K., Thwin, M.T., Deisseroth, K., and Kreitzer, A.C. (2010). *Regulation of parkinsonian motor behaviours by optogenetic control of basal ganglia circuitry*. Nature 466, 622-626.

Kroeger, D., Tamburri, A., Amzica, F., and Sik, A. (2010). *Activity dependent layer-specific changes in the extracellular chloride concentration and chloride driving force in the rat hippocampus*. J Neurophysiol 2010, 3.

Kuhlman, S.J., and Huang, Z.J. (2008). *High-resolution labeling and functional manipulation of specific neuron types in mouse brain by cre-activated viral gene expression*. PLoS ONE 3, e2005.

Kullmann, D.M., and Lamsa, K.P. (2007). *Long-term synaptic plasticity in hippocampal interneurons*. Nat Rev Neurosci 8, 687-699.

Kuner, T., and Augustine, G.J. (2000). *A genetically encoded ratio metric indicator for chloride: Capturing chloride transients in cultured hippocampal neurons*. Neuron 27, 447-459.

Lagali, P.S., Balya, D., Awatramani, G.B., Munch, T.A., Kim, D.S., Busskamp, V., Cepko, C.L., and Roska, B. (2008). *Light-activated channels targeted to on bipolar cells restore visual function in retinal degeneration*. Nat Neurosci 11, 667-675.

Lakatos, P., Chen, C.-M., O'Connell, M.N., Mills, A., and Schroeder, C.E. (2007). *Neuronal oscillations and multisensory interaction in primary auditory cortex*. Neuron 53, 279-292.

Lammel, S., Hetzel, A., Hackel, O., Jones, I., Liss, B., and Roeper, J. (2008). *Unique properties of mesoprefrontal neurons within a dual mesocorticolimbic dopamine system*. Neuron 57, 760-773.

Lamsa, K.P., Heeroma, J.H., Somogyi, P., Rusakov, D.A., and Kullmann, D.M. (2007). *Anti-hebbian long-term potentiation in the hippocampal feedback inhibitory circuit*. Science 315, 1262-1266.

Larkum, M.E., Nevian, T., Sandler, M., Polsky, A., and Schiller, J. (2009). *Synaptic integration in tuft dendrites of layer 5 pyramidal neurons: A new unifying principle*. Science 325, 756-760.

Larkum, M.E., Senn, W., and Luscher, H.R. (2004). *Top-down dendritic input increases the gain of layer 5 pyramidal neurons*. Cereb Cortex 14, 1059-1070.

Larsen, D.D., Wickersham, I.R., and Callaway, E.M. (2007). *Retrograde tracing with recombinant rabies virus reveals correlations between projection targets and dendritic architecture in layer 5 of mouse barrel cortex*. Front Neural Circuits 1, 5.

Lawrence, J.J. (2008). *Cholinergic control of gaba release: Emerging parallels between neocortex and hippocampus*. Trends Neurosci 31, 317-327.

Le Be, J.V., and Markram, H. (2006). *Spontaneous and evoked synaptic rewiring in the neonatal neocortex*. Proc Natl Acad Sci U S A 103, 13214-13219.

Lee, S., Yoon, B.E., Berglund, K., Oh, S.J., Park, H., Shin, H.S., Augustine, G.J., and Lee, C.J. (2010). *Channel-mediated tonic gaba release from glia*. Science 330, 790-796.

Leone, D.P., Genoud, S., Atanasoski, S., Grausenburger, R., Berger, P., Metzger, D., Macklin, W.B., Chambon, P., and Suter, U. (2003). *Tamoxifen-inducible glia-specific cre mice for somatic mutagenesis in oligodendrocytes and schwann cells*. Mol Cell Neurosci 22, 430-440.

Li, X., Gutierrez, D.V., Hanson, M.G., Han, J., Mark, M.D., Chiel, H., Hegemann, P., Landmesser, L.T., and Herlitze, S. (2005). *Fast noninvasive activation and inhibition of neural and network activity by vertebrate rhodopsin and green algae channelrhodopsin*. Proc Natl Acad Sci U S A 102, 17816-17821.

Lima, S.Q., and Miesenböck, G. (2005). *Remote control of behavior through genetically targeted photostimulation of neurons*. Cell 121, 141-152.

Lin, J.Y., Lin, M.Z., Steinbach, P., and Tsien, R.Y. (2009). *Characterization of engineered channelrhodopsin variants with improved properties and kinetics*. Biophys J 96, 1803-1814.

Lippincott-Schwartz, J., and Patterson, G.H. (2009). *Photoactivatable fluorescent proteins for diffraction-limited and super-resolution imaging*. Trends Cell Biol 19, 555-565.

Lisman, J.E. (1999). *Relating hippocampal circuitry to function: Recall of memory sequences by reciprocal dentate-ca3 interactions*. Neuron 22, 233-242.

Lisman, J.E., and Idiart, M.A. (1995). *Storage of 7 +/- 2 short-term memories in oscillatory subcycles*. Science 267, 1512-1515.

Liu, B.H., Li, P., Li, Y.T., Sun, Y.J., Yanagawa, Y., Obata, K., Zhang, L.I., and Tao, H.W. (2009a). *Visual receptive field structure of cortical inhibitory neurons revealed by two-photon imaging guided recording*. J Neurosci 29, 10520-10532.

Liu, B.H., Li, P., Sun, Y.J., Li, Y.T., Zhang, L.I., and Tao, H.W. (2009b). *Intervening inhibition underlies simple-cell receptive field structure in visual cortex*. Nat Neurosci 13, 89-96.

Llano, I., Leresche, N., and Marty, A. (1991). *Calcium entry increases the sensitivity of cerebellar purkinje cells to applied gaba and decreases inhibitory synaptic currents*. Neuron 6, 565-574.

Lorente De Nó, R. (1922). *La corteza cerebral del ratón*. Trab. Lab. Invest. Biol. (Madrid) 20, 41-78.

Lorente De Nó, R. (1938). *Architectonics and structure of the cerebral cortex*. In *Physiology of the nervous system*, J.F. Fulton, ed. (New York: Oxford University Press), pp. 291 - 330.

Lu, S.M., and Lin, R.C. (1993). *Thalamic afferents of the rat barrel cortex: A light- and electron-microscopic study using phaseolus vulgaris leucoagglutinin as an anterograde tracer*. Somatosens Mot Res 10, 1-16.

Lund, J.S. (1988). *Anatomical organization of macaque monkey striate visual cortex*. Annu Rev Neurosci 11, 253-288.

Lund, J.S., and Wu, C.Q. (1997). *Local circuit neurons of macaque monkey striate cortex: Iv. Neurons of laminae 1-3a*. The Journal of Comparative Neurology 384, 109-126.

Lyon, D.C., Nassi, J.J., and Callaway, E.M. (2010). *A disynaptic relay from superior colliculus to dorsal stream visual cortex in macaque monkey*. Neuron 65, 270-279.

Ma, W.P., Liu, B.H., Li, Y.T., Huang, Z.J., Zhang, L.I., and Tao, H.W. (2010). *Visual representations by cortical somatostatin inhibitory neurons - selective but with weak and delayed responses*. J Neurosci 30, 14371-14379.

Maass, W., Natschlager, T., and Markram, H. (2002). *Real-time computing without stable states: A new framework for neural computation based on perturbations*. Neural Computation 14, 2531-2560.

Magee, J.C., and Johnston, D. (1997). *A synaptically controlled, associative signal for hebbian plasticity in hippocampal neurons*. Science 275, 209-213.

Mainen, Z.F., and Sejnowski, T.J. (1996). *Influence of dendritic structure on firing pattern in model neocortical neurons*. Nature 382, 363-366.

Mann, E.O., Kohl, M.M., and Paulsen, O. (2009). *Distinct roles of gabaa and gabab receptors in balancing and terminating persistent cortical activity*. J. Neurosci. 29, 7513-7518.

Mann, E.O., and Mody, I. (2009). *Control of hippocampal gamma oscillation frequency by tonic inhibition and excitation of interneurons*. Nat Neurosci 13, 205-212.

Mann, E.O., and Paulsen, O. (2007). *Role of gabaergic inhibition in hippocampal network oscillations*. Trends in Neurosciences 30, 343-349.

Mann, E.O., Suckling, J.M., Hajos, N., Greenfield, S.A., and Paulsen, O. (2005). *Perisomatic feedback inhibition underlies cholinergically induced fast network oscillations in the rat hippocampus in vitro*. Neuron 45, 105-117.

Marinelli, S., Pacioni, S., Cannich, A., Marsicano, G., and Bacci, A. (2009). *Self-modulation of neocortical pyramidal neurons by endocannabinoids*. Nat Neurosci 12, 1488-1490.

Markram, H. (2006). *The blue brain project*. Nat Rev Neurosci 7, 153-160.

Markram, H. (2008). *Fixing the location and dimensions of functional neocortical columns*. HFSP J 2, 132-135.

Markram, H., Lubke, J., Frotscher, M., Roth, A., and Sakmann, B. (1997a). *Physiology and anatomy of synaptic connections between thick tufted pyramidal neurones in the developing rat neocortex*. J Physiol 500 (Pt 2), 409-440.

Markram, H., Lubke, J., Frotscher, M., and Sakmann, B. (1997b). *Regulation of synaptic efficacy by coincidence of postsynaptic aps and epsps*. Science 275, 213-215.

Markram, H., Toledo-Rodriguez, M., Wang, Y., Gupta, A., Silberberg, G., and Wu, C. (2004). *Interneurons of the neocortical inhibitory system*. Nat Rev Neurosci 5, 793-807.

Marr, D. (1982). *Vision: A computational investigation into the human representation and processing of visual information* (San Francisco: W. H. Freeman & Company).

Marr, D., and Poggio, T. (1976). *Cooperative computation of stereo disparity*. Science 194, 283-287.

Martin, K.A., and Whitteridge, D. (1984). *Form, function and intra cortical projections of spiny neurones in the striate visual cortex of the cat*. The Journal of Physiology 353, 463-504.

Martin, K.A.C. (2009). *The road ahead for brain-circuit reconstruction*. Nature 462, 411-411.

Martina, M., Schultz, J.H., Ehmke, H., Monyer, H., and Jonas, P. (1998). *Functional and molecular differences between voltage-gated k+ channels of fast-spiking interneurons and pyramidal neurons of rat hippocampus*. J Neurosci 18, 8111-8125.

Martinez, L.M., Wang, Q., Reid, R.C., Pillai, C., Alonso, J.-M., Sommer, F.T., and Hirsch, J.A. (2005). *Receptive field structure varies with layer in the primary visual cortex*. Nat Neurosci 8, 372-379.

Matsuzaki, M., Ellis-Davies, G.C.R., Nemoto, T., Miyashita, Y., Iino, M., and Kasai, H. (2001). *Dendritic spine geometry is critica l for ampa receptor expression in hippo campal ca1 pyramidal neurons*. Nat Neurosci 4, 1086-1092.

Metzger, D., Clifford, J., Chiba, H., and Chambon, P. (1995). *Conditional site -specific recombination in mammalian cells using a ligand-dependent chim eric cre recombinase* . Proc Natl Acad Sci U S A 92, 6991-6995.

Miesenböck, G., De Angelis, D.A., and Rothman, J.E. (1998). *Visualizing secret ion and synaptic transmission with ph-sensitive green fluorescent proteins*. Nature 394, 192-195.

Miesenböck, G., and Kevrekidis, I.G. (2005). *Optical im aging and control of ge netically designated neurons in functioning circuits*. Annu Rev Neurosci 28, 533-563.

Miesenböck, G., and Rothman, J.E. (1997). *Patterns of synaptic activity in neural net works recorded by light emission from synaptolucins*. Proc Natl Acad Sci U S A 94, 3402-3407.

Mikat, V., and Heckel, A. (2007). *Light-dependent rna interference with nucleobase -caged sirnas*. RNA 13, 2341-2347.

Miyawaki, A., Llopis, J., Heim, R., McCaffery, J.M., Adams, J.A., Ikura, M., and Tsien, R.Y. (1997). *Fluorescent indicators for ca2+based on green fluorescent proteins and calmodulin*. Nature 388, 882-887.

Mohanty, S.K., Reinscheid, R.K., Liu, X., Okamura, N., Krasieva, T.B., and Berns, M.W. (2008). *In-depth activation of channelrhodopsin 2-sensitized excitable cells with high spatial resolution using two-photon excitat ion with a near-infrared laser m icrobeam*. Biophys J 95, 3916-3926.

Monier, C., Chavane, F., Baudot, P., Graham, L.J., and Frégnac, Y. (2003). *Orientation and direction selectivity of synaptic inputs in visual cortical neurons: A diversity of com binations produces spike tuning*. 37, 663-680.

Monyer, H., and Lambolez, B. (1995). *Molecular biology and physiolog y at the single-cell level*. Curr Opin Neurobiol 5, 382-387.

Monyer, H., and Markram, H. (2004). *Interneuron diversit y series: Molecular and genetic tools to study gabaergic interneuron diversity and function*. Trends Neurosci 27, 90-97.

Mountcastle, V. (1997). *The columnar organization of the neocortex*. Brain 120, 701-722.

Mountcastle, V.B. (1957). *Modality and topographic prope rties of sing le neurons of cat's somatic sensory cortex*. J Neurophysiol 20, 408-434.

Mountcastle, V.B. (1978). *An orga nizing principle for cerebral functio n: The unit module and the distributed system* In *The mindful brain* V.B. Mountcastle, and G.M. Edelman, eds. (MIT Press), pp. 7 - 50.

Murayama, M., Perez-Garci, E., Nevian, T., Bock, T., Senn, W., and Larkum, M.E. (2009). *Dendritic encoding of sensory stimuli controlled by deep cortical interneurons*. Nature 457, 1137-1141.

Nagel, G., Brauner, M., Liewald, J.F., Adeishvili, N., Bamberg, E., and Gottschalk, A. (2005a). *Light activation of channelrhodopsin-2 in excitable cells of caenorhabditis elegans triggers rapid behavioral responses*. Curr Biol 15, 2279-2284.

Nagel, G., Szellas, T., Huhn, W., Kateriya, S., Adeishvili, N., Berthold, P., Ollig, D., Hegemann, P., and Bamberg, E. (2003). *Channelrhodopsin-2, a directly light-gated cation-selective membrane channel*. Proc Natl Acad Sci U S A 100, 13940-13945.

Nagel, G., Szellas, T., Kateriya, S., Adeishvili, N., Hegemann, P., and Bamberg, E. (2005b). *Channelrhodopsins: Directly light-gated cation channels*. Biochem Soc Trans 33, 863-866.

Nathanson, J.L., Jappelli, R., Scheeff, E.D., Manning, G., Obata, K., Brenner, S., and Callaway, E.M. (2009). *Short promoters in viral vectors drive selective expression in mammalian inhibitory neurons, but do not restrict activity to specific in hibitory cell-types*. Front Neural Circuits 3, 19.

Ni, H., Huang, L., Chen, N., Zhang, F., Liu, D., Ge, M., Guan, S., Zhu, Y., and Wang, J.H. (2011). *Upregulation of barrel gabaergic neurons is associated with cross-modal plasticity in olfactory deficit*. PLoS ONE 5, e13736.

Niell, C.M., and Stryker, M.P. (2008). *Highly selective receptive fields in mouse visual cortex*. J. Neurosci. 28, 7520-7536.

Nikolenko, V., Poskanzer, K.E., and Yuste, R. (2007). *Two-photon photostimulation and imaging of neural circuits*. Nat Meth 4, 943-950.

Nikolenko, V., Watson, B.O., Araya, R., Woodruff, A., Peterka, D.S., and Yuste, R. (2008). *Slm microscopy: Scanless two-photon imaging and photostimulation using spatial light modulators*. Frontiers in Neural Circuits 2.

Niwa, H., Yamamura, K., and Miyazaki, J. (1991). *Efficient selection for high-expression transfectants with a novel eukaryotic vector*. Gene 108, 193-199.

Ohki, K., Chung, S., Ch'ng, Y.H., Kara, P., and Reid, R.C. (2005). *Functional imaging with cellular resolution reveals precise micro-architecture in visual cortex*. Nature 433, 597-603.

Olshausen, B.A., and Field, D.J. (2005). *How close are we to understanding v1?* Neural Computation 17, 1665-1699.

Ormond, J., and Woodin, M.A. (2009). *Disinhibition mediates a form of hippocampal long-term potentiation in area ca1*. PLoS ONE 4, e7224.

Otsuka, T., and Kawaguchi, Y. (2009). *Cortical inh ibitory cell typ es differentia lly form intralaminar and interlaminar subnet works with excitatory neurons*. J. Neurosci. 29, 10533-10540.

Padgett, C.L., and Slesinger, P.A. (2010). *Gabab receptor coupling to g-proteins a nd ion channels*. In *Advances in pharmacology* (Academic Press), pp. 123-147.

Palmenberg, A.C. (1990). *Proteolytic proce ssing of picor naviral po lyprotein*. Annu Rev Microbiol 44, 603-623.

Pankratov, Y., Lalo, U., Krishtal, O., and Verkhratsky, A. (2002). *Ionotropic p2x purinoreceptors mediate synaptic tr ansmission in rat pyram idal neuro nes of layer ii/iii of somato-sensory cortex*. J Physiol 542, 529-536.

Pankratov, Y., Lalo, U., Krishtal, O., and Verkhratsky, A. (2003). *P2x receptor-m ediated excitatory synaptic currents in somatosensory cortex*. Molecular and Cellular Neuroscience 24, 842-849.

Papagiakoumou, E., Anselmi, F., Begue, A., de Sars, V., Gluckstad, J., Isacoff, E.Y., and Emiliani, V. (2010). *Scanless two-photon excitation of chan nelrhodopsin-2*. Nat Methods 7, 848-854.

Patterson, G.H., and Lippincott-Schwartz, J. (2002). *A ph otoactivatable gfp for selective photolabeling of proteins and cells*. Science 297, 1873-1877.

Paulsen, O., and Moser, E. (1998). *A model of hippoca mpal memory encodin g and retrieval: Gabaergic control of synaptic plasticity*. Trends in Neurosciences 21, 273-278.

Pavlov, I., Savtchenko, L.P., Kullmann, D.M., Semyanov, A., and Walker, M.C. (2009). *Outwardly rectifying ton ically active gabaa receptors in pyr amidal cells modulate neuronal offset, not gain*. J Neurosci 29, 15341-15350.

Pearce, R.A. (1993). *Physiological eviden ce for two distinct ga baa response s in rat hippocampus*. Neuron 10, 189-200.

Pei, Y., Rogan, S.C., Yan, F., and Roth, B.L. (2008). *Engineered gpcrs as tools to modulate signal transduction*. Physiology (Bethesda) 23, 313-321.

Pérez-Garci, E., Gassmann, M., Bettler, B., and Larkum, M.E. (2006). *The gabab1b isoform mediates long-lasting inh ibition of dend ritic ca2+ spikes in layer 5 som atosensory pyramidal neurons*. 50, 603-616.

Peterka, D.S. (2009). *(yuste lab), personal communication*.

Peters, A., and Harriman, K.M. (1988). *Enigmatic bipolar cell of rat visual cort ex*. The Journal of Comparative Neurology 267, 409-432.

Peters, A., and Regidor, J. (1981). *A reassessment of the form s of nonpyram idal neurons in area 17 of cat visual cortex*. The Journal of Comparative Neurology 203, 685-716.

Petersen, C.C., and Sakmann, B. (2001). *Functionally independent columns of rat somatosensory barrel cortex revealed with voltage-sensitive dye imaging*. J Neurosci 21, 8435-8446.

Petersen, C.C.H. (2007). *The functional organization of the barrel cortex*. Neuron 56, 339-355.

Petreanu, L., Huber, D., Sobczyk, A., and Svoboda, K. (2007). *Channelrhodopsin-2-assisted circuit mapping of long-range callosal projections*. Nat Neurosci 10, 663-668.

Petreanu, L., Mao, T., Sternson, S.M., and Svoboda, K. (2009). *The subcellular organization of neocortical excitatory connections*. Nature 457, 1142-1145.

Pinault, D. (1996). *A novel single-cell staining procedure performed in vivo under electrophysiological control: Morpho-functional features of juxtacellularly labeled thalamic cells and other central neurons with biocytin or neurobiotin*. J Neurosci Methods 65, 113-136.

Pitler, T., and Alger, B. (1992). *Postsynaptic spike firing reduces synaptic gabaa responses in hippocampal pyramidal cells*. J. Neurosci. 12, 4122-4132.

Porter, J.T., Johnson, C.K., and Agmon, A. (2001). *Diverse types of interneurons generate thalamus-evoked feedforward inhibition in the mouse barrel cortex*. J Neurosci 21, 2699-2710.

Pouille, F., and Scanziani, M. (2004). *Routing of spike series by dynamic circuits in the hippocampus*. Nature 429, 717-723.

Priebe, N.J., and Ferster, D. (2008). *Inhibition, spike threshold, and stimulus selectivity in primary visual cortex*. Neuron 57, 482-497.

Priebe, N.J., Mechler, F., Carandini, M., and Ferster, D. (2004). *The contribution of spike threshold to the dichotomy of cortical simple and complex cells*. Nat Neurosci 7, 1113-1122.

Pulver, S.R., Pashkovski, S.L., Hornstein, N.J., Garrity, P.A., and Griffith, L.C. (2009). *Temporal dynamics of neuronal activation by channelrhodopsin-2 and trpa1 determine behavioral output in drosophila larvae*. J Neurophysiol 101, 3075-3088.

Purves, D., Augustine, G.J., Fitzpatrick, D., Hall, W.C., LaMantia, A.S., McNamara, J.O., and Williams, S.M. (2004). *Neuroscience*, 3rd edn (Sunderland, MA: Sinauer Associates, Inc.).

Rajewsky, K., Gu, H., Kuhn, R., Betz, U.A., Muller, W., Roes, J., and Schwenk, F. (1996). *Conditional gene targeting*. J Clin Invest 98, 600-603.

Ren, J., Qin, C., Hu, F., Tan, J., Qiu, L., Zhao, S., Feng, G., and Luo, M. (2011). *Habenula "Cholinergic" Neurons corelease glutamate and acetylcholine and activate postsynaptic neurons via distinct transmission modes*. Neuron 69, 445-452.

Reyes, A., Lujan, R., Rozov, A., Burnashev, N., Somogyi, P., and Sakmann, B. (1998). *Target-cell-specific facilitation and depression in neocortical circuits*. Nat Neurosci 1, 279-285.

Richards, B.A., Voss, O.P., and Akerman, C.J. (2010). *Gabaergic circuits control stimulus-instructed receptive field development in the optic tectum*. Nat Neurosci 13, 1098-1106.

Rickgauer, J.P., and Tank, D.W. (2009). *Two-photon excitation of channelrhodopsin-2 at saturation*. Proceedings of the National Academy of Sciences 106, 15025-15030.

Rivera, C., Voipio, J., Payne, J.A., Ruusuvuori, E., Lahtinen, H., Lamsa, K., Pirvola, U., Saarma, M., and Kaila, K. (1999). *The k+/cl- co-transporter kcc2 renders gaba hyperpolarizing during neuronal maturation*. Nature 397, 251-255.

Rochefort, N.L., Garaschuk, O., Milos, R.-I., Narushima, M., Marandi, N., Pichler, B., Kovalchuk, Y., and Konnerth, A. (2009). *Sparsification of neuronal activity in the visual cortex at eye-opening* . Proceedings of the National Academy of Sciences 106, 15049-15054.

Romoser, V.A., Hinkle, P.M., and Persechini, A. (1997). *Detection in living cells of ca2+-dependent changes in the fluorescence emission of an indicator composed of two green fluorescent protein variants linked by a calmodulin-binding sequence*. Journal of Biological Chemistry 272, 13270-13274.

Rosenzweig, M., Brennan, K.M., Tayler, T.D., Phelps, P.O., Patapoutian, A., and Garrity, P.A. (2005). *The drosophila ortholog of vertebrate trpa1 regulates thermotaxis*. Genes Dev 19, 419-424.

Rothman, J.S., Cathala, L., Steuber, V., and Silver, R.A. (2009). *Synaptic depression enables neuronal gain control*. Nature 457, 1015-1018.

Sadato, N., Pascual-Leone, A., Grafman, J., Ibaez, V., Deiber, M.P., Dold, G., and Hallett, M. (1996). *Activation of the primary visual cortex by braille reading in blind subjects*. Nature 380, 526-528.

Sakata, S., and Harris, K.D. (2009). *Laminar structure of spontaneous and sensory-evoked population activity in auditory cortex*. Neuron 64, 404-418.

Sauer, J.F., and Bartos, M. (2010). *Recruitment of early postnatal parvalbumin-positive hippocampal interneurons by gabaergic excitation*. J Neurosci 30, 110-115.

Scanziani, M., and Hausser, M. (2009). *Electrophysiology in the age of light*. Nature 461, 930-939.

Schroder-Lang, S., Schwarzel, M., Seifert, R., Strunker, T., Kateriya, S., Looser, J., Watanabe, M., Kaupp, U.B., Hegemann, P., and Nagel, G. (2007). *Fast manipulation of cellular camp level by light in vivo*. Nat Meth 4, 39-42.

Schubert, D., Kotter, R., Luhmann, H.J., and Staiger, J.F. (2006). *Morphology, electrophysiology and functional input connectivity of pyramidal neurons characterizes a genuine layer va in the primary somatosensory cortex*. Cereb. Cortex 16, 223-236.

Schubert, D., Kotter, R., Zilles, K., Luhmann, H.J., and Staiger, J.F. (2003). *Cell type-specific circuits of cortical layer iv spiny neurons*. J. Neurosci. 23, 2961-2970.

Schubert, D., Staiger, J.F., Cho, N., Kotter, R., Zilles, K., and Luhmann, H.J. (2001). *Layer-specific intracolumnar and transcolumnar functional connectivity of layer v pyramidal cells in rat barrel cortex*. J. Neurosci. 21, 3580-3592.

Seidenbecher, T., Laxmi, T.R., Stork, O., and Pape, H.C. (2003). *Amygdalar and hippocampal theta rhythm synchronization during fear memory retrieval*. Science 301, 846-850.

Sejnowski, T.J., and Paulsen, O. (2006). *Network oscillations: Emerging computational principles*. J Neurosci 26, 1673-1676.

Senkowski, D., Schneider, T.R., Foxe, J.J., and Engel, A.K. (2008). *Crossmodal binding through neural coherence: Implications for multisensory processing*. Trends Neurosci 31, 401-409.

Shah, S., Jain, P.K., Kala, A., Karunakaran, D., and Friedman, S.H. (2009). *Light-activated rna interference using double-stranded sirna precursors modified using a remarkable regiospecificity of diazo-based photolabile groups*. Nucleic Acids Res 37, 4508-4517.

Shepherd, G.M., Pologruto, T.A., and Svoboda, K. (2003). *Circuit analysis of experience-dependent plasticity in the developing rat barrel cortex*. Neuron 38, 277-289.

Shepherd, G.M., Stepanyants, A., Bureau, I., Chklovskii, D., and Svoboda, K. (2005). *Geometric and functional organization of cortical circuits*. Nat Neurosci 8, 782-790.

Shepherd, G.M., and Svoboda, K. (2005). *Laminar and columnar organization of ascending excitatory projections to layer 2/3 pyramidal neurons in rat barrel cortex*. J Neurosci 25, 5670-5679.

Shi, Y., and Koh, J.T. (2004). *Light-activated transcription and repression by using photocaged serms*. ChemBioChem 5, 788-796.

Shu, Y., Hasenstaub, A., and McCormick, D.A. (2003). *Turning on and off recurrent balanced cortical activity*. Nature 423, 288-293.

Siegel, M.S., and Isacoff, E.Y. (1997). *A genetically encoded optical probe of membrane voltage*. Neuron 19, 735-741.

Silberberg, G., and Markram, H. (2007). *Disynaptic inhibition between neocortical pyramidal cells mediated by martinotti cells*. Neuron 53, 735-746.

Sineshchekov, O.A., Jung, K.H., and Spudich, J.L. (2002). *Two rhodopsins mediate phototaxis to low- and high-intensity light in chlamydomonas reinhardtii*. Proc Natl Acad Sci U S A 99, 8689-8694.

Sjulson, L., and Miesenböck, G. (2008). *Photocontrol of neural activit y: Biophysica l mechanisms and performance in vivo*. Chem Rev 108, 1588-1602.

Sohal, V.S., Zhang, F., Yizhar, O., and Deisseroth, K. (2009). *Parvalbumin neurons an d gamma rhythms enhance cortical circuit performance*. Nature 459, 698-702.

Söhl, G., Maxeiner, S., and Willecke, K. (2005). *Expression and functio ns of neuro nal gap junctions*. Nat Rev Neurosci 6, 191-200.

Soltesz, I. (2006). *Diversity in the neuronal machine* (New York: Oxford University Press).

Somogyi, P., and Klausberger, T. (2005). *Defined types of cortical in terneurone structure space and spike timing in the hippocampus*. The Journal of Physiology 562, 9-26.

Soriano, P. (1999a). *Generalized lacz expre ssion with t he rosa26 cre reporter strain* . Nature genetics 21, 70-71.

Soriano, P. (1999b). *Generalized la cz expression with the rosa26 cre reporter strain* . Nat Genet 21, 70-71.

Srinivas, S., Watanabe, T., Lin, C.S., William, C.M., Tanabe, Y., Jessell, T.M., and Costantini, F. (2001). *Cre reporter strains prod uced by tar geted insertion of eyfp and ecfp into the rosa26 locus*. BMC Dev Biol 1, 4.

Staley, K.J., and Mody, I. (1992). *Shunting of excitatory input to dentate gyrus granule cells by a depola rizing gabaa receptor-mediated post synaptic co nductance*. J Neurophysiol 68, 197-212.

Sun, Q.-Q., Huguenard, J.R., and Prince, D.A. (2006). *Barrel cortex microcircuits: Thalamocortical feedforward inhibition in spin y stellate cells is mediated by a sm all number of fast-spiking interneurons*. J. Neurosci. 26, 1219-1230.

Sun, W., and Dan, Y. (2009). *Layer-specific network oscillation and spatiot emporal receptive field in the visual cortex*. Proceedings of the National Academy of Sciences 106, 17986-17991.

Sussillo, D., and Abbott, L.F. (2009). *Generating coherent patterns of activit y from chaotic neural networks*. 63, 544-557.

Svoboda, K., Tank, D.W., and Denk, W. (1996). *Direct m easurement of coupling between dendritic spines and shafts*. Science 272, 716-719.

Swadlow, H.A. (2002). *Thalamocortical con trol of feed-forward inhibition in awake somatosensory 'barrel' cortex*. Philos Trans R Soc Lond B Biol Sci 357, 1717-1727.

Swadlow, H.A. (2003). *Fast-spike interneurons and feedforward inhibition in awake sensory neocortex*. Cereb Cortex 13, 25-32.

Swadlow, H.A., and Gusev, A.G. (2002). *Receptive-field construction in cortical inhibitory interneurons*. Nat Neurosci 5, 403-404.

Szabadics, J., Tamas, G., and Soltesz, I. (2007). *Different transmitter transients underlie presynaptic cell type specificity of gabaa,slow and gabaa,fast*. Proc Natl Acad Sci U S A 104, 14831-14836.

Szobota, S., Gorostiza, P., Del Bene, F., Wyart, C., Fortin, D.L., Kolstad, K.D., Tulyathan, O., Volgraf, M., Numano, R., Aaron, H.L., Scott, E.K., Kramer, R.H., Flannery, J., Baier, H., Trauner, D., and Isacoff, E.Y. (2007). *Remote control of neuronal activity with a light-gated glutamate receptor*. Neuron 54, 535-545.

Szymczak, A.L., Workman, C.J., Wang, Y., Vignali, K.M., Dilioglou, S., Vanin, E.F., and Vignali, D.A. (2004). *Correction of multi-gene deficiency in vivo using a single 'self-cleaving' 2a peptide-based retroviral vector*. Nat Biotechnol 22, 589-594.

Tan, E.M., Yamaguchi, Y., Horwitz, G.D., Gosgnach, S., Lein, E.S., Goulding, M., Albright, T.D., and Callaway, E.M. (2006). *Selective and quickly reversible inactivation of mammalian neurons in vivo using the drosophila allatostatin receptor*. Neuron 51, 157-170.

Thomson, A.M., and Bannister, A.P. (2003). *Interlaminar connections in the neocortex*. Cereb. Cortex 13, 5-14.

Thomson, A.M., Deuchars, J., and West, D.C. (1996a). *Neocortical local synaptic circuitry revealed with dual intracellular recordings and biocytin-filling*. J Physiol Paris 90, 211-215.

Thomson, A.M., and Lamy, C. (2007). *Functional maps of neocortical local circuitry*. Front Neurosci 1, 19-42.

Thomson, A.M., and Morris, O.T. (2002). *Selectivity in the inter-laminar connections made by neocortical neurones*. Journal of Neurocytology 31, 239-246.

Thomson, A.M., West, D.C., Hahn, J., and Deuchars, J. (1996b). *Single axon ipsps elicited in pyramidal cells by three classes of interneurones in slices of rat neocortex*. The Journal of Physiology 496, 81-102.

Thomson, A.M., West, D.C., Wang, Y., and Bannister, A.P. (2002). *Synaptic connections and small circuits involving excitatory and inhibitory neurons in layers 2-5 of adult rat and cat neocortex: Triple intracellular recordings and biocytin labelling in vitro*. Cereb. Cortex 12, 936-953.

Tian, L., Hires, S.A., Mao, T., Huber, D., Chiappe, M.E., Chalasani, S.H., Petreanu, L., Akerboom, J., McKinney, S.A., Schreiter, E.R., Bargmann, C.I., Jayaraman, V., Svoboda, K., and Looger, L.L. (2009). *Imaging neural activity in worms, flies and mice with improved gcamp calcium indicators*. Nat Meth 6, 875-881.

Toledo-Rodriguez, M., Blumenfeld, B., Wu, C., Luo, J., Attali, B., Goodman, P., and Markram, H. (2004). *Correlation maps allow neuronal elect rical properties to be predicted from single-cell gene expression profiles in rat neocortex*. Cereb Cortex 14, 1310-1327.

Toledo-Rodriguez, M., El Manira, A., Wallen, P., Svirskis, G., and Hounsgaard, J. (2005). *Cellular signalling properties in microcircuits*. Trends Neurosci 28, 534-540.

Tomita, H., Sugano, E., Isago, H., Hiroi, T., Wang, Z., Ohta, E., and Tamai, M. (2009). *Channelrhodopsin-2 gene transduced into retinal ganglion cells restores functional vision in genetically blind rats*. Exp Eye Res 90, 429-436.

Tonnesen, J., Sorensen, A.T., Deisseroth, K., Lundberg, C., and Kokaia, M. (2009). *Optogenetic control of epileptifor m activity* . Proceedings of the National Academy of Sciences 106, 12162-12167.

Traub, R.D., Bibbig, A., LeBeau, F.E.N., Cunningham, M.O., and Whittington, M.A. (2005). *Persistent ga mma oscillations in su perficial layers of rat a uditory neocortex: Experim ent and model*. J Physiol 562, 3-8.

Trauner, D. (2009). *Personal communication*.

Ts'o, D.Y., and Gilbert, C.D. (1988). *The organization of chromatic and spatial interactions in the primate striate cortex*. J Neurosci 8, 1712-1727.

Tsien, J.Z., Chen, D.F., Gerber, D., Tom, C., Mercer, E.H., Anderson, D.J., Mayford, M., Kandel, E.R., and Tonegawa, S. (1996a). *Subregion- and cell t ype-restricted gene knockout in mouse brain*. Cell 87, 1317-1326.

Tsien, J.Z., Chen, D.F., Gerber, D., Tom, C., Mercer, E.H., Anderson, D.J., Mayford, M., Kandel, E.R., and Tonegawa, S. (1996b). *Subregion- and cell type restricte d gene knockout in mouse brain*. 87, 1317-1326.

Tyler, C.J., Dunlop, S.A., Lund, R.D., Harman, A.M., Dann, J.F., Beazley, L.D., and Lund, J.S. (1998). *Anatomical comparison of the macaque and marsupial visual cortex: Co mmon features th at m ay reflect retent ion of essential cortical elem ents*. The Journal of Comparative Neurology 400, 449-468.

Tyzio, R., Cossart, R., Khalilov, I., Minlebaev, M., Hubner, C.A., Represa, A., Ben-Ari, Y., and Khazipov, R. (2006). *Maternal oxytocin triggers a tra nsient inh ibitory switch in gaba signaling in the fetal brain during delivery*. Science 314, 1788-1792.

Uematsu, M., Hirai, Y., Karube, F., Ebihara, S., Kato, M., Abe, K., Obata, K., Yoshida, S., Hirabayashi, M., Yanagawa, Y., and Kawaguchi, Y. (2008). *Quantitative che mical composition of cort ical gabaergic n eurons reve aled in transgenic venus-expressing rats* . Cereb Cortex 18, 315-330.

Volgraf, M., Gorostiza, P., Numano, R., Kramer, R.H., Isacoff, E.Y., and Trauner, D. (2006). *Allosteric control of an ionotropic gluta mate receptor with an optical switch* . Nat Chem Biol 2, 47-52.

von Engelhardt, J., Eliava, M., Meyer, A.H., Rozov, A., and Monyer, H. (2007). *Functional characterization of intrinsic cholinergic interneurons in the cortex*. J Neurosci 27, 5633-5642.

Walker, J.W., McCray, J.A., and Hess, G.P. (1986). *Photolabile protecting groups for an acetylcholine receptor ligand. Synthesis and photochemistry of a new class of o-nitrobenzyl derivatives and their effects on receptor function*. Biochemistry 25, 1799-1805.

Wang, H., Peca, J., Matsuzaki, M., Matsuzaki, K., Noguchi, J., Qiu, L., Wang, D., Zhang, F., Boyden, E., Deisseroth, K., Kasai, H., Hall, W.C., Feng, G., and Augustine, G.J. (2007). *High-speed mapping of synaptic connectivity using photostimulation in channelrhodopsin-2 transgenic mice*. Proceedings of the National Academy of Sciences 104, 8143-8148.

Wang, Y., Gupta, A., and Markram, H. (1999). *Anatomical and functional differentiation of glutamatergic synaptic innervation in the neocortex*. J Physiol Paris 93, 305-317.

Wang, Y., Toledo-Rodriguez, M., Gupta, A., Wu, C., Silberberg, G., Luo, J., and Markram, H. (2004). *Anatomical, physiological and molecular properties of martinotti cells in the somatosensory cortex of the juvenile rat*. The Journal of Physiology 561, 65-90.

Weaver, C.M., and Wearne, S.L. (2008). *Neuronal firing sensitivity to morphologic and active membrane parameters*. PLoS Comput Biol 4, e11.

Weiler, N., Wood, L., Yu, J., Solla, S.A., and Shepherd, G.M.G. (2008). *Top-down laminar organization of the excitatory network in motor cortex*. Nat Neurosci 11, 360-366.

Welker, E., Armstrong-James, M., Bronchti, G., Ourednik, W., Gheorghita-Baechler, F., Dubois, R., Guernsey, D.L., Van der Loos, H., and Neumann, P.E. (1996). *Altered sensory processing in the somatosensory cortex of the mouse mutant barrelless*. Science 271, 1864-1867.

Weston, A.D., and Hood, L. (2004). *Systems biology, proteomics, and the future of health care: Toward predictive, preventative, and personalized medicine*. J Proteome Res 3, 179-196.

White, E.L. (1989). *Cortical circuits. Synaptic organization of the cerebral cortex* (Boston: Birkhauser).

Wickersham, I.R., Finke, S., Conzelmann, K.K., and Callaway, E.M. (2007a). *Retrograde neuronal tracing with a deletion-mutant rabies virus*. Nat Methods 4, 47-49.

Wickersham, I.R., Lyon, D.C., Barnard, R.J., Mori, T., Finke, S., Conzelmann, K.K., Young, J.A., and Callaway, E.M. (2007b). *Monosynaptic restriction of transsynaptic tracing from single, genetically targeted neurons*. Neuron 53, 639-647.

Wieboldt, R., Gee, K.R., Niu, L., Ramesh, D., Carpenter, B.K., and Hess, G.P. (1994a). *Photolabile precursors of glutamate: Synthesis, photochemical properties, and activation of glutamate receptors on a microsecond time scale*. Proc Natl Acad Sci U S A 91, 8752-8756.

Wieboldt, R., Ramesh, D., Carpenter, B.K., and Hess, G.P. (1994b). *Synthesis and photochemistry of photolabile derivatives of gamma-aminobutyric acid for chemical kinetic investigations of the gamma-aminobutyric acid receptor in the millisecond time region*. Biochemistry 33, 1526-1533.

Wielaard, D.J., Shelley, M., McLaughlin, D., and Shapley, R. (2001). *How simple cells are made in a nonlinear network model of the visual cortex*. J. Neurosci. 21, 5203-5211.

Wilcox, M., Viola, R.W., Johnson, K.W., Billington, A.P., Carpenter, B.K., McCray, J.A., Guzikowski, A.P., and Hess, G.P. (1990). *Synthesis of photolabile precursors of amino acid neurotransmitters*. The Journal of Organic Chemistry 55, 1585-1589.

Wilson, R.I., Kunos, G., and Nicoll, R.A. (2001). *Presynaptic specificity of endocannabinoid signaling in the hippocampus*. Neuron 31, 453-462.

Womelsdorf, T., Fries, P., Mitra, P.P., and Desimone, R. (2006). *Gamma-band synchronization in visual cortex predicts speed of change detection*. Nature 439, 733-736.

Woolsey, T.A., and Van der Loos, H. (1970). *The structural organization of layer iv in the somatosensory region (si) of mouse cerebral cortex. The description of a cortical field composed of discrete cytoarchitectonic units*. Brain Res 17, 205-242.

Woolsey, T.A., Welker, C., and Schwartz, R.H. (1975). *Comparative anatomical studies of the sml face cortex with special reference to the occurrence of "Barrels" In layer iv*. J Comp Neurol 164, 79-94.

Wu, Y.I., Frey, D., Lungu, O.I., Jaehrig, A., Schlichting, I., Kuhlman, B., and Hahn, K.M. (2009). *A genetically encoded photoactivatable rac controls the motility of living cells*. Nature 461, 104-108.

Wyart, C., Bene, F.D., Warp, E., Scott, E.K., Trauner, D., Baier, H., and Isacoff, E.Y. (2009). *Optogenetic dissection of a behavioural module in the vertebrate spinal cord*. Nature 461, 407-410.

Xu, X., and Callaway, E.M. (2009). *Laminar specificity of functional input to distinct types of inhibitory cortical neurons*. J. Neurosci. 29, 70-85.

Xu, X., Olivas, N.D., Ievi, R., Ikrar, T., and Nenadic, Z. (2010a). *High precision and fast functional mapping of cortical circuitry through a combination of voltage sensitive dye imaging and laser scanning photostimulation*. J Neurophysiol 103, 2301-2312.

Xu, X., Roby, K.D., and Callaway, E.M. (2010b). *Immunochemical characterization of inhibitory mouse cortical neurons: Three chemically distinct classes of inhibitory cells*. The Journal of Comparative Neurology 518, 389-404.

Yazaki-Sugiyama, Y., Kang, S., Cateau, H., Fukai, T., and Hensch, T.K. (2009). *Bidirectional plasticity in fast-spiking gaba circuits by visual experience*. Nature 462, 218-221.

Yoshimura, Y., and Callaway, E.M. (2005). *Fine-scale specificity of cortical networks depends on inhibitory cell type and connectivity*. Nat Neurosci 8, 1552-1559.

Yoshimura, Y., Dantzker, J.L., and Callaway, E.M. (2005). *Excitatory cortical neurons form fine-scale functional networks*. Nature 433, 868-873.

Yuste, R., MacLean, J.N., Smith, J., and Lansner, A. (2005). *The cortex as a central pattern generator*. Nat Rev Neurosci 6, 477-483.

Zaitsev, A.V., Povysheva, N.V., Gonzalez-Burgos, G., Rotaru, D., Fish, K.N., Krimer, L.S., and Lewis, D.A. (2008). *Interneuron diversity in layers 2-3 of monkey prefrontal cortex*. Cereb. Cortex, bhn198.

Zemelman, B.V., Lee, G.A., Ng, M., and Miesenböck, G. (2002). *Selective photostimulation of genetically charged neurons*. Neuron 33, 15-22.

Zemelman, B.V., and Miesenböck, G. (2001). *Genetic schemes and schemata in neurophysiology*. Curr Opin Neurobiol 11, 409-414.

Zemelman, B.V., Nesnas, N., Lee, G.A., and Miesenböck, G. (2003). *Photochemical gating of heterologous ion channels: Remote control over genetically designated populations of neurons*. Proc Natl Acad Sci U S A 100, 1352-1357.

Zhang, F., Prigge, M., Beyriere, F., Tsunoda, S.P., Mattis, J., Yizhar, O., Hegemann, P., and Deisseroth, K. (2008). *Red-shifted optogenetic excitation: A tool for fast neural control derived from volvox carteri*. Nat Neurosci 11, 631-633.

Zhang, F., Wang, L.P., Boyden, E.S., and Deisseroth, K. (2006). *Channelrhodopsin-2 and optical control of excitable cells*. Nat Methods 3, 785-792.

Zhang, F., Wang, L.P., Brauner, M., Liewald, J.F., Kay, K., Watzke, N., Wood, P.G., Bamberg, E., Nagel, G., Gottschalk, A., and Deisseroth, K. (2007). *Multimodal fast optical interrogation of neural circuitry*. Nature 446, 633-639.

Zhang, J., Laiwalla, F., Kim, J.A., Urabe, H., Wagenen, R.V., Song, Y.-K., Connors, B.W., Zhang, F., Deisseroth, K., and Nurmikko, A.V. (2009). *Integrated device for optical stimulation and spatiotemporal electrical recording of neural activity in light-sensitized brain tissue*. Journal of Neural Engineering, 055007.

Zhao, J., Gover, T.D., Muralidharan, S., Auston, D.A., Weinreich, D., and Kao, J.P.Y. (2006). *Caged vanilloid ligands for activation of trpv1 receptors by 1- and 2-photon excitation*. Biochemistry 45, 4915-4926.

Zhao, S., Cunha, C., Zhang, F., Liu, Q., Gloss, B., Deisseroth, K., Augustine, G.J., and Feng, G. (2008). *Improved expression of halorhodopsin for light-induced silencing of neuronal activity*. Brain Cell Biol 36, 141-154.

Zhu, P., Narita, Y., Bundschuh, S.T., Fajardo, O., Zhang Schärer, Y.-P., Chattopadhyaya, B., Arn Bouldoires, E., Stepien, A.E., Deisseroth, K., Arber, S., Sprengel, R., Rijli, F.M., and

Friedrich, R.W. (2009). *Optogenetic dissection of neuronal circuits in zebrafish using viral gene transfer and the tet system*. Frontiers in Neural Circuits 3.

Zilles, K., and Wree, A. (1995). *Cortex: Areal and laminar structure*. In *The rat nervous system*, G. Paxinos, ed. (Academic Press), pp. 649-679.